BULLETIN
OF THE
CHEMICAL SOCIETY OF JAPAN

Vol. 33 No. 3 March 1960

OHIO STATE UNIVERSITY
MAY 4 1960
LIBRARY

CONTENTS

General and Physical

T. TANAKA: Heats of Formation of Lower Members of Dimethyl- and Methylisopropoxy-cyclopolysiloxanes 282

H. SANO: Studies on Organic Reagents for Inorganic Analysis. VI. Absorption Spectrum of Phenylfluorone-Metal Chelate and the Nature of the Chelating Bond 286

H. IMAI, S. CHAKI and S. INOUYE: Studies on the Vibrated Dropping Mercury Electrode. II. Electrocapillary Characteristics of the Current-Voltage Curve 296

A. SHIMADA: The Crystal Structure of Phenylarsonic Acid. 301

K. MAEDA: On the *d* Orbital of the Sulfur Atom in Thiophene. 304

K. ITO, K. INUKAI and T. ISOBE: Fluorine-19 Nuclear Magnetic Shielding in Some Monofluorinated Compounds. 315

M. KATO, T. NAKAGAWA and H. AKAMATU: Viscometric Study on Polystyrenesulfonic Acid Solutions. 322

H. HOTTA and A. TERAKAWA: Effect of Cupric Ion on Oxidation of Benzene Aqueous Solution by Cobalt-60 Gamma-rays. 335

K. KODERA and Y. ONISHI: The Molecular Cross-sectional Areas for the Determination of Specific Surface Areas of Solids. II. Titania and Silica 338

T. SAITO: The Molecular Structure of Hexachlorobenzene by Electron Diffraction 343

T. WATANABE: Studies on Thixotropy. I. On the Thixotropic Gelation Process 347

S. MIYAMOTO: The Effect of Metallic Ions on Surface Chemical Phenomena. III. Solubility of Various Metal Dodecyl Sulfates in Water 371

S. MIYAMOTO: The Effect of Metallic Ions on Surface Chemical Phenomena. IV. Surface Tension Measurement on Aqueous Solutions of Metal Dodecyl Sulfates. 375

H. SUZUKI: Relations between Electronic Absorption Spectra and Spatial Configurations of Conjugated Systems. V. Stilbene. 379

H. SUZUKI: Relations between Electronic Absorption Spectra and Spatial Configurations of Conjugated Systems. VI. Triphenylethylene, Tetraphenylethylene and Tolan. 389

H. SUZUKI: Relations between Electronic Absorption Spectra and Spatial Configurations of Conjugated Systems. VII. α-Substituted and α, α'-Disubstituted Stilbenes 396

H. SUZUKI: Relations between Electronic Absorption Spectra and Spatial Configurations of Conjugated Systems. VIII. Stilbene Derivatives with Methyl Groups on the Benzene Nuclei 406

H. SUZUKI: Relations between Electronic Absorption Spectra and Spatial Configurations of Conjugated Systems. IX. *p*-Phenylstilbene, *p, p'*-Diphenylstilbene, and their Related Compounds. 410

Analytical and Inorganic

B. SHARMA: Determination of Thallium(I) with Iodate in the Presence of Mercuric Ions and with Iodate and Permanganate via Bromide. 277

B. SHARMA: Preoxidation by Iodine Monochloride-Potassium Hydroxide and Use of Iodine Monochloride End Point in the Determination of Hydrazine, Thiocyanate, Thiosulfate and Glucose 279

(Continued on inside cover)

Published by the Chemical Society of Japan

THE CHEMICAL SOCIETY OF JAPAN

(NIPPON KAGAKUKAI)

Founded in 1948

Successor to the former Chemical Society of Japan founded in 1878 and to the Society of Chemical Industry, Japan founded in 1898.

OFFICERS

Munio KOTAKE, *President*, Osaka University, Osaka
Jurô HORIUTI, *Vice-President*, Hokkaido University, Sapporo
Teiji ICHIKAWA, *Vice-President*, Hiroshima University, Hiroshima
Eiichi IWASE, *Vice-President*, Institute of Physical and Chemical Research, Tokyo
Kenichi YAMAMOTO, *Vice-President*, Waseda University, Tokyo

BULLETIN OF THE CHEMICAL SOCIETY OF JAPAN

Editor: Yoshiyuki URUSHIBARA, The University of Tokyo, Tokyo
Assistant Editor: Saburo NAGAKURA, The University of Tokyo, Tokyo
Editorial Board:

Toshio ANDO	Kei MATSUZAKI	Tadao SHIBA
Genjiro HAZATO	Koji NAKANISHI	Osamu SIMAMURA
Kenichi HONDA	Shigeo OKUMURA	Tadashi SUEHIRO
Isao ICHISHIMA	Kazuo SAITO	Kenzi TAMARU
Masaji KUBO	Naoyasu SATA	Takeo WATASE
Hisao KUROYA	Tetsuro SEIYAMA	Tsuneo YOSHINO

(*Continued from outside cover*)

T. NOZAKI, H. BABA and H. ARAKI: Neutron Activation Analysis of Iodine in Silicon . . . 320

T. KIBA, I. AKAZA and O. KINOSHITA: Rapid Colorimetric Determination of Mercury by Tin(II)-Strong Phosphoric Acid Reduction Method . . . 329

S. OOI, Y. KOMIYAMA and H. KUROYA: The Crystal Structure of *trans*-$[Cr\ en_2\ Cl_2]Cl \cdot HCl \cdot 2H_2O$ . . . 354

K. NAITO: On the Mechanism of the Extraction of Uranyl Nitrate by TBP . . . 363

N. TANAKA and K. KATO: The Formation Constants of Metal Acetate Complexes. II. Polarographic Determination of the Formation Constants of Acetatocopper(II), Acetatolead(II) and Acetatozinc(II) Complexes . . . 417

Organic and Biological

C. ARAKI and S. HIRASE: Studies on the Chemical Constitution of Agar-agar. XXI. Reinvestigation of Methylated Agarose of *Gelidium Amansii* . . . 291

S. MORITA: Vapor Phase Oxidation of Alkyl Benzenes . . . 309

T. FUJITA and T. SATŌ: A Simple Method for the Preparation of Crystalline D-Mannose. . 353

Applied

Y. OGINO, M. OBA and H. UCHIDA: Catalytic Activity for Methanol Synthesis of Zinc Oxide-Chromium Oxide-Copper Oxide Catalysts and its Structural Dependency . . . 358

Short Communications

K. HIROTA, H. KUSUMOTO and T. UEDA: Confirmation of the Catalytic Deuteration of Methyl Groups of *p*-Xylene by the Use of the Infrared and NMR Methods . . . 423

A. NAKAMURA and N. HAGIHARA: Cyclopentadienyl Cobalt Cyclooctatetraene . . . 425

S. YAJIMA, S. ICHIBA, Y. KAMEMOTO and K. SHIBA: The Use of Recoil Fission Rare Gas for the Study of the Change in Crystal Structure . . . 426

M. ŌKI and H. IWAMURA: Intramolecular Interaction between Hydroxyl Group and π-Electrons. IX. The Energy of the Interaction in Benzyldimethylcarbinol . . . 427

S. FUJIWARA, H. SHIMIZU, Y. ARATA and S. AKAHORI: NMR Study of α,β-Unsaturated Fatty Acids . . . 428

K. TAMARU: Remarks on the Mechanism of Ammonia Synthesis . . . 429

S. MURAHASHI, S. NOZAKURA and Y. UTSUHARA: Polymerization of Styrene with the Ziegler-Natta Catalysts in the Presence of Molecular Hydrogen . . . 431

Determination of Thallium(I) with Iodate in the Presence of Mercuric Ions and with Iodate and Permanganate via Bromide

By Bechu SHARMA

(Received August 31, 1959)

Most of the current methods, to determine thallium(I), have certain inherent defects. Willm's method[1] based upon titration of thallium(I) in hydrochloric acid with permanganate has been used extensively, but various authors reported unfavorable results. The procedure used by Marshall[2] is tedious. Kolthoff[3], Zintl and Rienacher[4], however, titrated it accurately with bromate in hydrochloric acid using methyl orange as indicator. Willard and Young[5] determined it against ceric sulfate. Berry[6] titrated various thallous salts with iodate using iodine monochloride end point and reported low results by about 2%. Swift and Garner[7] employed iodine monochloride procedure in the determination of thallium(I) with iodate, permanganate and ceric sulfate, but precise results were obtained only with iodate. Recently a general application of the amperometric Dead Stop End Point to direct and indirect determination with iodate in the presence of mercuric ions has been reported. Arsenious oxide and hydrazine sulfate are used as direct primary standards and thiosulfate, thiocyanate and thiourea are determined by excessive iodate[8]. Investigations were therefore carried out to adopt the above procedure (iodate procedure in the presence of mercuric ions) in the determination of thallium. Oxidation titration of hydrazine sulfate with permanganate and ceric sulfate in hydrochloric acid via bromide has been carried out amperometrically using "Dead Stop End Point" written as D.S.E.P.[9] This also suggested a similar oxidizability of thallium.

1) Willm, *Bull. soc. chim. France*, **1863**, 352; *Ann.c him. phys.*, **5**, (1863).
2) H. Marshall, *J. Soc. Chem. Ind.*, **19**, 994 (1900).
3) I. M. Kolthoff, *Rec. trav. chim.*, **41**, 172 (1922).
4) E. Zintl and G. Rienacher, *Z. anorg. u. allgem. Chem.*, **153**, 276 (1926).
5) H. H. Willard and P. Young, *J. Am. Chem. Soc.*, **52**, 36 (1930).
6) A. J. Berry, *Analyst*, **51**, 137 (1926).
7) E. H. Swift and C. S. Garner, *J. Am. Chem. Soc.*, **58**, 113 (1936).
8) M. G. Bapat and B. Sharma, *Z. anal. Chem.*, **157**, 258 (1957).
9) M. G. Bapat and B. Sharma, *J. Sci. Res. (B.H.U.)*, **VII (2)**, 267 (1956—1957).

Experimental

A 0.1 N (0.025 M) solution of potassium iodate was prepared from E. Merck (G. R.) reagent. Its strength was checked against 0.1 N arsenious oxide prepared from E. Merck (G. R.) reagent using iodine monochloride end point. Approximately 0.1 N potassium permanganate solution, prepared from British Drag House (L. R.) reagent, was standardized against 0.1 N arsenious oxide. A 1% thallous acetate solution was prepared from B.D.H. reagent and its strength was determined against potassium iodate using iodine monochloride procedure.

Direct Titration Procedure. — An aliquot of iodate solution was transferred to a 100 ml. titrating vessel, 25～35 ml. of mercuric chloride (8～9%) solution was added followed by such a volume of 12 N hydrochloric acid as to adjust the overall acidity between 0.7～1.5 N. The contents of the vessel were cooled to 25°C completely. The reaction mixture was finally titrated against thallous acetate using the amperometric D.S.E.P. A potential of 0.1 V. was impressed across the indicator electrodes. The indicator current increased toward a maximum as the addition of thallous acetate solution was continued and finally decreased to a minimum at the equivalence point. As iodate is reduced to iodide, the equivalent weight in these titrations is 1/6 the formula weight.

Reverse Titration Procedure. — An aliquot of thallous acetate was taken in a titrating vessel, and mixed with 30～35 ml. mercuric chloride solution (8～9%) and 12 M hydrochloric acid (to maintain overall acidity between 1～2 N). The contents of the vessel were cooled to 25°C completely. The reaction mixture was finally titrated against standard iodate solution using the same electrometric end point. Near the equivalence point the indicator current showed a sudden increase in its value.

A series of experiments in which the acidity and mercuric chloride concentration were varied over a wide range, revealed that 1～2 N overall acid concentration and 25～35 ml. mercuric chloride gave accurate results. The results of one typical series of experiments are summarized in Tables I and II. Direct as well as reverse procedure may be extended to iodine monochloride end point (second end point), the acidity (hydrochloric acid) of the reaction mixture being raised at the iodide end point (first end point) to about 5～6 N.

Determination of Thallium(I) with Iodate and Permanganate via Bromide. —An aliquot of thallous

TABLE I. DIRECT TITRATION OF THALLIUM(I) WITH IODATE IN THE PRESENCE OF MERCURIC IONS

ml. of 0.025 M iodate	ml. of 8~9% mercuric chloride	Overall acidity N	ml. of thallous acetate		% Difference
			Reqd.	Calcd.	
2	30~35	0.5~1.5	2.78	2.75	1.00
4	30~35	0.5~1.5	5.55	5.50	0.91
5	30~35	0.5~1.5	6.95	7.00	0.71
6	30~35	0.5~1.5	8.30	8.25	0.60
8	30~35	0.5~1.5	11.06	11.00	0.55
10	30~35	0.5~1.5	13.82	13.75	0.51

TABLE II. REVERSE TITRATION OF THALLIUM(I) WITH IODATE IN THE PRESENCE OF MERCURIC IONS

ml. of thallous acetate	ml. of 8~9% mercuric chloride	Overall acidity N	ml. of 0.025 M iodate		% Difference
			Reqd.	Calcd.	
2	25~35	0.5~1.5	1.50	1.46	2.78
4	25~35	0.5~1.5	2.95	2.92	1.03
6	25~35	0.5~1.5	4.40	4.38	0.45
8	25~35	0.5~1.5	5.85	5.84	0.17
10	25~35	0.5~1.5	7.30	7.30	nil

TABLE III. DETERMINATION OF THALLIUM(I) WITH IODATE VIA BROMIDE IN HYDROCHLORIC ACID SOLUTION

ml. of thallium(I)	Wt. of potassium bromide in grams	Overall acidity N	ml. of 0.1 N iodate		% Difference
			Reqd.	Calcd.	
20	2~3	1.50	15.05	15.20	0.95
20	2~3	2.00	15.05	15.20	0.98
20	2~3	3.00	15.10	15.20	0.66
20	2~3	4.00	15.15	15.20	0.33
20	2~3	5.00	15.15	15.20	0.33

TABLE IV. DETERMINATION OF THALLIUM(I) WITH PERMANGANATE VIA BROMIDE IN HYDROCHLORIC ACID SOLUTION

ml. of thallium(I)	Wt. of potassium bromide in grams	Overall acidity N	ml. of permanganate solution		% Difference
			Reqd.	Calcd.	
20	2~3	2.0	12.60	12.65	0.39
20	2~3	3.0	12.65	12.65	nil
20	2~3	4.0	12.70	12.65	0.39
20	2~3	5.0	12.75	12.65	0.79
20	2~3	6.0	12.85	12.65	1.59

acetate was taken in a titrating vessel and 25~35 ml. 12 M hydrochloric acid was added to maintain the final acidity as indicated in Tables III and IV followed by 2~3 g. of potassium bromide. The reaction mixture was then titrated againt standard permanganate or iodate using the amperometric D.S.E.P. A potential of 0.1 V. was impressed across the indicator electrodes. The indicator current remained constant throughout the titration and finally at the equivalent point it showed a sudden increase in its value. Series of experiments in which the acidity was varied over a wide range revealed that the method is accurate for the determination of thallium(I) with iodate and permanganate via bromide at an overall acidity between 3~5 N. In the titration of thallous salt with permanganate at a high acid concentration (above 4 N), the amount of permanganate solution consumed was too high owing to (catalytic) oxidation of hydrochloric acid by permanganate.

Summary

Oxidation of thallium(I) is carried out with iodate in the presence of mercuric ions using the amperometric D.S.E.P. Thallium is oxidized to thallium(III) and iodate is quantitatively reduced to iodide. The procedure is valuable because it gives correct determination for thallium(I) at

a low acid concentration. Oxidation of thallium(I) with permanganate and iodate in hydrochloric acid via bromide is also found to be accurate and quantitative.

The author wishes to thank Professor S. S. Joshi for his kind interest in this work.

Chemical Laboratories
Banaras Hindu University
India

Pre-oxidation by Iodine Monochloride—Potassium Hydroxide and Use of Iodine Monochloride End Point in the Determination of Hydrazine, Thiocyanate, Thiosulfate and Glucose

By Bechu SHARMA

(Received August 31, 1959)

Iodate procedures introduced by Andrews[1] and later developed by Jamieson[2] and Lang[3], involve essentially the formation of iodine (+). Although applicable to a variety of common reductants, in a number of cases, iodate is not capable of bringing about direct oxidation. Thus ferrous iron and ferrocyanide bring about an apparent state of equilibrium which changes only slowly. Lang[3-4] proposed for such reductants a preoxidation by iodine monochloride solution prepared from iodide and iodate in the presence of chloride. Lang further found applicability of this method to an alkaline medium, wherein some cases hypoiodite acts more efficiently, e. g. for the determination of hydrogen peroxide[4] and formaldehyde[5]. An additional advantage of this procedure is that the back titrations can as well be followed with permanganate and ceric sulfate which are standared volumetric oxidizing agents. This point has been emphasized by Swift[6] and his coworkers in the determination of arsenic(III) wherein excessive iodine monochloride was followed in an acid medium. An earlier communication described the "iodine monochloride+sodium hydroxide" oxidation and iodine monochloride end point using iodate, permanganate and ceric sulfate for the determination of thiourea and its derivatives[7]. Subsequent investigations revealed that thiosulfate which is oxidized by alkaline hypoiodite could as well be determined. In an alkaline medium, thiosulfate is oxidized to sulfate which provides an advantage of a high conversion factor. The direct oxidation of thiocyanate by iodate, stops at cyanide stage alone while by alkaline hypoiodite it is converted into cyanate. Herein then, the modified procedure would provide an advantage of higher molecular ratio. Again, the oxidation of hydrazine sulfate, which is an ideal primary standard on account of its stability, ease of purification and various acidimetric and oxidimetric applications, was subjected to restricted conditions of acidity when titrated by iodine monochloride procedure. On the other hand, however, it could be easily oxidized by hypoiodite. Glucose is not oxidized by iodate in an acid medium, but iodine in weakly alkaline medium is capable of oxidizing it to gluconic acid. This principle was therefore applied to the determination of glucose as well. It may be pointed out that there are no direct titrimetric procedures for glucose, whose oxidation, except by iodine, hardly stops at the gluconic acid stage and the complete oxidation by drastic oxidants like permanganate and ceric sulfate in an acid medium and by ferricyanide in an alkaline medium, requires critical operative conditions for quantitative conversion into carbon dioxide and water.

1) L. W. Andrews, *J. Am. Chem. Soc.*, **25**, 756 (1903).
2) G. S. Jamieson, *Am. J. Sci.*, **33**, 352 (1912).
3) R. Lang, *Z. anorg. u. allgem. Chem.*, **142**, 229 (1925).
4) R. Lang, ibid., **142**, 280 (1925).
5) R. Lang, *Z. anal. Chem.*, **106**, 12 (1936).
6) E. H. Swift and C. H. Gregory, *J. Am. Chem. Soc.*, **52**, 901 (1930).
7) G. S. Deshmukh and M. G. Bapat, *Z. anal. Chem.*, **156**, 276 (1957).

Experimental

A 0.5 M iodine monochloride solution was prepared by dissolving 17.5 g. of potassium iodate, and 22.7 g. of potassium iodide in 250 ml. of water to which 150 ml. 12 M hydrochloric acid was added. The solution was titrated with iodate or iodide solution using carbon tetrachloride till the organic layer was colorless. A 0.1 M potassium thiocyanate solution was prepared and standardized as usual by titration with standard silver nitrate solution. Sodium thiosulfate solution was standardized against potassium dichromate as well as with 0.1 N potassium iodate using iodine monochloride end point. The latter was found to be a better check due to the oxidation of thiosulfate to sulfate, which was subsequently achieved by hypoiodite oxidation. A 0.1 N hydrazine sulfate solution was prepared from British Drng House (L.R.) reagent recrystallized from water twice and dried at 140°C. A 1% glucose solution was prepared from E. Merck (L.R.) sample and was standardized by iodimetric determination. Potassium permanganate and ceric sulfate solutions were prepared and standardized as usual. Except for glucose the following

TABLE I. OXIDATION OF HYDRAZINE BY IODINE MONOCHLORIDE+POTASSIUM HYDROXIDE

ml. 0.1 N (0.025 M) hydrazine sulfate	ml. 0.5 M iodine monochloride	Overall alkali %	Reaction time in min.	ml. 0.025 M iodate	Diff. %
(*a*) *Effect of excessive oxidant*					
10	3	1	5	9.60	4.00
10	4	1	5	9.80	2.00
10	5	1	5	9.95	0.50
15	10	1	5	14.95	0.33
(*b*) *Effect of hydrazine concentration*					
10	5	2	5	10.00	—
15	8	2	5	14.95	0.33
20	10	2	5	20.00	—
(*c*) *Test analysis*					
				ml. 0.1 N permanganate	
5	2	1	5	4.95	1.00
10	5	1	5	9.95	0.50
15	7	2	5	15.00	0.00
25	10	2	10	24.90	0.04

In all the experiments, hydrazine sulfate+iodine monochloride+potassium hydroxide was the order followed, in order to utilize the oxidant both in an acid and an alkaline medium.

TABLE II. OXIDATION OF THIOCYANATE BY IODINE MONOCHLORIDE+POTASSIUM HYDROXIDE

ml. 0.01 M thiocyanate	ml. 0.5 M iodine monochloride	Overall alkali %	Reaction time in min.	ml. 0.025 M iodate	Diff. %
(*a*) *Effect of excessive oxidant*					
10	2	1	5	7.20	−10.00
10	5	1	5	7.80	− 2.50
10	5	1	10	7.80	− 2.50
10	10	1	10	7.85	− 1.88
(*b*) *Effect of alkali concentration*					
10	2	3	10	7.50	− 6.25
10	4	4	10	7.80	− 2.50
10	5	4	10	7.90	− 1.25
10	5	6	10	7.95	− 0.62
(*c*) *Test analysis*					
5	3	4	10	3.95	− 1.25
7.5	5	5	10	5.90	− 1.56
10	10	5	10	7.95	− 0.62
10	10	5	10	7.95	− 0.62

The order of mixing was thiocyanate, iodine monochloride and alkali, in order to utilize the oxidant in acid and alkali medium.

general procedure was adopted. An aliquot of the reductant solution was taken in an Erlenmeyer flask to which an amount of iodine monochloride (at least 3/2 times that calculated on the reduction to iodide) and finally 25% (potassuim hydroxide solution were added to render the solution 1~2 N in alkali. Advantage of the addition of iodine monochloride was that the oxidant was available in an acid as well as in an alkaline medium. However, with thiosulfate, sulfur precipitates and the oxidation hardly goes to completion. The addition of alkali prior to iodine monochloride avoided this and the oxidation was found to be smooth. After being kept for 5~10 min. the solution was transferred to a 150 ml. beaker, acidified with 12 M hydrochloric acid to give an overall 5~6 N acidity and was titrated with iodate, permanganate or ceric sulfate by

TABLE III. OXIDATION OF THIOSULFATE BY IODINE MONOCHLORIDE+POTASSIUM HYDROXIDE

ml. 0.01 M thiosulfate	ml. 0.5 M iodine monochloride	Overall alkalinity %	Reaction time in min.	ml. 0.025 M iodate	Diff. %
(*a*) *Effect of excessive oxidant*					
5	2	1	5	3.80	− 5.00
5	3	1	5	3.80	− 5.00
5	4	1	5	3.85	− 3.75
10	10	1	10	7.85	− 1.88
(*b*) *Effect of alkali concentration*					
5	2	1	10	3.90	− 2.50
5	2	2	10	3.95	− 1.25
5	2	4	10	3.95	− 1.25
10	5	4	10	7.95	− 0.62
(*c*) *Test analysis*					
				ml. 0.1 M ceric sulfate	
5	2	4	15	3.95	− 1.25
7.5	4	4	10	5.95	− 0.83
10	8	4	10	7.95	− 0.62
10	10	4	10	7.95	− 0.62

Order of mixing.—Iodine monochloride+thiosulfate+alkali.—On slow addition of iodine monochloride to thiosulfate, part of sulfur separates, due to high acidity in contact with thiosulfate.

TABLE IV. OXIDATION OF GLUCOSE BY IODINE MONOCHLORIDE+POTASSIUM HYDROXIDE

ml. of 1% glucose	ml. 0.5 M iodine monochloride	Overall alkalinity %	Reaction time in min.	ml. 0.025 M iodate	Diff. %
(*a*) *Effect of excessive oxidant*					
10	3	Just alkaline to dissolve iodine*	5	10.70	3.17
10	5	〃	5	10.95	0.90
15	7	〃	10	16.40	1.05
15	8	〃	10	16.55	0.15
(*b*) *Effect of alkali concentration*					
10	3	1	5	10.60	4.07
10	5	2	5	10.75	2.71
10	5	2	10	10.75	2.71
(*c*) *Test analysis*					
10	5	as in (*a*)	10	10.95	0.90
15	10	〃	10	16.55	0.15
20	10	〃	10	22.00	0.45
20	10	〃	5	21.70	1.81

10 ml. of 1% glucose require 11.05 ml. 0.025 M iodate.

* As in the presence of excess of alkali, hypoiodite does not act smoothly on glucose, the order of mixing was "glucose+iodine monochloride", to which only just sufficient alkali was added to dissolve the liberated iodine. Finally little more alkali was added to convert iodine into hypoiodite.

the amperometric "Dead Stop End Point". The unit was the simple form of the one described by Foulk and Bawden[8]. One tenth volt was the impressed potential across the indicator electrodes between which a mechanical stirrer served to mix thoroughly the reaction mixture. The current measurements were made by a sensitive galvanometer with a lamp-and-scale arrangement. The current increased to a maximum and then decreased to a minimum where the conversion of iodine and iodide to iodine (+) was complete. In the oxidation of glucose, the control of alkalinity was most critical. This was achieved by careful addition of alkali to the mixture of glucose and iodine monochloride to the point where the iodine that separated just dissolved. The reverse order glucose-alkali-iodine-monochloride was found to give variable results. In glucose determination, the final titration was possible only with iodate because other oxidants, permangante and ceric sulfate, attacked the gluconic acid. The results of one typical series of experiments are summarized in Tables I—IV.

8) C. W. Foulk and A. T. Bawden, *J. Am. Chem. Soc.*, **48**, 2045 (1926).

Summary

The principle of hypoiodite (iodine monochloride+potassium hydroxide) pre-oxidation and iodine monochloride end point has been adopted to the determination of hydrazine, thiocyanate, thiosulfate and glucose. The availability of alternative standard titrating solutions (iodate, permanganate and ceric sulfate) and applicability over a range of reductant concentrations are essential features of this procedure.

The author wishes to thank Professor S. S. Joshi, for his kind interest in the work.

Chemical Laboratories
Banaras Hindu University
India

Heats of Formation of Lower Members of Dimethyl- and Methylisopropoxy-cyclopolysiloxanes

By Toshio TANAKA

(Received July 30, 1959)

From the investigation on the redistribution equilibrium between dimethylcyclopolysiloxanes and linear polysiloxanes catalyzed by sulfuric acid, it was concluded by Scott that the ring in the trimer of cyclosiloxanes had a slight strain, while the ring structures of tetramer and the polymer of larger size were probably free from strain. He attributed this strain to the deformation of normally large Si–O–Si angle in forming the small-membered ring[1]. Before and after that, it was indicated from X-ray[2,3] and electron[4] diffraction studies that the six-membered ring in the trimer was planer or nearly planar. While, the siloxane rings of the tetramer[5] and the octamer[6] were reported to have *zigzag* form from X-ray diffraction study, and the former ring was supposed to have *cradle* (rather than *crown*) form from electron diffraction study[7]. As the results of these studies, the difference between the molecular structures of the cyclic trimer and the cyclic tetramer exist in the Si–O–Si angle, which is 125° for the former and 140° for the latter, and it has been supposed that a value of about 140° would be probable for a strain free Si–O–Si valency angle[7].

In this paper, the heats of combustion of the members represented by C_n and D_n (see below) have been measured at 20°C and a constant volume, and the corresponding heats of combustion and formation in isobaric process have been calculated. From the results, it will be indicated

1) D. W. Scott, *J. Am. Chem. Soc.*, **69**, 803 (1947).
2) G. Peyronel, *Atti accad. nazl. Lincei. Rend., Classe sci. fis., mat. e nat.*, **15**, 402 (1953); **16**, 78, 231 (1954); *Chem. Abstr.*, **48**, 7971*b*, 10401*h* (1954).
3) W. L. Roth and D. Harker, *Acta Cryst.*, **1**, 34 (1948).
4) E. H. Aggarwal and S. H. Bauer, *J. Chem. Phys.*, **18**, 420 (1950).
5) H. Steinfink, B. Post and I. Fankuchen, *Acta Cryst.*, **5**, 802 (1954).
6) L. K. Frevel and M. J. Hunter, *J. Am. Chem. Soc.*, **67**, 2275 (1945).
7) M. Yokoi, This Bulletin, **30**, 100 (1957).

TABLE I. PHYSICAL CONSTANTS AND ANALYTICAL DATA OF C_n

Compound	b.p. °C/mmHg	d_4^{20}	n_D^{20}	Mol. wt. Found[a] (Calcd.)	MR_D Found (Calcd.)[b]	Si % Found (Calcd.)
C_3	67/1	0.9912	1.3973	348 (355)	86.23 (85.98)	23.80 (23.76)
C_4	97/1	1.0009	1.4023	— (473)	115.09 (114.64)	23.77 (23.76)

a) Cryoscopic measurement in benzene.
b) Calculated from bond refractivities by E. W. Warrick, *J. Am. Chem. Soc.*, **68**, 2455 (1946).

that the cyclotetrasiloxane and the cyclopentasiloxane are free from strain, while the cyclotrisiloxane will have a slight strain.

C_n: $\left[\begin{array}{l}CH_3\\ |\\ Si\cdot O\\ |\\ OC_3H_7\text{-}i\end{array}\right]_n$, $n=3,\ 4$; D_n: $\left[\begin{array}{l}CH_3\\ |\\ Si\cdot O\\ |\\ CH_3\end{array}\right]_n$, $n=4,\ 5$

Experimental

Materials.—The members of C_n were prepared by hydrolyzing methylisopropoxydichlorosilane with considerable dropping rate using pyridine as an acid acceptor and were characterized*. The physical constants and the analytical data are shown in Table I.

The members of D_n, supplied from Shin-etsu Chem. Ind. Co., have been rigorously fractionated through a semi-micro Stedman column of about 20 theoretical plates and the physical constants have been compared with them reported in the literature of the subject. The results are shown in Table II.

TABLE II. PHYSICAL CONSTANTS OF D_n[a]

Compound	b.p. °C/mmHg	d_4^{20}	n_D^{20}	Mol. wt. Found[b] (Calcd.)
D_4	70/18 [175/760]	0.9558 [0.9558]	1.3968 [1.3968]	291 (297)
D_5	80/8 [210/760]	0.9596 [0.9593]	1.3984 [1.3982]	362 (371)

a) The values in brackets are those reported in the publication; E. G. Rochow, "An Introduction to the Chemistry of the Silicones", 2nd Ed., John Wiley & Sons, Inc., New York (1951), p. 185.
b) Cryoscopic measurements in benzene.

Calorimetry.—The apparatus used in this experiment was described elsewhere[8]. Each liquid sample has been weighed in a gelatine capsule and it has been burned by electrical ignition, as described in the case of methylethoxypolysiloxane in the previous paper[9]. After the burning of the samples, a bulky product, consisting of silica and incomplete combustion products of a part, are yielded in the combustion vessel. The incomplete combustion products in the experiments of C_3, C_4 and D_4 have been found to contain amorphous carbon and, sometimes, a trace of carborundum**. In addition to these products, a polymer-like substance containing a silicon atom has been yielded in the combustion experiment of D_5, as in the case of 1,3,5,7,9-pentamethylcyclopentasiloxane[10]. The incomplete combustion products included in the silica have been determined in quantities and the thermal corrections for them have been calculated according to the method in the previous paper[9,10].

Results and Discussion

Five to six combustion experiments have been carried out with each liquid sample of the same material, and the results are shown in Table III, excepting that of D_5.

The result of the combustion experiment of D_5 is shown in Table IV.

In Table IV, the energy evolved per gram at 20°C and a constant volume is represented by $-\Delta U_B^{low}$, in which the thermal corrections for carbon and, sometimes, for carborundum have been made, but the correction for the polymer-like substance only is not taken into account;

TABLE III. EXPERIMENTAL RESULTS OF C_3, C_4 AND D_4

Compound	cal./g. Heat of combustion						Mean	Relative mean deviation %
C_3	6140	6133	6121	6126	6113	6138	6129	±0.14
C_4	6099	6077	6096	6088	6090	—	6090	±0.06
D_4	6357	6336	6355	6346	6332	—	6345	±0.09

* Details of the preparation of these compounds will soon be published by Dr. Ōkawara.
8) T. Tanaka and T. Watase, This Bulletin, **28**, 258 (1955).
9) T. Tanaka, ibid., **32**, 1258 (1959).
** In the combustion experiment of D_4, polymer-like substance, though only a trace in quantity, has sometimes been found in the combustion product, as in the case of D_5 described below, but such an experimental result of D_4 has been rejected here.
10) T. Tanaka, *Technol. Repts. Osaka Univ.*, **8**, 437 (1958).

TABLE IV. EXPERIMENTAL RESULTS OF D_5

Wt. of sample	$-\Delta U_B^{low}$	Amount of SiO_2 produced from the polymer-like substance		$-\Delta U_B^{high}$
g.	cal./g.	mg.	α(%)	cal./g.
0.45543	6326	1.90	0.52	6359
0.45763	6277	2.75	0.74	6323
0.44446	6317	2.03	0.56	6352
0.45899	6292	1.79	0.48	6322
0.45121	6311	1.48	0.41	6337
0.45404	6321	1.52	0.41	6347
Mean	6307			6340
Average value		6324		

$-\Delta U_B^{low}$, will be therefore considered as underestimated value for the heat of combustion of D_5. The third column in this table is the number of grams of silica produced from the polymer-like substance by the further ignition in the course of analysis of incomplete combustion product, and the fourth column indicated by α is its percentage for the amount of silica equivalent to the weight of the sample in each run. As the thermal correction for the formation of the polymer-like substance could not be evaluated exactly in this experiment, it has been calculated under the assumption that the amount of sample equivalent to the amount of silica produced from the polymer-like substance remained, not burned at all, and $-\Delta U_B^{high}$ in th last column of the Table IV has been obtained by the following expression:

$$-\Delta U_B^{high} = -\Delta U_B^{low}(1+\alpha\cdot 10^{-2}).$$

This will be evidently overestimated value for its heat of combustion. Accordingly, the average value of these $-\Delta U_B^{low}$ and $-\Delta U_B^{high}$ values has here been adopted as the reasonable one for the heat of combustion of D_5.

Table V is a summary of thermal data of C_n and D_n calculated from the combustion results.

Notations in this table are as follows: $-\Delta U_R$, the heat of combustion at standard constant volume process, where the reactants are one atmospheric pressure; $-\Delta H_f$, the heats of formation of the members of C_n and D_n in the liquid state from standard elements; $-\Sigma E$, the heats of formation of those in the gaseous state from mono-atomic gases. These energy values have been calculated by the method described in the previous paper[8]. In the calculation of $-\Sigma E$, values of 52.1, 59.2, 171.7 and 89.9 kcal./g.-atom have been adopted for the heats of atomization of hydrogen, oxygen, carbon and silicon, respectively, which are the same values used in the previous paper[8]. And then, values of 10.9[11] and 11.2[12] kcal./mol. have been used for the heats of vaporization of D_4 and D_5, respectively, and the corresponding energy values of C_3 and C_4 have been estimated to be 10.1 and 11.0 kcal./mol. from the Trouton's rule, respectively. The $-\Sigma E/n$ in the last column of the Table V, derived in this manner, will be considered as the sums of bond energies in structural units*** of $\left[\begin{matrix}CH_3\\ i\text{-}C_3H_7O\end{matrix}\!\!>\!Si\!<\!\begin{matrix}O\\ O\end{matrix}\right]$ for C_n and of $\left[\begin{matrix}CH_3\\ CH_3\end{matrix}\!\!>\!Si\!<\!\begin{matrix}O\\ O\end{matrix}\right]$ for D_n.

No Strain in the Cyclic-tetramer and -pentamer. —If the $-\Sigma E/n$ of D_5 in Table V, though involving a considerable uncertainty, will be accepted as the reasonable value for the sum of bond energies in its structural unit, this is somewhat higher than the corresponding value of D_4. Such an energy difference between these compounds will perhaps be attributed to the difference between their polymer sizes, as in the case of methylmethoxypolysiloxanes, $CH_3O\cdot[(CH_3)(CH_3O)SiO]_nCH_3$[9], and methoxy end-blocked dimethylpolysiloxanes, $CH_3O\cdot[(CH_3)_2SiO]_nCH_3$[13], in which the values of

TABLE V. HEATS OF COMBUSTION AND FORMATION OF C_n AND D_n

Compound	Mol. wt.	kcal./mol.				
		$-\Delta U_R$	$-\Delta H_c$	$-\Delta H_f$	$-\Sigma E$	$-\Sigma E/n$
C_3	354.63	2173	2177	601	4839	1613
C_4	472.84	2879	2885	819	6473	1618
D_4	296.63	1882	1887	518	3728	932
D_5	370.79	2344	2350	656	4670	934

11) R. C. Osthoff, W. T. Grubb and C. A. Burkhard, *J. Am. Chem. Soc.*, **75**, 2227 (1953).
12) D. F. Wilcock, ibid., **68**, 691 (1946).
*** For example, in D_n, the term of "structural unit" will be used for $[(CH_3)_2SiO_2]$, but not $[(CH_3)_2SiO]$, on the number of each chemical bond in the compounds.
13) T. Tanaka, to be published in *J. Inorg. & Nuclear Chem.*

$-E\left[\begin{matrix}C\\O\end{matrix}\!\!>\!Si\!<\!\!\begin{matrix}O\\O\end{matrix}\right]^{****}$ and $-E\left[\begin{matrix}C\\C\end{matrix}\!\!>\!Si\!<\!\!\begin{matrix}O\\O\end{matrix}\right]^{****}$ were found to be increasing with their polymer sizes, respectively.

If the value of 98.8 kcal./mol.[9,10] is here adopted for C–H bond energy in D_n, the values of $-E\left[\begin{matrix}C\\C\end{matrix}\!\!>\!Si\!<\!\!\begin{matrix}O\\O\end{matrix}\right]$ for D_4 and D_5 result in 339 and 341 kcal./mol., respectively. While, the corresponding values in methoxy end-blocked dimethylpolysiloxanes, which are linear compounds, were obtained to be 329, 335 and 336 kcal./mol. for the monomer, the dimer and the trimer, respectively[13]. The value of $-E\left[\begin{matrix}C\\C\end{matrix}\!\!>\!Si\!<\!\!\begin{matrix}O\\O\end{matrix}\right]$ in the cyclic tetramer is somewhat larger than that in the linear trimer, and the energy difference between them will be attributed to the difference between their polymer sizes and, if possible, partly to the difference between the cyclic and the linear structures. As the linear polysiloxanes under consideration will probably have no strain in their molecular structures, the ring structures of the cyclic-tetramer and -pentamer may also be free from strain. when one compares the $-E\left[\begin{matrix}C\\C\end{matrix}\!\!>\!Si\!<\!\!\begin{matrix}O\\O\end{matrix}\right]$ with those in the linear compounds.

Strain in the Cyclic Trimer.—The value of $-\Sigma E/n$ in C_3 is 5 kcal. lower than that in C_4, as shown in Table V. The energy difference will not by itself correspond to the strain per the structural unit of $\left[\begin{matrix}CH_3\\i\text{-}C_3H_7O\end{matrix}\!\!>\!Si\!<\!\!\begin{matrix}O\\O\end{matrix}\right]$ in C_3, because it must be taken into consideration that the value of $-\Sigma E/n$ in C_n will also increase with increasing of the polymer size, as in the case of D_n. Now, if it is assumed that the $-\Sigma E/n$ for C_3 should be 2 kcal. lower than that for C_4, by applying the energy difference in $-\Sigma E/n$ between D_4 and D_5, the extra lowering energy in C_3 comparing from C_4, 3 kcal. per the structural unit, will be due to the strain in the cyclic trimer; the ring of cyclic trimer, then, will be anticipated to have a strain corresponding to 9 kcal./mol. as a whole. However, the incremental change in $-\Sigma E/n$ between the cyclic-trimer (C_3) and -tetramer (C_4), attributed to the difference of their polymer sizes, will perhaps be larger than that between the cyclic-tetramer (D_4) and -pentamer (D_5), because the incremental change in energy between the neighboring members will be decreasing as their polymer sizes increase, as observed in the previous works on the linear polysiloxanes[9,13]. It has also been found in the previous paper[9] that the value of $-E\left[\begin{matrix}C\\O\end{matrix}\!\!>\!Si\!<\!\!\begin{matrix}O\\O\end{matrix}\right]$ in the first member of methylmethoxypolysiloxanes were 4 kcal. lower than that in the second member. As the cyclic trimer is the smallest-membered ring in the cyclopolysiloxanes, the larger part of the incremental change (5 kcal.) in $-\Sigma E/n$ between C_3 and C_4 may be attributed to the difference of their polymer sizes. Thus, the ring of the cyclic trimer will be considered to have a strain corresponding to a few or several kcal./mol. at most, being fairly smaller than 9 kcal./mol.

Though the Si–O–Si angle in the cyclic trimer has been considered to be subjected to a considerable distortion in comparing with its normal angle, the magnitude of energy due to strain obtained here seems to be too small. Such a slight strain in the six-membered ring will however be explained as due to the siloxane linkage having the nature represented by the term of "*ball and joined socket*", as explained previously by Roth and Harker[3].

The energy due to strain derived here comes out from the small difference between large quantities, so that it may not be a conclusive value. Notwithstanding, it may be said that the above results are parallel with the conclusions obtained from the investigation on redistribution equilibrium[1] and on molecular structures of cyclopolysiloxanes[2-7].

**** Sums of bond energies in the structural units of $CSiO_3$ and C_2SiO_2, in which C-H and C-O bonds are excepted, in methylmethoxypolysiloxanes and methoxy end-blocked dimethylpolysiloxanes, respectively. These sums were obtained under the assumption that the C-H and the C-O bond energies were not varied from molecule to molecule in the previous papers[9,13].

Summary

Heats of combustion of lower members of dimethyl- and methylisopropoxy-cyclopolysiloxanes have been measured at 20°C and a constant volume, and the corresponding heats of combustion and formation in isobaric process have been calculated. From the results, the heats of formation of structural units, $\left[\begin{matrix}CH_3\\CH_3\end{matrix}\!\!>\!Si\!<\!\!\begin{matrix}O\\O\end{matrix}\right]$ and $\left[\begin{matrix}CH_3\\i\text{-}C_3H_7O\end{matrix}\!\!>\!Si\!<\!\!\begin{matrix}O\\O\end{matrix}\right]$, of these compounds from mono-atomic gases have been derived, and it has been found that the ring structures

of the cyclic-tetramer and -pentamer would be free from strain. Further, the effect of distortion of Si-O-Si valency angle in the cyclic trimer on the heat of formation has been discussed.

The author wishes to express his sincere thanks to Professor T. Watase, Dr. R. Ōkawara and Dr. M. Kakudo for their helpful discussions, and to Mr. H. Mimura for his aid in a part of this work.

Department of Applied Chemistry
Faculty of Engineering
Osaka University
Miyakojima-ku, Osaka

Studies on Organic Reagents for Inorganic Analysis. VI. Absorption Spectrum of Phenylfluorone-Metal Chelate and the Nature of the Chelating Bond

By Hirotoshi SANO

(Received July 2, 1959)

For many organic dyes used for the colorimetry of metals, the color change is ascribable to the shift of the $\pi \rightarrow \pi'$ absorption spectra of the organic system caused by the chelating. With respect to the nature of such color change, there have been many papers published recently. Molecular orbital (LCAO) method was applied successfully by Belford, Martell and Calvin[1] to compute the effect of metal ion upon the β-diketone-metal chelate. The absorption spectra of metal oxalates were interpreted by Graddon[2] on the basis of a simple electrostatic effect. Dortashaeppi, Hürzeler and Treadwell[3] tried to apply a free electron gas model method to the alizarin chelates of several metals. Based on the amperometric titration data, the absorption spectra of alizarin S and its metal chelate were also discussed by Larsen and Hirozawa[4].

In the treatment of the problem, however, the effect of the nature of the chelating bond has been almost neglected, although it seems sometimes to have considerable influence on the absorption spectra. The author reported previously that the maximum wavelengths of the absorption spectra of phenylfluorone metal chelates shift toward the longer side with the decrease in the electronegativity of the metal chelated[5]. In this paper, the correlation of the maximum wavelength with the ionic character of the chelating bond was treated theoretically with the aid of the free electron gas model approximation.

Fundamental Consideration

The author has adopted Kuhn's free electron gas model method[6,7] for the present purpose, because the model can be conveniently applied to the subject although the value of the model must not be overestimated. According to Kuhn, the electron gas suffers a disturbance in the case of polyenes, unsymmetrical cyanines, etc., and the π-electrons are thought to be placed in a one-dimensional potential having a sine curve periodicity. The wavelength of absorption maximum is expressed by the following equation.

$$\frac{1}{\lambda_{max}} = \frac{V_0}{\boldsymbol{h}\cdot\boldsymbol{c}}\left(1-\frac{1}{N}\right)+\frac{\boldsymbol{h}}{8m\boldsymbol{c}}\cdot\frac{N+1}{L^2} \qquad (1)$$

where, L is the length of the path of the free π-electron measured along the conjugated chain, N, the number of π-electrons, m, the mass of the electron, $\boldsymbol{c}$, the velocity of light, $\boldsymbol{h}$, Planck's universal constant, and V_0, the amplitude of the sine-shaped potential along the chain.

1) R. L. Belford, A. E. Martell and M. Calvin, *J. Inorg. & Nuclear Chem.*, **2**, 11 (1956).
2) D. P. Graddon, ibid., **3**, 308 (1956).
3) Y. Dortashaeppi, H. Hürzeler and W. D. Treadwell, *Helv. Chim. Acta*, **34**, 797 (1951).
4) E. M. Larsen and S. T. Hirozawa, *J. Inorg. & Nuclear Chem.*, **3**, 198 (1956).
5) Part II of this series: H. Sano, This Bulletin, **30**, 790 (1957).
6) H. Kuhn, *Helv. Chim. Acta*, **31**, 1441 (1948); *J. Chem. Phys.*, **16**, 840 (1948).
7) H. Kuhn, *Z. Elektrochem.*, **53**, 165 (1949); *J. Chem. Phys.*, **17**, 1198 (1949).

Suppose that the dye is resonating between two limiting structures Ia and Ib. When each of the two structures makes the same contribution to the normal state of the dye, as seemed to be the case for symmetrical polymethine dyes, each conjugated C–C bond should have an equal bond length*, and the value of V_0 should be zero.

$$\cdots\underset{1}{C}=\underset{2}{C}-\underset{3}{C}=\underset{4}{C}-\underset{5}{C}=\cdots \leftrightarrow \cdots=\underset{1'}{C}-\underset{2'}{C}=\underset{3'}{C}-\underset{4'}{C}=\underset{5'}{C}-\cdots$$

Ia Ib

On the other hand, when Ia and Ib do not make equal contribution to the normal state, as seemed to be the case for polyene etc., a longer C–C bond (so-called "single bond") and a shorter bond (so-called "double bond") appear alternatively along the conjugated chain, and V_0 has a definite value.

If the mean bond length of the longer C–C bond and the shorter bond is represented with $\overline{R}'$ and $\overline{R}''$, respectively, the relation mentioned above is summarized as follows:

$$V_0=0, \text{ when } \overline{R}'-\overline{R}''=0 \quad (2)$$

$$V_0>0, \text{ when } \Delta R=\overline{R}'-\overline{R}''>0 \quad (3)$$

The Relation between V_0 and ΔR.—It was difficult to obtain theoretically the relation between V_0 and ΔR. Therefore, the problem was solved with the aid of empirical treatment. The difference between the mean "double-" and mean "single-" bond length in polyenes, ΔR, was obtained by calculation based on Coulson's semi-empirical theory[8], because few observed values for the bond length of polyenes were reported. The results are shown in Table I**.

TABLE I. CALCULATED VALUES OF $\overline{R}'$, $\overline{R}''$ AND ΔR

j	$\overline{R}'$, Å	$\overline{R}''$, Å	ΔR, Å
1	—	1.330	—
2	1.432	1.347	0.085
3	1.424	1.356	0.068
4	1.420	1.362	0.058
5	1.415	1.365	0.050
6	1.414	1.369	0.045
7	1.412	1.371	0.041
8	1.411	1.373	0.037
9	1.410	1.375	0.034
10	1.409	1.376	0.032
11	1.408	1.377	0.030
12	1.407	1.378	0.029
—	—	—	—
22	1.402	1.384	0.017

The values of V_0 calculated from the experimentally determined absorption maxima of a number of polyenes*** have been collected in Fig. 1, which shows the relationship between V_0 and the number of conjugated double bonds. It is found that the values of V_0 distribute in a narrow range hyperbolically with the increasing number of the conjugated double bonds.

Based on the values ΔR obtained in Table I and the values of V_0 estimated from Fig. 1, an empirical equation for the ΔR-relation is derived as follows:

$$V_0=3-3\left(1-\frac{\Delta R}{0.21}\right)^5 \quad (4)$$

Fig. 2 illustrates the value of V_0 as a function of ΔR.

In practice, the small value of V_0 is useful for the following discussion, because the value of V_0 is smaller than one electron volt in the dye-metal chelate. Therefore, Eq. 4 can be reduced to

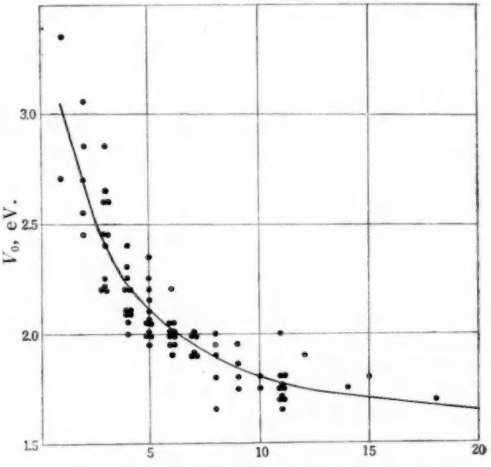

Fig. 1. Relation between V_0 and the number of conjugated double bond.

* This approximation is not strictly correct, but no objection is found in the following consideration, because the corresponding bond length in both structures strictly equal, namely, C_1-C_2, C_2-C_3, C_3-C_4,.....equal to $C_{1'}$-$C_{2'}$, $C_{2'}$-$C_{3'}$, $C_{3'}$-$C_{4'}$,....., respectively.

** The value of bond length for the "single" bond is underestimated, because the calculation used here includes no self-consistent treatment, whereas that of "double" bond is considered to be practically equal to the true value.

*** The absorption maxima were taken from the follwing: A. E. Gillam and E. S. Stern, "An Introduction to Electronic Absorption Spectroscopy in Organic Chemistry", Edward Arnold Publishers, Ltd., London (1954); Y. Urushibara, "Organic Chemistry II (Yûki Kagaku)", Kyôritsu Shuppan, Tokyo (1955).

8) C. A. Coulson, *Proc. Roy. Soc.*, **A169**, 413 (1939).

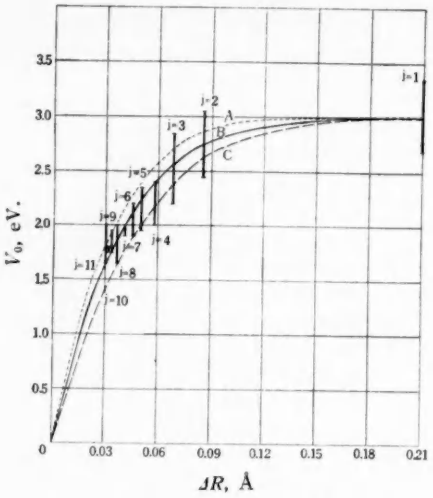

Fig. 2. Relation between V_0 and ΔR.
Curve A: $V_0=3-3(1-\Delta R/0.21)^6$
Curve B: $V_0=3-3(1-\Delta R/0.21)^5$
Curve C: $V_0=3-3(1-\Delta R/0.21)^4$

$$V_0 \simeq 71.4\Delta R - 680\Delta R^2 \qquad (5)$$

Deviation from Eq. 4 is 5%, at $\Delta R<0.03$Å, $V_0<1.8$ eV.,

or $$\Delta R \simeq \frac{V_0}{71.4}\left(1+\frac{680}{71.4^2}\cdot V_0\right) \qquad (6)$$

The Relation between V_0 and the Ionic Character of the Chelating Bond.—As is well known, a bond length, R, is expressed as follows:

$$R=R_1-(R_1-R_2)\frac{3x}{2x+1} \qquad (7)$$

where R_1 is the C–C bond length of pure single bond of ethane, R_2 is that of pure double bond of ethylene and $(1+x)$ is the bond order of the C–C bond in question based on the valence bond theory[9]. For instance, x should be expected to be 0.5 when ΔR is zero.

Suppose that $(1+x)$ represents the bond order of the "double" bond, the bond length, R'', is

$$R''=R_1-(R_1-R_2)\frac{3x}{2x+1}, \quad x>0.5 \qquad (8)$$

Similarly, the bond length corresponding to "single bond", R', is

$$R'=R_1-(R_1-R_2)\frac{3(1-x)}{3-2x} \qquad (9)$$

Then,

$$\Delta R=3(R_1-R_2)\frac{2x-1}{4-(2x-1)^2} \qquad (10)$$

substituting numerical data for R_1 and R_2 in Eq. 10, it is seen that

$$\Delta R=0.63\frac{2x-1}{4-(2x-1)^2}$$
$$(R_1: 1.54\text{Å}, R_2: 1.32\text{ Å}) \qquad (11)$$

By rewriting this expression it is seen that

$$x=\frac{1}{2}+\frac{2}{0.63}\Delta R-\frac{8}{0.63^3}\Delta R^3+\frac{64}{0.63^5}\Delta R^5-\cdots \qquad (12)$$

$$x\simeq\frac{1}{2}+\frac{2}{0.63}\Delta R, \qquad \Delta R<0.16\text{ Å} \qquad (12')$$

On the other hand, the value of x may be connected with the ionic character of the bond between the metal and the donor atom of the dye as follows:

In the four formulae, IIa and IIb represent two limiting structure of the metal-dye compound combined with a pure ionic bond, whereas IIIa and IIIb represent two limiting structures of compound combined with a pure covalent bond.

When the metal-donor bond has a pure covalency, the conjugated system is considered to be similar to that of polyene ($V_0=V_{0n}$, $\Delta R=\Delta R_n$, and $x=x_n$) which has the same number, N, of conjugated π-electron, whereas it becomes equal to that of symmetrical polymethine ($\Delta V_0=0$, $\Delta R=0$, $x=0.5$) when the bond is pure ionic.

On the whole, therefore, each of two structures, II and III, contributes to the normal state of the dye-metal compound, in proportion to the ionic character and covalent character, respectively. The mean bond order for "double" bonds of the dye-metal chelate, $1+x$, will be expressed as follows:

$$1+x=(1-i)(1+x_n)+1.5i \qquad (13)$$

where i is the ionic character. The value of x_n, the mean bond order of the polyene, is obtained from Table 1, Eq. 9 or 10, and the mean bond length $\bar{R}'$ or $\bar{R}''$ of the polyene, which possesses the same number of conjugated π-electron as the system. Based on Eqs. 6, 12′ and 13, the relation between i and V_0 can be derived as follows:

9) L. Pauling, "The Nature of the Chemical Bond", Cornell Univ. Press, Ithaca, N. Y. (1939).

$$1-i=(0.044\,V_0+0.006\,V_0^2)/(x_m-0.5) \quad (14)$$

The absorption maximum of the dye-metal complex is also connected with the ionic character of the dye-metal bond through V_0 in Eqs. 1 and 14.

Application to Experimental Results

It is necessary to know the conjugated system responsible for the absorption maximum of the dye anion to calculate the length of the conjugated chain, L, based on the number of π-electrons in the system. The phenylfluorone anion is considered to be resonating between IVa and IVb or Va and Vb, each of which makes the same contribution to the normal state of the anion, because of its symmetrical structure.

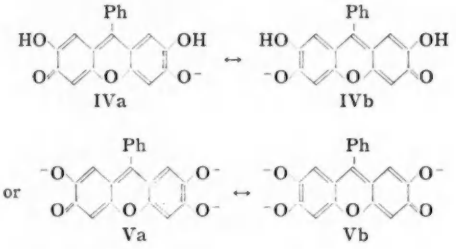

In the present study, L was calculated from the observed wavelength of the absorption maximum of the phenylfluorone anion (N=12, and V_0=0 based on the following equation,

$$\lambda_{max}=\frac{8mc}{h}\cdot\frac{L^2}{N+1} \quad (1')$$

and this value was used in calculating the value of V_0 for the metal chelates.

The possible structures of phenylfluorone metal chelate**** are

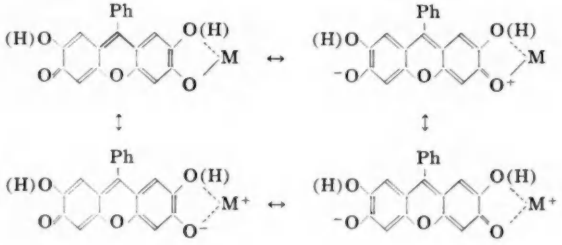

The wavelength of absorption maxima of the 2,3,7-trihydroxy-9-phenylfluorone chelates were shown in Table II together with other properties.

As is found in Table II, the shift of the absorption maximum is rather independent of the ionic radii of metals. This suggests that the electrostatic effect on the shift is not predominant in this case.

In the previous work[5] the author showed empirically that V_0 of each phenylfluoronate increased with the decrease in the ionic character estimated from the difference of electronegativity between metal and oxygen atoms. The value of the ionic character obtained through the process

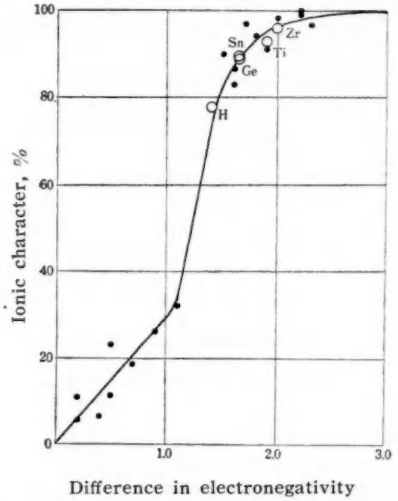

Fig. 3[10]. Relation between electronegativity difference and ionic character in the chelating bond.
○ Data obtained from metal phenylfluoronate.
● Values obtained from nuclear quadrupole coupling data by Dailey and Townes.

**** The infrared spectrum data of germanium phenylfluoronate support this structure: M. Shima, *J. Chem. Soc. Japan, Pure Chem. Soc. (Nippon Kagaku Zasshi)*, **79**, 1049 (1958).

TABLE II

Metal	λ_{max} Å	Reagent/Metal	V_0 (eV.)	i	Ionic radius[a] Å	Electronegativity[b]
H	4680	—	0.473	0.77_7	—	2.1
Ge	5080	2 : 1	0.246	0.88_3	0.53～0.52	1.8～1.9
Si	5100	—	0.236	0.89_2	0.71	1.8～1.9
Ti	5250	2 : 1	0.160	0.92_3	0.68	1.6
Zr	5400	4 : 1	0.0891	0.95_3	0.80～0.828	1.5
Ionic	5600	—	0	1.00_0	—	—

a) L. Pauling, *J. Am. Chem. Soc.*, **49**, 765 (1927); E. Kordes, *Z. physik. Chem.*, **B48**, 91 (1941).
b) H. O. Pritchard and H. A. Skinner, *Chem. Revs.*, **55**, 745 (1955).

mentioned above is shown in Fig. 3, together with the results obtained from the nuclear quadrupole coupling data by Dailey and Townes[11], for comparison.

The agreement between two independent results is too close to be accidental. This will be due to the fact that the metal-dye chelate has the structure in which the electrostatic effect by metal is negligibly small, and the effect of the perturbation caused by metal is predominant.

Some phenylfluorone derivatives which possess some substituent in the phenyl group react with metals, and the relationship among the absorption maxima of the metal chelates is similar to that in the phenylfluorone metal chelates[12].

Experimental

Metal solutions were prepared from metal oxides (germanium, titanium), chloride (tin), or oxychloride (zirconium), and standardized gravimetrically. These stock solutions contain sufficient amounts of hydrochloric acid to prevent the hydrolysis of metals, being free from foreign ions. A working solution was prepared by dilution of an aliquot of each stock solution with water or dilute hydrochloric acid.

Phenylfluorone solution was prepared by dissolving 0.120 g. of phenylfluorone in 150 ml. of ethanol containing 1 ml. of 5.0 N hydrochloric acid, and the resulting solution was diluted to 200 ml. with ethanol.

Absorbance values of the sample and the blank solution were measured with a Beckman Model DU spectrophotometer, using 1 cm. glass cells. Distilled water or blank solution was used as a reference solution. The absorption maxima show practically no variation with the change in the acidity of the solution or the amount of the dyes and metals in solution[14].

Summary

The absorption spectra of phenylfluorone-fourth group metal chelates were investigated by the acid of Kuhn's free electron gas model method. If the chelating bond formation does not cause an essential change in the π-electron system of the dye molecule, in the more ionic chelating bond, the absorption maximum of the chelate must be closer to the maximum wavelength of the dye anion. Based on the conception in valence-bond method and ionic-covalent resonance, it was theoretically and experimentaly shown that there was a certain relationship between the absorption maximum wavelength of the chelate and the ionicity of the chelating bond. (The ionicity of the bond was estimated from the difference of electronegativity between the metal and the terminal oxygen atom). The results obtained here for the relationship between the ionicity and the electronegativity difference show too close an agreement with the results obtained from the nuclear quadrupole coupling data by Dailey and Townes.

The author is indebted to Dr. Kenjiro Kimura, Professor Emeritus, and Professor Nobufusa Saito in this laboratory, for their generous encouragement in carrying out this study. The author is also grateful for a grant from the Ministry of Education.

Department of Chemistry
Faculty of Science
The University of Tokyo
Hongo, Tokyo

10) As the value of electronegativity, Dailey and Townes adopted the value reported by Huggins[13], but the author adopted here the value reported by Pritchard and Skinner as "best value" (see Table II). The value of electronegativity for the quadrupole spectrum data in Fig. 3 was rearranged in accordance with Pritchard and Skinner's scale.
11) B. P. Dailey and C. H. Townes, *J. Chem. Phys.*, **23**, 118 (1955).
12) H. Sano, This Bulletin, **30**, 672 (1957); **31**, 974 (1958).
13) M. J. Huggins, *J. Am. Chem. Soc.* **75**, 4123 (1953).
14) For other detailed procedures and experimental descriptions, see previous work of the present author[5].

Studies on the Chemical Constitution of Agar-agar. XXI[1]. *Re-investigation of Methylated Agarose of Gelidium Amansii*

By Choji ARAKI and Susumu HIRASE

(Received August 24, 1959)

It has been suggested by Araki[2], one of the present authors, that agar is a mixture of at least two different polysaccharides, one of which is termed agarose having a linear structure composed alternatively of β-D-galactopyranose and 3,6-anhydro-α-L-galactopyranose residues. The structure assignment to the agarose has been partly based on the fact that complete methanolysis of methylated agarose led to the isolation of methyl 2,4,6-tri-*O*-methyl-D-galactoside[3,4] and 2-*O*-methyl-3,6-anhydro-L-galactose dimethylacetal[5]. But the separation of the cleavage fragments was incomplete and the latter fragment was isolated only in a yield insufficient to interpret the whole molecule of agarose. This paper is concerned with the examination of the agarose structure by carefully re-investigating the methanolysis products of methylated agarose prepared from the *Gelidium amansii* agar.

Following the complete methanolysis of the methylated polysaccharide with 3% methanolic hydrogen chloride, the products were separated into neutral and acidic components by means of ion-exchange resins. The acidic component was obtained in too small a yield to be of structural significance. The mixture of neutral sugar derivatives was solved into its components by fractionation with petroleum ether followed by chromatography on charcoal-Celite columns. The mixture was found to contain methyl 2-*O*-methyl-3,6-anhydro-β-L-galactopyranoside in addition to the previously isolated 2-*O*-methyl-3,6-anhydro-L-galactose dimethylacetal and methyl 2,4,6-tri-*O*-methyl-D-galactoside. It was of significance to observe that, well in agreement with the fore-going Araki's formula of agarose, the 2-*O*-methyl-3,6-anhydro-L-galactose derivatives could be obtained in molar quantities equivalent to the 2,4,6-tri-*O*-methyl-D-galactose derivative.

The methyl 2-*O*-methyl-3,6-anhydro-β-L-galactopyranoside, a new compound, was obtained as crystals, melting at 67~69°C and showing a specific rotation $[\alpha]_D^{12}$ +66° in water. Its structure was assigned by the rotation, by the hydrolysis to give 2-*O*-methyl-3,6-anhydro-L-galactose, which was identified as crystalline 2-*O*-methyl-3,6-anhydro-L-galactonic acid and its methyl ester and amide, and by further methylation to give crystalline methyl 2,4-di-*O*-methyl-3,6-anhydro-β-L-galactoside. The finding of the methyl 2-*O*-methyl-3,6-anhydro-β-L-galactopyranoside among the methanolysis products of the methylated agarose accounts for the direct origin of methyl 2,4-di-*O*-methyl-3,6-anhydro-β-L-galactoside, which had been isolated[6] after methanolysis and subsequent re-methylation of the methylated polysaccharide.

If the agarose molecule were branched, it would be expected that either methyl di-*O*-methyl-D-galactoside or 3,6-anhydro-L-galactose dimethylacetal or both would be derived from units of branch points when the methylated polysaccharide was subjected to methanolysis. In spite of careful examination, however, neither of them could be detected among the methanolysis products under investigation. It is therefore convincing that the molecule is a chain as previously suggested by Araki[2]. As for the non-reducing end of the chain, repeated experiments failed to detect any of the fully methylated component sugars among the methanolysis products of the methylated polysaccharide with the exception of only one experiment, in which 2,3,4,6-tetra-*O*-methyl-D-galactose was isolated as its crystalline aniline derivative in a yield of twelve milligrams from fifteen grams of the methylated polysaccharide. This exception, however, suffers from the

1) Part XX: C. Araki and K. Arai, This Bulletin, **30**, 287 (1957).
2) C. Araki, This Bulletin, **29**, 543 (1956); *Memoirs Fac. Ind. Arts, Kyoto Tech. Univ.*, **5**, 21 (1956).
3) C. Araki, *J. Chem. Soc. Japan (Nippon Kwagaku Kwaishi)*, **58**, 1362 (1937).
4) E. G. V. Percival and J. C. Somerville, *J. Chem. Soc.*, **1937**, 1615.
5) C. Araki, *J. Chem. Soc. Japan (Nippon Kwagaku Kwaishi)*, **61**, 775 (1940).
6) (a) C. Araki, ibid., **59**, 304 (1938). (b) C. Araki and K. Arai, ibid., **61**, 503 (1940). (c) S. Hands and S. Peat, *Nature*, **142**, 797 (1938). (d) E. G. V. Percival, J. C. Somerville and I. A. Forbes, ibid., **142**, 797 (1938).

possibility that the polysaccharide molecule might have been degraded before or during the methylation process. Percival and his coworkers reported, that no tetra-*O*-methyl-D-galactose could be detected among the products of hydrolysis of the methylated polysaccharide[7]. Consequently, it may be still difficult at this time to decide whether D-galactose and 3,6-anhydro-L-galactose constitutes the non-reducing end of the molecule. In any case, since the end group, if present, would exist only in a trace quantity, it seems likely that agarose is a chain with a very high degree of polymerization, although the possibility is not completely excluded yet that the polysaccharide may have an endless, closed loop-structure.

In connection with the methylation data mentioned above, the information concerning the paper chromatography of the methylated derivatives of 3,6-anhydro-L-galactose is also reported here in. Cyclohexanol saturated with water was found to serve as an effective solvent for separating the anhydrosugar derivatives, the spots of which could be easily revealed when chromatograms were sprayed with an *o*-aminophenol reagent previously reported from this laboratory[8]. Table I shows the R_f values and the colors of spots observed by this method for some available samples of the anhydrosugar derivatives.

TABLE I. PAPER CHROMATOGRAPHY OF SOME 3,6-ANHYDRO-L-GALACTOSE DERIVATIVES

Compound	R_f	Color
Methyl 2-*O*-methyl-3,6-anhydro-β-L-galactopyranoside	0.77	brown
2-*O*-Methyl-3,6-anhydro-L-galactose dimethylacetal	0.67	brown
Methyl 2,4-di-*O*-methyl-3,6-anhydro-β-L-galoctoside	0.84	brown
2,4-Di-*O*-methyl-3,6-anhydro-L-galactose dimethylacetal	0.84	yellow
2,5-Di-*O*-methyl-3,6-anhydro-L-galactose dimethylacetal	0.84	brown

Filter paper used: Tōyō Filter Paper No. 52.
Developing solvent: cyclohexanol saturated with water.
Spraying reagent: *o*-aminophenol in aqueous ethanol acidified with phosphoric acid[8].

Experimental

General Procedure.—Evaporation and concentration of solutions were carried out below 40°C under reduced pressure. Specific rotations were measured in aqueous solutions unless otherwise stated. Melting points are uncorrected.

Paper Chromatography.—Paper chromatograms were run in cyclohexanol saturated with water and sprayed with *o*-aminophenol in aqueous ethanol acidified with phosphoric acid[8] for the purpose of identifying 3,6-anhydro-L-galactose derivatives; while, they were run in *n*-butanol-ethanol-water (4 : 1 : 2 V./V.) and sprayed with aniline hydrogen phthalate in moist *n*-butanol[9] for the purpose of identifying reducing D-galactose derivatives.

Methylated Agarose.—Methylated agarose was prepared by acetylating the *Gelidium amansii* agar with acetic anhydride and pyridine, extracting the agarose acetate from the resulting acetylation products with chloroform and then treating the agarose acetate repeatedly with dimethylsulfate and sodium hydroxide as previously described by Araki[10], one of the present writers. The methoxyl value found was 33.8% in reasonable agreement with the value 34.3% calculated for $[C_{12}H_{14}O_5(OCH_3)_4]_n$.

Methanolysis of Methylated Agarose and Separation of Neutral and Acidic Components.—Methylated agarose (15.0 g.) was suspended in 3% methanolic hydrogen chloride (100 ml.) and heated under reflux for 35 hr. The resulting brown solution was neutralized with silver carbonate, filtered and evaporated to a sirup. It was then dissolved in 0.2 N barium hydroxide solution (100 ml.) and heated for 2 hr. at 60°C to saponify the methyl ester of the acidic component. After removal of the excess of barium hydroxide by neutralization with carbon dioxide and subsequent filtration, the solution was allowed to pass through columns of Amberlite IR-120 (80 ml.) and IR-4B (100 ml.) in succession, and the columns were thoroughly washed with water. The effluent and washings were combined and evaporated to dryness, when the mixture of neutral sugar derivatives was obtained as a colorless sirup; yield, 15.2 g., $[\alpha]_D^{20}+60.0°$ (c 1.20).

The anion-exchange resin used above was transferred to a beaker, stirred with 2 N sulfuric acid (100 ml.) for a few minutes under ice-cooling to displace the acidic component, and re-transferred to a glass tube to form a column. After the excess of the liquid was allowed to drain from the column, the resin was washed with additional 40 ml. of 2 N sulfuric acid followed by water (600 ml.). All the effluents and washings were combined and immediately neutralized with a saturated barium hydroxide solution, the precipitates of barium sulfate were removed by filtration, and the filtrate was evaporated to dryness. The acidic component in a barium salt form was obtained as a thick sirup; yield, 0.42 g., $[\alpha]_D^{20}$ +2.7° (c 0.75). It showed positive color reactions both for ketose and uronic acid. But the yield was so small that no further investigation was carried out.

Fractionation of the Neutral Components with Petroleum Ether.—The mixture of the neutral

7) E. G. V. Percival and T. G. H. Thomson, *J. Chem. Soc.*, **1942**, 750.
8) S. Hirase, C. Araki and S. Nakanishi, This Bulletin, **26**, 183 (1953).
9) S. M. Partridge, *Nature*, **164**, 443 (1949).
10) C. Araki, *J. Chem. Soc. Japan (Nippon Kwagaku Kwaishi)*, **58**, 1338, 1351 (1937).

sugar derivatives (15.2 g.) obtained above was dissolved in water (80 ml.). The solution was continuously extracted with petroleum ether (b. p. 30~37°C) for 30 hr. in a Soxhlet's apparatus. The extract was evaporated to a thin sirup, which on standing crystallized partly; yield, 2.05 g., $[\alpha]_D^{22}$ +76.1° (*c* 0.71). The residual aqueous solution was also evaporated to a sirup; yield, 13.0 g., $[\alpha]_D^{22}$ +56.0° (*c* 1.0).

Chromatographic Separation of the Components Insoluble in Petroleum Ether.—One third quantity of the petroleum ether-insoluble components obtained above was chromatographed at 20~22°C on a column (5.2×22 cm.) packed with a mixture of charcoal (50 g.) and Celite (40 g.). The solvents used for elution were water and ethanol of successively increasing concentrations in water. The effluents were collected of every one liter in separate receivers and concentrated to give 100 ml. fractions, which were then examined both polarimetrically and paper chromatographically. The fractions showing the same contents were combined and evaporated to recover components, which were then purified by dissolution in acetone, filtration and re-evaporation to a constant weight. The total recovery amounted to 4.12 g. or 93% of the applied sample. The recovered components were determined for methoxyl content and specific rotation. The results are shown in Table II. None of the fractions showed on a paper chromatogram the presence of non-methylated or fully methylated 3,6-anhydro-L-galactose derivatives, which might be, derived from units of branch points or the non-reducing end of the methylated polysaccharide molecule, respectively.

Identification of the Components Insoluble in Petroleum Ether.—*(a) 2-O-Methyl-3,6-anhydro-L-galactose Dimethylacetal.*—Fraction II in Table II was a colorless sirup showing a refractive index n_D^{25} 1.4620 When examined on a paper chromatogram, it showed a single spot having R_f 0.67. The methoxyl value found was in good agreement with the value 41.90% calculated for $C_6H_9O_3 \cdot (OCH_3)_3$. The fraction was therefore considered to be pure 2-*O*-methyl-3,6-anhydro-L-galactose dimethylacetal. One of the present writers has reported $[\alpha]_D$ −13.79° and n_D^{25} 1.4647 about the previously isolated sample of 2-*O*-methyl-3,6-anhydro-L-galactose dimethylacetal[5].

Fraction III in Table II was a colorless sirup, which on standing crystallized partly. When examined on a paper chromatogram, it showed the presence of two spots having R_f 0.67 and 0.77, respectively, one agreed with the dimethylacetal obtained above, the other with methyl 2-*O*-methyl-3,6-anhydro-β-L-galactopyranoside. Since the optical rotations of these pure compounds are −30.7° and +66.0°, respectively, as reported herein, the fraction was considered to be a mixture of 28% of the dimethylacetal (0.14 g.)

TABLE II. CHROMATOGRAPHIC SEPARATION OF THE COMPONENTS INSOLUBLE IN PETROLEUM ETHER

	Receiver number	Solvent*	Yield g.	$[\alpha]_D^{22}$ ° (H_2O)	OCH_3 %	Identified component**
I	1— 3	W	nil	—	—	—
II	4— 8	2.5% E	1.10	−30.7	42.37	A
III	9—10	2.5% E	0.50	+40.3	38.15	A (28%) + B (72%)
IV	11—12	5 % E	0.19	+66.7	32.83	B
V	13—15	5 % E	0.22	+92.8	44.65	B (40%) + C (60%)
VI	16—21	7.5% E	0.77	+110.2	52.25	C
VII	22—28	10 % E	0.90	+110.9	52.32	C
VIII	29—33	15 % E	0.06	+111.0	52.35	C
IX	34—38	25 % E	0.25	−29.0	43.11	?
X	39—41	50 % E	0.13	+35.3	39.37	?

* W: Water; E: Ethanol.

** A: 2-*O*-Methyl-3,6-anhydro-L-galactose dimethylacetal;
B: Methyl 2-*O*-methyl-3,6-anhydro-β-L-galactopyranoside;
C: Methyl 2,4,6-tri-*O*-methyl-α, β-D-galactoside.

TABLE III. CHROMATOGRAPHIC SEPARATION OF THE COMPONENTS SOLUBLE IN PETROLEUM ETHER

	Receiver number	Solvent*	Yield g.	$[\alpha]_D^{22}$ ° (H_2O)	OCH_3 %	Identified components**
I	1— 3	2.5% E	—	—	—	—
II	4— 7	5 % E	0.60	+71.7	48.40	B (70%) + C (30%)
III	8— 9	5 % E	1.22	+88.9	52.22	C
	10—14	7.5% E				
	15—19	10 % E				
IV	20—24	15 % E	0.04	+96.0	—	C + D (?)
	25—28	30 % E				

* E: Ethanol.

** B: Methyl 2-*O*-methyl-3,6-anhydro-β-L-galactopyranoside;
C: Methyl 2,4,6-tri-*O*-methyl-α, β-D-galactoside;
D: Methyl 2,3,4,6-tetra-*O*-methyl-D-galactoside.

and 72% of the methyl glycoside (0.36 g.). This proportion is in agreement with that calculated on the basis of methoxyl values. For the actual separation, the fraction was re-chromatographed on a column (2.5×20 cm.) of charcoal-Celite at 20~22°C. The dimethylacetal was eluted from the column chiefly with 4% ethanol in water; yield, 0.10 g., $[\alpha]_D^{17}$ −30.3° (*c* 0.54), n_D^{25} 1.4615, OCH_3 41.27%; while, the methyl glycoside was removed from the column with 6% ethanol in water and was obtained as crystals; yield, 0.31 g., m. p. 65~67°C, $[\alpha]_D^{17}$ +66.0° (*c* 0.50). Admixture with the sample obtained from fraction IV described below showed no depression of the melting point.

For the identification of 2-*O*-methyl-3,6-anhydro-L-galactose dimethylacetal, the following experiments were carried out:

i) 2-O-Methyl-3,6-anhydro-L-galactose.— 2-*O*-Methyl-3,6-anhydro-L-galactose dimethylacetal (0.40 g.) in 0.02 N sulfuric acid (20 ml.) was heated in a boiling water bath for 2 hr., at which time the rotation of the solution reached a constant value ($[\alpha]_D$ −31°→−10°). The solution was neutralized with barium carbonate, filtered and evaporated to a sirup which was then dissolved in acetone. Filtration and evaporation of the acetone solution afforded 2-*O*-methyl-3,6-anhydro-L-galactose as a colorless sirup; yield, 0.35 g., $[\alpha]_D^{12}$ −14.3° (*c* 0.63), n_D^{25} 1.4870, OCH_3; found: 17.45% (calcd. for $C_6H_9O_4(OCH_3)$: 17.59%). It reduced a Fehling solution at room temperature and restored the color to a Schiff's reagent. One of the present writers has reported $[\alpha]_D^{24}$ +33.9° of the sugar[5]. The previously reported value in a positive direction seems to be ascribed to some contaminants.

ii) 2-O-Methyl-3,6-anhydro-L-galactonic acid.— The reducing sugar (0.30 g.) obtained above was dissolved in water (5 ml.) and bromine (0.4 ml.) was added dropwise during 4 hr. to the solution kept at 40°C. The treatment of the solution in the usual manner afforded 2-*O*-methyl-3,6-anhydro-L-galactonic acid; yield, 0.35 g., m. p. 137~140°C. Recrystallization twice from ethyl acetate furnished the pure compound; m. p. and mixed m. p. 141~142°C, $[\alpha]_D^{12}$ −70.3° (*c* 0.84). One of the present writers has reported m. p. 142°C and $[\alpha]_D^{12}$ −70.0° for 2-*O*-methyl-3,6-anhydro-L-galactonic acid[5].

Found: C, 43.63; H, 6.32; OCH_3, 16.34. Calcd. for $C_6H_9O_5(OCH_3)$: C, 43.75; H, 6.27; OCH_3, 16.15%.

iii) Methyl 2-O-methyl-3,6-anhydro-L-galactonate.—The acid obtained above was converted to the methyl ester by the reaction with methanolic hydrogen chloride in the usual manner. The resulting methyl ester was recrystallized from benzene, forming stout needles; m. p. 90~91°C, $[\alpha]_D^{12}$ −70.8° (*c* 1.06). One of the present writers has reported about m. p. 91°C[1,5] $[\alpha]_D^{10}$ −55.3°[5] and $[\alpha]_D^{24}$ −61.6°[1].

Found: C, 46.54; H, 7.02; OCH_3, 30.23. Calcd. for $C_9H_{14}O_6$: C, 46.60; H, 6.84; OCH_3, 30.12%.

iv) 2-O-Methyl-3,6-anhydro-L-galactonamide.— The amide was prepared from the methyl ester obtained above by the reaction with methanolic ammonia and purified by recrystallization from ethanol; m. p. 171~172°C, $[\alpha]_D^{12}$ −75.4° (*c* 0.53). Araki and Arai have reported m. p. 170~171°C and $[\alpha]_D^{23}$ −74.3° for the amide[1].

Found: C, 43.88; H, 6.95; OCH_3, 16.01. Calcd. for $C_7H_{13}O_5N$: C, 43.97; H, 6.85; OCH_3, 16.23%.

(b) Methyl 2-O-Methyl-3,6-anhydro-β-L-galactopyranoside.—Fraction IV in Table II crystallized completely on standing and melted at 64°C. It showed on a paper chromatogram as a single spot having R_f 0.77. This was combined with the crystals obtained by re-chromatography of fraction III described above and was recrystallized twice from petroleum ether, affording pure methyl 2-*O*-methyl-3,6-anhydro-β-L-galactopyranoside as elongated prisms; m. p. 67~69°C, $[\alpha]_D^{12}$ +66.0° (*c* 1.00).

Found: C, 50.49; H, 7.46; OCH_3, 32.55; mol. wt. (Rast), 190. Calcd. for $C_6H_9O_3(OCH_3)_2$: C, 50.52; H, 7.42; OCH_3, 32.65%; mol. wt., 190.2.

The structure assignment to this compound has been based on the following experiments:

i) 2-O-Methyl-3,6-anhydro-L-galactose.— The methyl glycoside (0.20 g.) obtained above was hydrolyzed with 0.02 N sulfuric acid (20 ml.) for 2 hr. during which time the specific rotation of the solution changed from +66° to −11°, the final value being in good agreement with that observed when 2-*O*-methyl-3,6-anhydro-L-galactose dimethyl-acetal was hydrolyzed. The resulting 2-*O*-methyl-3,6-anhydro-L-galactose was isolated in the same manner as described already; yield, 0.15 g., $[\alpha]_D^{12}$ −15.0° (*c* 0.50), n_D^{25} 1.4867; OCH_3 found 17.50%. The sugar was identified as 2-*O*-methyl-3,6-anhydro-L-galactonic acid and its methyl ester and amide in exactly the same manner as described already.

ii) Methyl 2,4-di-O-methyl-3,6-anhydro-β-L-galactoside.— Methyl 2-*O*-methyl-3,6-anhydro-β-L-galactopyranoside (0.08 g.) was dissolved in methyl iodide (4 ml.), silver oxide (3 g.) added, and the mixture was refluxed for 6 hr. The reaction mixture was diluted with dry acetone and filtered. Evaporation of the filtrate afforded methyl 2,4-di-*O*-methyl-3,6-anhydro-β-L-galactoside melting at 81~82°C, which was then recrystallized from petroleum ether; yield, 0.07 g., m. p. and mixed m. p. 83°C, $[\alpha]_D^{17}$ +76.7° (*c* 0.60). Methyl 2,4-di-*O*-methyl-3,6-anhydro-β-L-galactoside has been recorded as: m. p. 83°C and $[\alpha]_D^{24}$ +78.1°[6a]; m. p. 82~83°C and $[\alpha]_D$ +73.0°[6c] and m. p. 81°C and $[\alpha]_D$ +75.0°[6d].

Found: C, 53.02; H, 7.88; OCH_3, 45.45. Calcd. for $C_6H_7O_2(OCH_3)_3$: C, 52.93; H, 7.90; OCH_3, 45.59%.

(c) Methyl 2,4,6-Tri-O-methyl-α,β-D-galactoside.—All fractions VI—VIII in Table II were obtained as crystals with ill-defined melting points. Examination on paper chromatograms using the *o*-aminophenol reagent revealed no spot, indicating thereby the absence of any 3,6-anhydro-L-galactose derivative. The methoxyl values found were in good agreement with the value 52.52% calculated for $C_6H_9O_2(OCH_3)_4$. These fractions

were therefore composed entirely of methyl 2,4,6-tri-*O*-methyl-α,β-D-galactoside.

Fraction V in Table II showed a spot corresponding to methyl 2-*O*-methyl-3,6-anhydro-β-L-galactopyranoside on a paper chromatogram. When the fraction was hydrolyzed with 1 N sulfuric acid for 5 hr. at 98°C, the product showed a single spot corresponding to 2,4,6-tri-*O*-methyl-D-galactose on a paper chromatogram, the anhydrosugar derivative being completely destroyed during the hydrolysis. Fraction V was therefore a mixture of 40% of methyl 2-*O*-methyl-3,6-anhydro-β-L-galactopyranoside (0.09 g.) and 60% of methyl 2,4,6-tri-*O*-methyl-α,β-D-galactoside, the proportion being calculated on the basis of the methoxyl values.

i) 2,4,6-Tri-O-methyl-α-D-galactose.—Fractions VI—VIII were combined and hydrolyzed with 1 N sulfuric acid (20 ml.) for 4.5 hr. at 98°C. The reaction solution was then treated in the usual manner, when 2,4,6-tri-*O*-methyl-D-galactose was obtained; yield, 1.40 g., m. p. 104~105°C. Paper chromatographic examination indicated the presence of 2,4,6-tri-*O*-methyl-D-galactose only. Recrystallization, twice from ether, furnished the pure compound; m. p. and mixed m. p. 110~111°C, $[\alpha]_D^{15}$ +115.9° (initial)→+90.7° (after 24 hr., constant) (*c* 1.07). The physical constants are in good agreement with literature values[3,4].

Found: C, 48.56; H, 8.30; OCH_3, 41.78. Calcd. for $C_6H_9O_3(OCH_3)_3$: C, 48.64; H, 8.16; OCH_3, 41.90%.

ii) 2,4,6-Tri O-methyl-N-phenyl-D-galactosylamine.—The tri-*O*-methyl-D-galactose recovered from the mother liquor of recrystallization mentioned above was converted into its aniline derivative in the usual manner[3,4]; m. p. and mixed m. p. 174°C, $[\alpha]_D^{14}$ −120.0° (initial)→−82.0° (constant) in acetone (*c* 0.50).

(d) Unidentified Components.—Fractions IX and X in Table II seemed to be methylated disaccharide derivatives having molecular weight, respectively, 423 and 398. The structures will be studied in the subsequent paper.

Separation and Identification of the Components Soluble in Petroleum Ether.—*(a) Separation.*—The sirup (2.05 g.), which had been obtained by extracting the neutral components of the methanolysis products with petroleum ether, was chromatographed at 22~24°C on a column (5.0×15 cm.) packed with charcoal (40 g.) and Celite (28 g.) in exactly the same manner as in the separation of the components insoluble in petroleum ether. The results are shown in Table III.

(b) Identification.—Fraction II was a colorless sirup, showing a spot corresponding to methyl 2-*O*-methyl-3,6-anhydro-β-L-galactopyranoside on a paper chromatogram. When it was hydrolyzed with 1 N sulfuric acid for 5 hr. at 98°C, the resulting product showed a spot corresponding to 2,4,6-tri-*O*-methyl-D-galactose on a paper chromatogram, the anhydrosugar derivative being completely destroyed during the hydrolysis. From these facts, fraction II was considered to be a mixture of 70% of methyl 2-*O*-methyl-3,6-anhydro-β-L-galactopyranoside (0.42 g.) and 30% of methyl 2,4,6-tri-*O*-methyl-D-galactoside (0.18 g.), the proportion being calculated on the basis of the methoxyl values.

Fraction III was proved to be entirely methyl 2,4,6-tri-*O*-methyl-α,β-D-galactoside in exactly the same manner as in the case of fractions VI—VIII in Table II.

Fraction IV in Table III gave no spot on a paper chromatogram sprayed with an *o*-aminophenol reagent, indicating thereby the absence of any 3,6-anhydro-L-galactose derivative. On hydrolysis it produced 2,4,6-tri-*O*-methyl-D-galactose which was identified on a paper chromatogram. Fraction IV contained therefore methyl 2,4,6-tri-*O*-methyl-α,β-D-galactoside only. However, a similar fraction obtained from the other batch was found to contain methyl 2,3,4,6-tetra-*O*-methyl-D-galactoside in addition to the tri-*O*-methyl-D-galactose derivative as described below.

Confirmation of Methyl 2, 3, 4, 6-Tetra-*O*-methyl-D-galactoside.—From the other batch of methylated agarose (15 g.), there was obtained a fraction similar to fraction IV of Table III; yield, 0.07 g. Paper chromatographic examination indicated the absence of any 3,6-anhydro-L-galactose derivative. The sirup was hydrolyzed with 1 N sulfuric acid (1 ml.) for 4.5 hr. at 98°C and the product was isolated in the usual manner as a colorless sirup; yield, 62 mg. Examination on a paper chromatogram indicated the presence of both 2,4,6-tri-*O*-methyl-D-galactose and 2,3,4,6-tetra-*O*-methyl-D-galactose. The mixture was resolved into the components on a column (2.5×32 cm.) packed with filter paper powder, a 2-butanone-water azeotrope being used as a mobile phase. A faster moving fraction containing the tetra-*O*-methyl-D-galactose was obtained as a sirup; yield, 20 mg., $[\alpha]_D^{19}$ +44.0° (*c* 0.50). It was dissolved in ethanol (1 ml.), aniline (20 mg.) added, and the solution was refluxed for 3 hr., when 2,3,4,6-tetra-*O*-methyl-*N*-phenyl-D-galactosyl amine was obtained; yield, 12 mg., m. p. 186~189°C. Recrystallization from ethanol afforded the pure compound; m. p. and mixed m. p. 192°C, $[\alpha]_D^{13}$ −75.8° (initial) in acetone (*c* 0.132).

Found: OCH_3, 40.18. Calcd. for $C_{16}H_{25}O_5N$: OCH_3, 40.51%.

Yields of the Components.—As shown in Tables II and III, the yields of 2-*O*-methyl-3,6-anhydro-L-galactose dimethylacetal, methyl 2-*O*-methyl-3,6-anhydro-β-L-galactopyranoside and methyl 2,4,6-tri-*O*-methyl-α,β-D-galactoside are 3.72, 2.34 and 7.02 g., respectively, when calculated on the basis of the whole neutral components (15.2 g.). Consequently, the molar proportion of the sum of the former two to the last one is 1 : 1.03.

The authors wish to express their hearty thanks to Mr. K. Arai for micro-combustion and to Mr. T. Itō for assistance.

Institute of Chemistry
Faculty of Industrial Arts
Kyoto Technical University
Matsugasaki, Kyoto

Studies on the Vibrated Dropping Mercury Electrode. II. Electrocapillary Characteristics of the Current-Voltage Curve

By Hideo IMAI, Shōkichi CHAKI and Senkichi INOUYE

(Received June 8, 1959)

The theory of the limiting current of the vibrated dropping mercury electrode (VDME) has been given in the previous report[1], and it was shown that the limiting current increases about ten times when the mean velocity of the vibration is of the order of several centimeters per second. This result suggests the potentiality of the "VDME" method for improving the sensitivity of polarographic determinations. The surface charge density of the dropping mercury electrode (DME), however, exerts an influence on the velocity of the vibration, and accordingly, it controls the limiting current. Thus, the linear relation of the limiting current with the depolarizer concentration was not always obtained. Moreover, the remarkable effect of surface active materials on the limiting current and the effect of the vibration on the summit potential of a polarographic maximum or on potential of the electrocapillary maximum (the Lippmann-potential) were observed. These results are presented and discussed in this report.

Experimental

The apparatus used was described in the previous report[1] and was not modified in any detail.

All the reagents were of analytical grade, and were used after the recrystallization. The test solution was prepared in the same way as that described in the previous report[1].

When the reduction potential of a depolarizer was adjoining the Lippmann-potential, the plateau of the limiting current was not well-defined. On this occasion, the limiting current was measured at a potential optionally determined.

The increase in the current-sensitivity owing to the vibration was expressed by the ratio, (i_l/i_d), of the limiting current against the diffusion-controlled current measured at the same potential. All measurements were made at 25.0 ± 0.1°C.

1) H. Imai, S. Inouye and S. Chaki, This Bulletin, **32**, 994 (1959).

Results and Discussion

1. Variation of Limiting Current with Depolarizer Concentration.—This relation was investigated in the cases of the mercuric, thallous, cadmium, nickel and zinc ions. The concentration ranged from 0.005 to 10 mF. The test solution contained 0.1 F potassium chloride or potassium nitrate as the supporting electrolyte, and a small

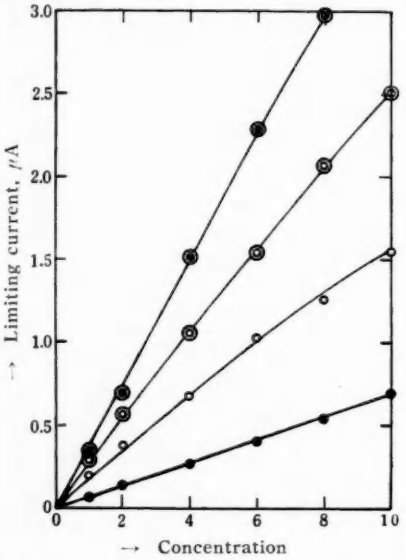

Fig. 1. The variation of the limiting current with the concentration of the zinc ion.
●: i_d of 10^{-3}, 10^{-4} and 10^{-5} F order
○: i_l of 10^{-3} F order
◎: i_l of 10^{-4} F order
◉: i_l of 10^{-5} F order
The value of the current in the ordinate must be multiplied by the factor of 100, 10 and 1 μA for the concentration order of 10^{-3}, 10^{-4} and 10^{-5} F, respectively. $E=0.38$ V./cm. (25 c. p. s.). $m=1.81$ mg./sec. $t=4.1_9$ sec. (open circuit). The supporting electrolyte=0.1 F KCl. The limiting current was evaluated at -1.2 V. vs. S. C. E.

TABLE I. THE VARIATION OF THE RATIO, i_l/i_d, WITH THE DEPOLARIZER CONCENTRATION (25°C)

Depolarizer concentration, mF	i_l/i_d				
	Hg^{2+} in KCl	Tl^{+} in KNO_3	Cd^{2+} in KCl	Ni^{2+} in KNO_3	Zn^{2+} in KNO_3
10	—	—	—	—	2.0
5	—	—	—	—	2.5
1	5.7	3.0	3.2	3.3	3.5
0.5	5.6	2.8	3.4	3.8	4.3
0.1	5.7	2.8	3.3	4.0	5.0
0.05	5.6	2.7	3.2	4.3	6.0
0.01	—	2.8	3.2	4.6	7.0
0.005	—	2.6	3.4	4.8	—
E, V./cm.	0.4	0.38	0.38	0.38	0.38
t, sec.	8.3	6.2	6.2	6.1	4.2
m, mg./sec.	0.74	1.33	1.34	1.48	1.81

E is the intensity of the a. c. electric field (25 c. p. s.), *t* is the life-time of the DME and *m* is the rate of mercury flow.

quantity of the sodium sulfite solution was added to remove the trace of dissolved oxygen.

In the cases of the mercuric ion, the thallous ion and the cadmium ion, the plateau of the limiting current was not obtained. This is because the surface charge density of the DME markedly varies near Lippmann-potential which is adjacent to the reduction potential of the depolarizer in question. On the contrary, the nickel ion and the zinc ion developed a fairly well-defined wave except for the increase of the residual current.

The variation of the ratio, i_l/i_d, with the depolarizer concentration is given in Table I.

In the former three depolarizers of Table I, the value of i_l/i_d does not appreciably change with the depolarizer concentration. On the contrary, the value of i_l/i_d is inversely proportional to the depolarizer concentration in the latter two depolarizers, and a curvilinear plot of the limiting current versus the concentration is obtained as is shown in Fig. 1.

In this connection, the variation of the life-time of the DME with the depolarizer concentration was investigated, and the result is illustrated in Table II.

TABLE II. THE VARIATION OF THE LIFE-TIME OF THE DME WITH THE CONCENTRATION OF THE ZINC ION (25°C)

Concentration of the zinc ion, mF	Life-time of the DME, sec.	
	Open circuit	At −1.2 V. vs. S. C. E.
8	4.5_6	4.4_2
1	4.5_6	4.3_7
0.2	4.5_7	4.3_4
0.01	4.5_7	4.2_4
0.001	4.5_7	3.8_4

In Table II the life-time measured in the open circuit is independent of the depolarizer concentration, while the life-time measured at the more negative potential than the reduction potential of the zinc ion increases as the depolarizer concentration is increased.

The increase of the life-time can be assigned to the increase of the surface tension of the DME.

The surface tension increases as the surface-charge density decreases and the decrease of the surface charge density results in the retardation of the vibration. Thus, the curvilinear relation of Fig. 1 is attributable to the effect of the reductant on the surface charge density of the DME.

2. Effect of Surface Active Materials.—*2-i. Variation of limiting current with concentration of surface active materials.*—The variation of the limiting current of 1 mF zinc ion with the concentration of the surface active material such as gelatine, methyl cellulose or polyoxyethylene lauryl ether (LEO, the mean molecular weight = 862) was investigated. The result is illustrated in Fig. 2. In every case the effect of the vibration diminishes by the addition of the surface active material, the limiting current being reduced to the value of the diffusion-controlled current by the addition up to about 0.01%. This effect is attributable to the retardation of the vibration due to the decrease of the surface-charge density. The effect of gelatine is more pronounced than that of methyl cellulose, and the difference of the curvilinear relation in Fig. 2 seems to relate to the adsorption mechanism of the surface

active material on the mercury surface.

2-ii. Current-voltage curve accompanied with adsorption and desorption of surface acitve material. — The effect of *n*-octyl alcohol on the current-voltage curve of 1 mF mercuric ion in 0.1 F potassium chloride was investigated. The limiting current markedly changes at two potentials which lie in the region of the anodic polarization and in the region of the cathodic polarization as is illustrated in Fig. 3. The potential of the current change at about −0.2 V. vs. S. C. E. and that of the current change at about −1.5 V. vs. S. C. E. correspond to the potential of the adsorption and that of the desorption of *n*-octyl alcohol, respectively, as is seen in comparison with the tensammetric curve appended in Fig. 3. From the fact that the limiting current changes with the adsorption or the desorption of the surface active material as is previously described in *2-i*, it is concluded that the change of the limiting current at about −0.2 V. vs. S. C. E. and that at about −1.5 V. vs. S. C. E. correspond to the decrease of the anodic current of the chloride ion owing to the adsorption of *n*-octyl alcohol and to the increase of the cathodic current of the mercuric ion owing to the desorption of *n*-octyl alcohol, respectively.

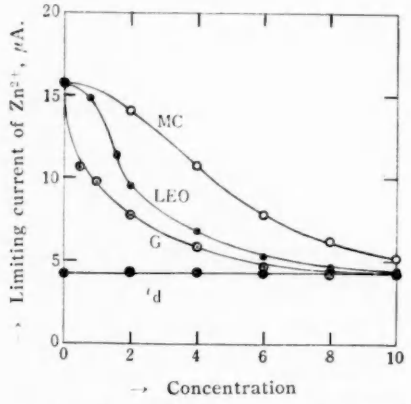

Fig. 2. The variation of the limiting current of the zinc ion with the concentration of the surface active material. The value of the concentration in the abscissa must be multiplied by the factor of 10^{-3} % for gelatine (curve G) and methyl cellulose (curve MC) or by the factor of 2.5×10^{-6} F for LEO. $(Zn^{2+})=1\times10^{-3}$ F. Refer the illustration given in Fig. 1 to the other experimental conditions.

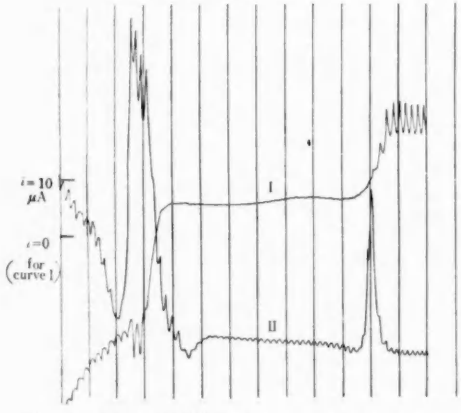

Fig. 3. The "VDME" current-voltage curve of the mercuric ion in the presence of *n*-octyl alcohol (curve I). $(Hg^{2+})=1\times10^{-3}$ F. The supporting electrolyte=0.1 F KCl. Curve II is the tensammetric curve of the same solution. The applied voltage starts from +0.2 V. vs. S. C. E., and each voltage interval corresponds to 0.15 V.

2-iii. Dependence of limiting current to frequency of vibration and to concentration of

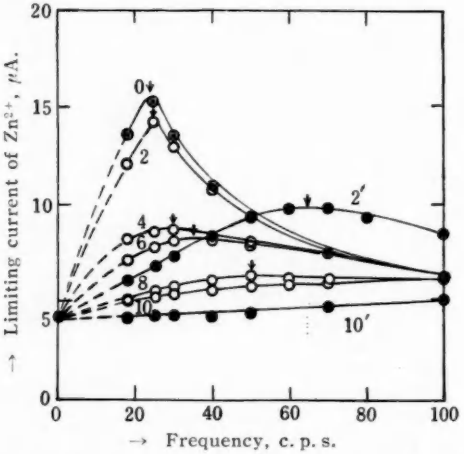

Fig. 4. The effect of the frequency of the a. c. electric field on the limiting current of the zinc ion in the presence of the surface active material. Curve 0 is obtained in the absence of the surface active material. Curves 2, 4, 6, 8 and 10 correspond to the concentration of methyl cellulose as great as 0.002, 0.004, 0.006, 0.008 and 0.01%, respectively. Curves 2' and 10' correspond to the concentration of gelatine as great as 0.002 and 0.01%, respectively. The maximum point of curve 10' appears at about 200 c. p. s. $(Zn^{2+})=1\times10^{-3}$ F. Refer the illustration given in Fig. 1 to the other experimental conditions.

surface active material.—The dependence of the limiting current of the zinc ion to the frequency of the vibration was investigated in the presence of gelatine or methyl cellulose of various concentrations. The result is illustrated in Fig. 4. Under the vibration of the frequency less than 20 c. p. s., the mercury droplet is shaken off by the violent vibration in the absence of the surface active material, and the effect of the vibration on the limiting current gradually decreases as the frequency of the vibration increases. Thus, the limiting current gives a maximum at about 25 c. p. s. In the presence of the surface active material, the frequency of the vibration, which gives the maximum limiting current, shifts toward higher frequencies as the concentration of the surface active material increases. In connection with this effect, the difference between gelatine and methyl cellulose is noticeable as is pointed out in *2-ii*.

3. Effect of Vibration on Maximum Wave.—It was found that the summit potential of the polarographic maximum of the first kind shifts toward more negative potentials by the vibration.

The test solution contained 1 mF mercuric ion in 0.01 F sodium sulfate solution, and the DME with the comparatively short life-time was preferable in order to obtain reproducible data. The effect of the vibration on the maximum wave of the mercuric ion is illustrated in Fig. 5, and the variation of the summit potential with the intensity of the a. c. electric field is given in Table III.

TABLE III. THE VARIATION OF THE SUMMIT POTENTIAL OF THE POLAROGRAPHIC MAXIMUM WITH THE INTENSITY OF THE a. c. ELECTRIC FIELD (E_1, E_2, E_3 and E_4 represent the potential given in Fig. 5.)

The intensity of the electric field, V./cm.	E_1	E_2	E_3	E_4
	V. vs. S. C. E.			
0	-0.37_5	-0.44_8	-0.43_5	-0.36_7
0.16	-0.39_2	-0.48_0	-0.44_2	-0.37_6
0.25	-0.43_0	-0.50_3	-0.47_7	-0.41_3
0.34	-0.49_5	-0.56_1	-0.56_5	-0.50_2

(25 c. p. s. square wave, $t=5.5_6$ sec.)

According to the theory[1] previously reported, the velocity of the vibration is a linear function of the intensity of the a. c. electric field. Accordingly, it seems to be probable that the velocity of the vibration pertains to the shift of the summit potential. In this connection, Heyrovsky and Vascautzanu[2] have pointed out the fact that the summit potential is shifted toward more negative potentials by increasing the mercury head. The authors' observation coincides with this

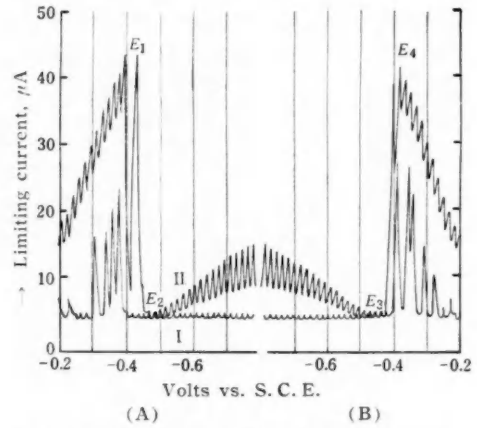

Fig. 5. The effect of the vibration on the summit potential of the maximum wave of 1×10^{-3} F Hg^{2+} in 0.01 F Na_2SO_4. The applied voltage is scanned from −0.2 V. to −0.8 V. vs. S. C. E. (A) or from −0.8 V. to −0.2 V. vs. S. C. E. (B). Curves I and II correspond to the cases when the intensity of the applied a. c. electric field is 0 and 0.34 V./cm., respectively. $t=8.0$ sec.

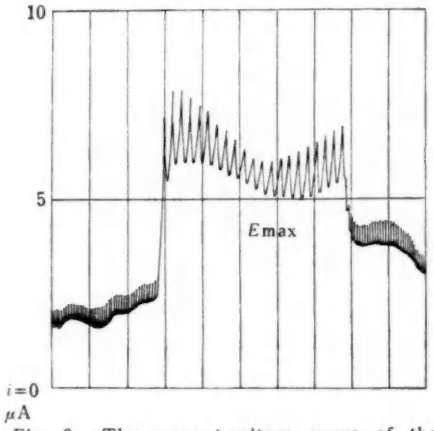

Fig. 6. The current-voltage curve of the mercuric ion under the violent vibration. The voltage starts from 0 V. vs. S. C. E. and each voltage interval corresponds to 0.1 V. $(Hg^{2+})=1\times10^{-4}$ F. The supporting electrolyte=0.1 F KCl. $E=0.38$ V./cm. $t=7$ sec. (open circuit).

2) J. Heyrovsky and E. Vascautzanu, *Collection Czechoslov. Chem. Communs.*, 3, 418 (1931).

effect with respect to the point that the possible change of the ζ-potential due to the movement of the surface of the mercury droplet results in the shift of the summit potential of the maximum.

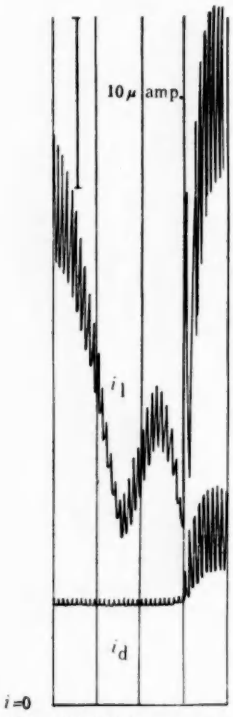

Fig. 7. The "VDME" current-voltage curve of the mercuric ion under the high rate of mercury flow. i_d is the diffusion-controlled current and i_l is the limiting current. $t=5.4_4$ sec. (open circuit). $m=1.34_7$ mg./sec. $(Hg^{2+})=1\times10^{-3}$ F. The supporting electrolyte=0.1 F KCl. The applied voltage starts from −0.7 V. vs. S. C. E. and each voltage interval corresponds to 0.1 V.

4. Anomalous Effect of Vibration on Current-Voltage Curve. — *4-i. Effect of violent vibration.*—The abrupt change of the limiting current was observed in the current-voltage curve of the mercuric ion under the application of the intense a. c. electric field (cf. Fig. 6). This change is caused by the change of the life-time of the DME. The mercury droplet is attached to the capillary orifice counteracting to the gravity and the vibration, and it is shaken off by the violent vibration caused by the coupled effect of the intense a. c. electric field and the increase of the surface charge density which is a function of the applied potential. Tachi and Okuda[3] have reported a similar phenomenon in the alternating current polarography.

4-ii. Effect of rapid rate of mercury flow. —Under the slow rate of the mercury flow, a minimum in the current-voltage curve is observed at the Lippmann-potential by the "VDME" method (cf. **1** and **4**). Under the rapid rate of the mercury flow, however, two minima were observed, the Lippmann-potential lying between them (cf. Fig. 7). It seems to be probable that this effect will be assigned to the variation of the ζ-potential at the mercury-solution interface with the flow of mercury on the surface of the DME.

The authors wish to express their hearty gratitude to Professor Mutsuaki Shinagawa for his valuable advice and encouragement.

Laboratory of Chemistry
Minami College
Hiroshima University
Minami, Hiroshima

3) I. Tachi and M. Okuda, This Bulletin, **27**, 310 (1954).
4) H. Imai, S. Inouye and S. Chaki, ibid., **31**, 767 (1958).

The Crystal Structure of Phenylarsonic Acid[1]

By Akira SHIMADA

(Received September 9, 1959)

The chemistry of organoarsenic compounds has an earlier growth than that of others among those of organometallic compounds, and this fact has again attracted much attention of chemists in recent days[2]. However, there are only a few structural studies of the organoarsenic compounds[3-10], and, hence, it may be of interest and importance in this field of chemistry to reveal the spatial configuration and orientation of the molecules in the crystal of phenylarsonic acid, $C_6H_5AsO(OH)_2$, which is one of the fundamental compounds in the organoarsenic compounds. The present work, which provides the first determination of the packing mode of organoarsonic acid, seems of interest also from the standpoint of the hydrogen-bond formation, in comparison with other organic acids.

Experimental

In a preliminary note, the crystallographic constants were already reported[1]; the crystal of this compound belongs to the orthorhombic system and the space group $D_2^4-P2_12_12_1$ with four chemical units in a unit cell, which has the following dimensions;

$a=10.42\pm0.02$, $b=14.92\pm0.02$, $c=4.70\pm0.02$ Å

The data mentioned above are in fairly good agreement with those recently reported by Bryden[11]. Oscillation and Weissenberg photographs were taken around the principal axes with Cu $K\alpha$ radiation. Intensities were obtained by the multiple-film technique in Weissenberg photographs and were estimated by visual comparison with a calibrated scale. They were corrected by means of the usual Lorentz and polarization factors, while the correction for absorption was evaluated under the assumption that the specimens were cylindrical rods. The absorption effect could not be neglected, especially for $(0\,k\,l)$ and $(h\,0\,l)$ spectra because of the rather high absorption coefficient ($\mu=60.3\,cm^{-1}$) of the crystals and because of their dimensions [cross section with rectangular dimensions: 0.20×0.25 mm. for $(h\,k\,0)$, 0.65×0.40 mm. for $(0\,k\,l)$, and 0.70×0.65 mm. for $(h\,0\,l)$].

Structure Determination

The structure has been determined by making use of the heavy-atom technique. Thus, the electron density projection $\rho(xy)$, favorable because of the short c axis, were fairly well resolved to reveal the configuration of the molecules, as described in the preliminary note[1]. The electron density projections $\rho(yz)$ and $\rho(xz)$ were easily constructed by the same method, referring to the refined electron density projection $\rho(xy)$. These projections were shown in Figs. 1—3, and the final coordinates are listed in Table I, their refinement being made by the difference syntheses at later stages. In the calculation of structure factors, McWeeny's scattering curves[12] of "valence states" for carbon atom and of $1/3(f^{\parallel}+2f^{-})$ for oxygen atom were used, while the scattering curve given by Berghuis et al.[13] was used for arsenic atom. Isotropic temperature factors were estimated to be 3.3 Å^2

TABLE I. ATOMIC COORDINATES

Atom	x/a	y/b	z/c
As	0.334_4	0.126_5	0.211_2
O_1	0.457	0.111	−0.032
O_2	0.192	0.109	0.079
O_3	0.372	0.060	0.499
C_1	0.338	0.249	0.320
C_2	0.429	0.313	0.218
C_3	0.424	0.400	0.332
C_4	0.336	0.423	0.531
C_5	0.249	0.360	0.633
C_6	0.242	0.271	0.520

1) A preliminary account has already appeared in This Bulletin, **32**, 309 (1959).
2) E. G. Rochow, D. T. Hurd and R. N. Lewis, "The Chemistry of Organometallic Compounds", John Wiley & Sons, Inc., New York (1957).
3) R. C. L. Mooney, *J. Am. Chem. Soc.*, **62**, 2955 (1940).
4) R. C. L. Mooney, *Phys. Rev.*, **61**, 739 (1942).
5) H. A. Skinner and L. E. Sutton, *Trans. Faraday Soc.*, **40**, 164 (1944).
6) J. Waser and V. Shomaker, *J. Am. Chem. Soc.*, **67**, 2014 (1945).
7) J. Donohue, G. Humphrey and V. Schomaker, ibid., **69**, 1713 (1947).
8) S. C. Nyburg and J. Hilton, *Acta Cryst.*, **8**, 358 (1955).
9) W. Schaffer, ibid., **9**, 401 (1956).
10) R. C. L. Mooney, ibid., **12**, 187 (1959).
11) J. H. Bryden, ibid., **12**, 558 (1959).
12) R. McWeeny, ibid., **4**, 513 (1951).
13) J. Berghuis, I. M. Haanappel, M. Potters, B. O. Loopstra, C. H. MacGillavry and A. L. Veenendaal, ibid., **8**, 478 (1955).

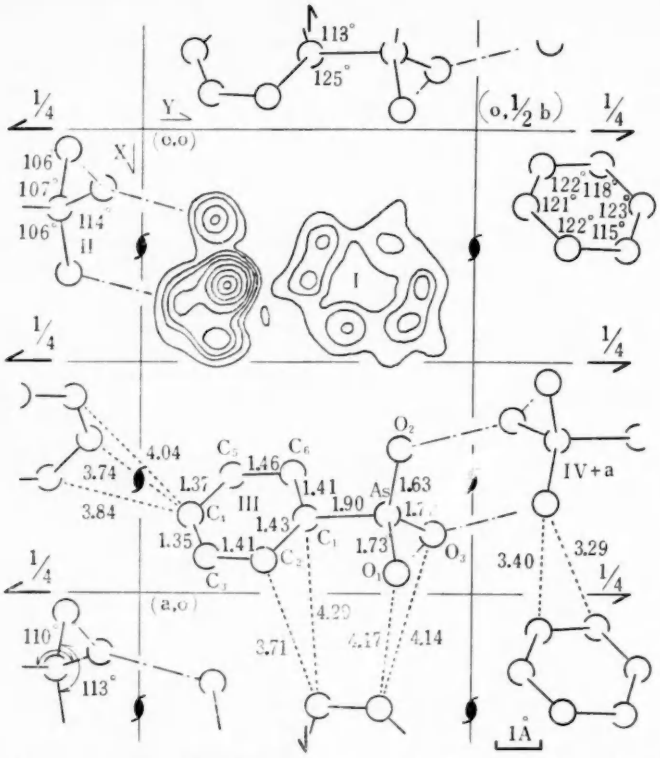

Fig. 1. The structure and the electron-density projection along the c axis, with bond angles, intra- and intermolecular distances (Å). Contours at intervals of 2 eÅ^{-2}, starting at 2 eÅ^{-2}, except at the arsenic atom, where contours above 8 eÅ^{-2} are at intervals of 10 eÅ^{-2}. Dot-dash lines indicate hydrogen bonds.

for all atoms in the case of $(h\,k\,0)$ and $(0\,k\,l)$, and 4.2 Å^2 in the case of $(h\,0\,l)$. R indices for the final coordinates were 18.0, 14.0 and 15.6%, for $(h\,k\,0)$, $(0\,k\,l)$ and $(h\,0\,l)$, respectively, excluding terms too weak to be observed.

Description of the Structure

The general nature of the structure is shown in Figs. 1—3, which are c, a and b axis projections for this compound. The aresenic atom is surrounded by a group consisting of three oxygen atoms, O_1, O_2 and O_3 of the arsonic acid and one carbon atom C_1 of the benzene ring. The average As–O distance is 1.69 Å, and the As–C distance is 1.90 Å. The disposition of bonds from the arsenic atom appears to be nearly tetrahedral, the angles between the bonds being about 110°. The benzene ring is planer and the averge distance between adjacent carbon atoms is 1.41 Å, individual values ranging from 1.35 to 1.46 Å.

Phenylarsonic acid, which has two active hydrogen atoms, forms two hydrogen bonds, one with a length 2.64 Å from the atom O_3 of molecule I to the atom O_2 of molecule II, the other with a length 2.49 Å from the atom O_3 of molecule I to the atom O_1 of molecule I+c (molecule displaced by the unit vector c). This arrangement of these two types of hydrogen bonds links molecules with each other to form endless chains along the twofold axis perpendicular to the (001) plane. The benzene rings are connected through the arsenic atom to these chains which are held together by the van der Waals force only. The shorter distances between neighboring molecules occur between O_2 of one molecule and C_2, O_3 and C_3 of adjacent molecules; these distances are 3.29, 3.39 and 3.40 Å, respectively. Other intermolecular distances exceed 3.71 Å.

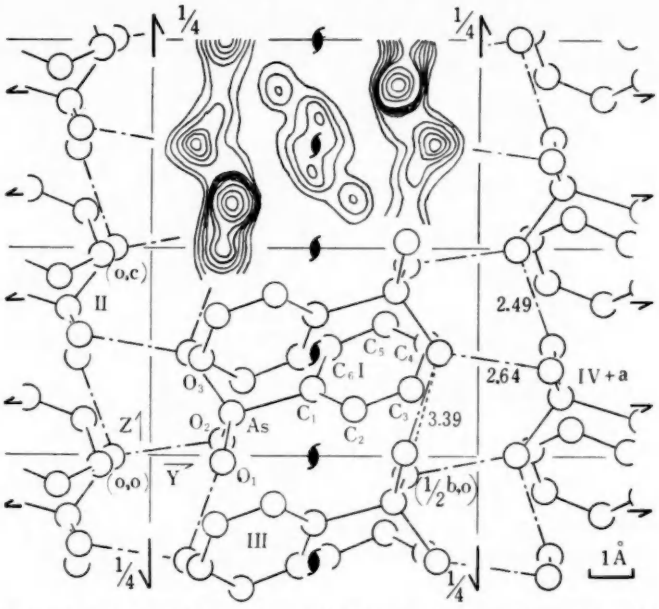

Fig. 2. The structure and the electron-density projection along the *a* axis, with intermolecular distances (Å). Contours at intervals of 2 eÅ^{-2}, starting at 4 eÅ^{-2}, except at the arsenic atoms, where contours above 16 eÅ^{-2} are at intervals of 10 eÅ^{-2}. Dot-dash lines indicate hydrogen bonds.

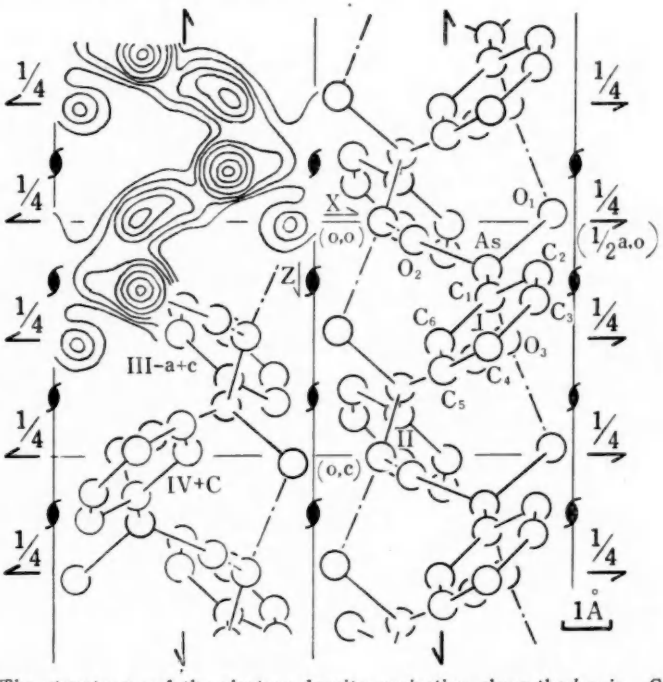

Fig. 3. The structure and the electron-density projection along the *b* axis. Contours at intervals of 3 eÅ^{-2}, starting at 5 eÅ^{-2}, except at the arsenic atoms, where contours above 11 eÅ^{-2} are at intervals 10 eÅ^{-2}. Dot-dash lines indicate hydrogen bonds.

This mode of packing the molecules would explain the cleavages along the planes parallel to the (110) and (100) planes.

The author wishes to express his sincere thanks to Professor I. Nitta and Professor T. Watanabé of Osaka University for their helpful advice, to Professor H. Nakata of Konan University for supplying the specimen, and to other members of this University for their encouragement.

Department of Chemistry
Faculty of Science
Konan University
Higashinada, Kobe

On the d Orbital of the Sulfur Atom in Thiophene

By Kôgorô MAEDA

(Received June 17, 1959)

The idea of *pd* hybridization in thiophene has been used successfully in accounting for the general similarity between thiophenes and their benzene analogues[1-3]. In hybridizing the *p*- and *d*-orbitals on the sulfur atom, the fundamental procedure was that the two hybridized orbitals which conjugate with $2p\pi$ orbitals on the carbon atoms are defined so as to be non-orthogonal to each other. A problem which has to be solved, however, results from adopting the *d* orbitals in bonding; it follows what values should be used for nuclear charge parameters of the *d* orbitals. If the use of the free atom parameter required by Slater's rule[4] for an electron in the *d* orbital is to be retained at all, the orbital becomes too diffuse and weakly bound to participate substantially in bonding. For example, when an electron of an unshared pair on the sulfur atom is considered to be in the *d* state, it bears the value 1 as the effective nuclear charge; this fact gives a small value of overlap integral with the $2p\pi$ orbital on the carbon atom, of the order of 0.1[5] and suggests the level of its energy much higher than the ground state. Under this condition, one might not expect the appreciable participation in bonding to occur through the hybridization, from the point of overlap criterion on bonding[6] and from balancing of energy. The eigenfunction of the electron, however, has its radial function whose maximum lies at 9 atomic units. The orbital, therefore, may be regarded as including the full carbon skeleton of thiophene, so that it would be impossible to avoid the influence of the nuclear charges of neighboring carbon atoms. The charges may distort the orbital, contracting it and allowing its participation in the hybridization, as suggested by Craig and Magnusson[7].

In this paper, the influence of perturbing potentials of the charges will be examined, and the possibility of the participation in the hybridization will be inquired into, following the treatment by Craig and Magnusson, who presented a model to represent *d* electrons in an octahedral molecule, and applied it to the consideration of actual examples.

Orbital Contraction.—Let us now consider the system in which a bivalent sulfur atom combines with two carbon atoms at an angle. In this model, a single *d* electron will be supposed to move in the field of the sulfur nucleus of charge Z_s, and upon this hydrogen-like atom system will be superposed a perturbation consisting of two positive charges of the carbon atoms of magnitude Z_c at the distance of σ atomic units. Furthermore, the central hydrogen-like atom will be considered to be surrounded, not by two hydrogen-like atoms of carbon, but just by point charges of magnitude Z_c. The actual potential of perturbation consists of the attraction of the surrounding nuclei minus the

1) H. C. Longuet-Higgins, *Trans. Faraday Soc.*, **45**, 173 (1949).
2) K. Kikuchi, *Sci. Repts. Tohoku Univ. Series I*, **40**, 133 (1956).
3) K. Kikuchi, ibid., **41**, 35 (1957).
4) J. C. Slater, *Phys. Rev.*, **36**, 57 (1930).
5) H. H. Jaffé, *J. Chem. Phys.*, **21**, 258 (1953).
6) D. P. Craig, A. Maccoll, R. S. Nyholm, L. E. Orgel and L. E. Sutton, *J. Chem. Soc.*, **1954**, 332.
7) D. P. Craig and E. A. Magnusson, ibid., **1956**, 4895.

coulomb repulsions of their electrons plus exchange terms; hence the dependence on distance of this composite potential will not follow the r^{-1} law at all closely. The system being thus too complicated, the point charge approximation is employed as approximation in this paper; the charge Z_c will be treated rather as a parameter relevant to making up for the imperfection of the approximation, values plausible in wider range being involved. As for the angle between two C-S bonds, θ, the following three cases will be considered apart from the thiophene in question, from a more general point of view, 90°, 120° and further 180°. For $Z_c=0$, the eigenfunction for d electron is, of course, that of the hydrogen-like atom of charge Z_s. As the d electron wave function, two of the usual Slater-type atomic functions are taken up for consideration, as follows:

$$\psi_{xz}=(\sqrt{2}/81\sqrt{\pi})\alpha^{7/2}r^2\exp(-\alpha r/3)\times\sin\vartheta\cos\vartheta\cos\varphi$$

$$\psi_{yz}=(\sqrt{2}/81\sqrt{\pi})\alpha^{7/2}r^2\exp(-\alpha r/3)\times\sin\vartheta\cos\vartheta\sin\varphi$$

where, α, as will be mentioned later, is a parameter to be determined with respect to energy. Further, the influence upon $3p$ Slater atomic function will be examined in comparison with the case of the d orbitals.

The potential by the outlying charges may be expanded as a sum in the usual $1/r$ series[8], which reduces to the following expressions for the three cases respectively.

$\theta=90°$:

$$V_{r<\sigma}=-(2Z_c/\sigma)-(Z_c/\sigma)(r/\sigma)\times(\cos\varphi+\sin\varphi)\sin\vartheta-(Z_c/2\sigma)(r/\sigma)^2(3\sin^2\vartheta-2)+\cdots\cdots$$

$$V_{r>\sigma}=-(2Z_c/r)-(Z_c/r)(\sigma/r)\times(\cos\varphi+\sin\varphi)\sin\vartheta-(Z_c/2r)(\sigma/r)^2(3\sin^2\vartheta-2)+\cdots\cdots$$

$\theta=120°$:

$$V_{r<\sigma}=-(2Z_c/\sigma)-(Z_c/\sigma)(r/\sigma)\times\cos(\varphi-\pi/3)\sin\vartheta-(Z_c/2\sigma)(r/\sigma)^2\{(15/4)\cos^2\varphi\sin^2\vartheta+(3\sqrt{3}/2)\sin\varphi\cos\varphi\sin^2\vartheta+(9/4)\sin^2\varphi\sin^2\vartheta-2\}+\cdots\cdots$$

$$V_{r>\sigma}=-(2Z_c/r)-(Z_c/r)(\sigma/r)\times\cos(\varphi-\pi/3)\sin\vartheta-(Z_c/2r)(\sigma/r)^2\times\{(15/4)\cos^2\varphi\sin^2\vartheta+(3\sqrt{3}/2)\sin\varphi\cos\varphi\sin^2\vartheta+(9/4)\sin^2\varphi\sin^2\vartheta-2\}+\cdots\cdots$$

$\theta=180°$:

$$V_{r<\sigma}=-(2Z_c/\sigma)-(Z_c/\sigma)(r/\sigma)^2\times(3\cos^2\varphi\sin^2\vartheta-1)+\cdots\cdots$$

$$V_{r>\sigma}=-(2Z_c/r)-(Z_c/r)(\sigma/r)^2(3\cos^2\varphi\sin^2\vartheta-1)+\cdots\cdots$$

Each expression shows that the perturbing potential has its symmetrical plane bisecting the angle between two C-S bonds, θ. The perturbation energy due to the outlying potential is given by $\int\psi V\psi d\tau$, where ψ and V are both shown above. Hence, after integrating over the angular parts excepting the radial one, it is found that the expressions for $3p_z$ orbitals have the same forms, and that the $3d_{xz}$ and $3d_{yz}$ orbitals are exposed respectively to the same fields of the outlying potentials when $\theta=90°$. Both of these can naturally be expected from their symmetric characters. In integrating with respect to the radial part, the terms higher than 2nd may be neglected because of their small contribution to the potential. Hence, the perturbation energy E' is given by the following, for example, for $3d_{xz}$ when $\theta=180°$;

$$E'=(8Z_c/81^2\times15)\int_0^\sigma\alpha^7r^6\{-2/6-(2/7)\times(r^2/\sigma^3)\}\exp(-2\alpha r/3)dr+(8Z_c/81^2\times15)\int_\sigma^\infty\alpha^7r^5\{-2-(2/7)\times(\sigma^2/r^2)\}\exp(-2\alpha r/3)dr$$
$$=-(2Z_c/\sigma)(2\alpha\sigma/3)^7(1/6)[\{6!(3/2\alpha\sigma)^7-A_6(2\alpha\sigma/3)+A_5(2\alpha\sigma/3)\}+(1/7)\{8!(3/2\alpha\sigma)^9-A_8(2\alpha\sigma/3)+A_3(2\alpha\sigma/3)\}]$$

where

$$A_n(\omega)=\int_1^\infty r^n\exp(-\omega r)dr$$

Hereupon, using the auxiliary function presented by Craig and Magnesson[7],

$$R^p_{nn}(\alpha\sigma)=(1/\sigma)(2\alpha\sigma/n)^{2n+1}\{1/(2n)!\}\times\{(2n+p)!(n/2\alpha\sigma)^{2n+p+1}-A_{2n+p}(2\alpha\sigma/n)+A_{2n-p-1}(2\alpha\sigma/n)\}$$

8) H. Eyring, J. Walter and G. E. Kimball, "Quantum Chemistry", John Wiley & Sons, Inc., New York (1944), p. 369.

$$E' = -(2Z_c/\sigma)\{\sigma K^0_{33}(\alpha\sigma) - (1/7)\sigma R^2_{33}(\alpha\sigma)\}$$

For $3d_{yz}$ when $\theta = 180°$,

$$E' = -(2Z_c/\sigma)\{\sigma K^0_{33}(\alpha\sigma) - (2/7)\sigma R^2_{33}(\alpha\sigma)\}$$

Similarly, when $\theta = 120°$, for $3d_{xz}$

$$E' = -(2Z_c/\sigma)\{\sigma K^0_{33}(\alpha\sigma) - (1/56)\sigma R^2_{33}(\alpha\sigma)\}$$

and also for $3d_{yz}$,

$$E' = -(2Z_c/\sigma)\{\sigma K^0_{33}(\alpha\sigma) - (1/8)\sigma R^2_{33}(\alpha\sigma)\}$$

As mentioned above, the $3d_{xz}$ and the $3d_{yz}$ orbitals have the same potentials of perturbation when $\theta = 90°$, and so their energies are given in the same form,

$$E' = -(2Z_c/\sigma)\{\sigma K^0_{33}(\alpha\sigma) - (1/14)\sigma R^2_{33}(\alpha\sigma)\}$$

In the case of the $3p$ orbitals, they have the same energies for three cases of the angle θ because of their symmetric characters, that is;

$$E' = -(2Z_c/\sigma)\{\sigma R^0_{33}(\alpha\sigma) - (1/5)\sigma R^2_{33}(\alpha\sigma)\}$$

The total energy is the sum of the perturbation energy E' and the unperturbed given by

$$W = (\alpha/3^2)(\alpha/2 - Z_s)$$

for the hydrogen-like orbital of free atom parameter Z_s.

The procedure to be performed now is to find the new value of effective nuclear charge for which the total energy is a minimum for given magnitude of σ, Z_c and Z_s, i.e. to minimize the energy with respect to the exponent α. The increase in α over Z_s corresponds to a contraction of the orbital and the decrease to an expansion, since Slater radial functions have their maxima at $r_m = n^2/\alpha$. As the value of Z_s, the following two are chosen, 1 and 2 for $3d$ orbital, and 5 and 6 for $3p$. The distance σ is assigned to three values, 4, 3 and 2 atomic units, the first two come from actual examples containing the sulfur atoms, and the last is taken for the purpose of comparison with the first two. With respect to the value of Z_c, it is difficult to determine the straightforwardly equivalent parameter of the outlying potential, because, as mentioned above, the real field is not truly coulombic but much more complicated. Furthermore, there is, in general, a considerable difference between so-called potential- and field-determined nuclear charges on the same atom[9]. Therefore, in this paper, three values are assumed, $Z_c = 1$, 2 and 3, which are of course treated as tentative parameters, and the last is introduced from the well-known value of Slater's rule for the $2p$ orbital of carbon. In finding the minimum of the total energy, it is necessary to evaluate the values of $\sigma R^k_{nn}(\alpha\sigma)$, which are tabulated in *Appendix*.

In Tables I and II are given the results. It is shown in these tables that the $3d$ orbitals are largely contracted, while the $3p$ orbitals are little affected by the outlying perturbing charges, and that the contraction is more sensitive to the bond distance σ than to the effective charge Z_c. The magnitude of the contraction is less for a greater bond distance and for a greater value of Z_c. This may be expected for the model employed here. Fig. 1 illustrates the rapid decrease in increment $(\alpha - Z_s)$ with increasing σ and

TABLE I. EFFECTIVE NUCLEAR CHARGE α of $3d$ ORBITAL WHEN $\theta = 180°$ AND $120°$

θ	Z_s	Z_c	$\sigma=2$	$\sigma=3$	$\sigma=4$
I. $3d_{xz}$					
180°	1	1	2.85	2.50	2.15
〃	〃	2	3.76	3.00	2.45
〃	〃	3	4.20	3.25	2.50
〃	2	1	3.66	2.96	2.64
〃	〃	2	4.25	3.48	2.93
〃	〃	3	4.50	3.65	3.10
120°	1	1	2.63	2.30	2.09
〃	〃	2	3.56	2.93	2.48
〃	〃	3	4.14	3.20	2.70
〃	2	1	3.40	2.94	2.58
〃	〃	2	4.14	3.42	2.90
〃	〃	3	4.60	3.60	3.05
II. $3d_{yz}$					
180°	1	1	2.30	2.10	1.95
〃	〃	2	3.12	2.68	2.24
〃	〃	3	3.78	3.05	2.62
〃	2	1	3.08	2.84	2.59
〃	〃	2	3.75	3.14	2.96
〃	〃	3	4.10	3.06	3.15
120°	1	1	2.54	2.20	1.98
〃	〃	2	3.45	2.80	2.51
〃	〃	3	3.90	3.16	2.65
〃	2	1	3.28	2.87	2.68
〃	〃	2	3.95	3.27	2.84
〃	〃	3	4.40	3.56	2.94

TABLE II. EFFECTIVE NUCLEAR CHARGE α of $3p_z$ ORBITAL

Z_s	Z_c	$\sigma=2$	$\sigma=3$	$\sigma=4$
5	1	5.47	5.22	5.15
〃	2	5.93	5.52	5.20
〃	3	6.20	5.55	5.24
6	1	6.32	6.13	6.00
〃	2	6.63	6.20	6.12
〃	3	6.90	6.25	6.18

9) For example, see: F. W. Brown, *Phys. Rev.*, **44**, 214 (1933).

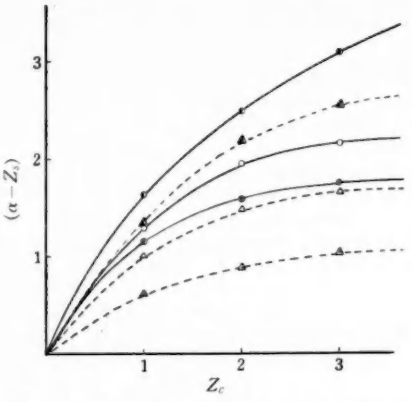

Fig. 1. Values of the increment $(\alpha - Z_s)$ for $3d_{xz}$ and $3d_{yz}$ orbitals when $\theta = 90°$.

—◐— $Z_c=1$ $\sigma=2$
—○— 〃 $\sigma=3$
—⊙— 〃 $\sigma=4$
--▲-- $Z_s=2$ $\sigma=2$
--△-- 〃 $\sigma=3$
--◬-- 〃 $\sigma=4$

Z, when $\theta = 90°$ (the case of thiophene[10]). The figure also shows that the increment of effective nuclear charge by the perturbation is little altered by Z_c in the range $Z_c = 2 \sim 3$ which are most plausible as the equivalent parameter, $\sigma = 3$ and 4 corresponding to the actual molecule containing the sulfur atom.

From these results, it might be inferred in any case that in hybridizing the *d* orbital on the sulfur atom as in thiophene the effective nuclear charge for the *d* orbital would not bear the free atom parameter, but it should bear at least a greater value, for example, $\alpha \fallingdotseq 3$ for that in thiophene. Of course, it must be emphasized that this discussion on the effective value for α is by all means tentative under the point charge approximation. Furthermore, the value of α appropriate to the real system should be determined precisely with respect to the whole energy of the molecule. The value obtained through the approximation, however, may be used as the first step of the calculation about the molecular energy.

On the other hand, for the $3p$ orbital, the free atom parameter may be used directly in calculating the molecular energy, because it is little affected by the surrounding nuclei. In general, the contraction of orbital is large only when the orbital with highly screened and loosely bound electrons lies under the perturbation. For the $2p\pi$ orbital of carbon, an argument similar to the case for $3p$ orbital can be applied as follows; the perturbation energy E' for the $2p$ orbital with nuclear charge $Z=3$ is given as

$$E' = -(2Z_c/\sigma)\{\sigma R^0_{22}(\alpha\sigma) - (1/5)\sigma R^2_{22}(\alpha\sigma)\}$$

when $\theta = 120°$. Using the values σR^0_{22} and σR^2_{22} (see *Appendix*), the perturbed nuclear charge can be obtained, which is given in Table III for $\sigma = 2$, 3 and 4 atomic units. It is seen that the orbital is not altered at all. The free atom parameter for the $2p$ orbital of carbon may be used securely as usual in the molecular energy calculation.

TABLE III. EFFECTIVE NUCLEAR CHARGE α OF $2p_z$ ORBITAL WHEN $\theta = 120°$

Z	Z_c	$\sigma=2$	$\sigma=3$	$\sigma=4$
3	1	3.26	3.14	3.07
〃	2	3.46	3.22	3.10
〃	3	3.64	3.33	3.14

It is of interest to notice that the radial maxima of the $3d$ orbitals contracted lie nearly at the bond distance σ.

Overlap Integral.—The overlap criterion[6] may be used conveniently in discussing the bond formation, because it is generally impracticable to calculate accurately the energy of formation of a bond between two centers, and, as much used and discussed by Mulliken and his collaborators[11], it gives some measure of the concentration of electronic charge between the nuclei. It can be used not only for the discussion of covalent bond, but also can be well applied to that of π bonding. An amount of increase in overlap integral means to strengthen the bond to some extent. Further the increase in overlap integral of a *d* orbital with an orbital on the neighboring atom will be associated by large contribution to the hybridization in which the *d* orbital participates, because the integral of the hybrid orbital may be written as a sum of those of participating orbitals.

The values of the integral for the contracted and unperturbed $3d\pi$ orbitals with the $2p\pi$ orbitals of carbon are summarized in Table IV, together with those for $3p\pi$ orbitals. In calculating these values, numerical tables given by Jaffé[5] and

10) Y. Schomaker and L. Pauling, *J. Am. Chem. Soc.*, **61**, 1779 (1939).

11) For example, F. S. Mulliken, *J. Phys. Chem.*, **56**, 295 (1952).

TABLE IV. OVERLAP INTEGRALS OF 3*d* ORBITALS WITH 2*p* ORBITALS OF CARBON, WHEN $\theta=90°$*

Z_s	Z_c	$\sigma=2$	$\sigma=3$	$\sigma=4$
I. $3d_{xz}$ and $3d_{yz}$				
1	0	0.109	0.129	0.127
1	1	0.438	0.425	0.290
1	2	0.537	0.428	0.309
1	3			
2	0	0.319	0.326	0.279
2	1	0.525	0.426	0.308
2	2	0.566	0.439	0.315
2	3			
II. $3p_z$				
5	0	0.492	0.242	0.109
5	1	0.484	0.241	0.099
5	2	0.477	0.220	0.098
5	3			
6	0	0.477	0.202	0.081
6	1	0.444	0.192	0.079
6	2	0.426	0.192	0.074
6	3			

* In calculating the overlap integral involving *d* orbital, one must pay some attention to the special symmetric character of the orbital; in this table are given only the values when $\theta=90°$, because both other cases may cause some confusion in the calculation. Cf. Ref. 2.

Mulliken et al.[12] were used. The results show that the values of integral for the contracted 3*d* orbitals are enlarged without exception. Although it does not necessarily signify a very great possibility of bonding by the *d* orbital, it may be said at least that such $d\pi-p\pi$ bonding is likely to be more commom and important than has ever been considered, and that, therefore, the participation of the *d* orbitals in the hybridization is more probable than expected through the direct employment of free atom parameter by Slater's rule. In an actual system such as the sulfur atom in thiophene, the extent to which the *d* orbital participates in bonding will be of the order same as, or less than, that of the 3*p* orbital, despite the greater value of the integral. Because the mixing coefficient of the *d* orbital in the hybridization is not great, and also the balancing of energy is unfavorable; this will be examined in the next section.

Balancing of Energy.—Slater's rule seems to be insufficient for the accurate calculation of energy levels of an atom, although it suffices for the discussion of orbital size and overlap of atoms. For example, according to the rule, one has the values 45 and 1.5 eV. for 3*p* and 3*d* orbitals on the sulfur atom, respectively. They are very different from spectroscopic data[13], though these data are not always precisely corresponding to the so-called valence states of the atom. Spectroscopically the ionization energy of the atom is 10.36 eV. and the difference between 3*p* and 3*d* states is about 8.5 eV.

The discussion dealing with the final determining factor in bonding, i.e. the energy, can not be free from some ambiguity, since the general relationships between the overlap and the bond energy, and between the effective nuclear charge and the energy level, are not yet well established. If one should be allowed to assume that the free atom parameters $Z_s=5.45$ and 1 may correspond to the energy values 10.36 and 1.86 eV., respectively, the levels of the contracted *d* orbitals will be settled at about 5 eV. above the ground state. Of course, this estimation is merely tentative. However, it might be said that the level of energy of the *d* orbital will be drawn to some extent near to that of the 3*p* orbital as the result of the contraction by the perturbation, so that the possibility of participation in the hybridization will become greater, setting aside the question of extra promotion energy suggested by Craig and Magnusson[7], who estimated the energy directly by Slater's rule. It is well known that the closer the two energy levels are drawn to each other, the greater the interaction between them[14].

All the discussions above are those under the point charge approximation. It is more or less inevitable that the results obtained in this paper are not so readily available for an accurate discussion of bond formation in the real system. Further, in thiophene, there are two other perturbing charges which are included by the diffuse *d* orbital on the sulfur atom.

Nevertheless, the results will be sufficiently valid for approximate and semi-quantitative discussion on the possibility of participation of the *d* orbital in hybridization.

Summary

The influence of neighboring atoms upon the diffuse *d* orbital on the sulfur atom

12) R. S. Mulliken, C. A. Rieke, D. Orloff and H. Orloff, *J. Chem. Phys.*, **17**, 1248 (1949).

13) C. E. Moore, *Natl. Bur. Standards (U. S.), Circ.* **467**, 181 (1949).

14) C. A. Coulson, "Valence", Oxford University Press, London (1952), p. 195.

and the possibility of the participation in the hybridization were examined. It might be expected that, with respect to the sulfur atom in thiophene, the participation of *d* orbitals in the hybridization would take place to a greater extent than predicted by the direct application of free atom parameter by Slater's rule, owing to the contraction by the perturbation of neighboring carbon atoms.

The author wishes to express his sincere thanks to Dr. S. Nagakura for his kind advice and helpful discussions. Thanks are also due to Dr. K. Saito for his kind inspection and revision of this manuscript.

Electrotechnical Laboratory
Tanashi P. O., Tokyo

Appendix THE VALUES OF AUXILIARY FUNCTIONS

$\alpha\sigma$*	σR^0_{22}	σR^2_{22}	σR^0_{33}	σR^2_{33}
1.5			0.1665	0.0082
2.0	0.4799	0.1693		
2.25			0.2498	0.0269
3.0	0.6702	0.2287	0.3323	0.0611
3.75			0.4133	0.1088
4.0	0.8046	0.4517		
4.5			0.4915	0.1698
5.0	0.8908	0.4958		
5.25			0.5656	0.2368
6.0	0.9417	0.4843	0.6341	0.3061
6.75			0.6961	0.3714
7.0	0.9701	0.4412		
7.5			0.7511	0.4286
8.0	0.9851	0.3863		
8.25			0.7988	0.4752
9.0	0.9928	0.3313	0.8394	0.5098
10.0	0.9966	0.2817		
10.5			0.9011	0.5433
11.0	0.9984	0.2396		
12.0	0.9993	0.2045	0.9416	0.5373
13.0	0.9996	0.1758		
13.5			0.9667	0.5053
14.0	0.9999	0.1524		
15.0	1.0004	0.1364	0.9817	0.4598
18.0			0.9949	0.3616
21.0			0.9987	0.2850
24.0			0.9997	0.2169
27.0			0.9999	0.1725

* The values for $\alpha\sigma$ in the table given by Craig and Magnusson should be multiplied by 1.5.

Vapor Phase Oxidation of Alkyl Benzenes[1]

By Shigeru MORITA

(Received September 7, 1959)

Phthalic anhydride is produced commercially by vapor phase oxidation of naphthalene. By the same process, maleic anhydride is obtained from benzene, anthraquinone from anthracene. Production of benzoic acid from toluene and of phthalic anhydride from *o*-xylene by the oxidation has been studied, but the oxidation of benzene which contains an alkyl group with a longer chain than the methyl group has not been examined.

It has been published that, based on liquid phase oxidation of ethyl benzene, the mechanism of vapor phase oxidation of alkyl benzenes is assumed to be as follows[2]:

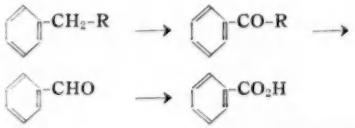

R: alkyl group

The author studied the mechanism of vapor phase oxidation of alkyl benzenes and others.

Experimental

Apparatus.—As shown in Fig. 1, a reactor was a steel U tube 18 mm. in diameter, immersed in a molten nitrate bath.

1) This is a summary of the report published in *J. Chem. Soc. Japan, Pure Chem. Sec.* (*Nippon Kagaku Zasshi*), **78**, 1746 (1957); **79**, 1081, 1230, 1406 (1958).

2) L. F. Marek and D. A. Hahn, "The Catalytic Oxidation of Organic Compound in the Vapor Phase", Am. Chem. Soc. Monograph No. 61, Chemical Catalog Co., New York (1932), p. 356.

TABLE I. PHYSICAL CONSTANTS OF SUBSTANCES

		°C	d_4^{20}
Toluene	b.p.	110.5	0.864
Ethyl benzene	b.p.	136.2	0.867
Styrene	$b.p._{40}$	44.5～45.5	0.908
n-Propyl benzene	b.p.	159.6	0.862
iso-Propyl benzene	b.p.	152.5	0.862
n-Butyl benzene	b.p.	183.2	0.860
sec-Butyl benzene	b.p.	173.5～173.8	0.862
tert-Butyl benzene	b.p.	170.0～170.5	0.866
sec-Amyl benzene	b.p.	192.0～192.8	0.862
3-Phenyl pentane	b.p.	191.0	0.864
tert-Amyl benzene	b.p.	189.0～189.5	0.873
n-Hexyl benzene	b.p.	225.4	0.857
2-Phenyl-*n*-hexane	b.p.	214	0.861
Dodecyl benzene	$b.p._{20}$	165～185	0.862
Phenyl cyclohexane	b.p.	235～236	0.943
Diphenyl	m.p.	70.3	—
Propiophenone	b.p.	218	1.005
Phenyl acetone	b.p.	216	1.004
Hydrocinnamic acid	m.p.	48	—
Cinnamic acid	m.p.	133	—
α-Hydrindone	m.p.	41	—
Butyrophenone	b.p.	220～221	0.988
Benzyl ethyl ketone	$b.p._{16}$	109～111	1.001
Benzyl acetone	$b.p._{13}$	115	0.985
γ-Phenyl butyric acid	m.p.	51	—
Tetralone	$b.p._{13}$	127	1.092

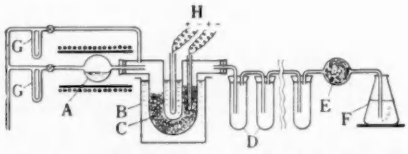

Fig. 1. Apparatus used for vapor phase oxidation.
A. Evaporator
B. Salt bath
C. Reactor
D. Air condensers and ice-cooled condensers
E. Glass wool
F. Water bubbler
G. Flowmeters
H. Thermocouples

Catalyst.—The Catalyst was, throughout the present experiments, a mixture of vanadium pentoxide and molybdenum trioxide on pumice stone, which was prepared from ammonium metavanadate (5 g.), ammonium molybdate (5 g.) and puric stone (100 ml.) by the method described before[3].

Experimental Conditions.—The air rate was 150 l./hr. and the feed rate of reactants 1.5 g./hr.; the range of reactor temperatures was 300～500°C and the volume of catalyst was 50 ml. Duration of an experimental run was 3 hr. Substances oxidized are listed in Table I.

Analysis of Reaction Products.—Oxidation products, mainly a mixture of phthalic and maleic anhydrides and benzoic acid, after having been dissolved in hot water (and filtered, if necessary,) were dried in vacuo and weighed. Then, using a portion of the dried product, the neutralization equivalent of the whole mixture was ascertained. Another portion of the product was taken, benzoic acid was removed completely by microsublimation apparatus at 65～70°C, and the neutralization equivalent of the remaining product was ascertained. From these values the amounts of phthalic, benzoic, and maleic acids were figured out.

The same procedure was repeated using a known mixture of three acids and the experimental values were found to be within 15% of the theoretical values.

Results and Discussion

Vapor Phase Oxidation of Monoalkyl Benzenes.—Toluene, ethyl benzene, propyl benzenes butyl benzenes, amyl benzenes, hexyl benzenes, and dodecyl benzenes were oxidized under the same conditions. The mole percentage yields of products are listed in Table II.

Table II shows that

1) Ethyl benzene is more easily oxidized

3) H. Sasayama, *J. Chem. Soc. Japan, Ind. Chem. Sec.* (*Kogyo Kagaku Zasshi*), **56**, 281 (1953).

TABLE II. EXPERIMENTAL RESULTS OF VAPOR PHASE OXIDATION OF ALKYL BENZENES

	Reaction temp. °C	Products		
		Phthalic anhydride mol. %	Benzoic acid mol. %	Maleic anhydride mol. %
Toluene	300	0	7	8
Toluene	350	trace	12	45
Ethyl benzene	300	0	35	12
Ethyl benzene	400	0	9	41
Styrene	300	0	35	5
Styrene	400	0	trace	49
n-Propyl benzene	350	18	6	34
n-Propyl benzene	400	24	2	35
iso-Propyl benzene	400	0	21	38
n-Butyl benzene	350	27	7	25
n-Butyl benzene	400	26	2	30
sec-Butyl benzene	350	35	9	23
sec-Butyl benzene	400	36	3	26
tert-Butyl benzene	400	trace	0	24
sec-Amyl benzene	350	23	5	22
sec-Amyl benzene	400	24	1	29
3-Phenyl pentane	400	20	2	30
tert-Amyl benzene	350	3	0	38
tert-Amyl benzene	400	4	trace	44
n-Hexyl benzene	350	14	1	50
n-Hexyl benzene	400	19	trace	65
2-Phenyl-*n*-hexane	350	7	3	25
2-Phenyl-*n*-hexane	400	35	1	26
Dodecyl benzene	400	17	1	45
Phenyl cyclohexane	400	8	2	20*
Phenyl cyclohexane	500	10	0	16
Diphenyl	400	14	2	35

* and 18 mol. % of diphenyl is produced.

than toluene. And benzoic acid and maleic anhydride are obtained from ethyl benzene in the same yields as that from styrene.

2) When the number of carbons in the longest chain of the alkyl group is three or more, for instance, *n*-propyl, *n*-butyl, *sec*-butyl, amyl, hexyl, etc., phthalic anhydride (25~36%), benzoic acid and maleic anhydride are obtained by vapor phase oxidation. When it is two or less, for instance, methyl, ethyl, *i*-propyl, no phthalic anhydride is obtained.

3) The yield of phthalic anhydride obtained from *n*-alkyl benzenes is lower than that from *sec*-alkyl benzenes, and that from *tert*-alkyl benzenes is very small.

4) No benzoic acid is obtained from *tert*-alkyl benzenes by vapor phase oxidation.

The Reaction Mechanism of Vapor Phase Oxidation of *n*-Propyl Benzene and *n*-Butyl Benzene. — *n*-Propyl benzene or *n*-butyl benzene has only one alkyl group. Oxidation of either of these two compounds produces phthalic anhydride in which the benzene ring has two side chains containing carbon atoms. This strange phenomenon, however, can not be explained by the mechanism that has been advocated by Marek, Hahn[2] and others so far.

The range of temperatures of vapor phase oxidation is 350~500°C and a reactant is passed with air through the vanadium pentoxide catalyst zone in vapor phase. Therefore, it is supposed that oxidation, pyrolysis and condensation would occur at the same time.

Concerning the above-mentioned strange reaction the author examined accordingly the following three mechanisms *a*, *b* and *c*.

Mechanism a. — *n*-Propyl benzene or *n*-butyl benzene would be oxidized to benzaldehyde. The two molecules of the aldehyde may be condensed to form anthraquinone as Parks[4] observed, and then this would be oxidized to from phthalic anhydride.

4) W. G. Parks et al., *Ind. Eng. Chem.*, **33**, 891 (1941); C. R. Downs, *J. Soc. Chem. Ind.*, **46**, 388, T (1927).

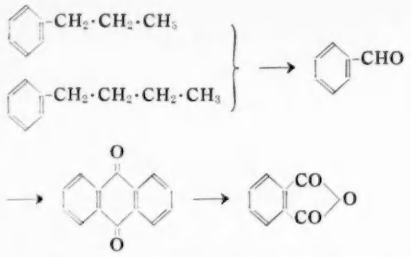

Mechanism b.—*n*-Propyl benzene or *n*-butyl benzene would be dissociated to form benzyl and ethyl or propyl radicals, as given in the papers by Szwarc[5], then the alkyl radical would be attached to the ortho position of benzyl radical to form dialkyl benzene[6]. This would be oxidized to phthalic anhydride.

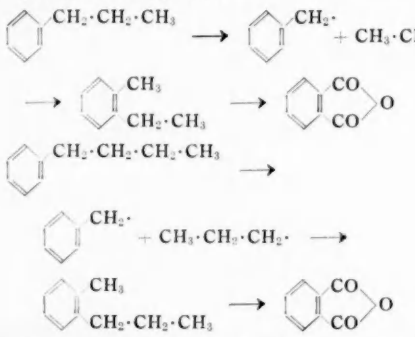

Mechanism c.—As already reported by Tonomura[7], Murphy[8] and Nametkin[9], *n*-propyl benzene or *n*-butyl benzene would produce hydrindene or tetralin by cyclization and then this would be oxidized to phthalic anhydride.

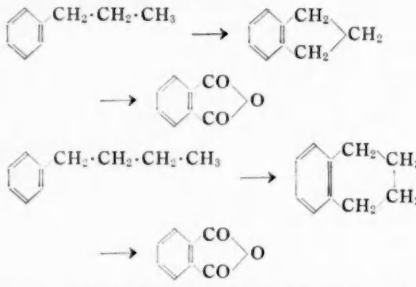

The author examimed these mechanisms.

On mechanism a.—Oxidation products of *n*-propyl benzene or *n*-butyl benzene contained no anthraquinone, and when the mechanism is true, ethyl benzene would have to produce phthalic anhydride through the same mechanisms. But the experimental results showed that no phthalic anhydride was produced from ethyl benzene. From these facts, it is supposed that this mechanism is not true.

On mechanism b.—If this mechanism is correct, ethyl benzene must produce phthalic anhydride by the oxidation. The experiments showed that ethyl benzene did not produce it, and therefore this mechanism is not correct. To ascertain this conclusion, ethyl benzene was oxidized in the vapor phase with air containing vapor of methanol or ethanol, etc., both of which are liable to form a free radical[10], but no phthalic anhydride was obtained.

On mechanism c.—*n*-Propyl benzene was passed through the pumice (carrier) bed which contained no vanadium pentoxide under the same conditions as those of the oxidation (temperature, air rate and feed rate). The ultraviolet spectrum of the product showed that it contained styrene but no hydrindene. Moreover, when this product was oxidized in the liquid phase with aqueous solution of potassium permanganate[11], only benzoic acid was found but no phthalic acid. As to *n*-butyl benzene, the spectrum showed the presence of alkenyl benzene (presumably propenyl benzene). Thus the mechanism *c* is incorrect.

With these three mechanisms, the formation of phthalic anhydride from *n*-propyl benzene or *n*-butyl benzene by the oxidation can not be explained.

The author studied the following reactions.

Mechanism d·1.—The first carbon atom attacked by oxygen in the alkyl group of *n*-propyl benzene, and *n*-butyl benzene.

Propiophenone $C_6H_5\cdot CO\cdot CH_2\cdot CH_3$, phenyl acetone $C_6H_5\cdot CH_2\cdot CO\cdot CH_3$, hydrocinnamic acid $C_6H_5\cdot CH_2\cdot CH_2\cdot CO_2H$, butyrophenone $C_6H_5\cdot CO\cdot CH_2\cdot CH_2\cdot CH_3$, benzyl ethyl ketone $C_6H_5\cdot CH_2\cdot CO\cdot CH_2CH_3$, benzyl acetone $C_6H_5\cdot CH_2\cdot CH_2\cdot CO\cdot CH_3$ and γ-phenyl butyric acid $C_6H_5\cdot CH_2\cdot CH_2\cdot CH_2\cdot CO_2H$ were oxidized in vapor phase under the same conditions. The experimental results are given in Table III.

5) M. Szwarc, *Chem. Revs.*, **47**, 75 (1950); C. H. Leigh et al., *J. Chem. Phys.*, **20**, 407 (1952).
6) V. N. Ipatieff et al., *J. Am. Chem. Soc.*, **75**, 3323 (1953).
7) S. Tonomura, *J. Sci. Research Inst.* (*Tokyo*), **21**, 794 (1942); **25**, 256 (1949).
8) M. T. Murphy et al., *J. Am. Chem. Soc.*, **71**, 3347 (1947).
9) S. S. Nametkin, *Chem. Abstr.*, **42**, 3339 (1948).
10) W. A. Waters, "The Chemistry of Free Radicals", Clarendon Press, Oxford (1948), p. 127.
11) S. P. Mulliken, "Identification of Pure Organic Compounds", Vol. I, John Wiley & Sons, Inc., New York, p. 197.

TABLE III. EXPERIMENTAL RESULTS OF VAPOR PHASE OXIDATION OF COMPOUNDS RELATED TO ALKYL BENZENE

Material	Reaction temp. °C	Products		
		Phthalic anhydride mol. %	Benzoic acid mol. %	Maleic anhydride mol. %
Propiophenone	300	0	45	39
Propiophenone	400	trace	2	49
Phenyl acetone	400	trace	20	42
Hydrocinnamic acid	400	20	2	44
Cinnamic acid	400	15	2	55
α-Hydrindone	400	77	0	11
Butyrophenone	300	trace	62	29
Butyrophenone	400	trace	6	42
Benzyl ethyl ketone	300	0	18	23
Benzyl ethyl ketone	400	0	6	43
Benzyl acetone	400	18	3	46
γ-Phenyl butyric acid	400	30	trace	22
Tetralone	400	62	trace	12

As shown in Table III, propiophenone, butyrophenone, phenyl acetone and benzyl ethyl ketone, of which C_1 or C_2 contains oxygen atom, produced no phthalic anhydride. While hydrocinnamic acid, benzyl acetone and γ-phenyl butyric acid whose C_3 or C_4 has an oxygen atom, produced phthalic anhydride in a yield of 20~30%. From these results, it is concluded that only when the oxidation was initiated at C_3 of *n*- propyl benzene or at C_3 or C_4 of *n*-buthyl benzene, phthalic anhydride was obtained. The waste gas of oxidation of *n*-propyl benzene had a strong odor of hydrocinnamic acid. *n*-Butyl benzene was passed with air through the catalyst bed which contained a very small quantity of vanadium pentoxide, and the presence of γ-phenyl butyric acid was confirmed by the ultraviolet spectrum of the product.

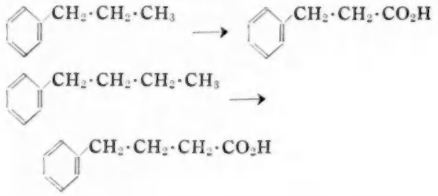

The mechanism given in *d·1* is different from the already published mechanism where only C_1 is oxidized in liquid phase or vapor phase oxidation.

Mechanism d·2.—On cyclization of hydrocinnamic acid and γ-phenyl butyric acid.

Hydrocinnamic acid produces hydrindone by cyclization in the presence of hydrogen fluoride[12], poly-phosphoric acid[13] or 80% phosphoric acid[14] catalyst, and tetralone is obtained from γ-phenyl butyric acid by the action of concentrated sulfuric acid[15]. However, it has not been reported that the cyclization takes place under conditions of vapor phase oxidation.

The author performed the experiment that a mixture of hydrocinnamic acid or γ-phenyl butyric acid vapor and air was passed through the bed of catalyst at 400°C which contained a very small quantity of vanadium pentoxide. Among the reaction products hydrindone and tetralone were identified as phenyl hydrazone and 2, 4-dinitrophenylhydrazone, respectively.

This indicates that cyclization took place. To ascertain this results, the reaction product was oxidized by aqueous solution of potassium permanganate, and phthalic acid was obtained.

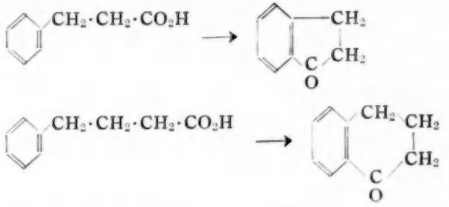

Mechanism d·3.—On vapor phase oxidation of hydrindone and tetralone.

By catalytic air oxidation hydrindone and tetralone gave phthalic anhydride in yields of 77, 62% and maleic anhydride 11, 12%, respectively. From these results (*d·1*, *d·2* and *d·3*), the mechanism through

12) F. Fieser et al., *J. Am. Chem. Soc.*, **61**, 2172 (1937).
13) M. R. Snyder et al., ibid., **72**, 2965 (1950); E. C. Horning, ibid., **73**, 5879 (1951).
14) J. C. Hillyer, *J. Org. Chem.*, **17**, 600 (1952).
15) K. Krollpfeiffer et al., *Ber.*, **56**, 620 (1922).

which phthalic anhydride is obtained by the oxidation of *n*-propyl benzene and *n*-butyl benzenes, is as follows:

n-propyl benzene → hydrocinnamic acid → α-hydrindone → phthalic anhydride

n-butyl benzene → γ-phenyl butyric acid → tetralone → phthalic anhydride

iso-Propyl benzene and *tert*-butyl benzene gave no phthalic anhydride by the oxidation. They have only two carbon atoms in the longest chain of the alkyl group, and therefore cyclization will be impossible to occur.

The yield of phthalic anhydride from *sec*-butyl benzene was higher than that from *n*-propyl benzene. This will probably be due to the fact that cyclization of hydrocinnamic acid takes place more easily when it has a substituent group than when it has none[16].

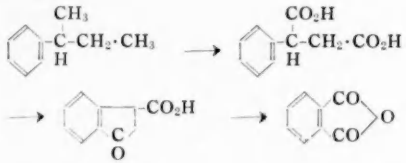

Vapor Phase Oxidation of Amyl Benzenes, Hexyl Benzenes and Dodecyl Benzenes and Others.—The number of carbons in the longest chain of these alkyl groups is at least 3 or more. For the same reason, phthalic anhydride is obtained by the oxidation of these alkyl benzenes (Table II). The product that was obtained by passing dodecyl benzene through the pumice stone (carrier) zone at 400°C, was separated by distillation into three fractions, boiling at about 162, 182 and 230°C, respectively. These produced benzoic acid by oxidation with aqueous solution of potassium permanganate and were absorbed by 90% sulfuric acid and their ultraviolet spectra were characteristic. These were possibly alkenyl benzene (the number of carbons of the alkenyl group was 4—6). As the result it is apparent that such long-chain alkyl benzene as dodecyl benzene is decomposed by heat into short-chain alkenyl benzenes and then phthalic anhydride is produced by oxidation through the above mentioned mechanism.

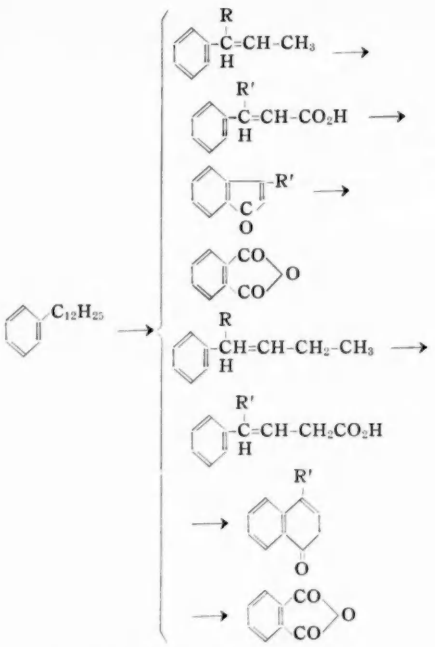

R: H, CH_3. R′: H, CO_2H.

Benzoic acid was not produced from *tert*-alkyl benzenes. This is possibly due to dissociation[17] into benzene nucleus and the alkyl group.

It is supposed that phenyl cyclohexane produced phthalic anhydride by oxidation through the following mechanism.

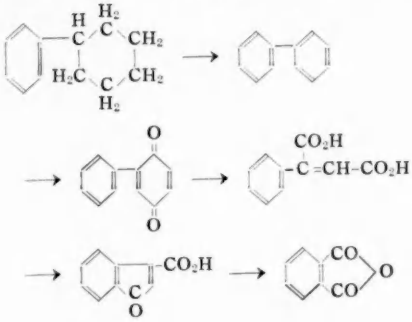

The author is particularly indebted to Professor S. Kimura of Kyoto University, Dr. T. Yoshida, Superintendent of Tobata Chemical Works and Mr. O. Hibino, Manager of the Laboratory Department of the Yawata Chemical Industry Co., Ltd.

Tobata Works
Yawata Chemical Industry Co., Ltd.
Yawata-shi, Fukuoka

16) Richter-Anschütz, "Organishe Chemie", Band II. Friedrich Cohen Bonn (1913), p. 615.
17) N. Tanaka et al., *J. Chem. Soc. Japan, Ind. Chem. Sec.* (*Kogyo Kagaku Zasshi*), **55**, 443 (1952).

Fluorine-19 Nuclear Magnetic Shielding in Some Monofluorinated Compounds

By Kazuo Ito, Kan Inukai and Taro Isobe

(Received July 20, 1959)

The chemical shifts in the proton magnetic resonance spectra of aromatic compounds have been studied by several authors both experimentally[1,2] and theoretically[2-8]. The magnetically non-equivalent nature of protons in these compounds has been essentially interpreted in terms of the interaction between a proton magnetic moment and diamagnetic currents induced on aromatic rings by an external magnetic field. On the other hand, Isobe, Inukai and Ito[9] have shown that the fluorine atoms in fluorobenzene, 1- and 2-fluoronaphthalenes are also magnetically non-equivalent. They have concluded tentatively that the non-equivalent nature of the fluorine atoms can not be attributed to the induced diamagnetic ring current mentioned above but may be attributed to the variation in polarity of the C–F σ-bonds. As a criterion for predicting such a variation in polarity of C–F bonds, the π-electron density of McWeeny's sense[10] has been suggested. Recently, however, Fukui and his coworkers[11] have proposed the qualitative assumption that the larger the π-electron conjugation of a fluorine atom with a neighboring atom or group of atoms and consequently the smaller the π-electron density on the fluorine atom, the more the fluorine nucleus is magnetically shielded. The ^{19}F chemical shifts in some aromatic fluoro compounds, including 1- and 2-fluoronaphthalenes, have been interpreted in terms of this assumption, although the variation in polarity of C–F σ-bonds has also been introduced in order to interpret the ^{19}F chemical shifts in *p*-nitrofluorobenzene and 1-fluoro-4-nitronaphthalene for which the assumption predicts results contradictory to those of the experiments.

In the present paper the ^{19}F NMR spectra of 2- and 3-fluoropyridines, 1-fluoropyrene[12] and cyclohexylfluoride are studied and the ^{19}F chemical shifts in these compounds, together with those in fluorobenzene, 1- and 2-fluoronaphthalenes, are discussed. The spectra of 9-fluoroanthracene and 12-fluorochrysene[12] have also been studied but no signal has been obtained.

Experimental

Materials.—The samples of 1-fluoropyrene and 12-fluorochrysene were kindly provided by Prof. G. M. Badger[13] of the University of Adelaide, South Australia, that of 9-fluoroanthracene by Dr. C. F. H. Allen[14], Eastman Kodak Co., Rochester, U. S. A. and that of cyclohexylfluoride by Dr. K. Okuhara of Government Industrial Research Institute, Nagoya, Japan, to whom the authors are much indebted. The samples of fluorobenzene[15], *m*-nitrofluorobenzene[16], 1- and 2-fluoronaphthalenes[15,17], 2- and 3-fluoropyridines[18] were prepared by the method of the Schiemann reaction. Since no NMR signal was found in 9-fluoroanthracene, the preparation of another sample of the compound was attempted by the general method of Garvey, Halley and Allen[14]. The reaction repeated under the conditions given was followed by some yellowing of the solution but no substance with the melting point specified for 9-fluoroanthracene was obtained.

Apparatus and Procedure.—The ^{19}F NMR spectra were measured with a Varian V-4300-B High Resolution Spectrometer operating at a fixed frequency of 40 Mc./sec. and equipped with a Varian Field Stabilizer. The sample was dissolved in

1) H. J. Bernstein and W. G. Schneider, *J. Chem. Phys.*, **24**, 468 (1956).
2) H. J. Bernstein, W. G. Schneider and J. A. Pople, *Proc. Roy. Soc. (London)*, **A236**, 515 (1956).
3) J. A. Pople, *J. Chem. Phys.* **24**, 1111 (1956).
4) G. Hazato, ibid., **27**, 605 (1957).
5) J. C. Waugh and R. W. Fessenden, *J. Am. Chem. Soc.*, **79**, 846 (1957).
6) K. Ito, ibid., **80**, 3502 (1958).
7) R. McWeeny, *Molec. Phys.*, **1**, 312 (1958).
8) C. E. Johnson, Jr. and F. A. Bovey, *J. Chem. Phys.*, **29**, 1012 (1958).
9) T. Isobe, K. Inukai and K. Ito, ibid., **27**, 1215 (1957).
10) R. McWeeny, ibid., **19**, 1614 (1951).
11) K. Fukui, S. Hattori, T. Yonezawa, R. Kusaka and H. Kitano, *J. Chem. Soc. Japan, Pure Chem. Sec.*, (*Nippon Kagaku Zasshi*), **80**, 541 (1959).
12) All compounds are numbered in accordance with A. M. Patterson and L. T. Capell, "The Ring Index", Reinhold Publishing Corp., New York (1940).
13) G. M. Badger and J. F. Stephens, *J. Chem. Soc.*, **1956**, 3637.
14) B. S. Garvey, Jr., L. F. Hally and C. F. H. Allen, *J. Am. Chem. Soc.*, **59**, 1827 (1937).
15) G. Balz and G. Schiemann, *Ber.*, **60**, 1186 (1927).
16) K. Inukai and Y. Maki, *J. Chem. Soc. Japan, Pure Chem. Sec.* (*Nippon Kagaku Zasshi*), **78**, 1305 (1957).
17) G. Schiemann, W. Gueffroy and W. Winkelmüller, *Ann.*, **487**, 270 (1930).
18) A. Roy and G. F. Hawkins, *J. Am. Chem. Soc.*, **69**, 2443 (1947).

about the same amount of another fluoro compound, *m*-nitrofluorobenzene in most cases, which provides an internal standard for determining the chemical shift δ of the sample defined as $\delta = 10^5 \times (H_c - H_r)/H_r$ where H_c is the applied magnetic field for the ^{19}F resonance in the sample and H_r is that for the reference. The chemical shift was determined by adjusting that of 1-fluoronaphthalene[9] to +1.32, refered to *m*-nitrofluorobenzene. The value of 1.32 was re-determined for the present work on the basis of the chemical shift of fluorobenzene[19] +0.33, agreeing with the previous one[9].

In the previous work[9], the δ-values obtained from the solutions, 1-fluoronaphthalene+*m*-nitrofluorobenzene, 2-fluoronaphthalene+*m*-nitrofluorobenzene and 1-fluoronaphthalene + 2-fluoronaphthalene, were found to be consistent in themselves. In the present work, the results obtained from the solutions, 2-fluoropyridine+*m*-nitrofluorobenzene, 3-fluoropyridine+*m*-nitrofluorobenzene and 2-fluoropyridine+3-fluoropyridine were, also consistent in themselves. Therefore, the bulk effects[20] for the chemical shifts were assumed to be insignificant in the present experiments.

A 33 mol. per cent solution of 9-fluoroanthracene in *m*-nitrofluorobenzene heated for increasing the solubility gave no signal except that of the solvent which was not greatly deformed compared with that of pure *m*-nitrofluorobenzene. Also no signal was obtained on a solution of 12-fluorochrysene in *m*-nitrofluorobenzene because of its low solubility. Both samples will be examined further.

Results and Discussion

It is known experimentally[21,22] that the magnetic shielding of an ^{19}F nucleus is quite sensitive to the nature of the bond between the fluorine atom in question and the atom to which the fluorine is bound. The simple and direct correlation[23] of ^{19}F magnetic shielding in para-substituted fluorobenzenes with the π-electron densities or Hamett's sigma constants for the para-position in the corresponding non-fluorinated compounds may also be attributed to the dependence of the shielding on the bonding nature of C–F bonds. On the other hand, Saika and Slichter[24] have shown theoretically that the ^{19}F magnetic shielding must have a close relation with the nature of the σ-bond by which the fluorine is bound to another atom. The qualitative extension of their theory suggests readily that a π-bond character in the bond by which the fluorine in question is bound to another atom would also have a significant effect on ^{19}F magnetic shielding. In order to discuss the present results, therefore, it would be necessary to take into account both σ- and π-bonding characters of C—F bonds. Since, however, correct estimations of σ- or π-bonding characters of C—F bonds in the compounds studied are very difficult, the following three molecular indexes which may serve as measures of σ- and π-bonding characters of C–F bonds are taken into account: (1) the π-electron density q on the ring carbon to which the fluorine in question is bound, (2) the π-electron "atom charge" density of McWeeny's sense[10] q' on the ring carbon mentioned above, and (3) the π-electron density q on the carbon atom of a CH_2^- group in a hypothetical molecule in which the fluorine atom of the fluoro compound studied is replaced by a CH_2^- group.

The π-electron densities on ring carbons may serve as a criterion for predicting chemical differences in these carbons and, consequently, differences in the σ-bonding nature of C–F bonds. The π-electron "atom charge" densities may also be usable from the same point of view. The latter, however, may be especially useful in alternant hydrocarbons in which the former fails to interpret chemical differences in ring carbons, being equal to unity on all carbons on the basis of the simple LCAO calculation. It would be worth noting that the π-electron "atom charge" densities on the 1- and 2-positions of naphthalene show a tendency consistent with the experimental observation[25]. The π-electron density on the carbon atom of the CH_2^- group in the hypothetical molecule mentioned above may serve as a measure of the π-conjugation of the fluorine atom substituted at the corresponding position. The smaller the π-electron density on the CH^-_2 group, the greater would be the π-conjugation of the fluorine atom with the remainder of the molecule.

The ^{19}F chemical shifts obtained in the present work are given in Table I, together with those of 1- and 2-fluoronaphthalenes. Three molecular indexes mentioned above are given in Tables II—IV, respectively. The parameters used in these tables for

19) H. S. Gutowsky, D. W. McCall, B. R. McGarvey and L. H. Meyer, ibid., **74**, 4809 (1952).
20) B. P. Daily and J. N. Shoolery, ibid., **77**, 3977 (1955); H. J. Bernstein and W. G. Schneider, *Nature*, **178**, 1328 (1956).
21) H. S. Gutowsky and C. J. Hoffman, *J. Chem. Phys.*, **19**, 1259 (1951).
22) L. H. Meyer and H. S. Gutowsky, *J. Phys. Chem.*, **57**, 481 (1953).
23) H. S. Gutowsky, D. W. McCall, B. R. McGarvey and L. H. Meyer, *J. Am. Chem. Soc.*, **74**, 4809 (1952).
24) A. Saika and C. P. Slichter, *J. Chem. Phys.*, **22**, 26 (1954).
25) S. C. Abrahams, J. M. Robertson and J. G. White, *Acta Cryst.*, **2**, 238 (1949).

TABLE I. ^{19}F CHEMICAL SHIFTS IN SOME MONOFLUORINATED COMPOUNDS

Compound	2-Fluoro-pyridine	Fluoro-benzene	2-Fluoro-naphthalene	1-Fluoro-pyrene	1-Fluoro-naphthalene	3-Fluoro-pyridine	Cyclohexyl-fluoride
δ	−4.27	0	0.16	0.97	0.99	1.25	5.63

TABLE II. THE π-ELECTRON DENSITIES ON RING CARBONS

Compound / Position	Pyridine 2	Benzene	Naphthalene 2	Pyrene 1	Naphthalene 1	Pyridine 3	Ref.
Simple LCAO with[e]							
$\delta_N=1$, $\delta_{C'}=0$	0.855	1.000	1.000	1.000	1.000	1.008	a)
$\delta_N=1$, $\delta_{C'}=0.1$	0.893	1.000	1.000	1.000	1.000	0.984	b)
Jaffe's parameters	0.970	1.000	0.989		0.999	0.977	c)
SCF LCAO		1.000	1.003		0.967		d)

a) K. Higashi and H. Baba, "Quantum Organic Chemistry (Ryoshi Yuki Kagaku)", Asakura Publishing Co., Tokyo (1956).
b) Calculated by the present authors.
c) H. H. Jaffe, *J. Chem. Phys.*, **20**, 279, 778, 1554 (1952).
d) C. M. Moser, *J. chim. phys.*, **52**, 24 (1955).
e) The Coulomb integral of a nitrogen atom is given by $\alpha_N=\alpha_C+\delta_N\beta_{CC}$ where α_C is the Coulomb integral of a carbon atom and β_{CC} is the resonance integral of a C–C bond. The Coulomb integral of the carbon atom bonded to the nitrogen atom is given by $\alpha_{C'}=\alpha_C+\delta_{C'}\beta_{CC}$.

TABLE III. THE π-ELECTRON "ATOM CHARGE" DENSITIES ON RING CARBONS

Compound / Position	Pyridine 2	Benzene	Naphthalene 2	Pyrene 1	Naphthalene 1	Pyridine 3
Simple LCAO with						
$\delta_N=1$, $\delta_{C'}=0$	0.644	0.756	0.757	0.771	0.767	0.784
$\delta_N=1$, $\delta_{C'}=0.1$	0.672	0.756	0.757	0.771	0.767	0.767[a]

a) If the inductive effect of nitrogen on β-carbon is taken into account as $\delta_C(\beta)=(0.1)^2$, this value takes 0.770

TABLE IV. THE π-ELECTRON DENSITY ON THE CARBON ATOM OF A CH_2^- GROUP SUBSTITUTED IN AN AROMATIC COMPOUND

Parent compound	Pyridine	Benzene	Naphthalene	Pyrene	Naphthalene	Pyridine
Position of substitution	2		2	1	1	3
Charge density on CH_2^-	1.499[a]	1.571[d]	1.529[d]	1.364[d]	1.450[d]	1.561[a]
	1.485[b]					1.542[b]
	1.464[c]					1.504[c]

a) Calculated with $\delta_N=1$, $\delta_{C'}=0$.
b) Calculated with $\delta_N=1$, $\delta_{C'}=0.1$.
c) Calculated with $\delta_N=2$, $\delta_{C'}=0.25$. This set of parameters was used by H. C. Longuet-Higgins and C. A. Coulson, *Trans. Faraday Soc.*, **43**, 87 (1947). These parameters would overestimate the electronegative effect of nitrogen (see Refs. 26 and 27), but were used here in order to show an extreme case.
d) Calculated by the method of H. C. Longuet-Higgins, *J. Chem. Phys.*, **18**, 265 (1950).

calculating the indexes of pyridine are their representative values[26,27]. The resonance integral of a C–N bond was assumed to be equal to that of a C–C bond, because small changes in resonance integrals have only negligible effects on the indexes in the tables. The values given in the second and the seventh columns of Table IV were calculated by the use of the mutual atom polarizabilities in a benzyl anion which are shown in Table V.

Fluorobenzene, 1- and 2-Fluoronaphthalenes, 1-Fluoropyrene and 3-Fluoropyridine. — The sequence of ∂-values for these compounds is, as shown in Table I, fluorobenzene < 2-fluoronaphthalene < 1-fluoropyrene, 1-fluoronaphthalene < 3-fluoropyridine. As seen from Table II, the π-electron density on the ring carbon to which the fluorine atom is bound fails to explain the

26) R. D. Brown, *Quart. Revs.*, **6**, 63 (1952).
27) L. E. Orgel, T. L. Cottrell, W. Dick and L. E. Sutton, *Trans. Faraday Soc.*, **47**, 113 (1951).

TABLE V. MUTUAL ATOM POLARIZABILITIES IN A BENZYL ANION

$r-s$[a]	$\pi_{r,s}\times\beta$
1—1′	−0.1324
2—1′	−0.0716
3—1′	−0.0099
4—1′	−0.1162
1′—1′	0.4116

a) 1′ denotes a CH_2^- group, 1 the carbon atom bonded to the CH_2^- group and 2, 3 and 4 denote the α, β and γ carbon atoms, respectively.

sequence of δ, because the densities in benzene, naphthalene and pyrene are all equal to unity. The π-conjugation of fluorine atoms, the rough measure of which is seen from Table IV, fails also to interpret the sequence of δ. As far as one restricts the attention only to fluorobenzene, 1- and 2-fluoronaphthalenes, one may find a possible interpretation in terms of the assumption[11] that the greater the π-electron conjugation of a fluorine atom with a neighboring atom or group of atoms, the greater the value of δ. However, this assumption fails also definitely to interpret the sequence of δ if one takes into account 1-fluoropyrene and 3-fluoropyridine. On the other hand, the sequence of the π-electon "atom charge" density (Table III), benzene<2-position of naphthalene < 1-position of naphthalene < 1-position of pyrene < 3-position of pyridine, shows a fairly good parallel tendency with the sequence of δ mentioned above. Although the parallelism between two sequences is not very good in pyrene, the π-electron "atom charge" density may be rather satisfactory for interpreting the sequence of δ compared with other indexes, in the sense that the "atom charge" densities of the 1-position of pyrene and the 1-position of naphthalene are fairly close to each other and that the "atom charge" density of the 3-position of pyridine can be larger than that of the 1-position of naphthalene within the reasonable limits[26,27] of parameters δ_N and δ_C (see Table III and footnote e) of Table II). Since the greater the value of q', the more ionic would be the C–F σ-bond, the increasing tendency of δ with q' is reasonable[24].

2-Fluoropyridine.—This compound has the smallest δ-value. This tendency can be interpreted in terms of any index given in Tables II—IV. However, the π-electon density would be rather worthless for this case too, because this index is very poor for interpreting the sequence of δ-values as discussed above. The effect of the π-conjugation of the fluorine atom substituted at the 2-position of pyridine is of interest from the point of view that the ^{35}Cl pure quadrupole resonance of 2-chloropyridine[28] has been explained, emphasizing the larger π-bonding character in the C-halogen bond at the 2-position compared with the π-bonding characters in those at other positions. The π-conjugation of the fluorine atom, however, may not be the main cause of the small δ-value of 2-fluoropyridine. Because, if it is so, the δ-value of 1-fluoronaphthalene must also very small contrary to the experiments. Therefore, the π-electron "atom charge" density and the inductive effect of nitrogen, which has the significant effect on proton NMR spectra of nitrogen heterocycles[29-31], would be responsible for the ^{19}F magnetic shielding of 2-fluoropyridine.

Cyclohexylfluoride.—This compound has a very great δ-value compared with that of benzene. It is obvious that this difference in δ is too great to be interpreted in terms of the diamagnetic ring current induced on benzene[2,3]. The assumption of Fukui et al. on the correlation of δ with the π-conjugation of the fluorine atom fails also to interpret the δ-value of this compound which is greater than that of fluorobenzene. A possible explanation is that the C–F bond in cyclohexylfluoride is more ionic than that in fluorobenzene. Such an explanation may be rather probable, since it is known that[32] the nature of the σ-bonding in a C(sp^3)–Cl bond is more ionic than that in a C(sp^2)-Cl bond and that[32,33] the ring hydrogens of benzene are more protonic than the hydrogens of C(sp^3)–H bonds.

In the arguments given above, it has been shown that the ^{19}F magnetic shielding of the compounds studied in the present work is correlated most probably with the π-electron "atom charge" density. Hereupon, it would be worth while to note

28) P. J. Bray, R. G. Barnes and S. L. Segel, *J. Chem. Phys.*, **28**, 99 (1958).
29) H. J. Bernstein and W. G. Schneider, ibid., **24**, 469 (1956).
30) L. H. Meyer, A. Saika and H. S. Gutowsky, *J. Am. Chem. Soc.*, **75**, 4567 (1953).
31) H. S. Gutowsky, R. L. Rutledge and M. Tamres, ibid., **76**, 4242 (1954).
32) Y. Kurita, *J. Japanese Chem.* (*Kagaku no Ryoiki*), **10**, 24 (1956). See also J. Duchesne, *J. Chem. Phys.*, **19**, 246 (1951).
33) H. W. Thompson, *Trans. Faraday Soc.*, **46**, 103 (1950); G. M. Barrow and D. C. McKean, *Proc. Roy. Soc.* (*London*), **A213**, 27 (1952); I. M. Mills and H. W. Thompson, ibid, **A228**, 287 (1955).

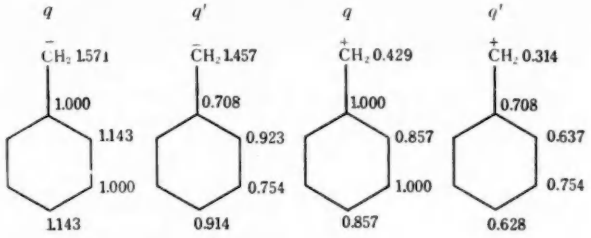

Fig. 1. The π-electron densities (q) and π-electron "atom charge" densities (q') in a benzyl anion and cation

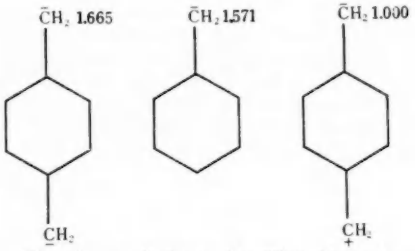

Fig. 2. π-electron densities in some carbions

that the ^{19}F magnetic shielding in substituted fluorobenzenes[23], which has been correlated simply with the π-electron density q, may also be correlated with the π-electron "atom charge" density q', because q and q' have the parallel tendency as shown in Fig. 1. On the other hand, Fig. 2 predicts that the π-conjugation of a fluorine atom, which is represented by CH_2^- in the figure, may be reduced by the para-substitution of $-E$ substituents (halogens, OH, NH_2, etc.) and is increased by that of $+E$ substituents (NO_2, CN, etc.). These predictions suggest that the assumption[11] of Fukui et al. may lead to the contradictory results with the experiments. The pure nuclear quadrupole resonance experiments on para-substituted chlorobenzenes[34] and iodobenzenes[35] have shown that the σ-bond character of a C–halogen bond is made more ionic by the para-substitution of $-E$ substitution and less ionic by that of $+E$ substituents, whereas the double-bond character of the C–halogen bonds is reduced by the para-substitution of $-E$ substituents and is increased by that of $+E$ substituents. These results support the interpretation of ^{19}F magnetic shielding in para-substituted fluorobenzenes in terms of q' or ionicity in C–F bonds, but do not support the interpretation of the same subject in terms of the assumption of Fukui et al. It would also be worth noting that the relative magnetic shielding of CF_4 and CF_3Cl, which has been one of the important experimental evidences for supporting the assumption of Fukui et al., is not necessarily interpreted merely by their assumption, but is also interpreted by the variation in polarity in C–F bonds as argued in the original paper[36].

34) H. C. Meal, *J. Chem. Phys.*, **24**, 1011 (1956); C. Dean, *Phys. Rev.*, **86**, 607 (1952); Y. Kurita, *Chemistry* (*Kagaku*), **12**, 556 (1957).
35) G. W. Ludwig, *J. Chem. Phys.*, **25**, 159 (1956).

Summary

The ^{19}F NMR spectra of 2- and 3-fluoropyridines, 1-fluoropyrene, cyclohexylfluoride, 9-fluoroanthracene and 12-fluorochrysene were studied. No signal was obtained for the latter two compounds. The magnetic shielding constants obtained were attempted, together with those for fluorobenzene, 1- and 2-fluoronaphthalenes, to be correlated with some molecular indexes. It was found that the π-electron density in McWeeny's sense (π-electron "atom charge" density) on the ring carbon atom, to which the fluorine in question is bound, is must probably correlated with the magnetic shielding of the fluorine nucleus. This result suggests that the variation in ^{19}F magnetic shielding constants in these compounds may be attributed mainly to the variation in polarity in C–F σ-bonds. It was noted that such an idea is supported by nuclear quadrupole resonance experiments.

Department of Chemistry
Nagoya University
Nagoya (*K. Ito*)

Government Industrial Research Institute,
Nagoya (*K. Inukai*)

Chemical Research Institute of
Non-Aqueous Solutions
Tohoku University
Sendai (*T. Isobe*)

36) L. H. Meyer and H. S. Gutowsky, *J. Phys. Chem.*, **57**, 481 (1953).

Neutron Activation Analysis of Iodine in Silicon

By Tadashi NOZAKI, Hideo BABA and Hidemaro ARAKI

(Received June 27, 1959)

The determination of trace impurities in silicon is of great importance in the research and industry of the semiconductor material. The neutron activation analysis has played an important role in this field, being used for many kinds of impurity and even in routine work[1]. Among the numerous reports, however, none, as far as listed in the "*Analytical Abstracts* (Society for Analyt. Chem. England)" up to Vol. 6 No. 3 (March, 1959) has dealt with halogens in silicon, though the semiconductor material has been purified through one of its halogen compounds. The present authors determined iodine in silicon purified by the iodide or the chloride method.

Natural iodine consists entirely of ^{127}I, which is activated by thermal neutrons into ^{128}I [$\sigma=6$ barn, $T_{1/2}=25$ min., β 2.12 (76%), etc., γ 0.45 (17%) etc.]. When more than a few p.p.m. of iodine is present with outany other appreciable amount of impurity that emits γ-rays or positrons, the γ-ray spectrometry with a multichannel pulse-height analyzer provides an easy method for quantitative analysis[2]. But when the iodine content is lower, chemical separation becomes necessary, because the photo-peak of ^{128}I is masked by the "Bremsung" of β-rays from ^{31}Si ($T_{1/2}=2.62$ hr., $E_{max}=1.48$ MeV.).

The separation method must be checked carefully, because iodine has many oxidation states, which involve complicated behavior of isotopic exchange, and because, molecular iodine as well as hydrogen iodide is volatile. The treatment of silicon with a mixture of hydrofluoric and nitric acid, a suitable process for many cases, cannot be used here. On the other hand, there is an advantageous rule that any kind of iodine oxide, at least in an ordinary concentration, reacts instantaneously and stoichiometrically with an excess of iodide in an acid solution to give molecular iodine. Fusion of the silicon with potassium hydroxide containing potassium iodide as the carrier, followed by treatment with sulfuric acid, and oxidation with sodium nitrite to molecular iodine, provides a method of chemical separation, the last being distilled and converted into silver iodide. Its usefulness was checked by the use of ^{131}I produced carrier free in silicon by the neutron irradiation of tellurium diffused in the silicon.

Experimental

Sample.—About 1 g. portion of metallic silicon, prepared by the thermal decomposition of silicon tetraiodide or by the reduction of silicon tetrachloride with zinc was used for each analysis. Details concerning each of the samples are described later.

Irradiation.—The sample and reference standard were put side by side in a poly ethylene capsule and irradiated in JRR-1 (Japan Research Reactor 1) under a thermal neutron flux of about 6×10^{11} n/cm^2·sec. The activity of ^{128}I reaches about 80% of its saturation by one hour irradiation.

Self-shielding Effect.—Thermal neutrons for which the absorption cross section of natural silicon is only 0.13 ± 0.03 barns, traverse one centimeter in this material, thereby decreasing the flux by only less than 1%. Thus with an ordinary quantity of the sample, the self-shielding effect can legitimately be neglected.

Chemical Separation of Iodine.—The irradiated silicon was immediately powdered in a special mortar made of iron. A weighed amount (about 0.8 g.) of the silicon powder was slowly added to potassium hydroxide (about 10 g.) which is maintained just above its melting point, and contained a known quantity (several milligrams) of potassium iodide as the carrier. When the vigorous reaction with the evolution of hydrogen became feeble, the mixture was carefully heated to complete the reaction rapidly. The fused matter was treated with 100 ml. of 5 N sulfuric acid containing a few milligram of sodium chloride and potassium bromide as a hold-back carrier. A solution of sodium nitrite was added to the product, and the liberated iodine distilled into a dilute solution of sodium sulfite. This distillate was treated again with sulfuric acid and sodium nitrite, and the molecular iodine was extracted with xylene, washed with dilute sul-

1) B. A. Thompson et al., *Anal. Chem.*, **30**, 1023 (1958).
2) T. Ichimiya et al., *Radioisotopes* (Jap. R. I. Association), **7**, 281 (1958).
3) For example, A. C. Wahl, "Radioactivity Applied to Chemistry", John Wiley & Sons, Inc., New York (1951), p. 32.

furic acid and water, and extracted back into an aqueous solution containing a small excess of sodium sulfite, from which silver iodide was precipitated by the addition of acetic acid, silver nitrate and nitric acid. The precipitate was filtered off through a glass filter (No. 3), washed with a very dilute nitric acid, water, ethanol and ether. The entire process required an hour, or, properly operated, slightly less, with a chemical yield of 50 to 70%.

Radioactivation Standard.—A weighed crop of potassium iodide in a polyethylene envelope was irradiated together with the silicon, and dissolved into a solution containing a known amount of inactive potassium iodide. A part of this solution was oxidized as above, and the molecular iodine extracted with xylene, washed with an aqueous potassium hydrogen sulfate and water, and similarly converted into silver iodide.

Counting.—A simple G-M counter with an end window tube served very conveniently, when the iodine content was more than 0.01 μg., while a 2π counter of gas flow type was used for less iodine. By the use of the latter, whose counting efficiency is several times higher than the former, 3/4 or more of the total disintegration could be detected by virtue of the back-scattering of the β-rays, when the sample was placed on such a heavy metal plate as tin, with negligible loss due to self-absorption. The activity was measured at short time intervals for about 150 min.

Check on the Chemical Process.—The chemical process was checked by the use of silicon containing ^{131}I, which was prepared by the irradiation of silicon doped with tellurium. The following reactions take place,

$$^{130}\mathrm{Te}\ (n,\gamma)\ ^{131}\mathrm{Te} \xrightarrow[25\ \mathrm{min.}]{\beta^-,\gamma} {}^{131}\mathrm{I} \xrightarrow[8.06\ \mathrm{d.}]{\beta^-,\gamma} {}^{131}\mathrm{Xe}\ \text{(stable)}$$

or, $$^{130}\mathrm{Te}\ (n,\gamma)\ ^{131\mathrm{m}}\mathrm{Te} \xrightarrow[30\ \mathrm{hr.}]{} {}^{131}\mathrm{Te} \longrightarrow {}^{131}\mathrm{I} \longrightarrow {}^{131}\mathrm{Xe}.$$

^{131}I emits various γ-rays, among which that of 0.364 MeV. is predominant, and with the irradiated tellurium the area covered by this photo-peak in the γ-ray spectrum decayed with the half-life of ^{131}I, while other peaks of lower energies due to other radioactive nuclides of tellurium (mostly of metastable state) survived longer. It would be reasonable to assume that the two radioisotopes, ^{129}I and ^{131}I, formed in the silicon, pass the so-called hot atom state and behave similarly throughout the chemical process.

Very pure silicon and a small quantity of metallic tellurium in an evacuated silica ampoule were heated over 1000°C for many hours, to cause the latter to diffuse into the former. The ampoule was kept in the reactor for a week. After several days, the silicon was washed with aqua regia and slightly etched with a mixture of hydrofluoric and nitric acids to remove surface contamination. The activity in the silicon was counted with a scintillation counter with a well-type crystal and a single channel analyzer (the region between 0.32 and 0.41 MeV.). The silicon without tellurium contained but negligible activity. After the same chemical process described above, the activity of ^{131}I in the silver iodide was measured under the same condition. The chemical yield being taken into account, the separation method was proved satisfactory within a standard error due to counting, which amounted to 3% in this case.

Results

The results are shown in the table, where I in the column of sample denotes that the silicons were purified by the iodide process, and Cl by the chloride process. The iodide process has been carried out in the Electrical Communication Laboratory in order to obtain semiconductor grade silicon. This method consists of converting a raw silicon into silicon tetraiodide, of purifying the iodide by various techniques, and of thermal decomposition of the iodide with continuous evacuation. The samples I-1 were silicons just after this stage. I-2 was obtained by keeping molten I-1 containing 4.5 p. p. m. of iodine in a silica vessel for an hour under an argon gas flow. I-3 were taken out of the tail of a single crystal made by the cooling method from I-1 containing 1.3 p. p. m. of iodine. The tail end of the crystal contained much more iodine (2.0 p. p. m.) than a part several millimeters above it (0.32 p. p. m.). These silicons were usually of type N. Floating zone refining has also been applied to obtain a material of higher quality. The samples denoted by Cl were silicons of transistor grade prepared by the chloride process in a certain foreign country, and this silicon is now widely used as the transistor material.

Sample	Number of different samples assayed	Iodine content (p. p. m.)
I-1	3	1.3, 4.5, 4.5
I-2	1	0.35
I-3	2	2.0, 0.32
Cl	2	0.005, 0.05

Discussion

After the chemical process, the decay curve of the silver iodide is usually straight on a semilog plot in accordance with the theoretical half-life. However, when the iodine content is lower than 0.01 μg. and the distillation is carried out carelessly, the separated silver iodide is contaminated with radioactive silica. Without the distillation, the precipitate

of silver iodide is by no means free from silica (about 10 μg. of silicon); without the extraction, about 1 μg. of silicon enters the precipitate.

When 0.002 μg. of iodine is present in silicon, it gives an activity of about 100 cpm to the 2π counter after the chemical treatments, and is enough for quantitative analysis and the measurement of the decay curve. If a reactor with a higher neutron flux were available, less iodine could be determined; however, the problem of decontamination from radioactive silicon would become more important. In such a case, repetition of the distillation would be necessary.

Determination of segregation constant of iodine and analysis of chlorine and bromine, with a slight modification of the method, in silicon are now under planning.

Summary

A trace quantity of iodine in silicon was determined by the neutron activation analysis. A chemical separation process, which involves potassium hydroxide fusion with potassium iodide as a carrier, was proved satisfactory by the use of ^{131}I produced by the neutron irradiation of tellurium diffused in silicon. By this method, the iodine was converted into silver iodide ready for counting and weighing within an hour, with a yield exceeding 50%. When it is assumed that a counting rate of 100 cpm is enough for accurate detection of activities, the limit of detection is 0.002 μg. of iodine with a neutron flux of 6×10^{11} n/cm^2 sec. and by the use of a 2π counter.

The authors acknowledge the help given by the members of the staff of Japan the Atomic Research Institute.

The Electrical Communication Laboratory
Nippon Telegraph and
Telephone Public Corporation
Musashino-shi, Tokyo

Viscometric Study on Polystyrenesulfonic Acid Solutions

By Masaaki KATO, Tsurutaro NAKAGAWA and Hideo AKAMATU

(Received August 17, 1959)

Among the physico-chemical properties of polyelectrolytes their flow property makes an important field of study from the viewpoint of polymer science and of electrolyte theory, and many theoretical and experimental investigations on viscosity behavior of various polyelectrolyte solutions have since been reported. Of these, however, comparatively few works have been done on polyelectrolytes of the sulfonic acid type.

It seems, therefore, to be interesting to compare the authors' viscosity data on the polystyrenesulfonic acid, which itself is a strong polymeric acid, with other workers' experimental and theoretical results previously reported, chiefly on sodium salts of polycarboxylic acids or polyquaternary halides.

This paper presents a viscometric study on polystyrenesulfonic acid in various solvents: water, water-dioxane mixed solvent, and aqueous solutions of sodium chloride and some other inorganic salts.

Part I. Viscosity Behavior of PSA Solution

Experimental

Samples.—For the preparation of polystyrenesulfonic acid, polystyrene pellets manufactured by the American Bakelite Company were used. Its viscosity-average molecular weight is about 180,000 from the viscosity measurement in benzene solution at 25°C.

The main feature of the sulfonation procedure is analogous to that of Neihof[1].

In a 500 cc. conical flask 10 g. of polystyrene pellets and 0.2 g. of silver sulfate as catalyst were taken. To this was added 200 cc. of concentrated sulfuric acid, and the flask was completely corked to exclude moisture and was immersed in a constant temperature bath at 100°C with frequent stirring for 20 hr. By this treatment, polystyrene is completely dissolved in concentrated sulfuric

1) R. Neihof, *J. Phys. Chem.*, **58**, 916 (1954).

acid and the content of the flask becomes brown in color and very viscous. The reaction product (i. e. mixture of polystyrenesulfonic acid, sulfuric acid and silver sulfate) is poured into cold distilled water. Then polystyrene sulfonic acid precipitates in the form of a white gummy mass, which is quickly washed with water several times until heat emergence is no longer felt. The precipitate of polystyrenesulfonic acid was then completely dissolved into 500 cc. of distilled water. The large excess of sulfuric acid present could be removed by prolonged dialysis of the aqueous solution using a cellophane membrane. The last trace of remaining sulfuric acid was removed by successive electrodialysis. The presence of sulfuric acid was detected by adding barium chloride solution to the dialyzed polystyrenesulfonic acid solution[2]; a white precipitate which does not dissolve on heating indicates the presence of sulfuric acid. Barium salt of polystyrenesulfonic acid appears also as white precipitate, but it dissolves away on heating. This test was negative after the electrodialysis for three days.

Another sample of polystyrenesulfonic acid was obtained by making the above-mentioned mixture (polystyrene, silver sulfate and conc. sulfuric acid) react in the dark and at the room temperature with frequent stirring for long days, and the following procedure was the same as above-described. The authors will hereafter refer to this as PSA-R and the sample prepared at 100°C as PSA-100.

Determination of the concentration was carried out by completely evaporating the weighed solution to dryness on a steam bath and then drying in an air oven at 110°C until the constant weight was reached.

The degree of sulfonation was determined by the back titration of the PSA solution, to which excess alkali was added, with hydrochloric acid using methyl red as an indicator. The results are:

91% for PSA-100
85% for PSA-R

where 100% is assumed for PSA having one sulfonic acid group on each benzene ring.

A solid sample of the polystyrenesulfonic acid was obtained by freeze-drying of the solution as a white cotton-like material. But throughout the present measurement, PSA as the state of aqueous solution was used.

The polystyrenesulfonic acid, thus prepared, is considered to have the structure shown below.

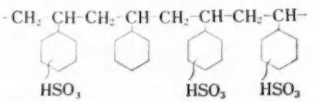

The degree of sulfonation depends, as was mentioned above, upon the condition of sulfonation.

Viscometers.—All our viscosity measurements were carried out at 30°C by using four viscometers of Ostwald type. Their flow time for water (ca. 2 cc.) is about 147, 153, 193 and 254 sec., respectively.

Effect of Rate of Shear. — Recently many investigators[3-6] have pointed out the pronounced shear dependence of the observed viscosity of linear chain polyelectrolyte solutions at low ionic strength. But, according to the results of our viscosity measurement with a horizontal capillary viscometer in the range of 80~1400/sec. of velocity gradient, our PSA sample exhibited

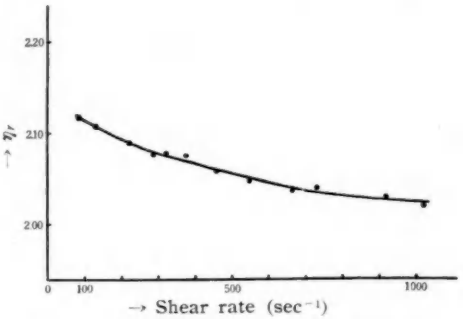

Fig. 1. Effect of rate of shear on relative viscosity. (0.0531%)

TABLE I. EFFECT OF RATE OF SHEAR ON RELATIVE VISCOSITY (0.385%)

Rate of shear q(/sec.)	Relative viscosity $\eta_r \times 10$
623	38.2
600	38.6
586	38.7
554	38.5
541	38.5
525	38.6
505	38.5
478	38.5
450	38.5
430	38.5
401	38.5
368	38.5
340	38.5
310	38.5
280	38.5
254	38.5
230	38.5
209	38.5
169	38.4
125.0	38.5
98.0	38.6
62.8	38.2
36.1	39.0

2) H. H. Waxman, B. R. Sundheim and H. P. Gregor, ibid., **57**, 969 (1953).

3) R. M. Fuoss and U. P. Strauss, *J. Polymer Sci.*, **8**, 593 (1952).

4) R. M. Fuoss and W. N. Maclay, ibid., **6**, 305 (1951).

5) A. Katchalsky and N. Sternberg, ibid., **10**, 253 (1953).

6) H. Fujita and T. Homma, ibid., **15**, 277 (1955).

only a very slight shear rate effect even in the absence of added electrolytes.

Fig. 1 shows an example* of the shear rate effect. Table I is another example** of viscosity measurement by varying the rate of shear. Here the influence of shear rate is not observed. (η_r is relative viscosity, and q is rate of shear.)

It may therefore be accepted that the following data are free from shear-rate dependence to the first approximation. The kinetic energy correction was negligible in all cases studied.

Results and Discussion

In Aqueous Solution.—The viscosity data obtained for the aqueous solutions are shown in Fig. 2, where reduced viscosity

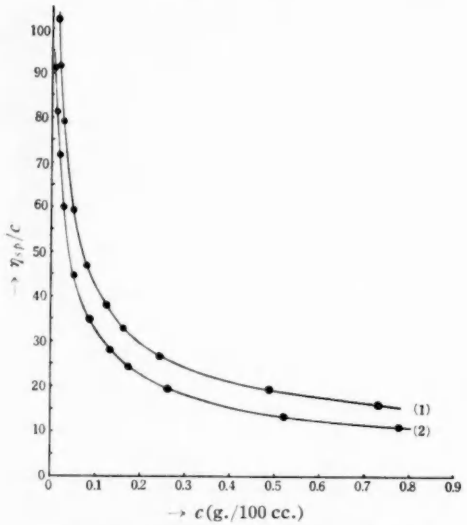

Fig. 2. Reduced viscosity vs. concentration curves.
curve (1) for PSA-100
〃 (2) for PSA-R

η_{sp}/c is plotted against concentration c (g./100 cc.). It is noticed that the PSA aqueous solutions have abnormally large η_{sp}/c value compared with ordinary non-polar polymer solutions in which η_{sp}/c is 2 or 3 at most. $\eta_{sp}/c-c$ plot exhibits a curve strongly concave upward, which is characteristic of polyelectrolyte solutions. In the experimental curves the tendency of decreasing in the low concentration range was not observed.

Considering that the reduced viscosity is a measure of the extention of a polymer coil in solution, the curves show that the size of a polymer becomes larger upon dilution. This phenomenon is generally explained as follows. As the concentration of PSA decreases, the negative net charge on a polyanion increases as a result of increasing dissociation of sulfonic acid groups, and so polymer chains extend more and more, due to the enhanced intramolecular repulsive force between like charges.

The relation between reduced viscosity and concentration of PSA is satisfactorily described by the formula

$$\frac{\eta_{sp}}{c} = \frac{A}{1+B\sqrt{c}} \qquad (1)$$

proposed by Fuoss[7,8]. Here, A and B are empirical constants. A has a meaning of intrinsic viscosity $[\eta]$, and B is a constant dependent on inter-ionic forces. The agreement of the experimental data with Eq. 1 is shown in Fig. 3. The value A is 400 for both PSA samples. The value B is

28 for PSA-100 and
41 for PSA-R

That the two PSA samples of different degrees of sulfonation have the same A value (400) is understandable by recalling that both PSA samples were prepared from the same polystyrene as a starting material and by assuming that no chain scission or cross-link formation through a

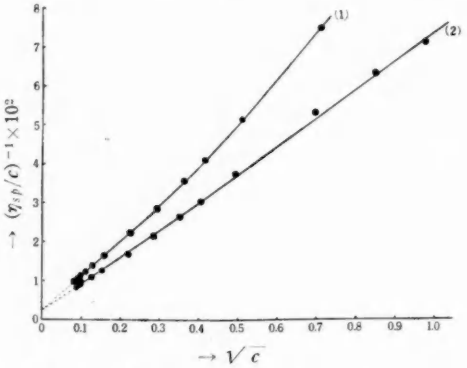

Fig. 3. Reciprocal reduced viscosity vs. $\sqrt{c}$ curves (Fuoss plot).
(1): for PSA-100
(2): for PSA-R

*,**) Samples from Koppers' polystyrene (viscosity-average molecular weight 3×10^5). Sulfonation for two weeks at room temperature. Degree of sulfonation 36.8 %. Viscosity measurement at 25°C.

7) R. M. Fuoss and G. I. Cather, *J. Polymer Sci.*, **4**, 97 (1949).
8) R. M. Fuoss, ibid., **3**, 603 (1948).

sulfone bridge during the course of sulfonation reaction occurred.

Water-Dioxane Mixed Solvent. — Viscosity data of PSA-R for water-dioxane mixed solvent of various mixing ratio are shown in Fig. 4.

η_{sp}/c vs. c relation in all the solvents studied is well described by Fuoss' Eq. 1 (cf. Fig. 5). The values A and B obtained are summarized in Table II together with the dielectric constant ε of the solvents. Values of ε of the mixed solvents are those borrowed from the published data on the ε-mixing ratio relationship by G. Åkerlöf and O. A. Short[9].

From Fig. 4 it is seen that the reduced viscosity decreases with the decrease of dielectric constant of solvent. This may be explained as follows. The dissociation $-SO_3H \rightarrow -SO_3^- + H^+$ is diminished as ε decreases, and consequently the negative net charge on a polyanion decreases, so that the polymer coil becomes more contracted in a low ε solvent than in a solvent of high ε. As the dioxane content in water increases, the Coulombic repulsive force between charged groups becomes stronger due to the decrease of dielectric constant of the medium. This effect to expand a polymer coil, however, may be less dominant than the effect of diminished dissociation of the sulfonic acid group.

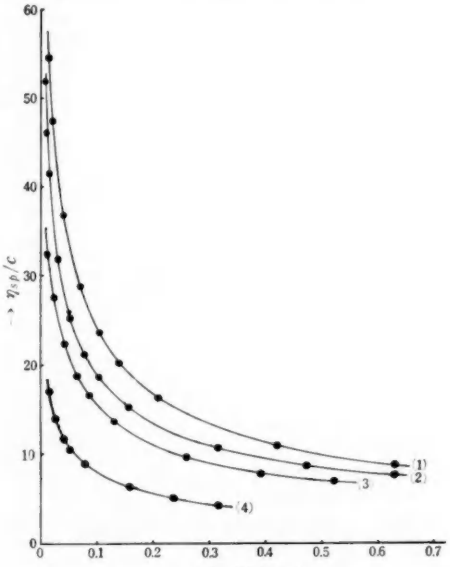

Fig. 4. Effect of dielectric constant of solvent on reduced viscosity.

PSA-R
(for ε=76.7 see Fig. 2)
(1) ε=58.9
(2) ε=40.9
(3) ε=32.4
(4) ε=16.9

TABLE II

ε	B	A	$1/\varepsilon^2\times10^3$
16.9	147	400	3.50
32.4	74.6	400	0.952
40.9	68.6	400	0.598
58.9	59.6	400	0.288
76.7	41.3	400	0.170

9) G. Åkerlöf and O. A. Short, *J. Am. Chem. Soc.*, 58, 1241 (1936).

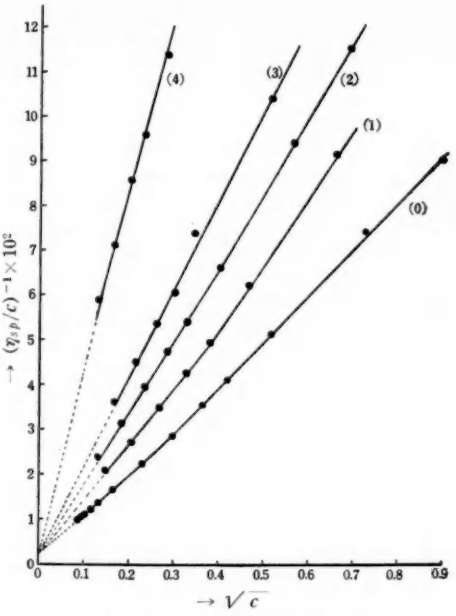

Fig. 5. Fuoss plot for the curves of Fig. 4.

PSA-R
(0) ε=76.7
(1) ε=58.9
(2) ε=40.9
(3) ε=32.4
(4) ε=16.9

Furthermore B vs. $1/\varepsilon^2$ plot is approximated by linear relation (cf. Fig. 6).

The parameter A has the same value 400 in any solvent. This may indicate that PSA molecule has the same size at infinite dilution in any solvent studied here.

In Sodium Chloride Aqueous Solution.—Plot of η_{sp}/c vs. c is shown in Figs. 7 and 8 for

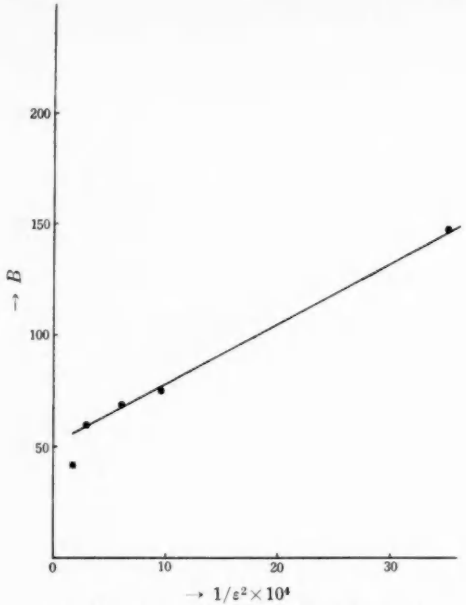

Fig. 6. Constant B of Fuoss' formula plotted against $1/\varepsilon^2$.

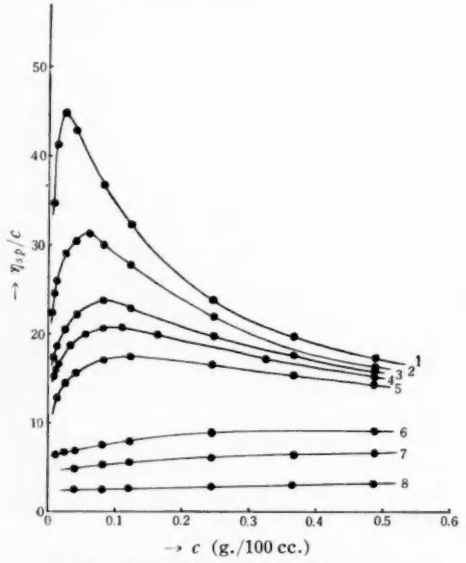

Fig. 7. Effect of salt on reduced viscosity. (PSA-100)

1) 0.000126 N NaCl aq. soln.
2) 0.000314 〃
3) 0.000628 〃
4) 0.000840 〃
5) 0.00126 〃
6) 0.00628 〃
7) 0.0126 〃
8) 0.0628 〃

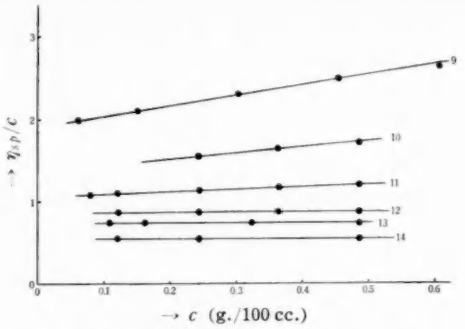

Fig. 8. Effect of salt on reduced viscosity. (PSA-100)

9) 0.0942 N NaCl aq. soln.
10) 0.2573 〃
11) 0.500 〃
12) 1.00 〃
13) 1.33 〃
14) 2.00 〃

solutions of PSA-100 in various concentration of aqueous sodium chloride in the range of 0.000126 to 2.00 N. Reduced viscosity is strongly affected by the presence of sodium chloride and diminished as the sodium chloride content in solution increases. When the sodium chloride concentration is small, the curves exhibit a maximum, which vanishes, however, with the increasing content of sodium chloride and the curves approach those for ordinary non-polar polymers. These behaviors of PSA are characteristic of many other polyelectrolytes. The qualitative explanation was given above. (See, for example, references 10 and 11).

Sodium chloride normality x and PSA normality c_m at the maximum of reduced viscosity are shown in Table III. PSA normality is greater by 10^1 than sodium chloride normality.

Values of intrinsic viscosity and sodium chloride concentration x (mol./l.) in solution are summarized in Table IV.

TABLE III

c at $(\eta_{sp}/c)_{max}$ (g./100 cc.)	$(\eta_{sp}/c)_{max}$	$x\times10^3$	$c_m\times10^3$
0.022	45.0	0.126	1.13
0.061	31.3	0.314	3.14
0.081	23.8	0.628	4.16
0.090	20.7	0.840	4.63
0.10	17.3	1.26	5.14

10) R. M. Fuoss and U. P. Strauss, *J. Polymer Sci.*, **3**, 602 (1948).
11) D. T. F. Pals and J. J. Hermans, *Rec. trav. chim.* **71**, 433 (1952),

TABLE IV

x	$[\eta]$	x	$[\eta]$	x	$[\eta]$
0.000126	25.0	0.00628	6.10	0.500	1.05
0.000314	18.0	0.0126	4.80	1.00	0.86
0.000628	15.7	0.0628	2.30	1.33	0.75
0.000840	13.3	0.0942	1.90	2.00	0.55
0.00126	8.82	0.2573	1.36		

$[\eta]$ values for low sodium chloride concentration are unreliable due to difficulty in extrapolating to zero concentration.

The relation between $[\eta]$ and x can be approximately described by the formula

$$[\eta]^{1/3} = a + \frac{b}{\sqrt{x}}$$

presented by Fuoss and Strauss[10] in the range of comparatively high sodium chloride concentration (Fig. 9).

In the Hermans-Overbeek theory[12] the polyion is considered as a sphere in which the separate charges are replaced by a continuous charge distribution, and the small ions are assumed to be governed by the Poisson-Boltzmann equation. Applying the result of the theory to the case in which the polymer coil is free-draining and the added salt concentration is not so low, it is concluded that $[\eta]$ vs. $1/\sqrt{x}$ relation is linear[11]. For the PSA sample a linear relation between $[\eta]$ and $1/\sqrt{x}$ is obtained in the range of concentration above ca. 0.006 N (Fig. 10).

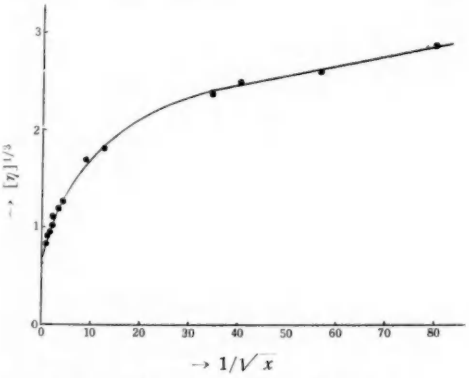

Fig. 9. Effect of salt concentration on the intrinsic viscosity (1).

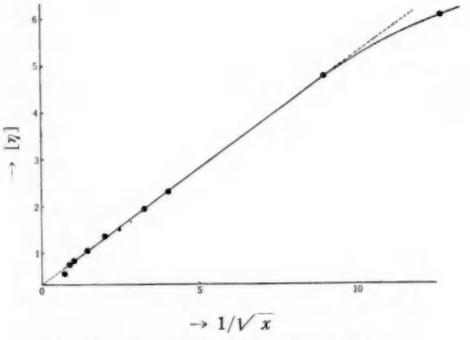

Fig. 10. Effect of salt concentration on the intrinsic viscosity (2).

12) J. J. Hermans and J. Th. G. Overbeek, ibid., **67**, 761 (1948).

In Sodium Bromide and Sodium Sulfate Aqueous Solution.—In sodium bromide and sodium sulfate aqueous solution the viscosity behavior of PSA-100 is nearly the same as in sodium chloride aqueous solution.

The effect of viscosity depression, i.e. the effect for inducing the contraction of polymer coil is strong in the order NaCl > NaBr ≈ Na_2SO_4, although the difference is very slight (Table V). No distinct lyotropic effect is observed here.

TABLE V. INTRINSIC VISCOSITY OF PSA-100 IN VARIOUS SOLVENTS

Solvent		$[\eta]$
Na_2SO_4	1.491 N aq. soln.	0.81
〃	0.745 〃	1.06
〃	0.373 〃	1.31
NaBr	2.93 N aq. soln.	0.39
〃	1.46 〃	0.82
〃	0.73 〃	1.23
NaCl	2.00 N aq. soln.	0.55
〃	1.33 〃	0.75
〃	1.00 〃	0.86
〃	0.50 〃	1.05

Part II. Viscosity Equation for PSA

As was stated in the previous part, PSA behaves like ordinary non-polar polymers in its viscosity character when the concentration of the added salt in the solution is high; here η_{sp}/c vs. c relation becomes linear. Hence in this circumstance it is possible to obtain Sakurada-Houwink's viscosity equation for PSA.

In this part it is aimed to prepare various PSA samples of the same charge density and different degrees of polymerization and to obtain the viscosity equation which holds between their degree of polymerization and their intrinsic viscosity in 0.52 N hydrochloric acid and 0.5 N sodium chloride aqueous solution.

For the preparation of PSA samples,

TABLE VI

PSA	$[\eta]$ of PS before sulfonation in benzene soln. at 25°C	P	$[\eta]$ of PSA in 0.5 N NaCl	$[\eta]$ of PSA in 0.52 N HCl
From Fract. 2	1.025	2534	1.41	1.64
〃 〃 4	0.672	1421	0.84	0.89
〃 〃 5	0.544	1063	0.61	0.67

polystyrene (average molecular weight = 180,000; American Bakelite Company) was fractionated into several fractions and these were sulfonated under the same condition as was described above.

As the authors have some evidence from the previous experiments (Part I) that neither chain scission nor sulfone bridge formation occurs during the course of sulfonation, the degree of polymerization of the fractionated polystyrenes before and after sulfonation was assumed to be unchanged. The degree of polymerization of the fractionated polystyrenes was determined from the viscosity measurement in benzene solution at 25°C.

Experimental Results

Fractionation of Polystyrene.—30 g. of polystyrene pellets was dissolved into 1.2 l. of methyl ethyl ketone in a 2 l. flask and the solution was filtered with a No. 4 glass filter. At room temperature, methanol was slowly added to the solution with stirring until the solution became turbid and then an additional 6 cc. of methanol was added. The flask was set in a thermostat and the bath temperature was raised up until the solution became clear. Then the bath was gradually cooled to the room temperature with stirring. At the room temperature the mixture was allowed to come to equilibrium, and the precipitate was separated by decantation and then an additional 11 cc. of methanol was added to the solution. This process was repeated six times. The amount of methanol used in each precipitation process was 6, 11, 16, 26, 40 and 150 cc., respectively. Each fraction was redissolved into toluene and reprecipitated by a great excess of methanol and finally dried up to a constant weight in vacuo at 50°C.

Sulfonation.—Silver sulfate and concentrated sulfuric acid were added to each fraction in the proportion polystyrene : Ag_2SO_4 : conc. H_2SO_4 = 10 : 0.2 : 110 by weight. Each mixture was put into a conical flask, which was compactly sealed to prevent the entrance of moisture. The flask was set in a thermostat at 50°C. The following procedure was the same as described in Part I.

It was expected that PSA's, of the same degree of sulfonation would be obtained, but this was unsuccessful. This may be ascribed to the fact that the texture or structure of the precipitated mass is different for each fraction. (There was no regularity between their reactivity and their molecular weight.) Only the PSA's prepared from Fractions No. 2, 4 and 5 had about the same degree of sulfonation, 85%, so that these PSA's were used for viscosity measurement. The viscosity data obtained are shown in Table VI and Fig. 11.

Viscosity Equation.—Molecular weight M of the fractionated polystyrene (before sulfonation) was determined by the viscosity formula by C. Bawn et al.[13]

$$[\eta] = 1.13\times10^{-4}\cdot M^{0.73}$$

(in benzene at 25°C, c in g./100 ml.)

which seems to be most reliable.

The relation between $\log[\eta]$ and $\log P$ of PSA is well approximated by a straight line and we obtained the following viscosity equations (cf. Fig. 11).

$$[\eta] = 6.35\times10^{-4}\cdot P \quad \text{(in 0.52 N HCl aq.)} \qquad (2)$$

$$[\eta] = 5.75\times10^{-4}\cdot P \quad \text{(in 0.50 N NaCl aq.)} \qquad (3)$$

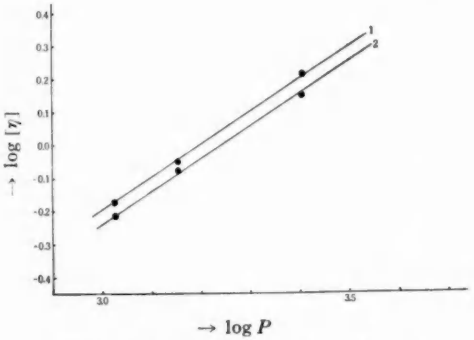

Fig. 11. Intrinsic viscosity vs. polymerization degree relation in salt solution.
1) in 0.52 N HCl
2) in 0.50 N NaCl

13) C. Bawn, R. Freeman and A. Kamaladin, *Trans. Faraday Soc.*, **46**, 1107 (1950).

Here P is the degree of polymerization of PSA. Eq. 2 is for 0.52 N HCl aqueous solution, and Eq. 3 for 0.50 N NaCl aqueous solution.

It is noticeable that $[\eta]$ is directly proportional to the first power of the degree of polymerization.

Calculating the degree of polymerization by Eq. 2 from the viscosity data obtained by Mock and Marshall[14] for vinyltoluene-styrene copolymer sulfonic acid ($P=2036$ by osmotic measurement in methyl ethyl ketone; $[\eta]=1.58$ in 0.54 N HCl at 25°C), $P=2490$ is obtained.

If the authors calculate the degree of polymerization of PSA-R used in the present study ($P=1730$ by viscosity measurement in benzene solution at 25°C before sulfonation; $[\eta]=1.07$ at 25°C in 0.5 N NaCl aq. soln.; degree of sulfonation=85%) by Eq. 3, $P=1860$ is obtained.

Hence Eq. 2 or 3 may be used for calculating roughly the degree of polymerization of highly sulfonated polystyrene-sulfonic acid from its intrinsic viscosity in 0.5 N HCl or 0.5 N NaCl aqueous solution.

The cost of this research has been partly defrayed from the Scientific Research Encouragement Grant from the Ministry of Education, to which the authors' thanks are due.

Department of Chemistry
Faculty of Science
The University of Tokyo
Hongo, Tokyo

14) R. A. Mock and C. A. Marshall, *J. Polymer Sci.*, **13**, 263 (1954).

Rapid Colorimetric Determination of Mercury by Tin(II)-Strong Phosphoric Acid Reduction Method

By Toshiyasu KIBA, Ikuko AKAZA and Osamu KINOSHITA

(Received August 28, 1959)

Tin(II)-strong phosphoric acid, a new powerful decomposing and reducing agent first described by the present authors[1], has been widely employed in this country for the determination of sulfur in various materials; e. g. sulfates[2], sulfide ores[3], iron and steel[4], organic compounds[5], rayon staple fiber, acetylcellulose[6] and proteins[7]. The reagent has also been applied for rapid determination of selenium in various forms. The selenium is reduced by the reagent into gaseous hydrogen selenide, which is absorbed in an alkaline solution, and then the amount is determined colorimetrically[8].

A further attempt was made by the present authors to reduce mercury in various compounds to the metallic state by treating the samples with tin(II)-strong phosphoric acid. The mercury was driven out from the reaction medium by heating and its vapor was carried in a current of carbon dioxide into an absorbing solution containing sulfuric acid and potassium permanganate. The mercury retained in the solution as mercury(II) ions was determined colorimetrically by the usual dithizone method. This new method is very rapid and simple, and moreover, the error caused by the volatillization of mercury during the digestion of the samples by ordinary methods is totally eliminated for the analysis is carried out in a closed system in carbon dioxide.

Experimental

Apparatus.—The apparatus used in this study is shown in Fig. 1. It is composed of two parts, a reaction vessel (A) and an absorbing part (B). The reaction vessel (A) is a round-bottomed flask of hard glass having a glass cap fitted to its top

1) T. Kiba et al., This Bulletin, **28**, 641 (1955).
2) T. Kiba, and I. Akaza ibid., **30** 53 (1957).
3) T. Kiba, I. Akaza and N. Sugishita, ibid., **30**, 972 (1957).
4) K. Kitagawa and Shibata, *Japan Analyst* (*Bunseki Kagaku*), **7**, 181 (1958).
5) T. Kiba and I. Kishi (present surname, Akaza), This Bulletin, **30**, 482 (1957); S. Ohashi, ibid., **28**, 645 (1955).
6) H. Terada and M. Yoshida, *J. Chem. Soc. Japan, Ind. Chem. Sec.* (*Kogyo Kagaku Zasshi*), **61**, 1301 (1958).
7) S. Akabori and T. Fujiwara, *Bull. Chem. Biolog.*, **40**, 1983 (1958).
8) T. Kiba, I. Akaza and H. Hachino, This Bulletin **32**, 641 (1959).

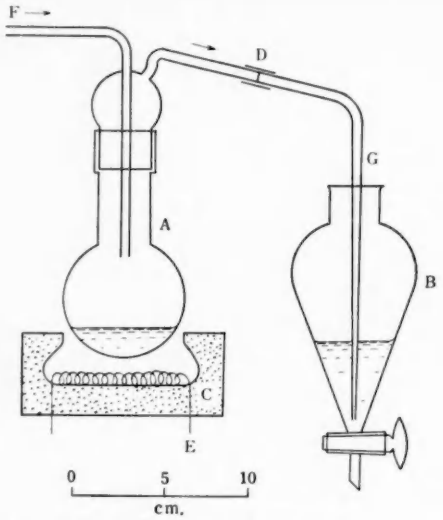

Fig. 1. Apparatus for reduction of mercury compounds and absorption of mercury vapor evolved.
A: Reaction vessel, a round bottomed flask.
B: A separatory funnel.
C: Electric heater.
D: Short piece of rubber tubing.
E: A.C. electric current regulated by a variable transformer.
F: Carbon dioxide gas introduced into A.
G: Gas-delivery tube.

and provided with an inlet and an outlet tube for the gas. The absorbing part (B) is a separatory funnel of about 100 ml. capacity. A gas delivery tube (C) is connected with a piece of rubber tubing (D) to the outlet arm of the reaction vessel (A) and inserted into the absorbing solution in the separatory funnel. A Kipp's apparatus is employed for the production of carbon dioxide, which is purified by three gas-washing bottles (not shown in Fig. 1) and introduced into the reaction vessel through the inlet arm. The solutions used for the purification of carbon dioxide are described later.

Photoelectric colorimeter.—A "Hirama photoelectric colorimeter" with 1 cm. cells was used with a filter of 517 mμ.

Reagents.—*Strong phosphoric acid.*—Four hundred grams of commercial ortho phosphoric acid of extra pure grade (d=1.7) is placed in a 300 ml. conical beaker, and dehydrated by heating on a 500 W. hot plate until a thermometer dipped in the liquid indicates 300°C. If the heating takes too long the liquid will become turbid and viscous and useless for the purposed in view. During the heating, the water vapor and the mist of phosphoric acid coming off should be rapidly removed from the neighborhood of the liquid surface, through a glass tube, one end of which is held near the surface of the liquid, the other end being connected to a suction pump. This saves much time in the dehydration.

Tin(II)-strong phosphoric acid.—Fifty grams of tin(II) chloride dihydrate of extra pure grade is placed in a 300 ml. conical beaker and on it is poured 250 g. of the strong phosphoric acid prepared as described above. The content is heated to 300°C within 30 min. in the manner of the preparation of the strong phosphoric acid. After cooling the tin(II)-strong phosphoric acid thus obtained, a very viscous and possibly slightly turbid liquid is produced, which may be stored in a closed vessel.

Carbon dioxide.—Carbon dioxide produced in the Kipp's apparatus is purified by passing through three gas-washing bottles containing, respectively, water, 2% vanadium(II) sulfate solution in 6 N sulfuric acid, 1% potassium permanganate solution in 10% sodium carbonate. This is introduced into the reaction vessel through a glass tube.

Standard mercuric chloride solution.—A 1.3539 g. portion of mercuric chloride of pure chemical grade dried in a vacuum desiccator is weighed accurately and dissolved in one liter of distilled water. This solution is used as a stock solution. One milliliter of the solution is diluted to 100 ml. with water before use. One milliliter of this diluted solution contains 10 μg. of mercury. According to Sandell[9] the mercuric ion is usually absorbed on the glass wall of the vessel, especially when the solution is extremely diluted. However, the effect is not noticeable when the diluted solution is employed soon after the preparation.

Dithizone chloroform solution.—A 0.001% (w/v) and a 0.005% (w/v) solution are prepared according to Sandell[9], and the former is used for 0 to 20 μg. of mercury and the latter for 0 to 50 μg. of the metal.

Hydroxylamine hydrochloride solution.—Twenty grams of hydroxylamine hydrochloride is dissolved in 65 ml. of water, and neutralized with aqueous ammonia using thymol blue as indicator. The solution is transferred into a separatory funnel and 10 ml. of 4% sodium diethyldithiocarbamate solution is added to it and mixed well. After a few minutes, 10 ml. of chloroform is poured into the vessel and the content is shaken vigorously to transfer the metal chelates into the organic layer. After the two layers are disengaged, the chloroform layer is rejected. To the aqueous layer, hydrochloric acid is added drop by drop till the red color of the indicator appears. This solution may be employed for the experiment.

Potassium permanganate solution.—A suitable amount of solid potassium permanganate of extra pure grade is dissolved in water and filtered through a glass-sintered crucible to make 0.1, 0.5 and 1 N solution.

Sulfuric acid.—Concentrated sulfuric acid of pure grade is diluted with water to a concentration of 10%.

Acetic acid solution.—6 N.

9) E. B. Sandell, "Colorimetric Determination of Traces of Metals", 2nd Ed., Interscience Publishers, Inc., New York (1950), pp. 441-452.

Ferric chloride solution.—Ferric chloride hexahydrate is dissolved in water to make a solution containing 10 mg. of iron(III) ion per ml.

Cadmium chloride solution.—Crystalline cadmium chloride is dissolved in water to make a solution containing 3.5 mg. of cadmium ion per ml.

Mercuric oxide.—Mercuric oxide of extra pure grade is used as a powder, and the mercury content was estimated by the ordinary potassium thiocyanate titration method as 97.30% pure.

Alumina.—As a diluent of solid samples, powdered alumina of utmost purity for chromatography is used.

Various samples containing mercury.—Commercial products, especially water-soluble insecticides and fungicides, are used as the samples of analysis, their mercury content having been determined by other methods.

Procedure.—Take an accurately measured sample containing mercury of 0 to 50 μg.—pipet a solution; weigh a solid—and put it into the reaction vessel (A in Fig. 1). The volume of the vessel should be varied according to the amount of the sample to be analyzed. Pour 5 to 10 ml. of the tin(II)-strong phosphoric acid over the sample. Put into the separatory funnel (B in Fig. 1) 5 ml. of 0.1 N potassium permanganate solution and 5 ml. of 10% sulfuric acid and mix well. Connect all the apparatus as shown in Fig. 1. Pass carbon dioxide very rapidly through the apparatus for two or three minutes to expel the air from the apparatus. The end of the gas-delivery tube (G) should reach the bottom of the separatory funnel. Reduce the flow of gas to a rate of one bubble per second, and heat the bottom of the reaction vessel by passing an electric current through the nichrome wire (E) placed in the diatomaceous block (C). Regulate the voltage of the current by a variable transformer. It is unnecessary to keep the temperature constant but it should be high enough to ensure that the content of the reaction vessel exhibits a white turbidity near the end of the reaction. After about fifteen minutes stop the heating, but continue the passing of the gas about five minutes longer.

Remove the separatory funnel, and pour into it about 15 ml. of 1 N sulfuric acid. To the colored solution add 1 ml. of 20% hydroxylamine hydrochloride solution to reduce the permanganate and, moreover, 2 ml. of 6 N acetic acid to stabilize the dithizonate which will be formed hereafter. Add 5 ml. of chloroform to the aqueous solution in the funnel and shake it vigorously for a while to saturate the aqueous phase with chloroform. After the layers are disengaged by standing the vessel for several minutes, reject the lower chloroform layer from the stem of the funnel. Then, add exactly 10 ml. of 0.05% dithizone-chloroform reagent using a pipet. Shake the vessel vigorously with an electric shaking machine for about two minutes. Allow the vessel to stand for several minutes and then drain the organic layer into an Erlenmyer flask containing unhydrous sodium sulfate as a dehydrant. Set it aside for a while till the water contained in the organic phase is absorbed and the layer becomes clear. Transfer the colored organic phase in a 1 cm. cell and read the absorbancy of the layer in a photoelectric colorimeter with a filter of 517 mμ. A blank test should be conducted with the dithizone-chloroform solution undergoing the same procedure without mercury.

Results and Discussion

Recovery of Mercury by This Method.—Employing an aliquot of the standard mercuric chloride solution, the determination of mercury in the amount between 5 and 50 μg. was made by carrying out all the procedure described above. Another aliquot of the standard solution was directly treated with dithizone-chloroform reagent and the absorbancy of the organic layer was read as described in the latter part of the procedure, which is similar to the ordinary method for the determination of mercury in solutions. The absorbancies measured on the same amount of mercury by the two methods are tabulated together in Table I, which shows good coincidence

TABLE I. COMPARISON OF THE ABSORBANCIES OF MERCURIC DITHIZONATE FOR THE SAME AMOUNT OF MERCURY

Amount of Hg μg./100 ml. $CHCl_3$	Absorbancy measured	
	Ordinary direct colorimetry	Via this reduction & evolution method
5	0.0928	0.0930
10	0.1722	0.1716
15	0.2580	0.2464
20	0.3172	0.3301
25	0.4205	0.4200
30	0.4878	0.4813
35	0.5695	0.5690
40	0.6475	0.6420
45	0.7190	0.7210
50	0.7975	0.7960

within the error unavoidable in colorimetry. The calibration curves obtained by the two methods can be represented by the following equations. In case ordinary colorimetry of the dithizone-chloroform phase was used:

$$y = 0.0168 + 0.01569\,x$$

and if colorimetry following this reduction and evolution method was used:

$$y = 0.0156 + 0.01569\,x$$

where y is the absorbancy measured and x the amount of mercury taken in micrograms. The numerical values in the equations were calculated by the method of the least squares from the experimental

data of more than two determinations of the same amount of the metal. In conclusion, it may be pointed out that only a negligible amount of mercury is lost in this reduction and evolution method, and a calibration curve prepared by the ordinary method with a standard solution of mercuric salt can be employed in this method as well.

Determination of Minute Amounts of Mercuric Oxide.—A definite amount of mercuric oxide was mixed with a large amount of alumina and the mixture was analyzed by the tin(II)-strong phosphoric acid method. Minute amounts of mercury could be determined by this method as shown in Table II.

TABLE II. DETERMINATION OF MERCURY IN MIXTURE OF MERCURIC OXIDE AND ALUMINA

Sample taken mg.	Hg content μg.	Hg found μg.
15.90	30.7	30.2
13.32	25.7	25.5
14.59	28.2	28.3
14.65	28.3	28.4
14.73	28.4	28.7

Determination of Minute Amounts of Mercury in Solution.—Because of their volatility, mercury compounds can not be dried or their solutions evaporated without affecting the analytical result. So the co-precipitation method was employed to concentrate the mercuric ion using ferric hydroxide or cadmium sulfide as gathering agent. A suitable volume of a solution containing 20 μg. of mercury as chloride, and a suitable volume of ferric chloride solution containing 10 mg. of iron(III) ion per ml. were placed together in the reaction vessel. Sodium hydroxide solution was added dropwise to complete the ferric hydroxide precipitate, and the mixture was set aside from two hours to overnight till the precipitate settled. The supernatant solution was sucked out by means of a suction pump through a filter stick, a short glass tube containing an asbestos plug near one end, the precipitate being allowed to remain in the reaction vessel. The precipitate caught on the asbestos plug was transferred from the filter stick into the reaction vessel by pushing out the plug with a slender glass rod inserted through the other end of the glass tube. The analysis of mercury caught in the ferric hydroxide precipitate was carried out according to the procedure in which the asbestos plug was completely decomposed by heating with tin(II)-strong phosphoric acid as shown by the clear solution obtained.

Cadmium sulfide can also be employed as the co-precipitant. In this case a suitable volume of a solution containing a minute amount of mercury and of cadmium chloride containing 3.5 mg. of cadmium per ml. were put together in the reaction vessel. The pH of the solution was adjusted to about 1 by adding hydrochloric acid, and then hydrogen sulfide was introduced into the solution to precipitate cadmium sulfide. After the solution was left for several hours to let the precipitate settle, it was filtered by means of the filter stick as described above, and the asbestos plug was transferred to the reaction vessel containing the precipitate. The analysis was then carried out according to the procedure.

Both the ferric hydroxide and the cadmium sulfide co-precipitation method give good recovery of mercury in the solution as shown in Table III. In these cases some problems remain about the reaction of tin(II)-strong phosphoric acid with ferric ions and the metallic sulfides. The ferric ion is reduced to the ferrous by the reagent intended for the reduction of the mercuric ion, and excessive consumption of the reagent occurs if a larger amount of iron(III) ion is present. But when only about ten milligrams of iron(III) is used for the co-precipitation, the amount of the tin(II) ion in the reagent used is far in excess of the need of the iron(III) ion, and the reduction of mercury is not hindered.

TABLE III. RECOVERY OF 20 μg. OF MERCURY BY COPECIPITATION METHOD

Ferric oxide was used as a collector:

Amount of Fe^{3+} mg.	Hg found μg.	Recovery %
10	19.9	99.5
20	19.2	96.0
30	19.7	98.5
30	19.7	98.5

Cadmium sulfide was used as a collector:

Amount of Cd^{2+} mg.	Hg found μg.	Recovery %
3.5	19.3	96.5
〃	19.5	97.5
〃	19.3	96.5
5	19.2	96.0
〃	18.6	93.0

When cadmium sulfide is treated with the tin(II)-strong phosphoric acid, gaseous

hydrogen sulfide is evolved at the same time, and the gas is carried with the carbon dioxide into the absorbing solution of potassium permanganate and sulfuric acid. The gas consumes the permanganate and the absorbing power of the solution for mercury vapor is markedly lowered. In this case a large amount of permanganate should be persent in the absorbing solution to oxidize the sulfide in the sample and keep adequate absorbing power for mercury vapor. This applies also to the analysis of mercury in sulfates. The question is what concentration of potassium permanganate should be kept in the absorbing solution for various amounts of sulfur in the sample. Fig. 2 shows the results of experiments

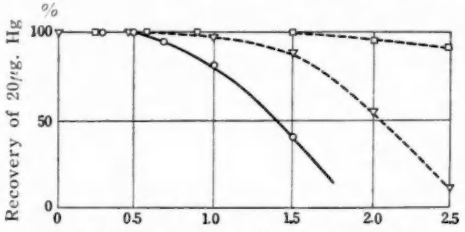

Fig. 2. Dependence of potassium permanganate concentration in the absorbing solution on the recovery of mercury.
Composition of the absorbing solution:
○: 5 ml. 0.1 N $KMnO_4$+5 ml. 10% H_2SO_4
▽: 5 ml. 0.5 N $KMnO_4$+5 ml. 10% H_2SO_4
□: 5 ml. 1 N $KMnO_4$+5 ml. 10% H_2SO_4

to estimate the concentration of permanganate for good recovery of mercury in the presence of various amounts of sulfur as sulfate. When 1 N potassium permanganate solution is used as 1:1 mixture with 10% sulfuric acid, less than 2.0 mg. of sulfur can be allowed to be present in the sample without any hindrance to the determination of 20 γg. of mercury.

Effect of Chloride for the Analysis.—The colorimetry of mercury dithizonate is usually dependent on the concentration of the chloride ion in the aqueous solution. In this evolution method, when a sample contains a large amount of chloride, the chloride is given off as hydrogen chloride and [absorbed in the absorbing solution. Many papers have been published on the dependence of the accuracy of the dithizone method on the chloride ion concentration, and a suitable pH range for the extraction of mercuric dithizonate by chloroform was reported[10]. However, when the amount of chlorides in the sample is not known, it is very difficult to make the absorbing solution in suitable composition for the colorimetric determination of mercury. In such cases the co-precipitation method is to be preferred.

Determination of Mercury in Organic Fungicides and Medicines.—Various methods have already been employed for the determination of mercury in organic compounds, but when the compounds are present mixed with large amounts of other substances or in the form of a solution of extremely low concentration, it is very hard to get an accurate result. Moreover, the decomposition of the compound is usually carried out by strong oxidizing acid with a reflux condenser, through which some of the mercury inevitably escapes during the treatment. If the tin(II)-strong phosphoric acid method is applied for the purpose, the powerful decomposing and reducing power of the reagent acts on the sample instantly, and the mercury vapor is evolved, leaving other interfering metals in the phosphoric acid medium. The procedure of the analysis is the same as in the case of inorganic substances.

Mercurochrome.—Crystals of mercurochrome were weighed and dissolved in water to give a solution containing 10 γg. of mercury per ml. Two or three milliliters of the solution was taken in the reaction vessel, and the analysis was carried out according to the procedure. The purity of the sample was estimated by iodometric titration using a large amount of the sample.

Ethylmercuric Phosphate.—A substance in tablet form having the trade name "Luberon" (Hokko Chemical Co.) which contains ethylmercuric phosphate among other substances, was employed for the analysis. A 0.4597 g. portion of the sample was dissolved in 1 l. of water, and 2 ml. of the solution was put in a run.

***p*-Toluolsulfonaniline Phenyl Mercury, Ethylmercuric Phosphate and Ethylmercuric Urea.**—A mixture of these compounds, some binding material, some surface active agent and coloring matter, is marketed with the trade name "Fumiron" (Hokko Chemical Co.). A 0.4952 g. portion of the sample was dissolved in 1 l. of water and 2 ml. of the solution was taken for analysis.

Methoxyethylmercuric Chloride.—A tablet having the trade name "Usplon" (Japan Special Fungicide Co.) which contains

10) T. Kato, N. Takei and A. Okagami, *Japan Analyst (Bunseki Kagaku)*, **5**, 689 (1956).

TABLE IV. DETERMINATION OF MERCURY IN VARIOUS FUNGICIDES AND MEDICINES

Sample		Taken	Diluted to	An aliquot for analysis,	Mercury	
Trade name	Compound contained	g.	l.	ml.	Found μg.	%
Luberon (Hg content denoted : 2.5%)	Ethylmercuric phosphate	0.4597	1	2	23.9 23.9 24.5 23.5	
					av. 23.95	……2.50
Fumiron (Hg content denoted : 2.5%)	*p*-Toluolsulfonaniline phenyl mercury Ethylmercuric phosphate Ethylmercuric urea	0.4952	1	2	24.0 25.5 25.4	
					av. 24.97	……2.52
Usplon (Hg content : 2.5%)	Methylethylmercuric chloride	0.4683	1	2	22.8 23.0 23.0	
					av. 23.93	……2.55
Mell (Tablet) (Hg content : 4.08%)	Dinaphthylmethane disulfonic acid phenyl mercury	0.3005	1	2	25.5 25.0 25.9	
					av. 25.47	……4.24
Mell (Powder) (Hg content : 0.15%)	〃	0.01993 0.01923 0.01555	— — —	— — —	27.5) 26.4 …… 21.4)	0.137
Thimerosal (Hg content : 48.3～49.7%)	Ethylmercuric sodium thiosalcylate	1.15081	2.5	2	22.8 22.8 22.8	
					av. 22.8	……49.5
Mercurochrome	Dibromohydroxy mercurifluorescein disodium salt	0.37411	10	2	20.9 20.1 20.9 20.6 20.3	
					av. 20.56	……25.88

2.5% of mercury was used as a sample. A 0.4683 g. portion of the sample was dissolved in 1 l. of water and 1 ml. of the solution was taken for analysis.

Dinaphtholmethane Disulfonic Acid Phenylmercuric Salt.—This compound is contained in "Mell" (Takeda Pharmaceutical Co.) which is solid in two forms. One is a tablet containing the compound in high concentration, and the other is a powder of lower concentration. A 0.3005 g. portion of the tablet was weighed and dissolved in 1 l. of water, 2 ml. of which was used for analysis. The powder was weighed and placed directly in the reaction vessel.

Ethylmercury Thiosalicylate.—A sample dried in a vacuum desiccator containing sulfuric acid was weighed (1.1508 g.) and dissolved in water to a concentration of 1 : 25000. Two milliliters of the solution was pipetted into the reaction vessel and the analysis was carried out.

The data obtained by the above analyses are tabulated together in Table IV. This shows good reproducibility, and a run of the analysis for each sample can be carried out within thirty minutes without any difficulty. Various methods have been proposed by other authors[11-14] for each sample, but some of them are not versatile enough for different substances and the others are very tedious. By the tin(II)-strong phosphoric acid method, analysis can be carried out with inorganic and organic compounds in various forms without any pre-treatments or precaution.

Summary

A simple and rapid method for the determination of a minute amount of

11) J. Kanazawa and R. Sato, ibid., **8**, 440 (1959).
12) D. Polley and V. L. Miller, *Anal. Chem.*, **24**, 1622 (1952).
13) V. L. Miller and and D. Polley, ibid., **26**, 1333 (1954); **27**, 1162 (1955).
14) H. Friedeberg, ibid., **27**, 305 (1955).

mercury in organic and inorganic compounds was established. This method uses the powerful decomposing and reducing power of tin(II)-strong phosphoric acid. In this method the sample is heated with the reagent in a round bottomed flask in a current of carbon dioxide. The mercury vapor evolved is carried with the carbon dioxide into an absorbing vessel which is a separatory funnel containing 10 ml. of 0.1 N potassium permanganate solution and 10 ml. of 10% sulfuric acid. The mercury vapor is oxidized again to the mercuric state and the ion is determined colorimetrically by the usual dithizone-chloroform method. After extracting the mercuric dithizonate with chloroform, the absorbancy of the organic layer is measured by a photoelectric colorimeter with a 517 mμ filter. Some organic compounds containing mercury and some inorganic mercuric compounds as mercuric chloride and mercuric oxide were analyzed by this method in extremely low concentrations, and satisfactory results were obtained. This method may be applied to various kinds of samples without special pre-treatments.

A part of the expenses for this study was defrayed by a grant from the Ministry of Education, to which the authors' thanks are due.

Department of Chemistry
Faculty of Science
Kanazawa University
Kanazawa

Effect of Cupric Ion on Oxidation of Benzene Aqueous Solution by Cobalt-60 Gamma-rays

By Hiroshi HOTTA and Akira TERAKAWA

(Received July 3, 1959)

The oxidation of benzene aqueous solution by Cobalt-60 gamma-rays has been studied by some investigators[1-4]. The yields of phenol and biphenyl are affected by the presence of some metallic ions[5-7]. The effect of cupric ions will be interpreted in the present paper.

Experimental

Triply distilled water was saturated with benzene purified by sulfuric acid and then by freezing, by shaking in a separate funnel. Then some solutions were aerated in a gas-wash bottle on covering the solution with benzene. Other inorganic reagents were used without further purification. The concentrations of initial benzene and produced phenol were measured directly by optical density at 253.5 and 270 mμ, respectively.

The solution in a test tube of hard glass (Hario Glass) was irradiated at the Cobalt-60 Irradiation Laboratory of Japan Atomic Energy Research Institute at room temperature (ca. 20°C). The dose, which was measured chemically as mentioned elsewhere[8], was changed not by its irradiation time, but by irradiation for one hour at various positions, namely, at various dose rates. Therefore, the abscissa of Fig. 1 gives the value of the dose in r as well as the value of dose rate in r/hr.

Results

The results of aerated benzene-saturated aqueous solution containing (a) 0.8 N sulfuric acid or (b) nothing are shown in Fig. 1. These curves were linear up to ca. $4\times10^4\,r$ for both solutions. The white precipitate, which smelled like biphenyl, was found in the solution irradiated by more than $7\times10^4\,r$, and was separated by means of a centrifuge for the measurement of optical density. The corresponding G-value of phenol is listed in Table I with the composition of each solution.

1) P. V. Phung and M. Burton, *Radiation Research*, **7**, 199 (1957).
2) K. C. Kurien, P. V. Phung and M. Burton, ibid., in press.
3) G. Stein and J. Weiss, *J. Chem. Soc.*, **1949**, 3241.
4) M. A. Proskyrnin, *Atomnaya Energiya (USSR)*, **5**, 321 (1958).
5) M. A. Proskyrnin and E. V. Barelko, *Nuclear Sci. Abstr.*, **13**, 1020 (1959).
6) J. H. Baxendale and D. Smithies, *J. Chem. Soc.*, **1959**, 779.
7) T. Yumoto, Y. Bono and T. Matsuda, *Mem. Gov. Ind. Research Inst. Nagoya* (in Japanese), **8**, 296 (1959).
8) H. Hotta, A. Terakawa and S. Ōno, to be published.

TABLE I. YIELD OF PHENOL

Name	Solute (in M)				Treatment	G-value	
	Cupric sulfate	Cupric chloride	Sulfuric acid	Benzene		At low dose	At high dose
a	0	0	0.4	Saturated	Aerated	2.63	0.33
b	0	0	0	Saturated	Aerated	2.63	(0.64)*
c	0.01	0	0.4	0.0115	Not-aerated	5.98±1.1	0.68±0.03
d	0	0.01	0.4	0.0132	Not-aerated	3.63±0.9	0.55±0.14
Burton[1]	0	0	0.4	Saturated	—	(2.64±0.04)**	(0.35±0.02)***

* Less reliable; ** Aerated; *** Oxygen-free.

The G-value of solution b) at a high dose was less reliable.

The results of benzene-saturated 0.8 N sulfuric acid solutions containing (c) 0.01 M cupric sulfate or (d) 0.01 M cupric chloride, which were not aerated, are also shown in Fig. 1. These curves were linear up to ca. 6×10^{1} r for both solutions. These solutions smelled somewhat like biphenyl at a higher does than that corresponding to the break point of the curve. However, nothing was found as precipitate even at the highest dose in spite of the presence of a break point. The corresponding G-value is greater than that in the absence of any cupric ion as listed in Table I.

The earlier result by Burton et al. is listed in the same table for reference[1].

According to the examination of the analytical method by Goodman and Steigman[9], the spectroscopic method without solvent extraction as employed in the present work unavoidably gives a higher G-value of phenol (ca. 29% higher). However, the following discussion might not be proved valueless qualitatively by this uncertainty. Kurien, Phung and Burton indicate that their initial G-value of phenol is very correctly 2.64[2], which is nearly equal to the present value.

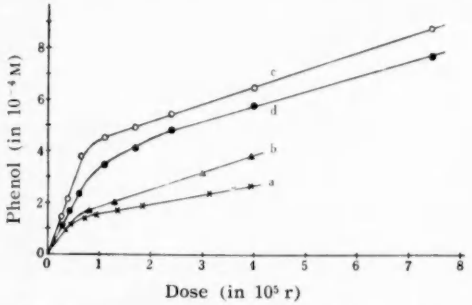

Fig. 1. Oxidation of aqueous benzene solutions. The name of each curve corresponds to the condition in Table. 1.

Discussion

According to Burton et al.[1,2], phenol and hydrogen peroxide are produced by irradiation of aerated aqueous solution saturated with benzene (like the present solutions a) and b). They interpret this fact with the following reactions:

$$H_2O \rightsquigarrow H,\ OH,\ H_2,\ H_2O_2 \qquad (0)$$

$$PhH + OH = Ph + H_2O \qquad (1)$$

$$Ph + O_2 = PhO_2 \qquad (2)$$

$$PhO_2 + H_2O = PhOH + HO_2 \qquad (3)$$

$$H + O_2 = HO_2 \qquad (4)$$

and $$2HO_2 = H_2O_2 + O_2 \qquad (5)$$

Furthermore, the reactions,

$$Ph + OH = PhOH \qquad (6)$$

$$Ph + Ph = Ph_2 \qquad (7)$$

$$PhH + H = PhH_2 \longrightarrow \text{Polymer} \qquad (8)$$

and $$Ph + H = PhH \qquad (9)$$

must be considered in the oxygen-free or -nearly free solution. Reactions 7 and 8 give some insoluble products. According to Baxendale and Magee[10], the reaction

$$Ph + H_2O_2 = PhOH + OH \qquad (10)$$

does not occur. Ph in the above equations denotes phenyl radical (C_6H_5).

The above interpretation is based on the assumption that, since the oxygen molecule scavenges all of the phenyl radical as well as H atoms, reactions 7 and 8 are suppressed by oxygen. The yield of phenyl depends not on the concentration of benzene but on that of oxygen. The concentrations at the break point of the curve are supposed to be about 1×10^{-2} M and 1×10^{-4} M for benzene and oxygen, respectively, from the former

9) J. Goodman and J. Steigman, *J. Phys. Chem.*, **62**, 1020 (1958).

10) J. H. Baxendale and J. Magee, *Discussions Faraday Soc.*, **14**, 160 (1953).

and the present experiments[1,11]. In a concentration of oxygen lower than this, phenol radicals are consumed by reactions 6—9[1,6]. The yield of phenol by the above reactions is at the highest $G_w(OH)=2.92$, which is the G-value of the OH radical induced from water. In fact, the experimental G-value supports this restriction, and indicates the partial re-hydrogenation of the phenyl radical to benzene by reaction 9, since the value is smaller than $G_w(OH)$.

In the presence of a cupric ion, the yield of phenol is larger than $G_w(OH)$, and no insoluble product is yielded even at the highest dose. The large yield of phenol can be interpreted by the following reactions,

$$Cu^{2+}+H=Cu^{+}+H^{+} \quad (11)$$

and then

$$Cu^{+}+H_2O_2=Cu^{2+}+OH^{-}+OH \quad (12)$$

The highest yield of phenol from this interpretation is $G_w(OH)+G(H_2O_2)=2.92+2.84=5.76$, where $G(H_2O_2)$ denotes the G-value of hydrogen peroxide by reaction 5 as well as reaction 0 and is estimated from datum by Phung and Burton[1]. Of course, a part of OH radicals may be consumed by the reaction

$$Cu^{+}+OH=Cu^{2+}+OH^{-} \quad (13)$$

This highest G-value is nearly equal to the present observed value of solution c) in Table I. The rate constant of reaction 11 is quantitatively confirmed to be great in the experiment of aqueous ferrous-cupric solution[8].

The concentration of benzene is not necessarily slight at the break point, and benzene should scavenge almost all of the OH radical by reaction 1 even after the break point as well as in the initial stage. Therefore, since the yield of phenyl radical is independent of oxygen, the fate of phenyl radicals, which are not dimerized to biphenyl by reaction 7 in virtue of the presence of the cupric ion, must be considered beside reaction 9. Moreover, reaction 11 suppresses reaction 9. Although reaction 11 suppresses also reaction 8, it is independent of phenyl radical. When the negative phenyl ion, Ph^{-}, is assumed to be a more stable form than phenyl radical, the promotion of re-hydrogenation to benzene without dimerization due to the cupric ion can be interpreted by the reactions,

$$Ph+Cu^{+}=Ph^{-}+Cu^{2+} \quad (14)$$

and then

$$Ph^{-}+H^{+}=PhH \quad (15)$$

through reaction 11. An analogous reaction is assumed for ferrous ion by Baxendale and Magee[10]. If almost all of the radical induced from water is scavenged by reactions 1 and 11 in the present condition, reactions 14 and 15 enable them to understand why no precipitate is found even at the highest dose in the presence of a cupric ion. The decomposition of phenol is slight according to Kurien, Phung and Burton[2]. There was no difference for the characteristics of absorption curve between 200~300 mμ for the solution through the whole range of dose.

Next, the effect of a chloride ion on the yield of phenol is noticed for solution d). A chloride ion is usually considered to react with OH radical in an acidic aqueous solution[12] as

$$Cl^{-}+H^{+}+OH=Cl+H_2O \quad (16)$$

and then

$$Cl+H_2O_2=Cl^{-}+H^{+}+HO_2 \quad (17)$$

or

$$Cl+H=Cl^{-}+H^{+} \quad (18)$$

Since reaction 16 competes with reaction 1, the yield of phenol is reduced. The reaction between phenyl and chloride radicals is ignored. The detailed study of the effect of chloride ions on the radiolysis of aqueous solution will be given in a later paper[8].

Since the present experiment is not exhaustive, the detailed study will follow.

Summary

The effect of a cupric ion on the radiolysis of benzene aqueous solution can be interpreted by the following reactions of a cuprous ion produced in reaction $Cu^{2+}+H=Cu^{+}+H^{+}$. That is, the larger yield of phenol than $G_w(OH)$ in the presence of oxygen is due to the increment of OH radical by reaction $Cu^{+}+H_2O_2=Cu^{2+}+OH^{-}+OH$, and no precipitation in the absence of oxygen is due to re-hydrogenation by reactions $Ph+Cu^{+}=Ph^{-}+Cu^{2+}$ and $Ph^{-}+H^{+}=PhH$, respectively.

Japan Atomic Energy Research Institute
Tokai, Ibaraki-ken

11) N. A. Lange, "Handbook of Chemistry", Handbook Publishers, Inc., Sandusky, Ohio (1956), p. 1091.

12) T. J. Sworski, *Radiation Research*, **2**, 26 (1955).

The Molecular Cross-sectional Areas for the Determination of Specific Surface Areas of Solids. II. Titania and Silica

By Kumasaburo KODERA and Yoshito ONISHI

(Received August 5, 1959)

As for the determination of the specific surface areas of solids by the B.E.T. method[1], it is generally experienced that the values obtained by different adsorbate gases do not always coincide among themselves. In the preceding paper[2], specific surface areas of carbon blacks were estimated by means of the B.E.T. method using several gases, and by comparing them with those from electron microscopy, the molecular cross-sectional areas of the gases which would give the consistent surface areas with different gases and also with those from electron microscopy were determined. In this paper, similar studies with titania and silica as adsorbents will be mentioned.

Experimental Method and Results

A series of ten commercial titania samples and five silica samples listed in column 2 of Table I were used. Nitrogen, argon, oxygen, carbon dioxide and *n*-butane were chosen as adsorbate gases, and the adsorption isotherms were measured as in the preceding paper. B.E.T. plots obtained from the isotherms are classified in four types from I to IV as shown in the preceding paper, in which, curves I and III are similar in form excepting that the former has a longer linear portion that the latter, curve II is a normal form with a length of linear portion being intermediate between I and III, and curve IV has a special form with shortest linear part. In Table I, types of isotherms are listed together with the appearance of the hysteresis in the measured pressure range, where "?" shows that the existence of hysteresis is not clear because the desorption isotherm was not measured in these cases. Estimated specific surface areas from the isotherms using the molecular cross-sectional areas[3] listed in column 4 of Table V, i.e. the values calculated from the densities of liquid state, are shown in Table II. Values under S_{N_2}/S in the table are ratios between the surface areas estimated by nitrogen and by other gases. Surface areas* calculated from $d_3 = K\sum nd^3/\sum nd^2$ determined by electron microscopy by Suito and Arakawa[4] are also listed in the table**. It should be noted that in the calculation an equation $S = 6/d_3\rho$ was used. This can be applied only for spherical or cubic particles. In this equation, S represents the specific surface area and ρ the specific gravity of the sample. Values of ρ used were 3.9 for anatase, 4.2 for rutile and 2.0 for silica.

In order to study the effect of the degree of crystallization or other surface states of the sample, surface areas of ten titania samples specially prepared under different conditions were measured by nitrogen, argon, oxygen and carbon dioxide, and the results are given in Table III. These samples were prepared by Kennedy's method[5], namely, titanium dioxide precipitated by hydrolysis of titanium tetrachloride was dried for five hr. at 100°C and then heated at different temperatures under the current of various gases***.

Discussion

From Table I, it is seen that the isotherms to which the B.E.T. equation can be applied most satisfactorily are those obtained by argon and oxygen, and then those by nitrogen and carbon dioxide; but for *n*-butane, about half of the isotherms are of special types. As in the case of carbon black in the preceding paper, the isotherms of nitrogen and argon generally show no hysteresis, whereas by other gases, hystereses of isotherms are seen in nearly half of the cases.

As are shown in Table II, the average values of S_{N_2}/S for argon at two temperatures are 1.26 and 1.25 and their standard deviations are small. For oxygen, the deviation is also small despite the rather great value for the carbon black but those for *n*-butane and carbon dioxide are great. In these the ratios in parentheses were excluded from the average. This

1) S. Brunauer, P. H. Emmett and E. Teller, *J. Am. Chem. Soc.*, **60**, 309 (1938).
2) K. Kodera and Y. Onishi, This Bulletin, **32**, 356 (1959).
3) P. H. Emmett and S. Brunauer, *J. Am. Chem. Soc.*, **59**, 1553 (1937).
* Ti-8, 9, 10 were measured by the present authors.

** '*d*' represents the particle diameter measured on an electron micrograph.
4) E. Suito and M. Arakawa, unpublished.
5) D. R. Kennedy, M. Ritchie and J. Mackenzie, *Trans. Faraday Soc.*, **54**, 119 (1958).
*** These samples have been prepared by Prof. I. Uei and Prof. F. Mashio of Kyoto Technical University.

Table I. Types of B.E.T. curves

No.	Samples	$N_2(-196°C)$		$Ar(-196°C)$		$Ar(-183°C)$		$O_2(-183°C)$		$CO_2(-78°C)$		$n\text{-}C_4H_{10}(0°C)$	
		Type	Hyst.	Type	Hyst.	Type	Hyst.	Type	Hyst.	Type	Hyst.	Type	Hyst.
Ti- 1	Ishihara A-100	I	–	II	–	II	–	II	–	III	–	II	+
〃 2	Ishihara R-810	I	–	I	–	II	–	II	–	II	–	II	–
〃 3	Tochigi TP-53	III	–	I	–	I	–	II	–	III	–	I	–
〃 4	Tochigi TP-53C	III	+	II	+	I	+	II	+	III	+	IV	+
〃 5	Furukawa Anatase-F	II	–	II	–	II	–	II	+	III	–	II	–
〃 6	Furukawa Rutile-F	II	–	II	–	II	–	II	+	II	–	II	+
〃 7	Chitan-kogyo Cronos	II	–	II	–	II	–	II	–	III	–	II	–
〃 8	TFM	II	?	II	?	II	?	II	?	III	+	—	—
〃 9	Titanox RA-Nc	II	?	II	?	II	?	II	?	III	?	—	—
〃 10	Unitane O-220	II	?	II	?	II	?	II	?	III	–	—	—
Si- 1	Hisil-101	III	–	II	–	II	–	II	?	III	–	IV	?
〃 2	Aerosil	III	–	II	–	II	–	II	?	III	+	IV	?
〃 3	Carplex 1120	III	+	II	–	II	–	II	?	III	+	IV	?
〃 4	Microsil B-55	III	–	II	–	II	–	II	?	III	+	IV	?
〃 5	Nisil F-1	III	–	II	–	II	–	II	?	II	+	IV	?

Table II. Specific surface areas measured by various gases

No.	$N_2(-196°C)$ S_{N_2} $m^2/g.$	$Ar(-196°C)$		$Ar(-183°C)$		$O_2(-183°C)$		$CO_2(-78°C)$		$n\text{-}C_4H_{10}(0°C)$		Electron microscope $m^2/g.$
		S, $m^2/g.$	S_{N_2}/S	S, $m^2/g.$	S_{N_2}/S	S, $m^2/g.$	S_{N_2}/S	S, $m^2/g.$	S_{N_2}/S	S, $m^2/g.$	S_{N_2}/S	
Ti- 1	9.48	7.60	1.25	7.71	1.23	8.06	1.17	6.95	1.36	7.18	1.32	8.93
2	6.41	5.32	1.21	5.32	1.21	5.45	1.18	4.29	1.49	4.33	1.48	3.40
3	8.14	6.47	1.26	6.57	1.24	7.09	1.15	6.28	1.30	5.91	1.38	8.58
4	7.61	5.90	1.29	5.91	1.29	6.31	1.21	4.90	1.55	5.27	1.45	8.67
5	10.97	8.60	1.28	8.90	1.23	9.22	1.19	6.13	1.79	7.70	1.43	8.82
6	8.57	6.88	1.25	7.21	1.19	7.20	1.19	3.87	(2.21)	5.48	1.56	6.53
7	9.88	7.88	1.25	7.99	1.24	7.97	1.24	5.69	1.74	7.02	1.41	8.82
8	16.90	13.70	1.23	13.55	1.25	13.70	1.23	9.78	1.73	—	—	9.50
9	8.89	7.03	1.26	7.06	1.26	7.00	1.27	6.21	1.43	—	—	6.14
10	8.50	6.68	1.27	6.80	1.25	6.84	1.24	4.71	1.81	—	—	6.14
Si- 1	93.3	73.9	1.26	73.9	1.26	79.4	1.18	68.7	1.36	61.6	1.51	100.0
2	118.7	92.7	1.28	94.0	1.26	97.3	1.22	82.8	1.44	88.2	1.35	77.3
3	86.0	67.8	1.27	69.0	1.25	73.4	1.17	65.3	1.32	55.6	1.55	126.4
4	117.8	91.0	1.29	91.4	1.29	97.4	1.21	87.9	1.34	74.0	1.59	64.9
5	24.7	19.3	1.28	19.9	1.24	20.2	1.22	8.5	(2.91)	15.6	1.58	—
Average			1.26		1.25		1.21		1.51		1.47	
Standard deviation			0.02		0.03		0.03		0.17		0.08	

TABLE III. SURFACE AREAS OF SPECIALLY PREPARED TiO_2

Heat treatments of samples			$N_2(-196°C)$	$Ar(-183°C)$		$O_2(-183°C)$		$CO_2(-78°C)$	
			$m^2/g.$	$m^2/g.$	S_{N_2}/S_{Ar}	$m^2/g.$	S_{N_2}/S_{O_2}	$m^2/g.$	S_{N_2}/S_{CO_2}
Vacuum	200°C	5 hr.	59.3	47.2	1.26	49.5	1.20	49.1	1.21
O_2	385	5	31.4	25.3	1.24	26.6	1.18	34.3	0.92
O_2	585	5	12.80	10.34	1.24	10.55	1.21	14.5	0.88
O_2	790	5	4.30	3.42	1.26	3.52	1.22	3.65	1.18
O_2	1000	3	2.82	2.29	1.23	2.46	1.15	2.15	1.31
N_2	900	3	6.85	5.48	1.25	5.70	1.20	—	—
N_2	1000	3	4.29	3.47	1.24	3.55	1.21	3.81	1.13
N_2-O_2(1:1)	1000	3	4.70	3.88	1.21	3.97	1.18	—	—
N_2-O_2(4:1)	1000	3	4.55	3.66	1.24	3.74	1.22	—	—
N_2-O_2(9:1)	1000	3	3.96	3.08	1.29	3.25	1.22	—	—
			Average		1.25		1.20	—	—

TABLE IVa. COMPARISON OF SURFACE AREAS FROM THE B.E.T. METHOD AND ELECTRON MICROSCOPY

Ratio of area by B.E.T. to area by electron microscopy

No.	N_2	$Ar(-196°C)$	$Ar(-183°C)$	O_2	CO_2	n-C_4H_{10}
Ti-1	1.06	0.85	0.86	0.90	0.78	0.81
2	(1.89)	(1.57)	(1.57)	(1.61)	(1.26)	(1.27)
3	0.95	0.75	0.77	0.83	0.73	0.69
4	0.88	0.68	0.68	0.73	0.57	0.61
5	1.25	0.98	1.01	1.05	0.70	0.87
6	1.31	1.05	1.10	1.10	0.59	0.84
7	1.12	0.89	0.91	0.90	0.65	0.80
8	1.77	1.44	1.43	1.44	1.03	—
9	1.45	1.15	1.15	1.14	1.01	—
10	1.39	1.09	1.11	1.11	0.77	—
Average	1.24	0.99	1.00	1.02	0.76	0.77
Molecular cross-section	13.1	13.9	14.4	13.8	22.4	41.7 Å²

TABLE IVb.

Si- 1	0.93	0.74	0.74	0.79	0.69	0.62
2	1.54	1.20	1.22	1.26	1.07	1.14
3	0.68	0.54	0.55	0.58	0.52	0.44
4	1.82	1.40	1.41	1.50	1.35	1.14
Average	1.24	0.97	0.98	1.03	0.91	0.84

anomaly for carbon dioxide has been observed also for the carbon black. From the comparison with the preceding paper, it is seen that the ratio in Table II is 7~11% greater than those for carbon black; therefore, the discrepancy between surface areas by nitrogen and those by other gases increased further.

With the titanias prepared under various conditions shown in Table III, nitrogen, argon, and oxygen give surface areas parallel to each other, i.e. the area ratios S_{N_2}/S are nearly constant, and equal to the values in Table II. This fact suggests that these gases give reliable areas despite the difference in the surface state of the samples. For carbon dioxide, however, ratios vary considerably, and in a few cases give values smaller than 1. Such deviations of ratios by carbon dioxide have been observed also for samples of carbon black, silica and other solids in our laboratory. It seems, therefore, that the adsorptions of carbon dioxide change considerably by some slight change in the surface state of the solid, thus, it is concluded that this gas is not suitable for use in the B.E.T. method.

For the reason mentioned above and for the same reason as in the preceding paper, argon may be taken as the standard gas. To determine the molecular cross-sectional areas of the standard gas and of the other gases, the specific surface areas estimated by the B.E.T. method, were compared with those from electron microscopy, the

TABLE V. MOLECULAR CROSS-SECTIONAL AREAS

Gas	Temp.	Van der Waals' const.	From liquid density	Livingston's	Present authors'		
					TiO_2, SiO_2	Carbon black[2]	Average
N_2	−196°C	15.4 Å²	16.2 Å²	15.4 Å²	12.9 Å²	14.2 Å²	—
Ar	−196	13.6	13.8	14.6	13.8	13.8	13.8 Å²
Ar	−183	13.6	14.4	15.5	14.3	14.4	14.4
O_2	−183	13.5	14.1	14.6	13.5	13.5	13.5
CO_2	− 78	16.5	17.0	19.5	20.4	20.8	20.6
n-C_4H_{10}	0	33.0	32.1	44.6	37.4	38.6	38.0

TABLE VI. MOLECULAR CROSS-SECTIONS CALCULATED FROM THE COMPARISON WITH THE ABSOLUTE METHOD

Gas	Temp.	Molecular cross-sections		Ratio	Literature
		From the liquid dens.	From the absolute method		
N_2	−196°C	16.2 Å²	16.2 Å² 16.27	1.00 1.00	6, 7, 8 9
Ar	−196	13.8	16.6 16.88	1.20 1.22	8 9
Ar	−183	14.4	18.19	1.26	9
O_2	−196	13.2	17.5	1.33	7
Kr	−196	15.3	19.5 21.78	1.28 1.42	6 9
CO_2	− 78	17.0	24.39	1.43	9

method independent of the former. The results are shown in Tables IVa and IVb, where figures represent ratios of surface areas estimated by the B.E.T. method and by electron microscopy. In the table, values of Ti-2 were excluded from the average, because it contained needle-like parallel piped particles. Since only a few samples of silica have been measured and the values in the table scatter rather badly, they were used only to verify those with the titanias. These scattered values for the silicas may be explained by the fact that they consist of far smaller particles than the titanias, so that the measurement of the particle diameters on an electron micrograph would yield more series errors. The values shown in the lowest part of Table IVa are obtained by dividing the molecular cross-sections from the liquid densities (column 4, Table V) by respective average ratios in the table. These values should give the consistent surface areas with those from electron microscopy. Since the molecular cross-sections of argon at −196°C thus obtained agree fairly well with both van der Waals' constant and that from liquid density, the value 13.8 Å² from the liquid density was employed as the standard as in the preceding paper. Molecular cross-sections for the other gases are calculated from this value and the values of S_{N_2}/S in Table II, and are shown in column 6 of Table V. From Table IVb it is seen that these values might be applied for silica as well. Since these values, except for that for nitrogen, agree very well with those for the carbon black, average values for both adsorbents can be used for both solids and are shown in the last column. It is seen that these values agree very well with those in Table IV. Agreement with those from the liquid densities also are fairly good, and the value for oxygen agrees with van der Waals' constant. The value for nitrogen, 12.9 Å², however, is considerably smaller than that for the carbon black, 14.2 Å², and deviation from the widely used value, 16.2 Å², from the liquid density is even greater. This deviation amounts to 26% and will be discussed below.

Beebe[6], Arnold[7], Corrin[8], and Pickering et al.[9] determined the molecular cross-sections of several gases for use in the surface area measurement by the B.E.T. method. In their studies, anatase used by Harkins and Jura[10] and determined to

6) R. A. Beebe, J. B. Beckwith and J. M. Honig, *J. Am. Chem. Soc.*, **67**, 1554 (1945).
7) J. R. Arnold, ibid., **71**, 104 (1949).
8) M. L. Corrin, ibid., **73**, 4061 (1951).
9) H. L. Pickering and H. C. Eckstrom, ibid., **74**, 4775 (1952).
10) W. D. Harkins and G. Jura, ibid., **66**, 1362 (1944).

TABLE VII. SPECIFIC SURFACE AREAS

No.	N_2 $m^2/g.$	Ar(−196°C) $m^2/g.$	Ar(−183°C) $m^2/g.$	O_2 $m^2/g.$	CO_2 $m^2/g.$	n-C_4H_{10} $m^2/g.$	B.E.T. mean $m^2/g.$	Elec. micro. $m^2/g.$
Ti- 1	7.55	7.60	7.71	7.72	8.42	8.50	7.92	8.93
2	5.10	5.32	5.32	5.22	5.20	5.12	5.21	3.40
3	6.48	6.47	6.57	6.79	7.61	7.00	6.82	8.58
4	6.06	5.90	5.91	6.04	5.94	6.24	6.02	8.67
5	8.74	8.60	8.90	8.83	7.43	9.11	8.60	8.82
6	6.83	6.88	7.21	6.89	(4.69)	6.49	6.86	6.53
7	7.87	7.88	7.99	7.63	6.89	8.31	7.76	8.82
8	13.45	13.70	13.55	13.12	11.85	—	13.13	9.50
9	7.08	7.03	7.06	6.70	7.52	—	7.08	6.14
10	6.77	6.68	6.80	6.55	5.71	—	6.50	6.14
Si- 1	74.3	73.9	73.9	76.0	83.2	73.0	75.7	100.0
2	94.5	92.7	94.0	93.1	100.3	104.3	96.5	77.3
3	68.5	67.8	69.0	70.2	79.1	65.8	70.1	126.1
4	93.8	91.0	91.4	93.2	106.5	87.6	93.9	64.9
5	19.7	19.3	19.9	19.3	(10.3)	18.5	19.3	—

have the specific surface area of 13.8 m^2/g.**** by their absolute method was chosen as a standard solid of the known surface area. They measured adsorption isotherms on this sample by several adsorbates, and calculated V_m by the B.E.T. equation. Dividing 13.8 m^2 by V_m they determined the cross-sectional area of adsorbate gas molecule. Areas thus obtained for various adsorbate gases are shown in Table VI together with the respective ratios to the areas from the liquid densities. These cross-sections have been proved by the above authors to give consistent surface areas for various solids examined, which include carbon black, rouge, rutile, etc. As are shown in column 5, the ratio of nitrogen is naturally 1, but all other values are greater than 1, i.e. from 1.20 to 1.43. From these ratios it is clear that, except for carbon dioxide and one of kryptons, the deviations of 26% for nitrogen mentioned above will nearly compensate deviations indicated by the ratios in the table, if 12.9 $Å^2$ were used for the cross-section of nitrogen. Moreover, ratios of the cross-sections of argon at two temperatures and carbon dioxide to that of nitrogen are 1.04, 1.12, and 1.50, respectively, by Pickering et al.[9], and 1.07, 1.12, and 1.58, respectively, by the present study. This fact also shows the agreement of the relative molecular cross-sections between both cases. Alexander et al.[11] measured surface area of six silica samples by the B.E.T. method, and determined their mean volume surface diameters (d_3) from electron microscopy. The ratios of the specific surface areas by nitrogen adsorption given in Table II in their paper and those calculated from d_3 in the same table give 1.27 on an average. Therefore, if the areas by electron microscopy are correct, the cross-section of nitrogen must be larger by 27% and agrees with the present study again.

From those discussed above the relative values of the molecular cross-sections estimated by the present authors are in fair agreement with those by the others, but from comparison with electron microscopy 16.2 $Å^2$ for nitrogen at −196°C seems to be too great and better agreement might be attained by choosing argon as a standard and giving 13.8 $Å^2$ for its cross-section at −196°C.

The specific surface areas of all the samples calculated by the cross-sections shown in column 8, Table V, are shown in Table VIII. The average value for each sample together with that from electron microscopy are also listed. In general, the surface areas from the different gases and from electron microscopy are in fair agreement with each other, except for a few cases which are shown in parentheses under carbon dioxide and excluded from the average. Especially for samples of titania, the agreement is satisfactory. Anomalous results obtained by carbon dioxide in certain cases may be explained by some difference in the surface state as in the case of the carbon black. Anomalous ratios in Table III for carbon dioxide are also explained similarly as was discussed above.

**** The same sample gave 13.9 $m^2/g.$ by the B. E. T. method using nitrogen as the adsorbate and by assuming 16.2 $Å^2$ for its molecular cross-section.

11) G. B. Alexander and R. K. Iler, *J. Phys. Chem.*, 57, 932 (1953).

Conclusion

For the estimation of the specific surface areas of titania and silica, argon, nitrogen, and oxygen are suitable for adsorbate gases and *n*-butane may also be available, but carbon dioxide must be used carefully as it gives unreliable results in some cases. The molecular cross-sectional areas given in Table V, column 6, are in fair agreement with those obtained for the carbon black except for that of nitrogen. The discrepancy by nitrogen would need further investigation, but for other gases, average values shown in column 8 may be expected to give consistent surface areas for many kinds of solids by different gases.

This research has been carried out by the research fund for science donated by the Ministry of Education.

Department of Chemistry
Faculty of Industrial Arts
Kyoto Technical University
Sakyo-ku, Kyoto

The Molecular Structure of Hexachlorobenzene by Electron Diffraction

By Takahide SAITO

(Received July 20, 1959)

An early electron diffraction investigation of the structure of haxachlorobenzene by the usual visual method was reported by Brockway and Palmer[1], observing the scattering in a range of q* less than 60 and using the trial and error method, led to the conclusion that the molecule has the planar configuration as a whole. In contrast with their opinion, Bastianssen and Hassel[2] re-investigated the molecule by the sector method and reported that the non-planar structure, illustrated in Fig. 1, is supported on the basis of interpretation of the peaks in the radial distribution curve, but they did not apply the trial and error method to their investigations. The above contradictory results are compared in Table 1, containing the distances of the principal atomic pairs**. Although it is generally recognized that the sector method is superior to the visual method, it is not perfectly meaningless to re-investigate the molecule by the visual method and the trial and error process, if it is possible to obtain the photographs with rings extending to higher scattering angle, that is, if it is possible to observe the rings of larger q values than the previous reports.

Experimental

The apparatus of electron diffraction is the same as that in the previous reports[3] and the diffraction can be easily observed over the broad range of q. The electron wavelength, about 0.055 Å, was calibrated with gold foil diffraction.

The sample was prepared by Holleman's method[4], m. p. 227°C. Measurements of the photographs were carried out by the usual visual method.

TABLE I. A COMPARISON OF TWO REPORTS

Investigater	θ	C-Cl	C'-Cl	C''-Cl	Cl-Cl	Cl'-Cl
Brockway, Palmer	0	1.70	2.69	4.00	3.11	5.39
Bastianssen, Hassel	12	1.72	2.68	3.99	3.15	5.39

The unit of interatomic distance is Å.
θ is the angle between the direction of C-Cl and the benzene plane.

1) L. O. Brockway and K. J. Palmer, *J. Am. Chem. Soc.*, **59**, 2181 (1937).
2) O. Bastianssen and O. Hassel, *Acta Chem. Scand.*, **1**, 489 (1947).
* $q=(10/\pi)s$, $s=(4\pi/\lambda)\sin\theta/2$, which λ is the wavelength.
** The term "principal" is used for the atomic pair having the larger values of nZZ/r, in which n is the number of the pair, Z is the atomic number and r is the length of atomic pair.
3) T. Yuzawa and M. Yamaha, This Bulletin, **26**, 414 (1953).
4) M. Holleman, *Rec. trav. chim.*, **39**, 763 (1920).

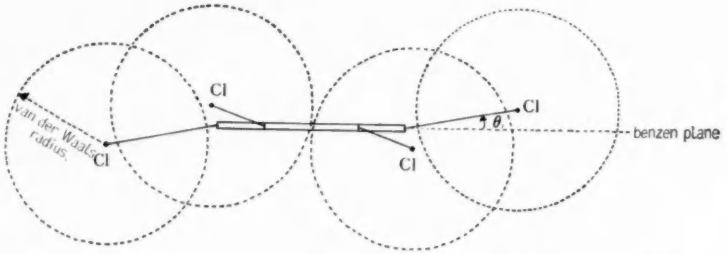

Fig. 1. The schema of deviation of Cl atoms from the benzene plane.

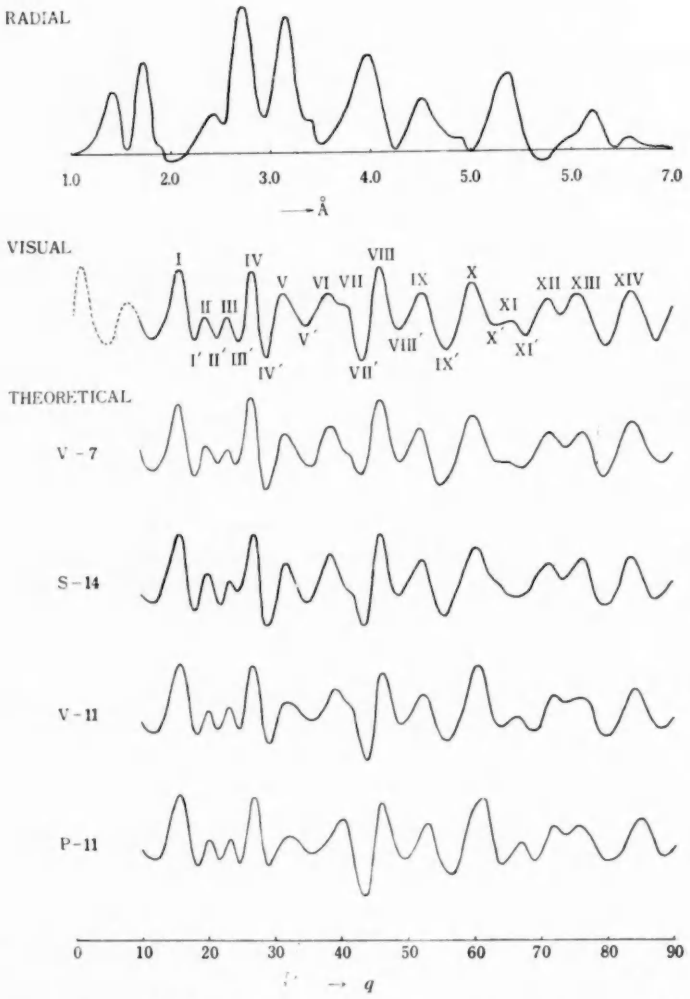

Fig. 2. The radial distribution curve, visual curve and various theoretical curves.

Procedure and Results

The experimental visual curve is shown in Fig. 2: fourteen maxima and ten minima have been observed in the range of q from 15 to 95. From the visual intensity curve, the radial distribution curve has been calculated according to the equation[5]

$$rD(r)=\sum_{q=1}^{q_{max}} I(q)\exp(-aq^2)\sin(\pi qr/10)$$

$$\exp(-aq^2_{max})=0.1$$

$$q=(10/\pi)s \qquad s=(4\pi/\lambda)\sin(\theta/2)$$

in which θ is the scattering angle and a is a constant. The radial curve shows remaining ghosts, but has clearly six principal peaks at 1.40, 1.72, 2.70, 3.99, 3.15 and 5.36 Å. They correspond to the interatomic distances of C–C, C–Cl, C′–Cl, C″–Cl, Cl–Cl and Cl′–Cl, respectively.

Theoretical intensity curve for the molecular models have been calculated by the use of the equation[5]

$$I(q)=\sum_i\sum_j (Z_iZ_j/r_{ij})\exp(-a_{ij}q^2)\sin(\pi qr_{ij}/10)$$

$$a_{ij}=(\pi^2/200)l^2_{ij}$$

where l_{ij} is the mean amplitude of the atomic distance r_{ij}. The coefficients of thermal vibration, a_{ij}, roughly estimated in reference to the calculated aliphatic data[6-8] is introduced into each model, for $q>30$. The values of coefficients are shown in Table II. The theoretical curves were calculated to cover the following ranges of the principal parameters: C′–Cl=2.66~2.72 Å, C″–Cl=3.94~4.02 Å, Cl–Cl=3.06~3.17 Å and Cl′–Cl=5.30~5.42 Å. In Fig. 2 are shown some of the theoretical curves, which agree comparatively well with the visual intensity curve and have the close

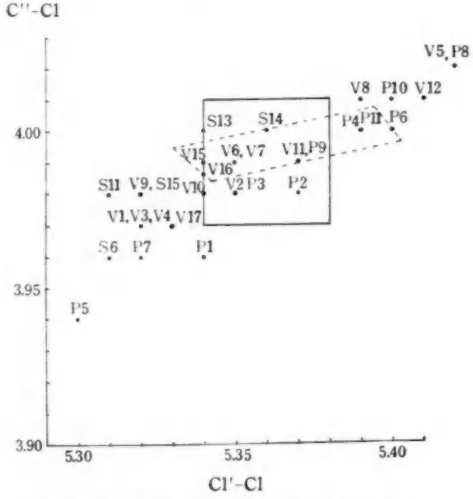

Fig. 3. The parameter chart of C″–Cl vs. Cl′–Cl.

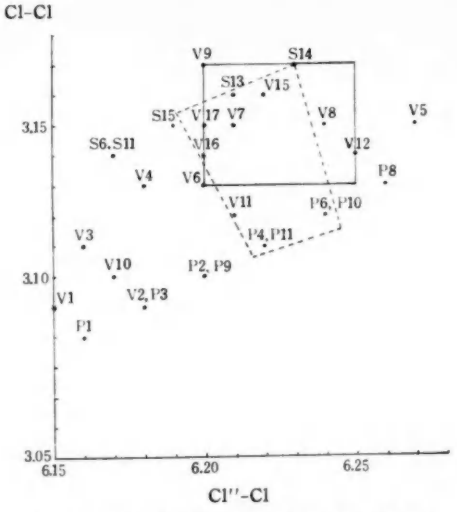

Fig. 4. The perameter chart of Cl–Cl vs. Cl″–Cl

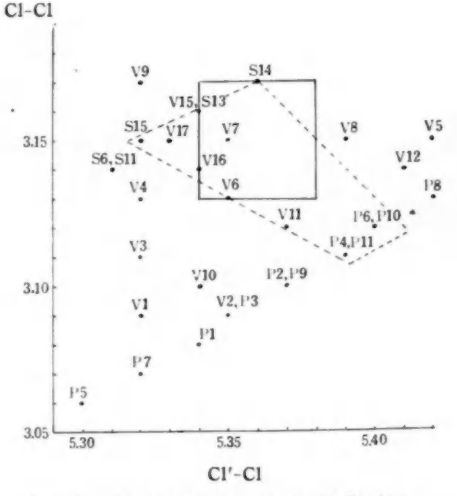

Fig. 5. The parameter chart of Cl–Cl vs. Cl′–Cl.

5) R. Spurr and V. Schomaker, *J. Am. Chem. Soc.*, **64**, 2693 (1942).

6) J. Karle, *J. Chem. Phys.*, **20**, 65 (1952).

7) Y. Morino, K. Kuchitsu and T. Shimanouchi, ibid., **20**, 726 (1952).

8) Y. Morino, K. Kuchitsu, A. Takahashi and K. Maeda, ibid., **21**, 1927 (1953).

TABLE II. THE COEFFICIENTS OF THERMAL VIBRATION TERMS

Atomic pair	a_{ij}	Atomic pair	a_{ij}
C-C	0	C''-Cl	0.00022
C'-C	0.00007	C-Cl	0.00033
C''-C	0.00015	Cl-Cl	0.00011
C-Cl	0	Cl'-Cl	0.00046
C'-Cl	0.00008	Cl''-Cl	0.00062

TABLE III. RESULTS OF QUOTED MODELS AND RADIAL DISTRIBUTION CURVE

Atomic pair	Model number				Radial
	V-7	S-14	P-11	V-11	
C-Cl	1.72	1.72	1.70	1.71	1.72
C-Cl	2.70	2.70	2.69	2.70	2.70
C-Cl	3.99	3.99	4.00	3.99	3.99
Cl-Cl	3.15	3.16	3.11	3.12	3.15
Cl-Cl	5.35	5.34	5.39	5.37	5.36
Av. of q_{calc}/q_{obs}	1.001	0.996	1.005	1.005	
Mean deviation	0.008	0.008	0.016	0.005	

V-7, S-14 and V-11 are the non-planar models. P-11 is the plane model.

values of parameters to those of the interatomic distances from the radial distribution curve.

The values of principal parameters of models are shown in Table III. No distinct differences in the theoretical curves to contribute to any decisive choice can be observed, and the observable, relatively small, difference are as follows: (1) the relative shapes and positions of max. V—VII; (2) the relationships of max. VI and min. XI. The theoretical curves of the non-planar models show the good agreements rather than the curves of the plane models in the shapes of the above respects and in the values of q_{calc}/q_{obs} and of interatomic distances.

Summary

The non-planar structure of hexachlorobenzene is fairly suitable rather than the planar structure and the values of principal interatomic distances are

C-Cl = 1.72±0.01 Å

C'-Cl = 2.69±0.02 Å

Cl-Cl = 3.15±0.02 Å

They are in agreement with Hassel's data.

The author thinks that the re-investigation of the molecular structure of hexachlorobenzene by the precise sector method is necessary.

The author has great pleasure in acknowledging his debts of gratutude to Professor A. Kotera and Professor K. Suzuki for their continued encouragement and advice, and to Dr. M. Igarashi and Dr. H. Sekine for their kind discussions and to Dr. K. Kuchitsu for his kindness in the calculations. A part of the cost of this research has been defrayed from the Scientific Research Encouragement Grant from the Ministry of Education, to which the author's thanks are due.

Department of Chemistry
Faculty of Science
Tokyo University of Education
Koishikawa, Tokyo

Studies on Thixotropy. I. On the Thixotropic Gelation Process*

By Takehiko WATANABE

(Received August 10, 1959)

A number of studies concerning thixotropy, have been carried out by various kinds of methods. Taking as an example the bentonite-water system, which may be regarded as a typical thixotropic system, the studies have been made by the analysis of flow curve[1-9], the measurement of time required for gelation[10-14], and by both the rate constant of thixotropic gelation and the maximum gel strength (maximum yield value) developed as a consequence of completion of gel formation[15-18].

The third method may be said to be the one by which the process of gel formation can be actually followed and expressed in proper terms. The author et al.[16] have also made studies on bentonite (Gumma Bentonite) and some other clays, employing a method of the same kind and found that the thixotropic gel formation of clays generally proceeds in two first order processes which take place successively. Later, as phenomena similar to the above, in the case of the surface film of high polymer, Tachibana et al.[19] found that the thixotropic recovery of the surface elasticity or the surface pressure proceeds also in two steps.

In the present experiments, the author has also made studies on other thixotropic systems than bentonite, e.g. vanadium pentoxide sol, graphite suspension, etc., and found that in any system, in which the form of dispersed particles is plate- or rod-like, the thixotropic gelation generally proceeds in two steps. The conditions, under which the thixotropic gel formation proceeds thus in two steps, are examined and discussed.

Experimental

Materials. — *Bentonite.* — Gumma Bentonite; a product from Gumma Prefecture, which was a finely ground powder, was used. A 10% aqueous suspension of the bentonite was let stand for 5 days and after the removal of the larger sized particles by sedimentation, the suspension (concn. about 5%) was collected and concentrated on a water bath at about 60°C.

Yamagata Bentonite: a 3% aqueous suspension of an original soil from Yamagata Prefecture which was eventually let stand for 5 years after preparation was used. The upper part of the suspension was first filtered by cotton wool and the filtrate (concn. about 1%) was concentrated.

Volclay (Wyoming Bentonite): after sedimentation of a 7% aqueous suspension of the powdery product for 5 days, its upper part (concn. about 3%) was taken and concentrated.

Tixoton: a product of the firm "Deutsche Bentonit" was used as an aqueous suspension.

The order of the capacity of swelling of the above four bentonites is as follows.

Yamagata Bentonite > Volclay > Tixoton > Gumma Bentonite.

The X-ray spectrographic analysis showed that Yamagata Bentonite contained no appreciable impurity, while Volclay contained small amounts of impurity which may be α-quartz and α-crystobalite, and Tixoton a small amounts of α-quartz and Gumma Bentonite a relatively large amount of α-crystobalite compared with the other three.

Kaolin.—Three kinds of products from Tochigi Prefecture (Kampaku mine), Korea and Hongkong, respectively, were used as aqueous suspensions.

Sericite. — The original powdery product from Niigata Prefecture was sieved through 250 mesh and used as an aqueous suspension.

* Presented in part at the Symposium on Colloid Chemistry of the Chemical Society of Japan, Kanazawa, October, 1957.

1) O. Kimura, *J. Chem. Soc. Japan, Pure Chem. Sec. (Nippon Kagaku Zasshi)*, **56**, 1346 (1935).
2) B. Tamamushi ibid., **61**, 280 (1940).
3) H. Akamatu, ibid., **63**, 1275 (1942).
4) T. Alfrey, Jr. and C. W. Rodewald, *J. Colloid Sci.*, **4**, 283 (1949).
5) P. Rehbinder, *Discussions Faraday Soc.*, **18**, 151 (1954).
6) H. van Olphen, "Proceedings of the Fourth National Conference on Clays and Clay Minerals", publication 456, National Academy of Sciences, National Research Council, Washington (1956), p. 204.
7) S. Peter and I. Stolle, *Z. physik. Chem. (Frankfurt)*, **11**, 251 (1957).
8) Sven-Eric Dahlgren, *J. Colloid Sci.*, **13**, 151, (1958).
9) H. Enneking, *Rheologica Acta*, **1**, 234 (1958).
10) E. A. Hauser, *Kolloid-Z.*, **48**, 57 (1929).
11) H. Freundlich, O. Schmidt and G. Lindau, *Kolloid-Beih.*, **36**, 43 (1932).
12) U. Hofmann, *Kolloid-Z.*, **125**, 86 (1952).
13) S. Ono and T. Watanabe, *J. Chem. Soc. Japan, Pure Chem. Sec. (Nippon Kagaku Zasshi)*, **74**, 463 (1953).
14) H. v. Platen and H. G. F. Winkler, *Kolloid-Z.*, **158**, 3 (1958).
15) H. Braune and I. Richter, ibid., **113**, 20 (1949).
16) T. Watanabe and S. Matsumoto, *J. Chem. Soc. Japan, Pure Chem. Sec. (Nippon Kagaku Zasshi)*, **76**, 1215 (1955).
17) A. Packter, *Kolloid-Z.*, **150**, 60 (1957).
18) T. Watanabe and Y. Takasaki, *Naturwissenschaften*, **45**, 334 (1958).
19) T. Tachibana and N. Okuda, presented at the 9th (1956) and the 10th (1957) Annual Meetings of the Chemical Society of Japan.

Vanadium pentoxide. An aqueous sol was prepared according to Biltz's method, and the heat treatment of the sol was carried out at 96°C for 10 hr. as suggested by Sato[20]. Afterwards the sol was let stand for one month.

Graphite. — Flaky powder was used as an aqueous suspension.

In the case of experiments with the suspension in the electrolyte solution, the electrolyte solution was added to the above aqueous suspension until its requisite concentration was attained.

Organophilic Bentonite.—Gumma Bentonite was converted into an organophilic bentonite by cation-exchange reaction using oleyl-picolinium chloride or lauryl-picolinium chloride as cation active agent. A dried powdery product was obtained and used as a benzene suspension.

Apparatus and Procedure. — The measurement of yield value of the above mentioned suspensions was carried out using Du Noüy torsion balance. The length and diameter of the torsion wire are 40 and 0.025 cm., respectively. A small glass sphere (diameter about 0.7 cm.) is hung from the hook of the apparatus with a thin palladium wire (diameter 0.1 mm.). The force which causes the glass sphere to move upward, is given by twisting the torsion wire and is read on the dial scale.

In kinetic studies, measurements should be carried out at constant temperature. In the present experiments, however, all the measurements were made at room temperature, since the characteristics of the observed phenomena and also the maximum yield value are only slightly influenced by the change of temperature in the neighborhood of room temperature.

Experiments have been made as follows. The suspension is taken into a test tube (inner diameter 2.1 cm.) and thoroughly shaken or stirred. Then the glass sphere is immersed into the suspension about 3 cm. below the meniscus. Then, force is added until the glass sphere begins to show a minute upward movement (about 1/60 mm.). The preceding procedure should be performed within 30 sec. after stopping the stirring. The moment at which the above procedure was done, is regarded as the starting point of the experiment. Then, at 5 min. intervals, the force is superimposingly added in the same manner as stated above. In this experiment, the yield value (unit, dyn./cm^2) is expressed with the value obtained by dividing the force with the equatorial cross-section of the glass sphere. The yield value is taken versus the value obtained in the same manner as the above only with the dispersion medium. To observe the upward movement of the glass sphere, a small mirror was attached to the top of the hook and its movement was observed under twenty times enlargement using a lamp and scale. In the course of the application of the additional force, no upward movement of the glass sphere is observed until the total amount of the force has exceeded a certain amount. The force with which the upward movement of the glass sphere of about 1/60 mm. (i.e. that of 0.3 mm. on the scale) is brought about, is used to evaluate the yield value. It was observed that if the excess of force which caused the upward movement was removed immediately after the movement had been induced, the glass sphere returned to the position before the movement. Therefore, it may be said that the experiment has been carried out under the condition where the deformation applied to the suspension is within elastic limit.

With some of the samples used, experiments were also made using the torsion wire of 15 cm. besides one of 40 cm. In these cases, sensibility to detect a minute deformation was poor so that the amount of the added force became inevitably about two times greater than the case of 40 cm. Therefore, after the cessation of the additional increase of the force at the point where the upward movement of 0.3 mm. on the scale had been observed, a further gradual upward movement of 0.3~0.5 mm. was followed during the ensuing interval of about one minute. This movement may be a visco-elastic flow accompanied with the deformation over elastic limit induced by the force above stated.

Results

Experiments have been made with the various kinds of suspensions stated above. In Fig. 1 the yield value is plotted versus

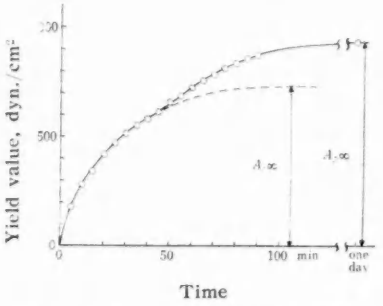

Fig. 1. The process of thixotropic gel formation (result obtained with 3.4% Yamagata Bentonite aqueous suspension).

the setting time. The curve shows that the increase of yield value with time proceeds in two processes which take place successively. The first process starts to develop immediately after the cessation of stirring or shaking. The second one reveals itself successively after some development of the first.

The increase of the yield value varies according to the first order kinetics for each separate process. These may be expressed as follows:

20) K. Sato, "Symposium on Colloid Science (Kōshitsu-gaku Ronsō", Kawade Shobō, Tokyo (1943), p. 93.

$$k_1 = \ln \frac{A_{1\infty}}{A_{1\infty} - A_t} \cdot \frac{1}{t}$$

$$k_2 = \ln \frac{A_{2\infty}}{A_{2\infty} - A_t} \cdot \frac{1}{t}$$

where A_t is the yield value at time t and $A_{1\infty}$ is the maximum yield value of the first process which is obtained from the curve as shown in Fig. 1. $A_{2\infty}$ is the maximum yield value of the second process. k_1 and k_2 are the rate constants for the first and the second processes, respectively. Similar plots such as that shown in Fig. 1 were generally obtained with the system where the dispersed particles have plate- or rod-like forms. In Table I the systems in which the increase of the yield value proceeds in two steps are collected. In the system to which an electrolyte was added, the two step process was detected, when no marked coagulation of the dispersed particles was observed. On the other hand, in the case where marked coagulation was observed, for example, Gumma Bentonite in 0.01 M $FeCl_3$, the process of the thixotropic gel formation was completed in a single step. The same phenomenon was also observed with the thixotropic sol of ferric oxide in 0.1 M NaCl.

TABLE I. THE SYSTEMS IN WHICH THE THIXOTROPIC GEL FORMATION PROCEEDS IN TWO STEPS

Dispersed particles	Medium*
Gumma Bentonite	Water, 0.1 M NaCl, 0.4 M NaCl, 0.1 M LiCl
Yamagata Bentonite	Water
Volclay	Water, 0.1 M NaCl, 0.01 M $FeCl_3$, 0.005 M $Th(NO_3)_4$
Tixoton	Water, 0.1 M NaCl, 0.01 M $FeCl_3$, 0.005 M $Th(NO_3)_4$
Organophilic Bentonite	Benzene
Kaolin	Water
Sericite	Water
Vanadium pentoxide	Water
Graphite	Water, 0.1 M NaCl, 0.05 M $FeCl_3$

* The resulting preparations may contain small amounts of some ions other than those listed, which are due to the nature of the dispersed particles.

For some systems, experiments were carried out at several concentrations of dispersed particles. These results are shown in Table II. And the relation between $A_{1\infty}$ or $A_{2\infty}$ and the concentration (C) was derived as shown in Table III.

Another experiment was made by using torsion wires of 15 and 40 cm., respectively. For example, results obtained with 3.1%

TABLE II. EXPERIMENTAL RESULTS WITH YAMAGATA BENTONITE-, VOLCLAY-, AND VANADIUM PENTOXIDE-WATER SYSTEMS

(Temp., room temp. i.e. in the neighborhood of 15°C)

System	Concn. of disperesed particles g./100 g.	$k_1 \times 10^2$ min^{-1}	$A_{1\infty}$ dyn./cm²	$k_2 \times 10^2$ min^{-1}	$A_{2\infty}$ dyn./cm²
Yamagata	3.7	2	870	3	1000
Bentonite-water	3.4	4	730	4	930
	3.1	3	690	4	910
	2.9	2	600	3	800
	2.7	3	520	4	750
Volclay-water	9.3	2	650	6	760
	8.8	3	540	6	700
	8.4	2	430	6	620
Vanadium	2.3	6	1100	5	1600
pentoxide-water	2.1	4	930	7	1200
	1.9	4	740	7	920
	1.8*	8	690	—	—

* Complete in a single step.

TABLE III. RELATIONS BETWEEN THE MAXIMUM YIELD VALUE OF THE FIRST STEP ($A_{1\infty}$) OR THE SECOND ($A_{2\infty}$) AND CONCENTRATION (C)

System	Relations
Yamagata Bentonite-water	$A_{1\infty} \propto C^2$ & $A_{2\infty} \propto C$
Volclay-water	$A_{1\infty} \propto C^4$ & $A_{2\infty} \propto C^2$
Vanadium pentoxide-water	$A_{1\infty} \propto C^2$ & $A_{2\infty} \propto C^3$

TABLE IV. DATA OBTAINED WITH THE SAME SUSPENSION (3.1% YAMAGATA BENTONITE) USING A DIFFERENT LENGTH OF TORSION WIRE

Wire length, cm.	$k_1 \times 10^2$, min^{-1}	$A_{1\infty}$, dyn./cm^2	$k_2 \times 10^2$, min^{-1}	$A_{2\infty}$, dyn./cm^2
40	3	690	4	910
15	6	1500	3	2100

Yamagata Bentonite aqueous suspension are shown in Table IV. The difference of the value of k_2 between the two cases is small but that of k_1 is cosiderable. The latter may be due to the following conditions. In the case of 15 cm. wire, the visco-elastic flow has been observed in each measurement as stated above, and consequently the thixotropic gel formation proceeds under small shearing motions which facilitate the formation of the gel structure, i.e. the phenomenon of rheopexy has been observed. In the case of 40 cm. wire such an experimental condition was not established so that the phenomenon of rheopexy was not observed.

Discussion

In the first place, let us consider the bentonite suspension. As a structure of thixotropic gel, it is adopted in such a network structure that plate-like particles link with each other in a short distance at the junction point. Furthermore as a model of structure, the 'house of cards' structure which was proposed by Hofmann[12] and whose existence in a xerogel was proved by Weiss et al.[21], is recommended.

In the present experiments, it was observed that the dependence on the concentration of $A_{1\infty}$ was different from that of $A_{2\infty}$. This fact can not be explained with the assumption that the yield value of the gel is determined by all the particles in the structure. Therefore, it must be assumed that the particular group of particles contributes to the yield value of the gel. Such a particular particle group which plays the part of a mechanical unit to the yield value, is named 'structural unit' (abbr. S. U.). Further, the particle group which acts as S. U. is classified into two types, i. e. one is the particle group forming linear ribbon and another is that of cross-linkage.

In the structure, the particles are linked at such small distances at any junction point that the steric hindrance caused by the interaction of linking particles must be taken into consideration. In these circumstances, the steric conditions such as freedom of rotation or flexibility around the junction point, may be the same as each other, in any particle group, so far as the co-operation between particles is concerned.

Considering the steric conditions, the association of plate-like particles may be classified into three types as follows.

P-1 association : Two adjacent particles are linked with each other at one point.

P-2 association : Two adjacent particles are linked at two or more points belonging to one straight line.

P-3 association : Two adjacent particles are linked at three or more points so that they are associated with surface-to-surface linkage.

By the third type of association a voluminous structure can not be expected to be formed, so that the discussions are undertaken leaving the third type out of consideration.

Next, it may be assumed that the magnitude of the cohesive force at junction points of S. U., remains constant in a given system unless the range of concentration studied is great. Therefore, as a first approximation, it may be assumed that the contribution to the yield value of each of the same kind of particle group, i. e. the strength of (b) the corresponding S. U. is constant, and the yield value (A) of any system will be determined by the number (N_s) of the S. U. in unit volume as follows:

$$A = bN_s \qquad (1)$$

In this case, the evaluation of the value of N_s is necessary. At first, probability of permanent junction between adjacent particles (abbr. probability of junction) will be considered. The probability of junction where a given particle in a gel is linked to an adjacent one with P-1 association, will be determined by the number of free dispersed particles in unit volume (N_p) which may exist when the gel is transformed to sol by stirring etc. In other words, the probability of junction will vary as the concentration of the dispersed particles (C). Generally, the probability of junction between a particle and

21) A. Weiss, R. Fahn and U. Hofmann, *Naturwissenschaften*, **39**, 351 (1952); *Ber. deut. keram. Ges.*, **30**, 21 (1953).

its adjacent l particles with P-1 association will vary as C^l, where $l \ll N_p$ and l is a positive integer.

The probability of junction will be evaluated in the case of P-2 association. In this case, the above probability will be determined by the following two probabilities. The one is that of orientation of the particle in sol state to the position where the particle can be linked with P-2 association to a given particle. The other is that of formation of junction between particles. The two probabilities will be proportional to N_p, i. e. C. Therefore, the discussed probability of junction should vary as $C \times C = C^2$. Generally, the probability of junction between a particle and its adjacent m particles in the same manner as stated above will vary as C^m, where m is a positive integer.

Let us consider the linear ribbons which act as S. U. The linear ribbons are formed from the aligned particles and in order to act as S. U. they must also be linked to two or more other linear ribbons. In general the linear ribbons are not formed from exactly equal numbers of particles. However, in the present case, the cohesive force between particles is considered to remain constant, so that the yield value may be determined by the number of junction points between particles in unit volume of the gel. The assumptions are made on the way whereby the linear ribbons are formed, i. e. how many particles are separately linked with what type of association to any one particle. And the relations between the yield value and the concentration in the case where the assumed linear ribbons act as S. U., are derived on the basis of the knowledge on the probability of junction above stated. The results are shown in Table V.

The consideration will be given to the cross-linkage. Cross-linkage is a particle group which plays the part of junction between the linear ribbons in structure. When it contributes to the yield value as S. U., it may be expected that one of the particles forming cross-linkage, could not move in accordance with the deformation of the gel under the applied force, but would behave as if it were restricted at a fixed position. Therefore, the characteristics of the cross-linkage are determined by two factors. One of them is the number of effective linear ribbons linked to the above fixed particle and the other is the type of association between particles forming the cross-linkage. In addition, it may be assumed that the degrees of steric hindrance of the junction points between the particles forming a cross-linkage must be the same as each other and further they must be the same as, or higher than, that of forming the linear ribbons participating in the cross-linkage. According to the above considerations, the relations between the yield value and the concentration of the gel are derived from the knowledge of the probability of junction and shown in Table VI. In this table the necessary type of association of the particles forming linear ribbons is also listed.

Considering the process of development of gel structure which is applicable for the two cases of Yamagata Bentonite and Volclay, it must be assumed that S. U. in

TABLE V. THE RELATION BETWEEN THE YIELD VALUE (A) AND THE CONCENTRATION (C) OF THE GEL IN WHICH THE LINEAR RIBBON ACTS AS STRUCTURAL UNIT

Nomenclature of structural unit	Mode of formation of linear ribbon	Relations between A and C
L-1	P-1 association $l=1$	$A \propto C$
L-2	$l=2$	$A \propto C^2$
L-3	$l=3$	$A \propto C^3$
L-4	P-2 association $m=1$	$A \propto C^2$
L-5	$m=2$	$A \propto C^4$

TABLE VI. THE RELATION BETWEEN THE YIELD VALUE (A) AND THE CONCENTRATION (C) OF THE GEL IN WHICH THE CROSS-LINKAGE ACTS AS STRUCTURAL UNIT

Nomenclature of structural unit	Mode of formation of cross-linkage	Relations between A and C	Necessary type of association of linear ribbon
M-1	P-1 association $l=2$	$A \propto C^2$	P-1
M-2	$l=3$	$A \propto C^3$	P-1
M-3	$l=4$	$A \propto C^4$	P-1
M-4	P-2 association $m=1$	$A \propto C^2$	P-1
M-5	$m=2$	$A \propto C^4$	P-1, P-2

the first step of gel formation is cross-linkage and that of the second is linear ribbon. Therefore, in the case of Yamagata Bentonite having $A_{1\infty} \propto C^2$ and $A_{2\infty} \propto C$, the S. U. for the first step is M-1 or M-4 in Table VI and that of the second is L-1 in Table V, since the linear ribbons of this sample must be formed from the particles linked together by P-1 association. Also in the case of Volclay, the linear ribbons are formed by P-2 association, and the S. U. of the first step is M-5 and that of the second is L-4, since this sample shows the relation, $A_{1\infty} \propto C^4$ and $A_{2\infty} \propto C^2$.

According to the above considerations, it may be explained that the thixotropic gel formation of bentonite will proceed as follows. During the first step, some of the dispersed particles align to form linear ribbons, and the latter further cross-link with neighboring ones to develop into a loose gel structure. In the second step, many particles or linear ribbons having no part in the formation of the first loose gel structure, begin to participate in structure to complete a rigid gel structure. On the other hand, in the first step, the increase of yield value is proportional to the increase in number of cross-linkage and the latter will be accelerated under small shearing motions so that the phenomenon of rheopexy will markedly appear. In the second step, both the increase in number of cross-linkage and that of linear ribbons participating in the formation of the cross-linkage, will simultaneously occur and these will lead to the increase of continuity of the linear ribbons in the gel structure so that the linear ribbons will come to act as S. U. Therefore, though the cross-linkage acting as S. U. in the first step, does not decrease in number nor disappear, its contribution to the yield value as S. U. gradually diminishes in the second step. Moreover, the rheopectic phenomenon can not be observed distinctly in the second step, since the rate of increase of yield value of this step is not determined by the rate of increase of the cross-linkage as in the case of the first step.

In the case of vanadium pentoxide sol, the experimental facts may be explained as follows. It is not necessary to make such a distinction between P-1 and P-2 association as in the case of bentonite, since the vanadium pentoxide particle has a thin rod-like form. It may be assumed that the particle group which acts as S. U. both in the first and in the second step, is the particle group forming cross-linkage. During the first step, a loose gel structure may be developed, in which the dispersed particles are linearly associated and a relatively small number of cross-linkage or entanglement can be seen between the linear chains of particles, and in the second step, it reaches another structure, i. e. a rigid gel structure which may be due to the appreciable increase of cross-linkage between chains. The difference in structure between the loose and rigid one is due to the variance in number of linear chains participating in the formation of the cross-linkage which acts as S. U. The number of linear chains linked to the fixed particle of the cross-linkage is two in the former structure and is three in the latter one, since this sample shows the relation, $A_{1\infty} \propto C^2$ and $A_{2\infty} \propto C^3$. In the course where the rigid gel structure is developed from the loose one, cross-linkage which contributes to the yield value proportional to C^2 is transformed to the cross-linkage proportional to C^3, according to the increase in number of linear chains linked to form the cross-linkage.

Summary

(1) In this system, in which the form of dispersed particles is plate- or rod-like, the thixotropic gelation generally proceeds in two steps.

(2) During the first step of thixotropic gel formation, a loose gel structure may be developed and a rigid gel structure in the second step.

(3) In the case of bentonite, the structural unit which contributes to the yield value of the gel in the first step is cross-linkage and that of the second is linear ribbon.

(4) In the case of vanadium pentoxide, the structural unit is cross-linkage both in the first and in the second step.

The author would like to express his gratitude to Professor Sôzaburo Ono for his kind guidance and discussion throughout this work and to Mr. Yoshiyuki Takasaki for his kind assistance in the experiment.

Laboratory of Biophysical Chemistry
College of Agriculture
University of Osaka Prefecture
Sakai, Osaka

A Simple Method for the Preparation of Crystalline D-Mannose

By Toshihito FUJITA and Tetsuo SATŌ

(Received August 18, 1959)

In the recent studies on the reaction of carbohydrates with boric acid, the present authors have required a large quantity of crystalline D-mannose. This is usually obtained by the hydrolysis of polysaccharides, such as mannan and glucomannan[1].

A better source of the sugar are the corms of *Amorphophallus* konjac, which contain mannose as glucomannan and are commercially available as "Konjac Flour". According to the previous methods[2] for the preparation of the sugar from this source, D-mannose is isolated in the form of its crystalline phenylhydrazone, purified as easily crystallizable methyl-*α*-D-mannoside, and then the glycoside is hydrolyzed to free sugar. This phenylhydrazone method is quite expensive, and not suitable for preparation on a large scale.

The phenylhydrazone method is based on the unusual low solubility in water of mannose phenylhydrazone. *N*-phenylmannosylamine, like the hydrazone, is insoluble and easily crystallized from an aqueous solution[3]. Moreover, the *N*-glycoside is very easily hydrolyzed under neutral conditions in the presence of formaldehyde or benzaldehyde. The authors have used *N*-phenyl-D-mannosylamine in isolating D-mannose from "Konjac Flour" and made certain improvements for the preparatory purpose of D-mannose.

The "Konjac Flour" has been hydrolyzed with concentrated or with dilute acid solution. The best results bave been obtained by refluxing it in 1 N acid solution. From the acid hydrolysate D-mannose has been isolated as crystalline *N*-phenylmannosylamine, and the *N*-mannoside has been readily hydrolyzed to free sugar in the usual manner[4]. The yield of sugar from this method is nearly equal to that of the phenylhydrazone method.

Experimental

Preparation of *N*-Phenyl-D-mannosylamine.—*Procedure-A.*—One hundred grams of "Konjac Flour" was mixed with 60 ml. of cold 75% sulfuric acid under cooling, allowed to stand overnight at room temperature and then added to 1 liter of water. The diluted solution was refluxed for 6 hr. The solution was neutralized with barium carbonate to pH 4~5 and the precipitate was filtered off. The filtrate was decolorized with active charcoal and concentrated to 100 ml. in vacuo. Aniline (16 ml.) in 100 ml. of ethanol was added to it. The mixture was kept overnight in a refrigerator. The crystals formed were collected and recrystallized from 50% ethanol. Yield 24 g., m.p. 180~181°C. It was identified with an authentic sample[3].

Procedure-B.—"Konjac Flour" (100 g.) was suspended in 1 liter of 1 N sulfuric acid and the mixture was boiled for 10 hr. under refluxing. The dark brown solution was neutralized to pH 4~5 with barium carbonate. The *N*-mannoside was obtained as described above. Yield, 33 g.

Isolation of D-Mannose from *N*-Phenyl-D-mannosylamine.—Fifty grams of *N*-phenyl-D-mannosylamine was dissolved in water at 60~70°C and 35% formaldehyde (25 ml.) was added to it. A white precipitate was soon deposited. The mixture was allowed to stand for 24 hr. at room temperature. The white resinous substance was removed and the filtrate was evaporated to a thick sirup. The colorless sirup was dissolved in methanol and *n*-propanol (1 : 1) and seeded with *α*-D-mannose. The crystals were separated and recrystallized from ethanol or acetic acid. Yield, 30 g. (85%), m.p. 130~131°C. $[\alpha]_D^{30}$: 28.4° →+13.3° (*c* 3.9, in water).

Found: C, 40.18; H, 6.84. Calcd. for $C_6H_{12}O_6$: C, 40.00; H, 6.71%.

Laboratory of Organic Chemistry
Tokyo Institute of Technology
Meguro-ku, Tokyo

1) J. Sowden, "The Carbohydrates", Academic Press, Inc., New York (1957), p. 94.

2) K. Nishida and H. Hagima, *J. Agr. Chem. Soc. Japan* (*Nippon Nōgei-kagaku Kaishi*), **6**, 1065 (1930); C. Araki, "Experiments in Chemistry" (*Kagaku Zikkengaku*)", Vol. II, Kawade Shobō, Tokyo (1942), p. 154.

3) G. P. Ellis and J. Honeyman, "Advances in Carbohydrate Chemistry", Vol. 10, Academic Press, New York (1955), p. 95.

4) L. Berger and J. Lee, *J. Org. Chem.*, **11**, 91 (1946).

The Crystal Structure of trans-[Cr en$_2$Cl$_2$]Cl·HCl·2H$_2$O

By Shun'ichiro OOI, Yoshimichi KOMIYAMA and Hisao KUROYA

(Received September 22, 1959)

The crystal structures of the two cobalt(III)-complexes, which are of the type *trans*-[Co en$_2$X$_2$]X·HX·2H$_2$O (X=Cl, Br)[1], were determined by Saito, Kuroya and their collaborators during the past several years[2,3]. In connection with this, it seems really interesting and important to investigate the crystal structures of the chromium(III)-analogues, which have a great resemblance to the cobalt(III)-complexes in various respects; particularly, it may be very instructive to examine what discrepancies can be found between the bond lengths M–N and M–X in these compounds, where M denotes a central metallic ion and N a nitrogen atom of the coordinated ethylenediamine molecule.

The present authors took up the *trans*-dichloro-bis-ethylenediamine-chromium(III) chloride hydrochloride dihydrate, *trans*-[Cr en$_2$Cl$_2$]Cl·HCl·2H$_2$O, in the first place, and made an attempt to analyze the crystal structure of this compound by means of X-rays. This paper is to report the results obtained.

Experimental

The crystal of [Cr en$_2$Cl$_2$]Cl·HCl·2H$_2$O was prepared by the method of Pfeiffer et al.[4] The crystals are bluish-green tablets and show marked dichroism like the crystals of [Co en$_2$Cl$_2$]-Cl·HCl·2H$_2$O. From oscillation and Weissenberg photographs the unit cell dimensions were found to be:

$$a=10.97,\quad b=7.88,\quad c=9.12\,\text{Å},\quad \beta=111.5°.$$

The space group was determined to be No. 14 $P2_1/c$ from the systematic extinctions of reflections. The unit cell contains two formula units ($\rho_{\text{calcd}}=1.59$, $\rho_{\text{obs}}=1.54$ g./cm^3). The photographs were taken with Cu$K\alpha$ radiation using multiple film technique. All intensities were estimated visually by comparison with standard scales. The usual correction factors were applied by means of a chart given by Cochran and relative $|F_o|$ values were obtained.

Structure Determination

The structure determination was carried out using $(h\,k\,0)$ and $(h\,0\,l)$ reflections from Weissenberg data. It was observed that the intensity of each reflection is similar to the corresponding one of the cobalt-analogue at low-angle reflections. This had been expected from the dichroism mentioned above and the crystallographic data, and the outline of the crystal structure was determined without difficulty.

At the stage of refinement, the method of successive difference syntheses was employed. The atomic coordinates obtained are shown in Table I. These parameters gave the reliability index $R=\sum||F_o|-|F_c||/\sum|F_o|$ of 0.131 and 0.121 for $(h\,k\,0)$ and $(h\,0\,l)$ respectively, excluding (100) reflection which could not be observed with full certainty. Calculated and observed structure factors are listed in Table II. In the calculation of structure factors, atomic scattering factors listed in the International Table (1935) were used. Overall temperature factors of the form exp $[-B(\sin\theta/\lambda)^2]$, where $B=2.7$ Å^2, were applied in the final calculation of structure factors. Final electron density projections on (010) and (001) are shown in Figs. 1 and 2.

TABLE I. FINAL ATOMIC COORDINATES

	x/a	y/b	z/c
Cr	0	0	0
Cl(1)	0.050	0.038	0.269
Cl(2)	0.345	0.387	0.272
N(1)	0.100	−0.235	0.042
N(2)	0.185	0.106	0.023
C(1)	0.227	−0.200	0.037
C(2)	0.288	−0.022	0.100
O	0.478	0.150	0.538

1) N. Fogel and S. D. Christian reported in *J. Am. Chem. Soc.*, **80**, 2356 (1958) that the dichloro-complex should be given a composition formula [Co en$_2$Cl$_2$]Cl·HCl·6H$_2$O instead of [Co en$_2$Cl$_2$]·Cl·HCl·2H$_2$O. However, no other formula than the latter can give any satisfactory agreement between the measured and calculated values of density, and furthermore, between $|F_o|$ and $|F_c|$, i. e., the observed and calculated intensities of X-ray diffraction.

2) A. Nakahara, Y. Saito and H. Kuroya, This Bulletin, **25**, 331 (1952).

3) S. Ooi, Y. Komiyama, Y. Saito and H. Kuroya, ibid., **32**, 263 (1959).

4) P. Pfeiffer et al., *Ber.*, **37**, 4255 (1904).

TABLE II. OBSERVED AND CALCULATED STRUCTURE AMPLITUDES

h k l	F_o	F_c	*h k l*	F_o	F_c	*h k l*	F_o	F_c
100	39.2	68.4	480	<5.2	−2.4	1130	9.6	9.6
200	38.4	51.6	490	4.8	−4.4	1140	<3.6	−0.8
300	70.0	72.4				1150	5.2	4.0
400	36.4	33.6	510	23.2	16.8			
500	9.6	5.2	520	28.0	28.8	1210	3.2	−2.8
600	42.4	42.8	530	<3.6	3.6	1220	<3.6	−1.6
700	21.6	−27.6	540	11.2	14.0	1230	<3.6	−4.0
800	4.0	−0.4	550	23.2	−22.0			
900	4.4	10.0	560	13.2	10.8	002	19.2	16.8
1000	<5.4	−9.2	570	29.2	−28.4	004	114.3	114.9
1100	10.4	8.0	580	6.0	3.6	006	14.8	−13.3
1200	2.4	4.4	590	10.0	−8.8	008	28.4	26.8
						0010	<4.0	−2.0
020	75.2	72.4	610	23.6	−12.0			
040	21.2	11.6	620	30.8	26.4	102	<4.0	0.4
060	9.6	12.4	630	27.2	−27.6	10$\bar{2}$	47.2	40.8
080	23.2	22.8	640	14.0	−22.4	104	<4.0	−3.6
0100	7.6	6.4	650	19.2	−23.2	10$\bar{4}$	96.4	96.8
			660	7.2	7.2	106	15.6	18.8
110	12.4	−19.2	670	2.8	−3.6	10$\bar{6}$	<5.6	6.4
120	59.2	64.4	680	18.4	18.8	108	<5.6	−5.6
130	64.4	−61.2				10$\bar{8}$	41.2	43.2
140	77.2	78.0	710	38.4	−33.6	1010	<4.0	10.4
150	10.8	12.8	720	19.6	15.6	10$\bar{1}\bar{0}$	<4.0	−1.6
160	17.6	11.6	730	22.0	−21.2			
170	15.2	16.8	740	28.8	28.0	202	<5.6	2.4
180	<5.2	0.4	750	11.2	−7.6	20$\bar{2}$	19.2	23.2
190	<3.6	−2.4	760	18.0	14.8	204	37.6	37.2
			770	<3.6	−0.4	20$\bar{4}$	51.6	54.4
210	43.6	44.8	780	6.0	2.4	206	<5.6	−7.2
220	52.0	49.6				20$\bar{6}$	32.0	32.8
230	14.0	−8.8	810	<5.2	6.4	208	8.8	10.0
240	42.8	40.8	820	<5.2	−6.0	20$\bar{8}$	23.2	17.6
250	21.2	−20.8	830	19.6	18.8	2010	<4.0	−4.8
260	28.0	25.2	840	8.8	6.0	20$\bar{1}\bar{0}$	<4.0	9.2
270	28.4	−26.8	850	18.0	−19.2			
280	9.6	4.8	860	18.0	9.6	302	44.8	−48.4
290	<3.6	−3.2	870	10.8	−12.0	30$\bar{2}$	98.0	−96.8
						304	20.8	24.0
310	18.4	−15.2	910	9.6	−13.2	30$\bar{4}$	74.4	69.6
320	76.0	76.4	920	8.0	−9.2	306	<5.6	−4.8
330	38.4	−33.6	930	8.4	−8.4	30$\bar{6}$	29.6	−29.6
340	28.0	22.8	940	6.0	−4.0	308	<5.6	6.8
350	9.6	−9.2	950	<5.2	−0.4	30$\bar{8}$	48.8	50.8
360	15.2	8.8	960	<3.6	0.8	30$\bar{1}\bar{0}$	<5.6	−2.4
370	20.4	−20.4	970	<3.6	0.4			
380	17.2	16.0				402	59.6	60.4
390	5.6	−6.4	1010	6.0	4.8	40$\bar{2}$	44.4	46.0
			1020	<5.2	−5.2	404	<5.6	−4.0
410	5.2	−4.4	1030	<5.2	−2.0	40$\bar{4}$	35.2	38.0
420	38.8	38.4	1040	20.0	15.2	406	29.2	42.4
430	24.8	−27.6	1050	<3.6	−3.6	40$\bar{6}$	16.8	−16.8
440	37.6	37.2	1060	10.4	7.6	408	<4.0	−2.8
450	12.4	−13.6				40$\bar{8}$	33.2	25.6
460	31.2	32.0	1110	6.8	7.2	40$\bar{1}\bar{0}$	14.8	−14.0
470	10.0	−8.0	1120	5.6	0.8			

hkl	F_o	F_c	hkl	F_o	F_c	hkl	F_o	F_c
502	10.4	12.0	70$\bar{4}$	6.8	−8.4	1002	33.6	42.0
50$\bar{2}$	32.4	35.6	706	19.6	25.2	100$\bar{2}$	46.0	46.8
504	14.0	12.0	70$\bar{6}$	16.8	14.4	1004	<4.0	−7.2
50$\bar{4}$	30.0	35.2	708	26.4	23.2	100$\bar{4}$	12.0	−16.0
506	11.2	12.8	70$\bar{1}\bar{0}$	<4.0	6.4	1006	32.4	26.4
50$\bar{6}$	32.0	38.4				100$\bar{8}$	<5.6	−1.6
508	<4.0	6.8	802	22.8	26.4	100$\bar{1}\bar{0}$	9.6	6.0
50$\bar{8}$	19.2	18.0	80$\bar{2}$	35.2	35.2			
50$\bar{1}\bar{0}$	10.0	12.4	804	6.8	10.4	1102	6.8	8.4
			80$\bar{4}$	7.2	−15.6	110$\bar{2}$	32.8	34.4
602	25.2	22.0	806	8.0	15.6	110$\bar{4}$	<5.6	1.2
60$\bar{2}$	10.4	−11.6	80$\bar{6}$	17.6	13.3	1106	36.4	34.0
604	11.2	17.2	808	11.2	−18.0	1108	<4.0	−5.2
60$\bar{4}$	46.8	51.6	80$\bar{1}\bar{0}$	9.2	7.6			
606	18.8	17.2				120$\bar{2}$	17.6	10.0
60$\bar{6}$	6.8	−8.4	902	20.4	20.2	120$\bar{4}$	12.0	10.4
608	38.8	42.8	90$\bar{2}$	16.8	14.0	1206	12.0	9.2
60$\bar{1}\bar{0}$	<5.6	−4.8	904	<4.0	4.4	1208	6.0	5.6
			90$\bar{4}$	24.0	24.4			
702	40.4	40.8	906	9.6	8.4	130$\bar{2}$	16.0	22.8
70$\bar{2}$	38.0	38.8	908	19.6	16.8	130$\bar{4}$	<4.0	−7.2
704	14.4	−26.4	90$\bar{1}\bar{0}$	<4.0	−5.2	130$\bar{6}$	31.6	27.6

Fig. 1. Electron density projected along the *b*-axis. Contours are drawn at intervals 10 e. Å^{-2} for peaks Cr and Cl (heavy lines) of 2 e. Å^{-2} for other peaks, zero-electron level being broken.

Results

The crystal structure determined is isomorphous with $[Co\ en_2Cl_2]Cl\cdot HCl\cdot 2H_2O$ and consists of the following elements: $[Cr\ en_2Cl_2]^+$, Cl^- and $[H_2O\cdots H\cdots H_2O]^+$. The configuration of the complex is as follows. Two enantiomorphous ethylenediamine molecules, taking *gauche* form, are coordinated to a chromium atom with their four nitrogen atoms. The arrangement of nitrogen atoms around the chromium atom is square coplanar. On a line approximately perpendicular to the plane are two chlorine atoms and these are coordinated to the central metal atom. The calculated bond lengths and angles are shown in Table III. The interatomic distance O···O of $[H_2O\cdots H\cdots H_2O]^+$ was found to be 2.56 Å.

A trial was made for the estimation of some coordinate standard deviations by

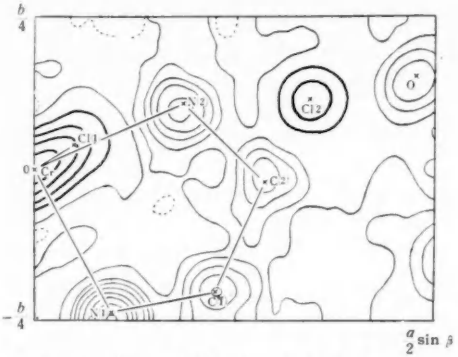

Fig. 2. Electron density projected along the *c*-axis. Contours are drawn in the same manner as Fig. 1.

TABLE III. BOND LENGTHS AND ANGLES

Cr–Cl(1)	2.33 Å
Cr–N(1)	2.11
Cr–N(2)	2.13
N(1)–C(1)	1.44
N(2)–C(2)	1.48
C(1)–C(2)	1.57
N(1)–Cr–N(2)	85.2°
Cr–N(1)–C(1)	105.8
Cr–N(2)–C(2)	108.3
N(1)–C(1)–C(2)	116.5
N(2)–C(2)–C(1)	106.8

TABLE IV. ESTIMATED COORDINATE STANDARD DEVIATIONS (VALUES IN ANGSTROM UNITS)

	Cl	N(1)	N(2)
$\sigma(X^*)$	0.013**	0.022	0.039
$\sigma(y)$	0.010	0.054	0.032
$\sigma(z)$	0.012	—***	—***

* X is the axis normal to the yz-plane.
** 0.013 was estimated from the data for $(h\,0\,l)$, 0.012 from those for $(h\,k\,0)$.
*** $\sigma(z)$ for N(1) and N(2) could not be estimated because of the required tedious calculation**** due to mutual overlaps of atomic peaks (see Fig. 1).
**** D.W.J. Cruickshank, *Acta Cryst.*, **5**, 511 (1952).

the method of Cruickshank[5], and the results are listed in Table IV. Regarding the bond lengths of chromium to nitrogen atoms, 2.11 and 2.13 Å are found for Cr–N(1) and Cr–N(2), respectively. These values are greater than the corresponding ones in the cobalt-analogue by ca. 0.1 Å. On this value, then, "significance tests"[3] were tried. At a rough approximation with $\sigma(z)$ of N(1) and N(2) ignored, the standard deviations of bond lengths $\sigma(l)$'s could be calculated from the data given in Table IV.

$$\sigma(\text{Cr–N(1)}) = 0.049, \quad \sigma(\text{Cr–N(2)}) = 0.037 \text{ Å}.$$

Similar treatments on the data of cobalt-analogues gave

$$\text{N(1)}: \sigma(X) = 0.068, \quad \sigma(y) = 0.084 \text{ Å},$$

and $$\text{N(2)}: \sigma(X) = 0.100, \quad \sigma(y) = 0.108 \text{ Å},$$

from which were obtained the values:

$$\sigma(\text{Co–N(1)}) = 0.080, \quad \sigma(\text{Co–N(2)}) = 0.099 \text{ Å}.$$

The values of $|l_1 - l_2|/\{\sigma(l_1)^2 + \sigma(l_2)^2\}^{1/2}$ were estimated to be 1.4 for Cr–N(1) and Co–N(1), and 1.2 for Cr–N(2) and Co–N(2), where l_1 and l_2 are bond lengths of Cr–N and Co–N, respectively. According to the levels given by Cruickshank, these values indicate that the difference between l_1 and l_2 is not significant.

The bond length found for Cr–Cl(1) is 2.33 Å which is the same as that found in the cobalt-analogue, and the estimated σ(Cr–Cl(1)) is 0.012 Å. The cell dimensions of cobalt-analogue are

$$a = 10.68, \quad b = 7.89, \quad c = 9.09 \text{ Å}, \quad \beta = 110.4°,$$

and a is shorter than that of the present crystal by ca. 0.3 Å which is apparently beyond the experimental error while no remarkable discrepancies can be found between the values of b's, c's and β's, respectively, of the two paired coordination compounds of Cr(III) and Co(III).

Thus, it has been evidenced that the substitution of metal causes the deformation of the unit cell. It is probably not unduly bold to consider that the effect of a metal substitution takes place first of all in the nearest neighbor of the metal. However, since the accuracy is not high enough as can be seen above, the authors' opinion is that it is going too far to give a definite conclusion to this problem.

The present authors wish to express their sincere thanks to Professor Y. Saito for his kind advice and encouragement throughout this work. Part of the cost of this investigation was defrayed from the Fund for Scientific Resarch Expenditure of the Ministry of Education, to which the authors' thanks are also due.

Institute of Polytechnics
Osaka City University
Kita-ku, Osaka

5) D. W. J. Cruickshank and A. P. Robertson, *Acta Cryst.*, **6**, 698 (1953).

Catalytic Activity for Methanol Synthesis of Zinc Oxide-Chromium Oxide-Copper Oxide Catalysts and its Structural Dependency

By Yoshisada OGINO, Masaaki OBA and Hiroshi UCHIDA

(Received September 19, 1959)

Because of their higher catalytic activity for methanol synthesis than that of zinc oxide-chromium oxide catalysts, three component catalysts, consisting of oxides of zinc, chromium, and copper, are in industrial use in this country. A few papers[1-3] have already appeared dealing with the catalysts. However, only the papers by Natta and Ivanov described the catalysts from a structural view point, and dependency of catalytic activity upon catalyst structures has remained unclarified as yet. The present study attempts to assemble a number of experimental data in this respect, and to approach complete understanding of the promoting action of copper oxide in the three component catalysts.

In this paper a preparative procedure somewhat different from the usual ones is proposed. The major part of the determinations on catalyst structures as well as on catalytic activity are made on the catalysts prepared by the procedure.

Experimental

Preparations of a series of zinc oxide-chromium oxide-copper oxide catalysts of varying chemical compositions were made by a procedure somewhat different from the usual ones: namely, a commercial zinc oxide powder was kneaded with a chromic acid solution, in which an appropriate amount of cupric oxide had been dissolved, into a paste, which was allowed to dry at room temperature. The resulting cake was crushed, and screened to 2 to 2.5 mm. granules. Another catalyst, denoted by catalyst R, manufactured by a usual procedure was also prepared. According to the procedure, a mixture of powders of zinc oxide and copper oxide was kneaded with a chromic acid solution into a paste, which was then treated similarly to finished catalyst granules.

Chemical compositions of the catalysts used in this study are listed in Table I. Because of rather poor solubility of copper oxide in a chromic acid solution, a catalyst of Cu/Zn ratio in excess of 0.25 could not be obtained.

Catalytic activity for the methanol synthesis was determined according to the same procedure as described in the previous paper[4]. Among the by-products of the synthesis, formaldehyde was determined by a chemical analysis, while water and higher alcohols were determined by means of a gas chromatography.

Catalyst bed density was determined on the catalyst after the synthesis as follows: an amount of the catalyst granules was placed in a graduated cylinder, which was vibrated by hand till no more reduction in volume of the catalyst bed was observed. The density is given by the value of catalyst weight (g.) divided by volume (cc.) at the end of the vibration.

Specific surface area of the catalyst was determined from nitrogen adsorption data plotted according to the BET theory. In addition, volumes were measured by the water- and the mercury-displacement method[5], from values of which true and bulk densities, and pore volume could be evaluated.

Some of the catalysts, the raw as well as the reduced ones, were subjected to an X-ray study by means of a Geiger-counter spectrometer using filtered K_α ray.

TABLE I. CATALYST COMPOSITION

Catalyst	No. 1	No. 2	No. 3	No. 4	No. 5	No. 6	No. 7
Cr/Zn, mol.	0.39	0.39	0.44	0.49	0.49	0.49	0.49
Cu/Zn, mol.	0.09	0.16	0.17	0.08	0.13	0.16	0.21
Catalyst	No. 8	No. 9	No. 10	No. 11	No. 12	No. 13	R
Cr/Zn, mol.	0.49	0.55	0.55	0.65	0.65	0.65	0.49
Cu/Zn, mol.	0.25	0.13	0.16	0.21	0.16	0.25	0.16

1) M. R. Fenske and P. K. Frolich, *Ind. Eng. Chem.*, **21**, 1052 (1929).
2) G. Natta and his coworkers, "Catalysis", III, Rheinhold Publishing Corp., New York (1955), p. 375.
3) K. N. Ivanov. ibid., p. 375.
4) H. Uchida and Y. Ogino, This Bulletin, **31**, 49 (1958).
5) A. J. Juhola and E. O. Wiig, *J. Am. Chem. Soc.*, **71**, 2078 (1949).

Results

Catalytic Activity for Methanol Synthesis. — Some of the results are exemplified in Fig. 1 which, for the sake of comparison, includes the authors' previous results[6] on a zinc oxide-chromium oxide catalyst. Besides the well-known fact that an addition of copper oxide is very effective in improving the catalytic activity of a zinc oxide-chromium oxide catalyst, the figure reveals that a zinc oxide-chromium oxide-copper oxide catalyst exists in either one of two states, A or B, of different activities. State-A appears immediately after reduction of the raw catalyst at temperatures lower than 280°C, and it is not until the reduced catalyst is heated above this temperature that catalytic activity is decreased to a lower level. Being heated beyond 280°C, the catalyst suffers a rapid activity decline until a steady state, state-B, is established. There is little tendency to further decrease in activity, even though the catalyst in state-B heated as high as 360°C.

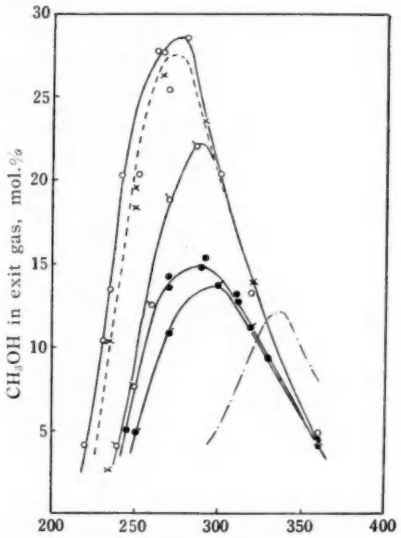

Fig. 1. Methanol concentration as a function of reaction temperature at 150 kg./cm² and S. V. of 1.10⁴.
○, cat. No. 6 (state A), ◬, cat. No. 6 (B), ×, cat. No. 6 (A'), ●, cat. R (A), ▲, cat R (B), —·—·, a zinc oxide-chromium oxide catalyst.

6) Y. Ogino, M. Oba and H. Uchida, This Bulletin, 32, 284 (1959).

Fig. 1 also indicates that after slow oxidation at low temperatures the catalyst in state-B recovers the activity to such a level that it is approximate to the initial activity in state-A (catalyst in state-A'). Being compared with catalyst No. 6, catalyst R of the same chemical composition as, but of a different manufacturing procedure from, catalyst No. 6 gives a considerably lower activity.

It is more desirable to express catalytic activity in terms of the rate constant of the synthesis than the methanol concentration in the exist gas. The reason for this is the difficulties of arranging experiments at a constant space velocity (based on catalyst bed volume after the synthesis), since the catalyst bed volume is apt to shrink, during the synthesis, in an extent that can not exactly be predicted before the synthesis. Usually the extents of shrinkage are in the range of 15 to 25% of the original bed volume of the raw catalyst. The rate constant can be calculated from a methanol concentration by the aid of the rate equation proposed by the present authors[1].

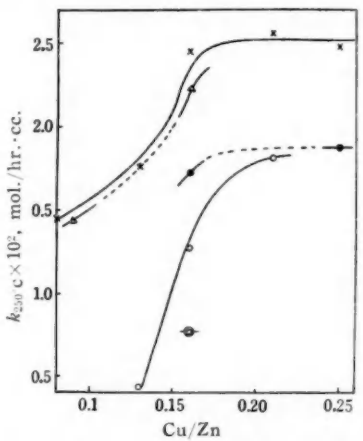

Fig. 2. Catalytic activity as a function of Cu/Zn ratio.
×, Cr/Zn=0.49, △, Cr/Zn=0.89,
●, Cr/Zn=0.65, ○, Cr/Zn=0.55,
◌, cat. R.

The activity thus defined is plotted as a function of chemical composition of the catalysts in Fig. 2. Regarding a series of catalysts of Cr/Zn ratio of 0.49 with varying Cu/Zn ratios, curves in the figure show a rapid initial increase in activity with increasing Cu/Zn ratio, followed by a portion with a smaller slope, and finally

no further increase in the range of Cu/Zn ratios higher than 0.17, while with a series of catalysts with the fixed Cu/Zn ratio of 0.16 and with varying Cr/Zn ratios they show a maximum activity appearing at the Cr/Zn ratio of 0.49.

By-products, such as water and isobutanol, are extremely small in amount (less than 0.7%) in the products at temperatures lower than 270°C, and it makes little difference, whether the catalyst is in state-A or state-B. At higher temperatures the amounts become greater, e. g. attaining to contents of 10% water and 1.4% isobutanol in the product at 360°C. There have been found no alcohols other than isobutanol. Very small quantities of formaldehyde (less than 0.1%) have always been found in the products of the present study.

Catalyst Bed Density. — The catalyst bed density after the synthesis is plotted against the chemical composition of the catalyst in Fig. 3, in which it may be seen that the bed density rises with Cr/Zn ratio up to the high value of 1.47 for a catalyst of an appropriate composition. In contrast to this, catalysts of the usual manufacturing procedures, such as catalyst R and a pelleted catalyst in an industrial use, give lower bed densities of 0.808 and 1.15, respectively.

Naturally the catalyst bed density parallels the bulk density of catalyst granules. It is not because the true density

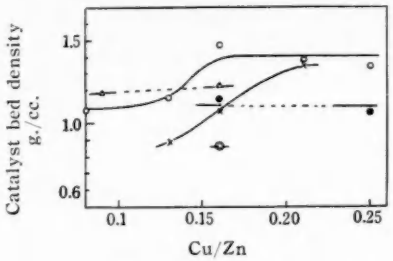

Fig. 3. Catalyst bed density as a function of Cu/Zn.
○, Cr/Zn=0.49, △, Cr/Zn=0.39,
×, Cr/Zn=0.55, ●, Cr/Zn=0.65,
◎, cat. R.

of catalyst granules is high, but because the pore volume in the granules is extremely small, that the present catalyst gives a high value of the bulk density (refer to Table III). As shown in the table, the bulk density of a raw catalyst can not be correlated directly to that of a reduced one, since the raw one contains an appreciable indefinite quantity of crystallization water.

Specific Surface Area. — Specific surface areas of the raw and the reduced catalysts are summarized in Table II. The table discloses that the specific surface area is enlarged remarkably by reduction of the raw catalyst to state-A, and further, but in less degree, by subsequent reduction to

TABLE II. CATALYST BED DENSITY AND SPECIFIC SURFACE AREA

Catalyst		No. 1	No. 2	No. 3	No. 4	No. 5	No. 6
Catalyst bed density, g.*/cc.		1.297	1.231	1.423	1.082	1.328	1.470
Specific surface area (raw), $m^2/g.$		—	10.85	0.54	8.90	5.65	1.69
Specific surface area (reduced), $m.^2/g.$	A	112	132	133	115	113	113
	B	—	—	—	124	151	147

Catalyst		No. 7	No. 8	No. 10	No. 11	No. 12	R
Catalyst bed density, g.*/cc.		1.381	1.328	1.067	1.361	1.162	0.808
Specific surface area (raw), $m^2/g.$		1.08	0.24	9.20	—	5.67	26.5
Specific surface area (reduced), $m.^2/g.$	A	104	113	104	101	116	94
	B	120	151	120	—	140	137

* With reduced catalysts.

TABLE III. DENSITIES AND PORE VOLUME OF CATALYSTS No. 6 AND R

Catalyst		Bed density g./cc.	Density g./cc.	Bulk density g./cc.	Pore volume cc./g.	Average pore dia. Å
No. 6 (raw)		1.78	3.4122	3.0883	0.0307	728
R (raw)		1.03	2.9813	1.1849	0.5085	768
No. 6 (reduced)	A	1.47	4.7325	3.042	0.1190	21
	B	1.43	5.4079	2.806	0.1725	23
R (reduced)	A	0.808	4.9221	2.9716	0.1333	28
	B	0.799	5.4477	1.8609	0.3538	52

state-B. The present catalysts give much higher surface areas than the zinc oxide-chromium oxide catalysts in the authors' previous paper.

A high extent of specific surface area once obtained on a catalyst in state-B is diminished, by slow oxidation of state-B to state-A, to a smaller area which is approximate to the former area of the catalyst in state-A, with simultaneous recovery of the activity.

Loss and Gain of Oxygen with Reduction and Oxidation of Catalyst.—The different states of a catalyst, state-A, −B, and −A′, appeared to be related to different oxygen contents of the catalyst. In this respect, changes in weight of catalyst No. 6 with repeated reduction and oxidation have been pursued in some detail. The results are given in Fig. 4, in which changes in

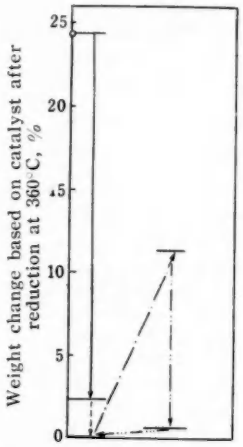

Fig. 4. Changes in weight of catalyst with reduction and oxidation.
○, raw catalyst, ——, reduction at 250°C, ------, reduction at 360°C, —·—·, oxidation at room temperature, —··—··, reduction at 250°C, ——···, reduction at 360°C.

weight are expressed in per cent increase based on the catalyst weight in state-B. By reduction of the raw catalyst at 250°C, decrease in weight takes place to a remarkable extent, the major part of which is presumably due to release of crystallisation water from the raw catalyst. Subsequent reduction from state-A to state-B accompanies the further decrease in weight, whose major part may probably be due to loss of oxygen[7]. After slow oxidation of the resulting catalyst in dry air at room temperature, gradual take-up of oxygen takes place till it, after a week, attains to as great an amount as 11.3% weight increase. The major part of the oxygen can readily be liberated by reduction at 250°C, and state-A′ is established. On the other hand, it should be emphasized that the gradual oxygen take-up is also observed for zinc oxide-chromium oxide catalysts, though it is of a much smaller amount, e. g. 2.4% increase for a catalyst of Cr/Zn ratio of 0.5.

Catalyst Structure Revealed by X-ray Diffraction Patterns. — Among the catalysts, catalysts No. 6 and R were subjected to an X-ray examination. Both of the raw catalysts gave diffraction lines due to zinchydroxychromates Iβ and IIβ, with no signs of oxides of copper. With catalyst No. 6 the latter hydroxychromate develops to greater crystallites than the former one, whereas with catalyst R the situation is the opposite. In this respect the authors' previous paper reported that a catalyst of Cr/Zn ratio of 0.49, with no copper, consisted of zinchydroxychromate Iβ alone, and that zinchydroxychromate IIβ, together with zinchydroxychromate Iβ, appeared only in a catalyst of the smaller ratio. In the present catalysts of high Cr/Zn ratios, zinchydroxychromate IIβ may gradually appear, because the part of chromic acid is consumed by the preferential combination with copper oxide to produce copper chromate. However, no evidence of either copper chromate or cupric chromite has been found in the diffraction diagram, even after the sintering of the catalyst at 600°C[8]. The results also show that in the manufacturing of the present catalysts chromic acid tends to combine with copper oxide more readily than it does in that of catalyst R.

After the synthesis, catalysts No. 6 and R gave no diffraction lines other than the diffused ones due to cuprous oxide[9]. This does not necessarily indicate that the crystallite, such as those of oxides of zinc and chromium or those of zinc chromite, are completely absent in the catalyst

7) The decreases are in the range of 1~3.5% for individual catalyst of the present series. No definite relationship between the extent of decrease and chemical composition has been found.

8) Refer to Stroupe's paper: J. D. Stroupe, *J. Am. Chem. Soc.*, **71**, 589 (1949).

9) The crystallites of cuprous oxide may perhaps be produced, during the taking of the diagram, by reoxidation of copper crystallites produced by reduction, though necessary care, such as the leaching of the specimen in methanol, has been taken.

granules, but that the crystallites are too finely dispersed to be detected by an X-ray examination. The diffration lines of cuprous oxide remain essentially unchaned, whether the catalysts are in state-A or state-B. From the diffusivity of the diffraction lines, a rough calculation of the width of cuprous oxide crystallites was made by the aid of Scherrer's formula. The width has proved to be about 50 Å.

Discussion

Catalytic Activity and Catalyst Bed Density.—Fig. 5. presents the relationship between the catalytic activity and the catalyst bed

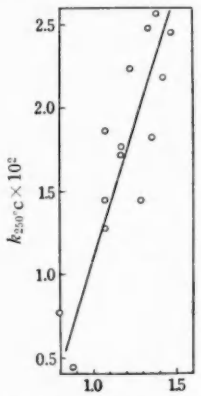

Fig. 5. Relationship between catalytic activity and catalyst bed density.

density, and an approximate proportionality has been found existing between them. The present catalyst owes the fact that it has such a high catalytic activity mainly to the high catalyst bed density. The high catalyst bed density is characteristic of the catalysts made by the present procedure.

Specific Surface Area and Specific Catalytic Activity.—With the present catalysts, hardly any relationship between catalytic activity and the extent of the specific surface area has been found. On the other hand, specific activity, namely, activity expressed per unit surface area, tends to increase slowly with copper content throughout the range of the present study (refer to Fig. 6). The tendency, however, is only a minor factor influencing the catalytic activity which is considered on the basis of unit volume of the catalyst bed or unit mass of the catalyst granules. Catalyst R gives a very low specific activity.

Activation Energy and Frequency Factor of Synthesis.—Arrhenius' plots are linear with slopes corresponding to an activation energy of 16.6 kcal./mol. for individual catalysts in state-A, and another one of 21.9 kcal./mol. for individual ones in state-B, respectively. Present values of the activation energy are much lower than those of zinc oxide (34.6 kcal./mol.) and zinc oxide-chromium oxide catalysts (e. g. 27.4 kcal./mol. for a catalyst of the Cr/Zn ratio of 0.5).

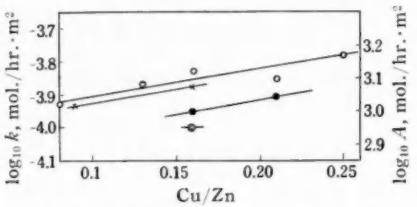

Fig. 6. Specific catalytic activity or frequency factor per unit surface area as a function of Cu/Zn.
○, Cr/Zn=0.49, ×, Cr/Zn=0.39,
●, Cr/Zn=0.55, ◎, cat. R.

By the choice of an adequate scale for the ordinate, the same straight line as cited in Fig. 6 can reveal the relationship between the frequency factor based on unit surface area and the Cu/Zn ratio, since the catalysts give a constant activation energy independently of the varying Cu/Zn ratios[10]. In contrast to the present catalysts, the zinc oxide-chromium oxide catalysts usually showed much higher values of the frequency factor per unit surface area (e. g. 0.5^{-2} mol./hr.·m² for the catalyst of Cr/Zn ratio of 0.5). This enables the authors to expect a steep rise of the frequency factor with decreasing Cu/Zn ratios in a range of the extremely low ratios, when the above mentioned straight line relationship is also taken into account. No experimental data, however, are available to demonstrate the expectation as yet.

The catalyst always changes its state from A to B with simultaneous increase of both the activation energy and the frequency factor per unit surface area.

State-A and State-B of Catalyst.—It is not because of the sintering of the catalyst granules that a decrease in catalytic

10) From the results, a premise is possible that all active centers are alike, appearing more frequently on the catalyst surface with increasing copper content.

activity appears with the change of the catalyst state from state-A to B, but it is because of a decrease in specific catalytic activity per unit catalyst surface. This is apparent from the rather larger specific surface area for the catalyst in state-B. At first sight, the sintering of copper crystallites, as revealed by the appearance of the diffraction lines due to cuprous oxide in the diagram, seemed to have a great influence upon the specific catalytic activity. This, however, can not be true, because the same diffraction lines appear in the diagram of the catalyst in state-A' of an activity approximate to state-A.

Among structural factors of the catalyst here investigated, only the oxygen content of catalysts seems to have an influence upon the specific catalytic activity. Oxygen of this kind is remarkably increased in amount by an addition of copper oxide. It is increased to such an extent that it is much greater than that estimated to be produced by the reduction of cupric oxide to copper. The oxygen may thus come partly from copper oxide, but also from some other kinds of oxides of high oxidation stage at which the oxygen is rather loosely bound, namely, oxide of chromium. In this respect, the X-ray diffraction diagram has revealed that, by an addition of copper oxide, crystallites of chromium oxide or zinc chromite become more finely dispersed in the catalyst. Chromium oxide in extremely fine dispersion is reasonably expected to be capable of being oxidized more readily to high valency states (refer to the papers of Selwood[11] and others[12,13]).

Summary

A preparative procedure in which copper oxide is introduced into the catalyst by a different way from the usual ones has presented the catalyst of high catalytic activity for the methanol synthesis. The catalyst owes its high catalytic activity to three structural factors, namely, a high catalyst bed density, a larger extent of specific surface area, and a great amount of oxygen loosely bond in catalyst oxides, among which the first factor plays the most important role. The last is effective in improving the specific catalytic activity based on unit surface area, and is in a close relation to the two states, A and B, of different catalytic activities.

The authors of this paper wish to thank Mr. S. Kato of Tokyo Institute of Technology for taking X-ray diagrams.

Government Chemical Industrial Research Institute, Tokyo
Shibuya-ku, Tokyo

11) P. W. Selwood, "Advances in Catalysis", Vol. III, Academic Press, Inc., New York (1951), p. 42.
12) Y. Matsunaga, This Bulletin, **31**, 58, 145 (1958).
13) S. Sida et al., Abstracts of the 7th Annual Meeting of the Chemical Society of Japan, (1954), p. 157.

On The Mechanism of the Extraction of Uranyl Nitrate by TBP (Partition Study)*

By Keiji NAITO

(Received July 23, 1959)

The TBP (tri-*n*-butyl phosphate) extraction has been extensively employed for the uranium refining and the reprocessing of reactor spent fuel. A number of researches on this subject have appeared[1], and the mechanism of the uranium extraction by TBP was already proposed by Moore[2] as follows:

$$UO_2^{2+}(aq.) + 2NO_3^-(aq.) + 2TBP(org.) \rightleftarrows UO_2(NO_3)_2(TBP)_2(org.) \quad (1)$$

The more rigorous analysis for the mechanism of TBP extraction was made by McKay et al.[3-5] and the mechanism of uranium extraction was confirmed as Eq. 1 proposed by Moore.

* This study was presented at the 1st Symposium on Atomic Energy, Tokyo, January 13, 1957, and the 1st Symposium on Radiochemistry, Tokyo, December 21, 1957.
1) For example, R. I. Smith, TID-3502.
2) R. L. Moore, AECD-3196 (1951).
3) K. Alcock et al., *Trans. Faraday Soc.*, **52**, 39 (1956).
4) T. V. Healy and H. A. C. McKay, ibid., **52**, 633 (1956).
5) E. Hesford and H. A. C. McKay, ibid., **54**, 573 (1958).

The extraction of the nitric acid by TBP was also observed by Moore[2] and the following mechanism was proposed,

$$HNO_3(aq.) + TBP(org.) \rightleftarrows HNO_3 \cdot TBP(org.) \quad (2)$$

The formation of the complex $HNO_3 \cdot TBP$ was supported by McKay et al.[3] and the behavior of uranium on the TBP extraction from a nitric acid solution was concluded as a result of the competition of uranium and nitric acid[4].

The object of the present work is to propose a method of analysis to confirm the formation of a complex and to apply this analysis to the extractions of uranyl nitrate and nitric acid with TBP. The discussion for the extraction behavior of uranium from nitric acid solution by TBP is the second object of this work and thirdly the thermochemical functions for this kind of complex formation are to be determined.

Experimental

Reagents.—The reagents used in these experiments are as follows:

A) TBP.—The TBP (tri-*n*-butyl phosphate) was used after vacuum distillation.

B) Uranyl nitrate.—Uranyl nitrate was obtained from British Drug Houses Ltd. and was used after recrystallization.

C) Diluents.—As diluents, carbontetrachloride and kerosene were used. Boiling point range of kerosene used in the experiments is 190~260°C, specific gravity (15/4°C) is 0.8094.

Equipment and Method.—The Measurements of the distribution equilibrium were always made at constant temperature using a thermostated water bath. The separatory funnels were specially designed in order to be easily dipped into the water bath. The method for the measurement of distribution coefficients was the following. The necessary volumes of both aqueous and organic phases were put into a separatory funnel, which was dipped in the water bath. After the temperature had reached equilibrium, shaking of about one minute was repeated at intervals of fifteen or twenty minutes. Both phases were separated rapidly after an equilibrium time of about three or four hours. A centrifuge was used in the case where the separation was difficult. The distribution coefficients of both uranium and nitric acid were obtained by analyzing both in the aqueous phase.

The methods of analysis are the following. For uranium, the alkaline peroxide method[6] was adopted and a Hitachi EPU-2 spectrophotometer was used for the determination (at $\lambda = 400\ m\mu$). For nitric acid, the uranium peroxide precipitation method[7] was taken.

Notation.—C_M and C'_M denote the equilibrium concentrations of a species M in aqueous and organic phases respectively. $Kd(M)$ denotes the distribution coefficient of the species M ($=C'_M/C_M$). a_M is the activity of the species M in aqueous phase or organic phase, and f_M is its activity coefficient.

Results and Discussion

Distribution Equilibrium.—Prior to a discussion about the extraction mechanism, a general survey of distribution equilibrium of uranium between the aqueous and TBP phase was made. The results of the measurement can be summarized briefly as the following.

(a) In case nitric acid is added, the distribution coefficient of uranium is constant when the uranium concentration is low and the nitric acid concentration is kept constant, on the other hand, when nitric acid is absent, a constant distribution coefficient can not be obtained.

(b) The uranium concentration in organic phase increases with the uranium concentration in aqueous phase and reaches a constant which corresponds to the uranium concentration of $UO_2(NO_3)_2 \cdot (TBP)_2$ in organic phase as pointed out by Moore[2].

(c) The distribution coefficients of uranium increases with the nitric acid concentration in aqueous phase and reaches a maximum value, and then decreases gradually. Fig. 1 shows the influence of nitric acid concentration upon the distribution coefficient of uranium at various uranium concentrations.

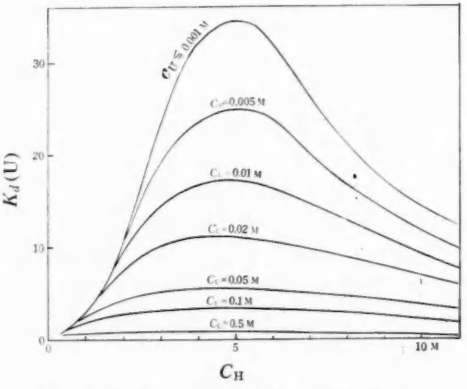

Fig. 1. Influence of nitric acid concentration upon the distribution coefficient of uranium at various concentrations.

6) C. J. Rodden and J. C. Warf, "Analytical Chemistry of the Manhattan Project", (National Nuclear Energy Series VIII-1(1950)).

7) R. E. Connik, MDDC-1245 (1945).

(d) The distribution coefficient of uranium is nearly proportional to the square of the TBP concentration in the organic phase when the concentrations of uranium and nitric acid are low and the nitrate concentration is held constant.

(e) The distribution coefficient of uranium decreases with the increase of temperature.

(f) The distribution coefficient of nitric acid coexisting with uranium decreases gradually with the increase of the uranium concentration in aqueous phase, but in the case where the nitric acid concentration is low the distribution coefficient of uranium reaches a maximum value and then decreases gradually.

(g) The influence of the nitric acid concentration in the aqueous phase on the distribution coefficient of nitric acid is markable when the uranium concentration is low. However, this influence becomes smaller with the increase of the uranium concentration in aqueous phase, and finally the distribution coefficient of nitric acid becomes nearly constant against the concentration of nitric acid in aqueous phase when the uranium concentration is higher than 0.1 M (Fig. 2).

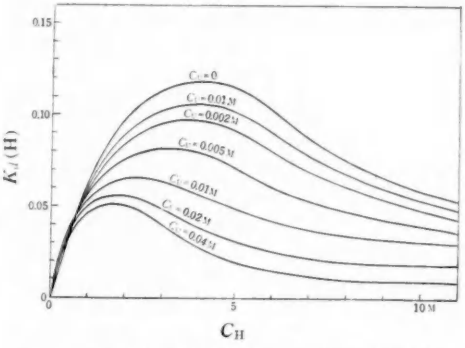

Fig. 2. The distribution coefficient of nitric acid coexisting with uranium.

From the above-mentioned distribution equilibrium of uranium, several pieces of information about the mechanism of the extraction of uranium can be obtained.

Facts b) and d) indicate that formation of the uranium complex with TBP in organic phase is likely. Therefore, it is possible to expect the following complex formation reaction considering the salting-out effect of nitrates on the extraction of uranium,

$$\mu UO_2^{2+}(\text{aq.}) + 2\mu NO_3^-(\text{aq.}) + \nu TBP(\text{org.}) \rightleftarrows [UO_2(NO_3)_2]_\mu(TBP)_\nu(\text{org.}) \quad (3)$$

where μ and ν are positive integers. The determination of μ and ν will be discussed later.

It is estimated from fact e) that this reaction should be an exothermic reaction.

Facts c) and f) also suggest that nitric acid is extracted together with uranium by TBP and both of these extraction reactions take place competitively.

Method of Analysis for an Extraction Mechanism.—Although there are several types of mechanisms by which a solute in aqueous phase can be extracted by organic solvent, one is the " mass-action " reaction between the solute ions and the organic solvent molecules as shown by Eq. 3.

This kind of extraction mechanism such as Eq. 3 is written as the following general expression,

$$\mu M^{n+}(\text{aq.}) + (n/m)\mu X^{m-}(\text{aq.}) + \nu S(\text{org.}) \rightleftarrows (MX_{n/m})_\mu S\nu(\text{org.}) \quad (4)$$

where

M_mX_n = inorganic solute (M^{n+} = cation, X^{m-} = anion)

S = organic solvent (extractant)

μ and ν = positive integers.

The purpose of the analysis is to obtain the value of μ and ν respectively without contradiction. The equilibrium constant (K) for Eq. 4 is given as

$$K = (a_{\text{complex}})/(a_M)^\mu(a_X)^{(n/m)\mu}(a_S)^\nu, \quad (5)$$

where a is the activity in aqueous phase or in organic phase and $a = fC$.

When the concentration of the solute is low, the ratio of the number of bonded solvent molecules to that of free solvent molecules is very small, so that Eq. 5 becomes

$$K = (f_{\text{complex}})(C_{\text{complex}})/(f_MC_M)^\mu(a_X)^{(n/m)\mu}(a_S^0)^\nu \quad (6)$$

where a_S^0 is the activity of the extractant solvent which corresponds to the initial concentration of extractant solvent in organic phase. In Eq. 6, f_{complex} is determined by the concentration of solvent in organic phase so that both f_{complex} and a_S^0 are constant at constant concentration of solvent.

If it is assumed that all M ions in organic phase are related to the formation of the complex, the following relation is obtained :

$$C_{complex}=C_M'/f' \quad (7)$$

Then from Eqs. 6 and 7, considering the relation: $C_{complex}/C_M=Kd(M)$

$$Kd(M)=\text{const.}\ (f_M{}^{\mu}/f_{complex})\cdot (C_M)^{\mu-1}(a_X)^{(n/m)\mu}(a_S{}^0)^{\nu} \quad (8)$$

From Eq. 8, the integers in Eq. 4 are determined experimentally as follows.

(1) Determination of μ.—In the case where the salting-out agent is absent, the activity a_X can be replaced with the concentration C_X, and f_M becomes unity, and C_X is determined uniquely by C_M as $(n/m)C_M$. When the distribution coefficient of M is measured at constant solvent concentration, $f_{complex}$ and $a_S{}^0$ are constant, as has been stated, so that Eq. 8 becomes

$$Kd(M)\cong\text{const.}\ (C_M)^{(1+n/m)\mu-1} \quad (9)$$

Thus by plotting $\log Kd(M)$ against $\log C_M$ the slope of the line indicates the value of $(1+n/m)\mu-1$, from which μ can be determined.

In the case where the salting-out agent exists, C_X is determined by both C_M and the concentration of the salting-out agent. If one adds a large amount of salting-out agent compared with C_M (which is low), both C_X and the ionic strength of the aqueous solution are mainly determined by the concentrationof the salting-out agent. Thus, when the distribution coefficient of M is measured at constant solvent concentration keeping the concentration of salting-out agent constant, Eq. 8 becomes

$$Kd(M)\cong\text{const.}\ (C_M)^{\mu-1} \quad (10)$$

because f_M and a_X are constant at costant ionic strength of the aqueous phase and $f_{complex}$ and $a_S{}^0$ are constant at constant solvent concentration. Thus, by plotting $\log Kd(M)$ against $\log C_M$ one can determine μ from the slope of the line.

(2) Determination of ν.—When the distribution coefficient of M is measured, keeping the aqueous phase concentration of M constant, and also keeping the concentration of the salting-out agent constant (if the salting-out agent exists), Eq. 8 becomes

$$Kd(M)\cong\text{const.}\ ((f_S{}^0)^{\nu}/f_{complex})(C_S{}^0)^{\nu} \quad (11)$$

where $f_S{}^0$ is the activity coefficient for $C_S{}^0$. Unfortunately both $f_S{}^0$ and $f_{complex}$ are the function of the solvent concentration $C_S{}^0$, and the determination of these activity coefficints for various solvent concentrations is not easy. However, if the measurement is made at low solvent concentration, the slope which is obtained by plotting $\log Kd(M)$ against $\log C_S{}^0$ roughly indicates the value of ν, because the deviation from the ideal solution becomes smaller according to the dilution of the solution.

The above-mentioned method is applicable to any reaction of the type of Eq. 4; however, it should be noticed that this method stands upon the assumption that all M ions in organic phase are combined with the solvent molecules. If this assumption does not exist, the method of analysis will become more complicated. On the other hand, when one can determine the integers μ and ν without contradiction under this assumption, one recognizes the validity of this assumption. An attention should be given to the case in which the successive complex formation by anion takes place according to the increase of the anion concentration, for example,

$$UO_2{}^{2+}+NO_3{}^- \rightleftarrows UO_2(NO_3)^+,$$

$$UO_2(NO_3)^+ + NO_3{}^- \rightleftarrows UO_2(NO_3)_2$$

Since the above-mentioned method of analysis is adopted for a low concentration region of the solute, this method can be applied without correction in case the salting-out agent is absent. In the case salting-out agent is added, the successive formation of the complex by anion will be expected, but the method is still applicable without correction, because the ionic strength of the solution is kept nearly constant. However, if an anionic complex such as $UO_2(NO_3)_3{}^-$, $UO_2(NO_3)_4{}^{2-}$, etc., is formed, the treatment must be changed.

Although this kind of method of analysis was used at first by Moore[2], the treatment was not rigorous. Eq. 11 was also derived by McKey et al.[5] and ν was called the solvation number. It is important, however, to confirm the existence of "mass-action" reaction for the solvent extraction process by applying the above-mentioned analysis.

Mechanisms of the Extraction for Uranium and Nitric Acid.—*(1) Uranyl nitrate extraction by TBP.*—The integers μ and ν in Eq. 3 were determined by applying the above-mentioned method in the following way.

μ is determined easily as $\mu=1$ from fact a) and Eq. 10 in case the salting-out agent exists. However, in case the salting-out agent is absent, no linear relation between $\log Kd(U)$ and $\log C_U$ was observed while a linear relation was expected from Eq. 9. This means that the mechanism of extraction in this case is not consistent with

the mechanism postulated in Eq. 3, and uranyl nitrate must be hydrolyzed, especially in the low concentration region and in the case where no acid exists, so that the mechanism of extraction must change.

ν was determined as $\nu = 2$ by applying Eq. 11. The linear relation between $\log[Kd(\mathrm{U})/(a_{NO_3})^2]$ and $\log C^0_{TBP}$ was observed as $\nu = 2$ for the low TBP concentration region.

Accordingly one obtained the same mechanism as that proposed by Moore for uranyl nitrate extraction by TBP. Though the same result was obtained, it should be noticed that the existence of this mechanism was confrimed beyond doubt by this analysis and this mechanism does not exist when the hydrolysis of uranium takes place.

On the extraction of uranium from a nitric acid solution by TBP, it was already observed that nitric acid coexisting with uranium is not only effective as a salting-out agent, also extractable together with uranium by TBP, so that the mechanism of the extraction of nitric acid should also be studied in order to clarify the mechanism of the extraction of the U–HNO_3–TBP system.

(2) Nitric acid extraction by TBP.—One can expect the reaction of nitric acid with TBP molecules as expected in the case of uranyl nitrate extraction, then

$$\mu H^+(\mathrm{aq.}) + \mu NO_3^-(\mathrm{aq.}) + \nu TBP(\mathrm{org.}) \rightleftarrows (HNO_3)_\mu(TBP)_\nu(\mathrm{org.}) \qquad (12)$$

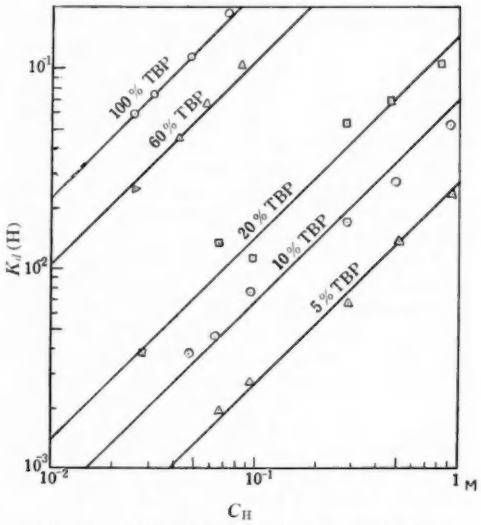

Fig. 3. Determination of μ in case the salting-out agent is absent.

The integers μ and ν in Eq. 12 can be determined as follows.

(a) Determination of μ.—In the case where the salting-out agent exists, μ is determined by Eq. 10. The result of the measurement of Kd(H) for dilute nitric acid when sodium nitrate is added as a salting-out agent shows that Kd(H) is constant independent of C_H when the concentration of salting-out agent is kept constant. Then, by applying to Eq. 10, μ is determined as $\mu = 1$.

In the case where the salting-out agent is absent, μ is determined by Eq. 9, Fig. 3 was obtained by plotting Kd(H) againts $\log C_H$ at 25°C for TBP-kerosene system. The existence of a linear relation is observed and the slope of this line is 1 independently with TBP concentration. An essentially the same result was obtained when the diluent is carbon tetrachloride. Then, from Eq. 9, μ is determined again as $\mu = 1$.

(b) Determination of ν.—The value of ν is determined by using Eq. 11. Fig. 4 was obtained by plotting $\log Kd$(H) against $\log C^0_{TBP}$ at 25°C, where the diluent is carbon tetrachloride. In this figure, the lines A and A′ are for the case no

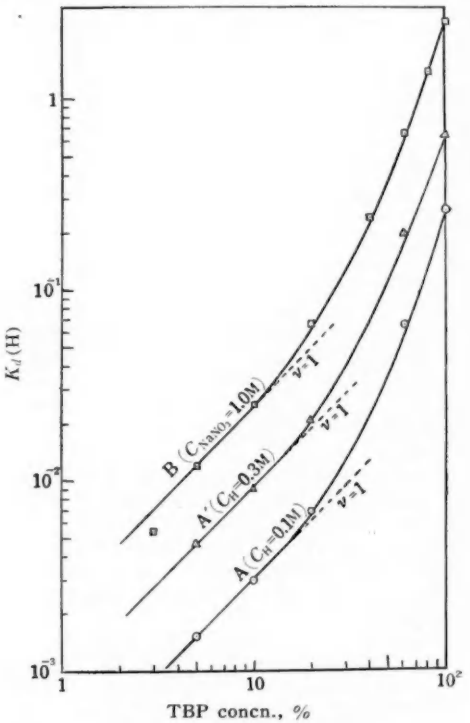

Fig. 4. Determination of ν.

salting-out agent exists and the line B is for the case the salting-out agent exists (1 M $NaNO_3$). It is noteworthy that both A (A') and B give nearly the same results. For a region where the TBP concentration is low, the linear relations are obtained and slopes are 1 for each case. The essentially the same results are obtained in case the diluent is kerosene. Then, from Eq. 11, ν is determined as $\nu=1$.

However, in a region where the TBP concentration is higher, the slopes are changing from one to two. It is not clear at the present stage whether this is based upon the change of activity coefficients ($f_S^0/f_{complex}$) in Eq. 11 or the formation of a complex $HNO_3(TBP)_2$.

As a result of above-mentioned analysis for the HNO_3–TBP system, the mechanism of the nitric acid extraction by TBP was confirmed as

$$H^+(aq.) + NO_3^-(aq.) + TBP(org.) \rightleftarrows HNO_3 \cdot TBP(org.) \quad (13)$$

On the other hand, Moore proposed Eq. 2 as the mechanism of nitric acid extraction by TBP. This mechanism was derived from the fact that Kd(H) is nearly constant, independent of the nitric acid concentration in the case of uranium extraction. However, as shown in fact g) this is true only in case the uranium concentration is higher than about 0.1 M, and his observation was made just in this range ($C_U=0.1\sim0.4$ M). So it is not suitable to discuss the mechanism of nitric acid extraction basing only on this fact. It may be reasonable to interpret this fact as a result of the competition of uranium and nitric acid as will be discussed later.

Competition of Uranium and Nitric Acid.—It has been clarified that both uranium and nitric acid are extracted according to the above-mentioned mechanisms. With these mechanisms, the behavior of both uranium and nitric acid during the extraction process should be interpreted as follows.

(1) Simultaneous partition of uranium and nitric acid.—In case uranium is extracted from a nitric acid solution by TBP, the distribution equilibria of Eqs. 1 and 13 should be established simultaneously. Then, one obtains the following simultaneous equations,

$$K(U) = [f_{complex}(U)/(f_{\pm}(U))^3] \cdot [Kd(U)/C_{NO_3}^2(a_{TBP})^2] \quad (14)$$

$$K(H) = [f_{complex}(H)/(f_{\pm}(H))^2] \cdot [Kd(H)/(C_{NO_3})(a_{TBP})] \quad (15)$$

where K(U) and K(H) are the equilibrium constants of uranium for Eq. 1 and of nitric acid for Eq. 13, $f_{\pm}$(U) and $f_{\pm}$(H) are the mean activity coefficients of uranyl nitrate and of nitric acid.

When the concentrations of both uranium and nitric acid are low, if one keeps the ionic strength of solution constant, the activity coefficient in aqueous phase is kept nearly constant, and the activity coeficients of the complex in organic phase are nearly constant because the concentration is very low. In such a case, the following relation is obtained :

$$\log Kd(H) \cong (1/2) \log Kd(U) + \text{const.} \quad (16)$$

This relation was confirmed by Fig. 5

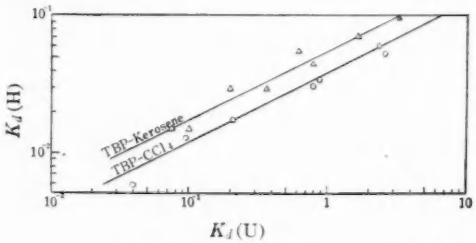

Fig. 5. Existence of simultaneous partition of both uranium and nitric acid.

which was obtained from the measurements under the uranium concentration range : 0.005~0.05 M, and the nitric acid concentration range : 0.1~1 M and at TBP 20%, 25°C. Though this measurement was made at various ionic strengths, the linear relationship is still observed in both the TBP–CCl_4 system and the TBP-kerosene system, and the slopes are both 1/2.

By this analysis, it was confirmed that when uranium is extracted from a nitric acid solution by TBP, both the extraction reaction of uranium shown by Eq. 1 and the extraction reaction of nitric acid shown by Eq. 13 take place simultaneously.

(2) The influence of the nitric acid concentration upon Kd(U).—In the distribution equilibrium of uranyl nitrate, Kd(U) has its maximum value against the change of C_H as shown by fact c). This can be interpreted as a result of the competition of both uranium and nitric acid in the following way.

In the case where the concentration is low, if one replaces the activity by the concentration in order to make the discussion simple, the following simultaneous equations exist approximately,

$$K(U) \cong Kd(U)/C_H^2(C^0_{TBP}-C_H')^2 \quad (17)$$

$$K(\mathrm{H}) \cong C_{\mathrm{H}}'/C_{\mathrm{H}}^{2}(C^{0}_{\mathrm{TBP}} - C_{\mathrm{H}}') \qquad (18)$$

where C^{0}_{TBP} represents the initial concentration of TBP in organic phase. From Eqs. 17 and 18 by eliminating C_{H}',

$$Kd(\mathrm{U}) = K(\mathrm{U})\,[C_{\mathrm{H}}C^{0}_{\mathrm{TBP}}/(1+K(\mathrm{H})C_{\mathrm{H}}^{2})]^{2} \qquad (19)$$

Eq. 19 gives the relation between Kd(U) and C_{H} in a region where the uranium concentration is low. It can easily be shown from Eq. 19 that Kd(U) increases with the increase of C_{H}, reaches a maximum value, then decreases gradually. Furthermore, the maximum value of Kd(U) is obtained from Eq. 19 as $K(\mathrm{U})(C^{0}_{\mathrm{TBP}})^{2}/4K(\mathrm{H})$ at $C_{\mathrm{H}}=1/\sqrt{K(\mathrm{H})}$. If one takes $K(\mathrm{U})=27$, $K(\mathrm{H})=0.08$ as the values of equilibrium constants respectively at 25°C, TBP 20% (these values were obtained tentatively as the equilibrium constants), one obtains as the calculated values: $Kd(\mathrm{U})_{\max}=45$ at $C_{\mathrm{H}}=3.5$ M. These correspond to the following experimental values: $Kd(\mathrm{U})_{\max}=34$ at $C_{\mathrm{H}}=5$ M. Considering that this calculation was made using the concentration instead of the activity, the agreement seems to be fairly good.

In case the uranium concentration is higher, although the calculation becomes more complicated, one can obtain a similar result.

Accordingly, it was confirmed that fact c) is interpreted as the result of the competition of both uranium and nitric acid as was pointed out by Moore[2] and McKay[4,8]. From this point of view, facts f) and g) are also interpreted as the result of the competition of both.

(3) Nitric acid and sodium nitrate as salting-out agent. — On the extraction of uranium from a nitric acid solution, it was clarified that both uranium and nitric acid are extracted by TBP competitively. Accordingly, it is interesting to observe the behavior of the extraction of uranium when the salting-out agent which is not extractable by TBP is added.

Sodium nitrate was chosen as one of those agents that are suitable for this purpose. The salting-out effects of both nitric acid and sodium nitrate for diluted uranyl nitrate are shown in Fig. 6 which was made at 25°C, TBP 20% (in the case of sodium nitrate, 0.5 M nitric acid is added in order to prevent the hydrolysis of uranium).

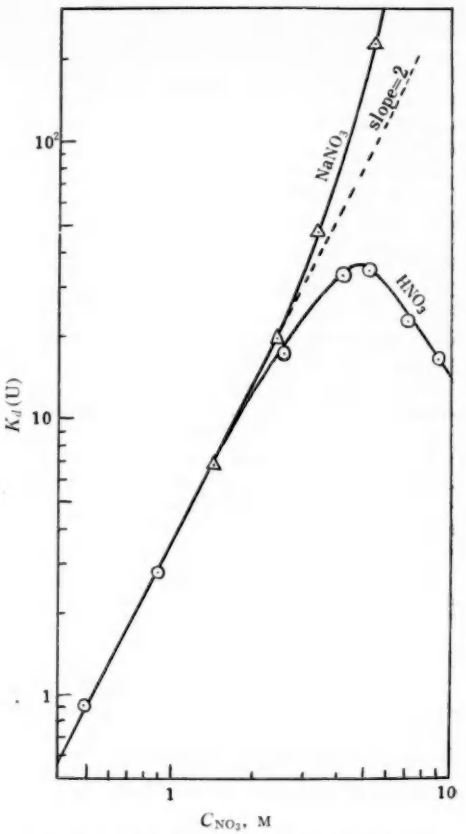

Fig. 6. The salting-out effect of both nitric acid and sodium nitrate for diluted uranyl nitrate.

It is obvious from Fig. 6 that, in the case of nitric acid, Kd(U) has the maximum at C_{NO_3} of nearly 5 M; and in the case of sodium nitrate, Kd(U) increases monotonously and is nearly proportional to the square of C_{NO_3}.

When the salting-out agent is not extracted by TBP and contributes only to the increase of the concentration of NO_3^-, one obtains the relation: $Kd(\mathrm{U}) = \text{const.} \times (C_{NO_3})^2$ from Eq. 14 by ignoring the activity coefficient. Then Kd(U) is nearly proportional to $(C_{NO_3})^2$. It can also be understood from this analysis that little sodium nitrate is extracted by TBP and is effective only as a salting-out agent for the uranium extraction.

However, it is noteworthy that when the concentration of nitric acid is low, nitric acid is also effective mainly as a salting-out agent. This is observed from

8) H. A. C. McKay, "Int. Conf. Peaceful Uses of Atomic Energy", United Nations, (1955), p./441.

Fig. 6 and is also derived from Eq. 19 as $Kd(\mathrm{U}) = \mathrm{const.}(C_{\mathrm{H}})^2$ by considering C_{H} is small. This relation just corresponds to the relation $Kd(\mathrm{U}) = \mathrm{const.}(C_{\mathrm{NO_3}})^2$, therefore, nitric acid is effective mainly as a salting-out agent when its concentration is low.

Rough Determination of the Thermochemical Functions of the Reaction of Uranyl Nitrate and TBP.—Although the existence of the complex with TBP such as $UO_2(NO_3)_2(TBP)_2$, $HNO_3 \cdot TBP$ was confirmed, the nature of these complexes remains uncertain. At first the measurement of the thermochemical functions was tried.

ΔH^0, ΔF^0 and ΔS^0 are defined as the enthalpy change, the Gibbs' free energy change and the entropy change respectively for Eq. 1 when the activities of each species of Eq. 1 are unity. These thermodynamical functions are determined roughly by using the distribution coefficient as the following.

(1) Enthalpy change.—By applying a thermodynamical relation for the reaction of Eq. 1

$$(\partial \ln K(\mathrm{U})/\partial T)_P = \Delta H^0/\boldsymbol{R}T^2 \qquad (20)$$

The equilibrium constant $K(\mathrm{U})$ is given as Eq. 14. If one keeps both the concentration of salting-out agent and the concentration of TBP constant, the equilibrium constant $K(\mathrm{U})$ becomes

$$K(\mathrm{U}) = \mathrm{const.}\,[f_{\mathrm{complex}}/(f_{\pm}(\mathrm{U}))^3 \times (f_{\mathrm{TBP}})^2]\,Kd(\mathrm{U}) \qquad (21)$$

When the concentration is low, the temperature dependence of the activity coefficient is very small, so that one can obtain the following relation from Eqs. 20 and 21

$$(\partial \ln Kd(\mathrm{U})/\partial T)_P \cong \Delta H^0/\boldsymbol{R}T^2 \qquad (22)$$

If one assumes that ΔH^0 is constant for the integration range, from Eq. 22

$$\ln Kd(\mathrm{U}) \cong \mathrm{const.} - \Delta H^0/\boldsymbol{R}T \qquad (23)$$

Thus by plotting $\log Kd(\mathrm{U})$ vs. $1/T$ the slope of the line indicates the value $-\Delta H^0/\boldsymbol{R}$, from which ΔH^0 can be obtained.

The measurement of the distribution coefficient of uranium was made at 10, 25 and 50°C, respectively. The concentration of uranium in this measurement is low enough to neglect the temperature dependence of the activity coefficient and to keep the concentration of TBP constant.

The linearity between $\log Kd(\mathrm{U})$ and $1/T$ was observed obviously in both the TBP–CCl_4 system and the TBP-kerosene system, and the slopes in both systems were exactly the same. Then, the enthalpy change ΔH^0 was obtained by measuring the slope of the line as

$$\Delta H^0 = -4.3\ \mathrm{kcal.}\ (10 \sim 50^\circ\mathrm{C})$$

This value has nearly the same order of the bonding energy of the hydrogen bond, so that it can be estimated that the bond strength or stability of this complex should be of nearly the same order as those of the hydrogen bond.

(2) Gibbs' free energy change.—Gibbs' free energy change ΔF^0 for the reaction of Eq. 1 is given as

$$\Delta F^0 = -\boldsymbol{R}T \ln K(\mathrm{U}) \qquad (24)$$

The equilibrium constant $K(\mathrm{U})$ is given as Eq. 14 and it is necessary to know the value of the activity coefficient of each species in order to calculate the $Kd(\mathrm{U})$. Unfortunately the activity coefficient of the organic phase is not clear though the activity coefficient of the aqueous phase is available. However, in organic phase, the activity coefficients of each species can be considered as nearly unity so far as the concentration is very low.

It is necessary to make the solution acidic in order to prevent the hydrolysis of uranium, otherwise the mechanism of extraction will change as has been stated already. Therfore, the measurement of the distribution equilibrium of uranium must be made under slightly acidic condition.

The equilibrium constant was calculated by using activity coefficients of uranyl nitrate and nitric acid in aqueous phase and by assuming the activity coefficients of the complex and TBP in organic phase as unity.

The results obtained are the following: $Kd(\mathrm{U})$ are 25.6, 25.2, 21.6 and 20.2 when the initial concentrations of nitric acid are 0.05, 0.1, 0.2 and 0.3 M, respectively. So one can observe that the equilibrium constant of uranium decreases gradually according to the increase of the concentration of nitric acid. This is considered as the result of the extraction of nitric acid into organic phase which causes the deviation of the activity coefficient in organic phase from unity.

Accordingly the following value is obtained as the rough value of $Kd(\mathrm{U})$ at 25°C by extrapolating to the zero nitric acid concentration: $K(\mathrm{U}) = 27$ (25°C). From this $K(\mathrm{U})$ value, one obtains Gibbs' free energy change of Eq. 1 by using Eq. 24 as

$$\Delta F^0 \cong -2.0 \text{ kcal. } (25^\circ\text{C})$$

This small change of ΔF^0 suggests that uranium can be transferred easily between aqueous and TBP phases by changing the concentration of salting-out agent.

(3) Entropy change.—The entropy change ΔS^0 for Eq. 1 is given as

$$\Delta S^0 = (\Delta H^0 - \Delta F^0)/T \qquad (25)$$

If $\Delta H^0 \cong -4.3$ kcal. which was obtained as the average value for 10~50°C is used as the value at 25°C, the entropy change at 25°C is obtained as

$$\Delta S^0 = -7.7 \text{ e. u. } (25^\circ\text{C})$$

Summary

The method of analysis using the distribution coefficient to confirm the mechanism of extraction was proposed and the formation of the complex $UO_2(NO_3)_2 \cdot (TBP)_2$ and $HNO_3 \cdot TBP$ was confirmed. The extraction behavior of uranium from a nitric acid solution was concluded as a result of the competition of uranium and nitric acid. The thermochemical functions ΔH^0, ΔF^0 and ΔS^0 for the complex formation reaction:

$$UO_2^{+2}(\text{aq.}) + 2NO_3^-(\text{aq.}) + 2\text{TBP(org.)} = UO_2(NO_3)_2(\text{TBP})_2(\text{org.})$$

were determined roughly from the measurement of the distribution coefficient as follows: $\Delta H^0(25^\circ\text{C}) \cong -4.3$ kcal., $\Delta F^0(25^\circ\text{C}) \cong -2.0$ kcal., $\Delta S^0(\sim 25^\circ\text{C}) \cong -7.7$ e.u.

The author would like to express his gratitude to Dr. K. Kimura, Dr. T. Nakai, Dr. K. Oshima and Dr. R. Hara for their invaluable assistance and advice in this work. He also thanks Mr. T. Suzuki for his help during the experiment.

Japan Atomic Energy Research Institute
Tokai, Ibaraki

The Effect of Metallic Ions on Surface Chemical Phenomena. III. Solubility of Various Metal Dodecyl Sulfates in Water

By Shigeru MIYAMOTO

(Received August 26, 1959)

In the preceding paper[1] a study was made of the effects of various inorganic electrolytes on the stability and type of emulsions stabilized with sodium dodecyl sulfate. Added polyvalent cations were found to cause phase inversion of the emulsions. These effects can hardly be explained without taking into consideration the properties of corresponding metal dodecyl sulfates formed as the consequence of the reaction of sodium dodecyl sulfate with these cations. In order to understand the nature of the effect of metallic ions in these systems it is, therefore, necessary to investigate fully the properties of various metal dodecyl sulfates, more generally metal alkyl sulfates in aqueous solutions.

Some studies have been reported regarding their properties up to the present. Nishizawa and Tomizuka[2] studied the compositions and crystallographic habits of hexadecyl sulfates of potassium, sodium, ammonium, magnesium and calcium. They also made reference qualitatively to the solubility of these compounds in various solvents. Ueno, Yokoyama and Iwakura[3] found that solubilities of ammonium-, sodium- and potassium dodecyl sulfates and hexadecyl sulfates decrease in this order. They studied also the foam formation, surface tension, interfacial tension at oil-water interface and detergent action of these metal dodecyl sulfates. Yoshizaki and Terashima[4] studied the change of foam volume on aqueous solutions of sodium hexadecyl sulfate with the course of time. Measurement of foam of ammonium-, magnesium- and calcium dodecyl sulfate and hexadecyl sulfate

1) S. Miyamoto, *Mem. Fac. Sci. Kyushu Univ., Series C, Chem.*, in press.
2) K. Nishizawa and T. Tomizuka, *J. Chem. Soc. Japan, Ind. Chem. Sec.* (*Kogyo Kagaku Zasshi*), **35**, 1368 (1923).
3) S. Ueno, S. Yokoyama and Y. Iwakura, ibid., **38**, 1333 (1935).
4) T. Yoshizaki and H. Terashima, ibid., **55**, 350 (1952).

solutions was made by Nakashima[5]. Lottermoser et al.[6] synthesized metal alkyl sulfates and undertook measurements of conductance, potential, surface tension and interfacial tension of their aqueous solution. These authors gave consideration to the change of dissolved state with the change of concentration of the solution. Further, Giers and Boido[7] measured cloud point, viscosity, pH, contact angle, wetting speed and foaming property of ammonium-, sodium-, potassium-, magnesium-, calcium- and zinc dodecyl sulfates. As regards solubility, sodium dodecyl sulfate, tetradecyl sulfate and hexadecyl sulfate were studied by Hutchinson et al.[8] at various temperatures. On the solubility of metal alkyl sulfates, however, only a few data have been reported. The solubility of calcium dodecyl sulfate was given as 0.03~0.04% at 25°C by Lenher[9], 0.00457 mol./1000 g. H_2O at 50°C by Tartar and Cadle[10] and 0.5 g./l. at 53°C and 1.0~5.0 g./l. at 54°C[11].

In the preceding paper reported by the author[1] values of solubility of sodium-, calcium-, barium-, aluminum-, iron- and thorium dodecyl sulfates were given at 25°C. It seems, however, that further studies are necessary to obtain full knowledge regarding the values of solubility of many other metal dodecyl sulfates. So one has conducted the measurements of solubility of calcium-, strontium-, lead-, barium-, copper, manganese-, magnesium- and cobalt dodecyl sulfates at various temperatures. It is the purpose of the present paper to report the results of the solubility measurement of these metal dodecyl sulfates and to undertake some discussions concerning them.

Experimental

Materials.—Metal dodecyl sulfates were synthesized from pure sodium dodecyl sulfate (abbreviated as SDS) which was synthesized from pure dodecyl alcohol and a guaranteed reagent of concentric sulfuric acid according to the method described in the papers already reported[1,12]. Pure dodecyl alcohol used was obtained by fractional distillations in vacuo. Synthesized SDS was freed from unsulfated dodecyl alcohol by extraction with ethyl ether for about forty hours in a Soxhlet extractor. The purity of the SDS sample was ascertained from the absence of the minimum in the curve representing surface tension of its aqueous solutions versus its concentration and also from results of elementary analysis of the sample. From these results[1], it was found that the SDS sample was highly pure surface-chemically. Metal dodecyl sulfates were precipitated from SDS aqueous solution by adding concentrated aqueous solutions of magnesium-, calcium-, strontium-, barium-, cupric-, lead-, manganous- and cobaltous chlorides. All these electrolytes had been purified before they were used for the preparation of corresponding metal dodecyl sulfates. The precipitated metal dodecyl sulfates were taken out by filtration by a glass filter and then they were recrystallized further three times except in the case of barium salt which was found to be soluble only in small amount even at high temperatures. Washing with water was carried out fully after every recrystallization. Readily soluble metal dodecyl sulfates were washed with cold water. After purification, they were brought into the air-dried state. Elementary analysis and metal content analysis were conducted on these air-dried samples.

Method.—Measurements of solubility were performed as usual by weighing the amounts of solute contained after drying up known weights of the saturated solution at 50°C. It was found that long periods of time were necessary to attain true equilibrium of solubility, so the bottle containing the sample was shaken to accelerate the attainment of equilibrium. The process of attainment of equilibrium is shown in Fig. 1 with magnesium-, calcium-, strontium-, lead- and barium dodecyl sulfates.

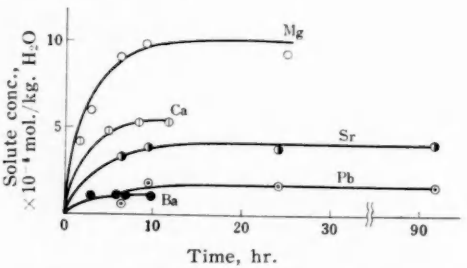

Fig. 1. Attaiment of equilibrium of the solubility in solution of Mg-, Ca-, Sr-, Pb- and Ba dodecyl sulfates in water with the course of stirring time.

Results

At first, elementary analyses of carbon, hydrogen and metal contents of air-dried metal dodecyl sulfates were carried out

5) H. Nakashima, ibid., **56**, 611 (1953).
6) A. Lottermoser and F. Püschel, *Kolloid-Z.*, **63**, 175 (1933); A. Lottermoser and F. Stoll, ibid., **63**, 49(1933).
7) S. Giers and D. Boido, *Soap Chem. Specialities*, **30**, 38, 179 (1954).
8) E. Hutchinson, K. E. Manchester and L. Winslow, *J. Phys. Chem.*, **58**, 1124 (1954).
9) S. Lenher, *Am. Dyestuff Reptr.*, **22**, 663 (1933).
10) H. V. Tartar and R. D. Cadle, *J. Phys. Chem.*, **43**, 1173 (1939).
11) K. Kanamaru, "Surface Active Agents (Kaimen Kassei Zai)", Maki Shoten, Tokyo (1955), p. 47.
12) R. Matuura, H. Kimizuka, S. Miyamoto and R. Shimozawa, This Bulletin, **31**, 532 (1958).

TABLE I. RESULTS OF ELEMENTARY ANALYSIS AND METAL CONTENT ANALYSIS OF AIR-DRIED METAL DODECYL SULFATES

Metal		Metal content %	Elementary analysis C, %	H, %
Ca	Found	9.33	49.10	8.65
	Calcd. as $Ca(DS)_2$	9.38	49.19	8.60
Sr	Found	14.22	46.95	8.11
	Calcd. as $Sr(DS)_2$	14.18	46.59	8.15
Ba	Found	20.53	43.36	7.77
	Calcd. as $Ba(DS)_2$	20.57	43.12	7.55
Pb	Found	28.04	38.90	6.89
	Calcd. as $Pb(DS)_2$	28.09	39.04	6.83
Mn	Found	9.33	49.10	8.65
	Calcd. as $Mn(DS)_2$	9.38	49.19	8.60
Mg	Found	3.67	43.43	9.47
	Calcd. as $Mg(DS)_2 \cdot 6H_2O$	3.77	43.48	9.35
Co	Found	8.65	41.23	8.95
	Calcd. as $Co(DS)_2 \cdot 6H_2O$	8.45	41.29	8.96
Cu	Found	—	43.09	8.86
	Calcd. as $Cu(DS)_2 \cdot 4H_2O$	—	43.23	8.78

TABLE II. VALUES OF SOLUBILITY (mol./1000 g. H_2O) OF METAL DODECYL SULFATES AT VARIOUS TEMPERATURES (THOSE OF GREATER SOLUBILITY)

Temp., °C	$Cu(DS)_2 \cdot 4H_2O$	$Mn(DS)_2$	$Co(DS)_2 \cdot 6H_2O$	$Mg(DS)_2 \cdot 6H_2O$
5.0	1.99×10^{-2}	2.12×10^{-3}	—	—
10.0	2.46×10^{-2}	4.15×10^{-3}	—	6.39×10^{-4}
13.0	—	5.26×10^{-3}	—	—
15.0	3.48×10^{-2}	6.35×10^{-3}	8.08×10^{-4}	8.06×10^{-4}
16.0	—	1.75×10^{-2}	—	—
17.0	—	8.92×10^{-1}	—	—
20.0	—	8.99×10^{-1}	9.01×10^{-4}	9.27×10^{-4}
23.0	4.12×10^{-2}	—	9.78×10^{-4}	9.58×10^{-4}
25.0	6.53×10^{-2}	—	2.53×10^{-3}	9.58×10^{-4}
25.8	9.30×10^{-1}	—	—	—
26.5	9.68×10^{-1}	—	—	—
28.0	—	—	9.81×10^{-3}	4.98×10^{-3}
31.0	—	—	4.17×10^{-2}	4.46×10^{-2}

TABLE III. VALUES OF SOLUBILITY (mol./1000 g. H_2O) METAL DODECYL SULFATES AT VARIOUS TEMPERATURES (THOSE OF SMALLER SOLUBILITY)

Temp., °C	$Ca(DS)_2$	$Sr(DS)_2$	$Pb(DS)_2$	$Ba(DS)_2$
25.0	4.61×10^{-4}	4.05×10^{-4}	1.76×10^{-4}	1.15×10^{-4}
35.0	7.31×10^{-4}	5.39×10^{-4}	1.21×10^{-4}	1.74×10^{-4}
40.0	9.33×10^{-4}	—	—	—
45.0	—	8.10×10^{-4}	2.81×10^{-4}	2.55×10^{-4}
50.0	1.62×10^{-3}	—	—	—
51.0	2.09×10^{-2}	—	—	—
52.6	2.30×10^{-2}	—	—	—
54.0	—	—	1.18×10^{-3}	—
55.0	2.45×10^{-2}	1.09×10^{-3}	3.43×10^{-3}	—
58.0	—	—	6.37×10^{-2}	—
60.0	—	1.40×10^{-3}	6.54×10^{-2}	—
65.0	—	3.59×10^{-3}	7.82×10^{-2}	5.06×10^{-4}
65.5	—	3.59×10^{-2}	—	—
66.0	—	6.25×10^{-2}	—	—
67.0	—	7.46×10^{-2}	—	—
70.0	—	—	—	6.74×10^{-4}
75.4	—	—	—	8.02×10^{-4}
100.0	—	—	—	1.66×10^{-3}

and the results are shown in Table I. From these results the compositions of metal dodecyl sulfates were determined. That is, they were found to have the following formulae. $Ca(DS)_2$, $Sr(DS)_2$, $Ba(DS)_2$, $Pb(DS)_2$, $Mn(DS)_2$, $Mg(DS)_2 \cdot 6H_2O$, $Co(DS)_2 \cdot 6H_2O$ and $Cu(DS)_2 \cdot 4H_2O$, where the abbreviation DS represents the dodecyl sulfate radical.

Values of solubility of these metal dodecyl sulfates were obtained at various temperatures and they are shown in Table II (greater solubility) and Table III (smaller solubility).

It has been well known that soaps have the Krafft point above which their solubilities increase enormously. The Krafft point has also been observed generally with the surface active agents such as sodium alkyl sulfates[5], sodium alkyl sulfonates[13], anisidine sodium sulfonates, alkyl pyridinium halides and alkyl trimethylammonium halides[14]. Metal dodecyl sulfates are considered to be surface active agents also, so they are expected to have a Krafft point. To examine whether they have a Krafft point or not, plots of logarithms of solubility versus reciprocals of temperature were drawn as shown in Fig. 2. In this figure, the intersections of two straight lines are seen, which show the Krafft points. The values of Krafft points thus obtained are shown in Table IV.

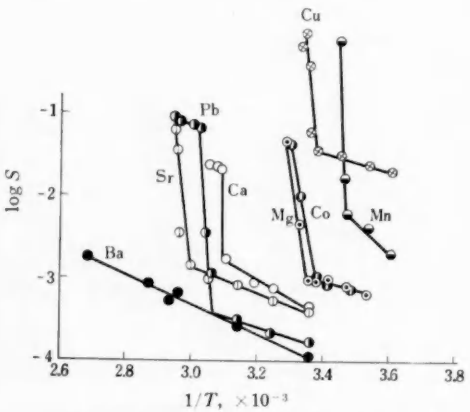

Fig. 2. Relation between the logarithms of solubility of various metal dodecyl sulfates and the reciprocals of absolute temperature.

13) H. V. Tartar and K. A. Wright, *J. Am. Chem. Soc.*, **61**, 539 (1939).
14) N. K. Adam and K. G. A. Pankhurst, *Trans. Faraday Soc.*, **42**, 523 (1946).

TABLE IV. KRAFFT POINTS OF VARIOUS METAL DODECYL SULFATES

Substance	Krafft point, °C
$Mn(DS)_2$	16
$Co(DS)_2 \cdot 6H_2O$	23
$Cu(DS)_2 \cdot 4H_2O$	24
$Mg(DS)_2 \cdot 6H_2O$	25
$Ca(DS)_2$	50
$Pb(DS)_2$	53
$Sr(DS)_2$	64
$Ba(DS)_2$	—*

* Krafft point of $Ba(DS)_2$ was not observed below 100°C.

Discussion

From the results of the composition of various metal dodecyl sulfates shown in Table I it is confirmed that calcium-, barium, magnesium- and cupric dodecyl sulfates have the same formulae as those already given by Lottermoser et al.[6] It is noted that some of them have crystalline water. All metal dodecyl sulfates examined were found to have the two dodecyl sulfate radicals in their molecules, presumably showing no hydrolysis of the cations contained in them throughout the process of preparation.

The values of solubility of metal dodecyl sulfates examined were found to increase rapidly with the increase of temperature above the respective Krafft point, except for the case of barium dodecyl sulfate as shown in Fig. 2. The Krafft point could be obtained as the intersect of two straight lines in the diagrams of logarithms of solubility versus the reciprocals of temperature. This method of obtaining the Krafft point has been known to be applicable to many surface active substances in general. From their behaviors in solution, metal dodecyl sulfates are considered to be also a group of the surface active substances.

The values of solubility of magnesium-, calcium-, strontium- and barium dodecyl sulfates in water below the respective Krafft point decrease in this order, which is the same order as that of the values of solubility in water of the inorganic metal sulfates having these cations and also the same as the order of increase of ionic radii of these cations. This series of gegenions is also applied to the values of Krafft point of these metal dodecyl sulfates. These correspondences are, however, not to be extended to manganese-, lead-, cobalt- and copper dodecyl sulfates. As a whole, the Krafft points of various metal dodecyl

sulfates seem to become higher as their solubilities decrease. At a temperature above the Krafft point the micelles of a surface active substance may be formed in the aqueous solution as explained by Murray and Hartley[15]. It has been found from the surface tension vs. concentration diagrams that the critical concentration for micelle formation of the solution of metal dodecyl sulfates of divalent cations is almost the same irrespective of the difference in the kind and type of gegenions. (The details of the surface tension measurement will be reported in a separate paper.) A sparingly soluble metal dodecyl sulfate can let its concentration reach the critical concentration for micelle formation at higher temperatures than more soluble metal dodecyl sulfate.

15) R. C. Murray and G. S. Hartley, ibid., **31**, 183 (1935).

Summary

Calcium, strontium-, barium-, lead-, manganese-, magnesium-, cobalt- and copper dodecyl sulfates were synthesized and their compositions were determined from the results of their elementary analysis and metal content analysis. Further, the solubility of these metal dodecyl sulfates was measured at various temperatures. From these data, these metal dodecyl sulfates except barium salt were found to have the Krafft points, values of which were shown also.

The author expresses his sincere gratitude to Professor R. Matuura of Kyushu University for his guidance and encouragement.

Department of Chemistry
Faculty of Science
Kyushu University
Hakozaki, Fukuoka

The Effect of Metallic Ions on Surface Chemical Phenomena. IV. Surface Tension Measurement on Aqueous Solutions of Metal Dodecyl Sulfates

By Shigeru MIYAMOTO

(Received August 26, 1959)

In the preceding paper[1a], the effect of metal ions on the properties of the emulsion stabilized with sodium dodecyl sulfate was investigated and in connection with it the solubility of various metal dodecyl sulfates was studied[1b]. Metal dodecyl sulfates should be formed in many systems containing sodium dodecyl sulfate and metal ions as a result of a reaction of the former with the latter. They were supposed to constitute also a group of surface active substances from the existence of their Krafft points measured by the temperature change of their solubilities in water. To explain the Krafft point, the presence of micelles of the solute has been assumed. It is therefore expected that metal dodecyl sulfates begin to form the micelles at a relatively narrow concentration range, referred to as critical micelle concentration (abbreviated as cmc) as is the case with sodium dodecyl sulfate.

In the present paper, measurements of surface tension were performed to examine how far they lower the surface tension of their aqueous solution and whether or not they would actually show cmc as expected from the Krafft phenomena. Although Lottermoser and Stoll[2] made the surface tension measurements of aqueous solutions of dodecyl sulfates of silver, magnesium, copper, zinc and iron(II), their data were obtained with the samples synthesized from impure sodium dodecyl sulfate as illustrated from the presence of the minimum in the diagram of surface tension of its aqueous solution versus concentration. So it seems to be necessary to undertake measurements with pure samples in order to obtain further knowledge of properties of metal dodecyl sulfates, on which only

1) (a) S. Miyamoto, *Mem. Fac. Sci. Kyushu Univ., Series C, Chem.*, in press.
(b) S. Miyamoto, This Bulletin, **33**, 371 (1960).

2) A. Lottermoser and F. Stoll, *Kolloid-Z.*, **63**, 49 (1933).

a few studies have been made up to the present[3].

Experimental

Metal dodecyl sulfates were synthesized from pure sodium dodecyl sulfate and then purified as described in the preceding paper[1a,b].

Measurements of surface tension of aqueous solutions of metal dodecyl sulfates were conducted with a Du Noüy's tensiometer at various temperatures kept constant with a water thermostat. The sample solution was contained in a bottle having a narrow neck and this was immersed in the thermostat up to the brim. The solution had been heated to a temperature above the temperature of the measurement of surface tension. In the measurement of surface tension, the ring of the tensiometer was suspended by a thin platinum wire from the bar of the tensiometer and was made to have contact with the surface of the solution prior to the measurement of surface tension. After the attainment of equilibrium of temperature of the solution with that of the thermostat, the measurement was started. At high temperatures, the measurement had to be carried out as rapidly as possible to avoid evaporation of the solvent.

From the data of surface tension, the cmc of each metal dodecyl sulfate solution could be determined and it was compared with the one measured by the dye titration method. The dye titration method was conducted by using pinacyanol chloride and rhodamine 6G and observing the change of their color with the change of the detergent concentration.

Results and Discussion

The values of surface tension of aqueous solutions of various metal dodecyl sulfates at various temperature are shown graphically in Fig. 1—7 as a function of their concentration. It is seen that every curve represents a kink and no minimum near the kink point. The absence of the minimum is considered to show the absence of more surface active impurities than these metal dodecyl sulfates. The value of cmc can be obtained as the concentration at the kink point of every curve. These values of cmc of various metal dodecyl sulfates at various temperatures are shown in Table I. It can be seen from Table I that the temperature dependence of the value of cmc of each

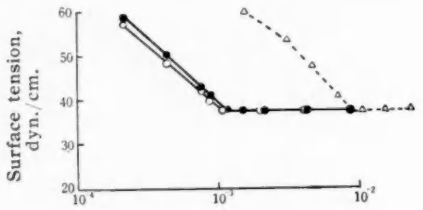

Fig. 1. Relation between surface tension and concentration of magnesium dodecyl sulfate solutions at 40°C (○) and 54°C (●). The dotted line represents the curve obtained with sodium dodecyl sulfate at 54°C.

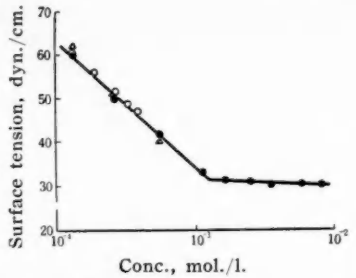

Fig. 2. Relation between surface tension and concentration of calcium dodecyl sulfate. Measurements of surface tension were conducted at 25°C (○), 35°C (△) and 54°C (●).

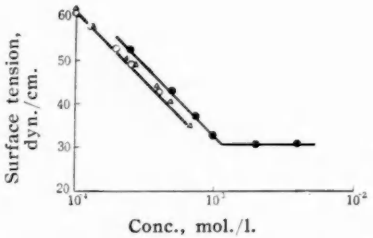

Fig. 3. Relation between surface tension and concentration of strontium dodecyl sulfate. Measurements of surface tension were conducted at 25°C (○), 54°C (△) and 67°C (●).

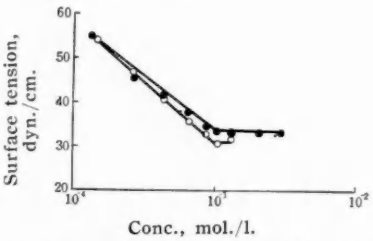

Fig. 4. Relation between surface tension and concentration of lead dodecyl sulfate. Measurements of surface tension were conducted at 54°C (○) and 67°C (●).

3) Literatures cited in 1b.

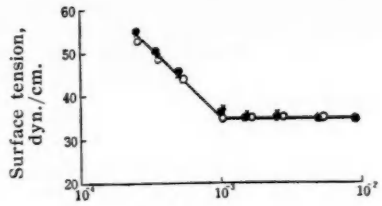

Fig. 5. Relation between surface tension and concentration of manganese dodecyl sulfate. Measurements of surface tension were conducted at 25°C (×), 40°C (○) and 54°C (●).

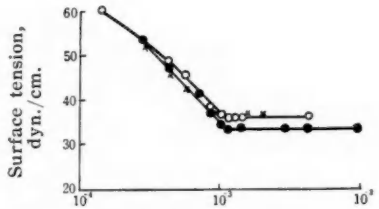

Fig. 6. Relation between surface tension and concentration of cobaltous dodecyl sulfate. Measurements of surface tension were conducted at 25°C (×), 40°C (○) and 54°C (●).

metal dodecyl sulfate of divalent cation is not so remarkable and also the values of dodecyl sulfates of various cations are almost the same, independent of the kind and type of cations contained in the molecules of these metal dodecyl sulfates.

These metal dodecyl sulfates were found to have their Krafft points as already reported[1b]. It is generally accepted with surfactant solutions that only at the temperatures above the Krafft point the micelles are formed. It seems true for some metal dodecyl sulfates studied in the

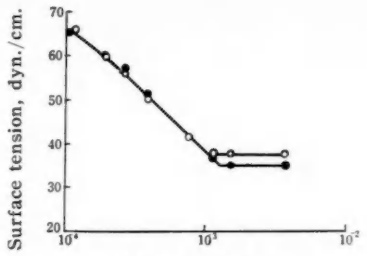

Fig. 7. Relation between surface tension and concentration of cupric dodecyl sulfate. Measurements of surface tension were conducted at 25°C (○) and 40°C (●).

present experiment. For example, calcium dodecyl sulfate was found to show its cmc at 54°C, as illustrated by the kink point of the surface tension-concentration curve (Fig. 2), but at 35°C which is below its Krafft point 50°C, the solution was saturated before its cmc had been reached. Referring to the diagram of Fig. 2 in the preceding paper[1b], it is found that the solubility of magnesium-, calcium-, strontium- and cobalt dodecyl sulfates at each Krafft point is nearly equal to the cmc of each solution which has been determined in the present experiment. In the case of lead salt, however, the solubility at its Krafft point is a little smaller than its cmc, and copper- and manganese salts show considerably larger solubilities than their corresponding value of cmc. It is not clear at the present why these metal dodecyl sulfates show anomalous behaviors. It will be necessary to make measurements of the existence of micelles over a much wider range of temperatures in order to elucidate the relation between the Krafft point and the micelle formation with these metal dodecyl sulfates.

As mentioned above, the dependence of

TABLE I. VALUES OF cmc (mol./l.) OF METAL DODECYL SULFATES AT VARIOUS TEMPERATURES DETERMINED BY SURFACE TENSION MEASUREMENTS

Subst.	cmc (mol./l.)			
	25°C	40°C	54°C	67°C
NaDS	7.4×10^{-3}	—	9.2×10^{-3}	—
$Mg(DS)_2\cdot6H_2O$	8.8×10^{-4}	1.1×10^{-3}	1.1×10^{-3}	—
$Ca(DS)_2$	—	—	1.3×10^{-3}	—
$Sr(DS)_2$	—	—	—	1.1×10^{-3}
$Pb(DS)_2$	—	—	1.0×10^{-3}	9.8×10^{-4}
$Mn(DS)_2$	1.1×10^{-3}	1.1×10^{-3}	1.1×10^{-3}	—
$Co(DS)_2\cdot6H_2O$	8.3×10^{-4}	9.7×10^{-4}	1.1×10^{-3}	—
$Cu(DS)_2\cdot4H_2O$	1.0×10^{-3}	1.2×10^{-3}	—	—

the values of cmc of various metal dodecyl sulfates on the kind of divalent cations contained in them is not explicitly found, the cmc being all nearly 1×10^{-3} mol./l. On the contrary, the values of cmc of alkali metal dodecyl sulfates measured by the electrical conductance method have been reported by Meguro et al.[4] to vary with the kind of alkali metal cations; i. e. they reported 7.8, 8.9 and 10.5 millimol./l. as the values of cmc of potassium-, sodium- and lithium dodecyl sulfates, respectively. These authors explained the dependence of cmc on the kind of monovalent cations as being due to the difference in hydration of these monovalent cations. This explanation might be applied also to the case of the metal dodecyl sulfates having the divalent cations examined in this experiment, but actually this effect seems so small that it can hardly be detected in this experiment. Metal dodecyl sulfates having divalent cations show far smaller values of cmc than those of the metal dodecyl sulfates having monovalent cations. This fact shows that the former sulfates have a less hydrophilic nature because of the two hydrocarbon chains for a metal, than the latter ones, and thus they have a tendency to form their micelles in solutions more easily. This may be a reason for the independence of their cmc's on the kind of divalent gegenions.

The value of surface tension of the solution above cmc is nearly constant. It ranges only from 31 to 37 dyn. per cm., depending on the temperature and the kind of metal dodecyl sulfates. In general a salt which is more soluble in water shows a larger value of saturation surface tension.

The cmc of a surface active substance has well been known to be obtained by the dye titration method as well as by the surface tension measurement. To examine the possibility of obtaining the values of cmc of the metal dodecyl sulfates by the dye titration method, measurements were conducted using pinacyanol chloride or rhodamine 6G as the indicator of the dye titration method. It was found that this method can also be applied to metal dodecyl sulfates. The values of cmc of the various metal dodecyl sulfates thus obtained are shown in Table II.

From Table II, the values of cmc obtained by pinacyanol chloride and rhodamine 6G are seen to be in good agreement with each other.

TABLE II. VALUES OF cmc (mol./l.) OF VARIOUS METAL DODECYL SULFATES* AT 40°C OBTAINED BY THE DYE TITRATION METHOD USING PINACYANOL CHLORIDE AND RHODAMINE 6G

Subst.	cmc (mol./l.) By pinacyanol chloride	By rhodamine 6G
NaDS	6.1×10^{-3}	6.1×10^{-3}
$Mg(DS)_2\cdot6H_2O$	1.0×10^{-3}	1.1×10^{-3}
$Ca(DS)_2$	1.3×10^{-3} (at 54°C)	—
$Mn(DS)_2$	1.2×10^{-3}	1.1×10^{-3}
$Co(DS)_2\cdot6H_2O$	1.0×10^{-3}	1.3×10^{-3}
$Cu(DS)_2\cdot4H_2O$	1.2×10^{-3}	1.3×10^{-3}
$Zn(DS)_2\cdot6H_2O$	1.1×10^{-3}	1.1×10^{-3}

* Measurements were not performed on strontium- and lead dodecyl sulfates because of their high Krafft points.

Comparing the values obtained by the dye titration method with those shown in Table I, obtained from surface tension measurements, it is found that these two methods of measuring cmc give values approximately coinciding with each other.

As described above, metal dodecyl sulfates with divalent cations are found to lower the surface tension of their solutions exceedingly and have far smaller cmc values than those of the salts of monovalent cations. Relatively soluble salts such as cupric-, manganese-, cobaltous- and magnesium dodecyl sulfates, therefore, may be useful for many purposes based on their strong surface activity.

Summary

The surface tension of aqueous solutions of various metal dodecyl sulfates with divalent cations was measured at various temperatures with a Du Noüy's tensiometer. The values of surface tension were observed to decrease steeply with the increase of their concentrations up to their cmc's, which are all nearly equal to 1×10^{-3} mol./l. These values of cmc of the metal dodecyl sulfates with divalent cations were found to be practically independent of temperature and the kind of these cations. Further, the dye titration methods were also performed to obtain the values of cmc of these metal dodecyl sulfates using pinacyanol chloride and rhodamine 6G. The values of cmc obtained by these methods were found to coincide with those from the surface tension measurements.

4) K. Meguro, T. Kondo, O. Yoda, T. Ino and N. Ohba, *J. Chem. Soc. Japan, Pure Chem. Sec.* (*Nippon Kagaku Zasshi*), 77, 1236 (1956).

The author wishes to express his sincere thanks to Professor R. Matuura of Kyushu University for his encouragement and guidance.

Department of Chemistry
Faculty of Science
Kyushu University
Hakozaki, Fukuoka

Relations between Electronic Absorption Spectra and Spatial Configurations of Conjugated Systems. V. Stilbene

By Hiroshi SUZUKI

(Received August 15, 1959)

Previously[1] the present author explained successfully the hypsochromic shifts of the conjugation band observed in the ultraviolet absorption spectra of *cis*-stilbene and of some α-alkyl- and α,α'-dialkylstilbenes as compared with *trans*-stilbene by correlating those with the most probable spatial configurations of the molecules on the basis of the calculations by the simple LCAO molecular orbital method. Thus, he determined by his calculations the relation between the interplaner angle θ (that is, the angle through which the plane of each phenyl group rotates out of the plane of the central essentially double bond) and the electronic transition energy correspondinng to the conjugation band, and clarified the fact that the perfect coplanarity of the molecular configuration is not prerequisite to an occurrence of conjugation and hence not prerequisite to the appearance of the conjugation band and that the conjugation band is progressively shifted toward shorter wavelengths with increasing θ. He showed also that the value of the interplanar angle of a given compound of the type concerned can satisfactorily be computed from the position of the conjugation band and vice versa. Further, he showed that the earlier interpretations[2,3] of these hypsochromic shifts in terms of "partial chromophores" are to be rejected.

The calculations were carried out on the basis of the assumption that the absorption maximum at about 294 mμ in the spectrum of *trans*-stilbene in solution was due to the transition in the planar molecule of *trans*-stilbene. According to the X-ray crystal analysis by Robertson and Woodward[4], *trans*-stilbene in the crystalline state has a nearly planar or probably completely planar configuration. Strictly speaking, however, it seems that there is no evidence to indicate that the most probable configuration of *trans*-stilbene in solution is also planar. The observation by Wiegand and Merkel[5] that the absorption curve of *trans*-stilbene in solution is closely similar to that of 2-phenylindene in which one of the phenyl groups of *trans*-stilbene may be considered to be maintained in the coplanar or nearly coplanar position with the central ethylenic bond by the methylene bridge is somewhat interesting in this connection, but it should not be considered as a proof of the planarity of the whole configuration of *trans*-stilbene in solution. As already discussed in the first part[6] of this series, biphenyl is probably non-planar in solution, while it is known to be planar in the crystalline state. In view of this fact, the spectrum of *trans*-stilbene in solution should not be considered without sufficient consideration to be due to the planar molecule.

In this part of the series, the results of measurements of the spectra of *trans*-stilbene in various solvents and in the crystalline state carried out from these considerations are reported, and these spectra as well as the vapor spectrum of *trans*-stilbene are discussed with special emphasis on the relation of the spectra to the spatial configuration of the molecule.

1) H. Suzuki, This Bulletin, **25**, 145 (1952).
2) R. N. Jones, *J. Am. Chem. Soc.*, **65**, 1818 (1943).
3) E. A. Braude, *J. Chem. Soc.*, **1949**, 1902.
4) J. M. Robertson and I. Woodward, *Proc. Roy. Soc. (London)*, **A162**, 568 (1937).
5) C. Wiegand and E. Merkel, *Ann.*, **550**, 175 (1942).
6) H. Suzuki, This Bulletin, **32**, 1340 (1959).

TABLE I. SOLUTION SPECTRA OF *trans*- AND *cis*-STILBENES

Solvent		A-band		B-band		$\varepsilon_\beta/\varepsilon_T$
		λ_{max}, mμ	ε	λ_{max}, mμ	ε	
trans-Stilbene						
n-Heptane	α	(320.5)	16000	(236)	10400	0.949
	β	306.9	26500	△228.5	16200	
	γ	△294.1	27950	(222)	15500	
	δ	(283)	24500			
Ethanol (95%)	α	321.0	16980	236	11150	0.977
	β	307.3	27200	△228.8	16400	
	γ	△294.5	27850	222.5	15370	
	δ	(284)	25200			
Methanol	α	319.5	17380	236.1	11200	0.975
	β	306.8	27350	△228.3	16500	
	γ	△294.0	28050	(222)	15500	
	δ	(283)	24150			
Chloroform	α	(323.5)	16400			0.989
	β	309.9	27150			
	γ	△297.9	27450			
	δ	(286.5)	23200			
Carbon tetrachloride	α	(324.5)	15500			0.988
	β	311.8	24750			
	γ	△299.4	25050			
	δ	(290)	22100			
Benzene	α	(324.5)	15400			1.010
	β	△311.2	25600			
	γ	298.8	25340			
	δ	(289)	21700			
Mixed alcohols[7] (−130°C)	α	326.2	25000			1.711
	β	311.2	38500			
	γ	297.5	22500			
cis-Stilbene						
Ethanol (100%)[7]		280	10450	224	24400	

Wavelengths in parentheses denote inflections.
Symbol △ denotes the most intense maximum of the fine structure.

Further, on the basis of the results, the relation between the spectrum and the spatial configuration of *cis*-stilbene is discussed by application of the usual method.

Spectra of *trans*-Stilbene in Various States

Solution Spectra of *trans*-Stilbene.—Data of the spectra of *trans*-stilbene in various solvents measured at room temperature are given in Table I, in which data of the spectrum of *trans*-stilbene at low temperature as well as those of *cis*-stilbene measured by Beale and Roe[7] are also included for comparison. The notation of the absorption bands is according to Beale and Roe. The A-bands are considered to be the conjugation bands. In addition to the bands shown in Table I, the spectrum of *trans*-stilbene in *n*-heptane exhibits a band at about 201.5 mμ (ε = 23900), and that in ethanol at about 201.0 mμ (ε = 23800). These are termed the C-bands.

The absorption curves of the spectra of the *n*-heptane solution and of the benzene solution of *trans*-stilbene are shown in Fig. 1 as the representatives of the solution spectra of *trans*-stilbene. In Fig. 1 the curve of the spectrum of *cis*-stilbene is also shown for comparison. The spectra of *trans*-stilbene in the other solvents resemble that in *n*-heptane on the whole, although especially the A-α-band in the spectrum in carbon tetrachloride as well as in chloroform is somewhat more diffuse than in the spectra in *n*-heptane and in alcohols.

It is notable that th A-band has a fine structure. The somewhat similar pattern of fine structure is seen also in the B-band. Beale and Roe[7] have concluded that the fine structure originates in the stretching frequency of the ethylenic bond. On the

7) R. N. Beale and E. M. F. Roe, *J. Chem. Soc.*, **1953**, 2755.

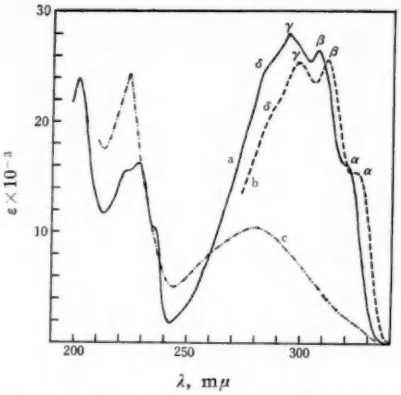

Fig. 1. Solution spectra of *trans*- and *cis*-stilbenes (cf. Table I).
a ——, *trans*-stilbene in *n*-heptane.
b – – –, *trans*-stilbene in benzene.
c –·–·–, *cis*-stilbene in ethanol.

other hand, in sharp contrast to *trans*-stilbene, *cis*-stilbene as well as α- and α, α'-substituted stilbenes which will be treated in a later part of this series shows no fine structure. These compounds are considered to be non-planar as will be shown later. Accordingly it would be expected that an appearance of fine structure might be related to the planarity of the molecular configuration or to its rigidity as the hypotheses proposed by Wiegand and Merkel[8] and by Kortüm and Dreesen[9]. However, such a relation has not yet been established.

In comparison with *n*-heptane, methanol exerts almost no, or a very small, hypsochromic effect, and ethanol exerts a small bathochromic effect. The magnitude of the bathochromic shift is considerably greater in chloroform, and is extraordinarily great in carbon tetrachloride as well as in benzene.

The great bathochromic effect of benzene may be especially noteworthy. According to Bayliss[10], a magnitude of wavelength displacement of a band of a nonpolar molecule by a nonpolar solvent is related to the refractivity of the solvent. The refractivity of benzene is slightly greater than that of *n*-heptane. However, it seems that the great bathochromic effect of benzene relative to *n*-heptane can not be attributed wholly to the difference of refractivity alone.

In this connection, it may be noted that the distribution of intensity among the vibrational bands of the A-band varies considerably with the solvent. The ratio of the intensity of the β-band to that of the γ-band for each solvent is listed in the last column of Table I. It is seen that the ratio increases in the order *n*-heptane < ethanol ≈ methanol < chloroform ≈ carbon tetrachloride < benzene. It may be noteworthy that while in solvents other than benzene the γ-band is the most intense maximum of the A-band, in benzene the β-band is the most intense maximum.

These facts appear to suggest the presence of a special interaction between the π-orbitals (or π-electrons) of the solute molecule and those of benzene. This problem will be discussed in somewhat greater detail in a later part of this series.

Solution Spectra of Some *p*-Substituted *trans*-Stilbenes. — The special solvent effect of benzene is seen also in the spectra of some *p*-substituted *trans*-stilbenes. The results of measurements of the spectra of *p*-methoxy-*trans*-stilbene and of *p*-nitro-*trans*-stilbene in *n*-heptane as well as in benzene are shown in Table II and Figs. 2 and 3. These spectra, especially those in *n*-heptane, bear a certain similarity in shape to that of *trans*-stilbene, showing similar patterns of fine structure. The magnitudes of the bathochromic displacements of the bands associated with the change of solvent from *n*-heptane to benzene are considerably

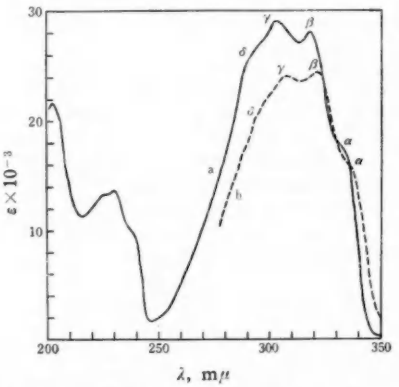

Fig. 2. Solution spectra of *p*-methoxy-*trans*-stilbene (cf. Table II).
a ——, in *n*-heptane.
b – – –, in benzene.

8) (a) C. Wiegand and E. Merkel, *Ann.*, **557**, 242 (1947). (b) E. Merkel and C. Wiegand, *Naturwissenschaften*, **34**, 122 (1947). (c) E. Merkel and C. Wiegand, *Z. Naturforsch.*, **3b**, 93 (1948).
9) G. Kortüm and G. Dreesen, *Chem. Ber.*, **84**, 182 (1951).
10) N. S. Bayliss, *J. Chem. Phys.*, **18**, 292 (1950).

TABLE II. SOLUTION SPECTRA OF *p*-SUBSTITUTED *trans*-STILBENES

Solvent		A-band		B-band	
		λ_{max}, mμ	ε	λ_{max}, mμ	ε
p-Methoxy-trans-stilbene					
n-Heptane	α	(332.5)	17700	(238)	9830
	β	317.8	28100	△230.0	13600
	γ	△302.7	28950	(225)	13250
	δ	(291)	25800		
Benzene	α	(337)	15700		
	β	△322.0	24500		
	γ	307.7	24100		
	δ	(295.5)	21000		
p-Nitro-trans-stilbene					
n-Heptane	α	(363)	14200	262.0	7860
	β	△345.0	23820	△240.0	11760
	γ	332.0	23420	△233.7	11760
	δ	(318)	17850	(215)	13770
Benzene	(β)	△350.5	17420		

Wavelengths in parentheses denote inflections.
Symbol △ denotes the most intense maximum of the fine structure.

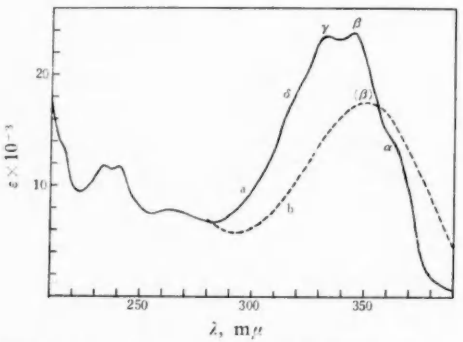

Fig. 3. Solution spectra of *p*-nitro-*trans*-stilbene (cf. Table II).
a ——, in *n*-heptane.
b ----, in benzene.

great (about 5 mμ) also with these compounds. Furthermore, in the spectra of *p*-methoxy-*trans*-stilbene a marked redistribution of intensity between the β-band and the γ-band occurs, quite similarly to the one observed in the spectra of *trans*-stilbene. It is also noteworthy that the fine structure of the A-band of *p*-nitro-*trans*-stilbene disappears almost completely in the spectrum in benzene.

Crystal Spectra of *trans*-Stilbene. — The spectrum of *trans*-stilbene in the crystalline state was measured by the pressed KCl-disk technique. The values of the molecular extinction coefficients were not reproducible and were considerably smaller than th corresponding values in the solution spectra. Thus, the former values varied from about 1/3 to about 1/30 of the latter ones from disk to disk. This fact may be considered to indicate the dependence of the extinction values on the condition of dispersion of the micro-crystals or the sizes of the micro-crystals, in view of the somewhat similar phenomenon observed by Weigl[11] in his study on the absorption spectra of some crystalline cationic dyes. In addition, this lowering of the extinction values may be partly due to the possible loss of the organic substance during grinding and evacuation of the press, as stated by Dale[12]. In spite of this, the reproducibility of the positions of the absorption maxima and inflections was almost completely satisfactory except for the α-band of the A-band. As representatives the results of measurements on the two disks of different thicknesses made from the same mixture (cf. *Experimental*) are shown in Table III and Fig. 4.

The crystal spectra differ considerably in the shape of the absorption curve from the solution spectra. In the crystal spectra the most intense maximum in the fine structure of the A-band is the δ-band, neither the γ-band as in the spectra in *n*-heptane etc., nor the β-band as in the spectrum in benzene. In this connection it may be of interest that in the solution spectrum measured by Beale and Roe[7] at low temperature (−130°C) the β-band is the most intense one, the fine structure being much more sharply resolved.

11) J. W. Weigl, ibid., **24**, 364 (1956).
12) J. Dale, *Acta Chem. Scand.*, **11**, 650 (1957).

TABLE III. CRYSTAL SPECTRA OF *trans*-STILBENE MEASURED BY THE KCl-DISK TECHNIQUE

Disk*		A-band		B-band	
		λ_{max}, mμ	A	λ_{max}, mμ	A
(*a*)	α	(327.5)	0.276	(241.5)	0.407
	β	(312.5)	0.430	△233.0	0.478
	γ	(298.5)	0.502	(225.5)	0.470
	δ	△287.0	0.511		
	ε	(276)	0.460		
(*b*)	α	(332)	0.090	242	0.195
	β	(313)	0.182	△233.5	0.216
	γ	(298.5)	0.245	(225.5)	0.190
	δ	△286	0.273		
	ε	(276)	0.254		

* See *Experimental*.
Symbol A represents the absorbance.
Wavelengths in parentheses denote inflections.
Symbol △ denotes most intense maximum of fine structure.

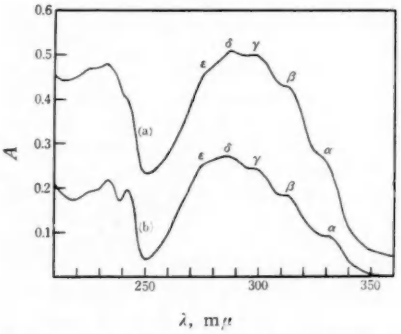

Fig. 4. Crystal spectra of *trans*-stilbene measured by the KCl-disk technique (cf. Table III).

The bands in the crystal spectrum are at longer wavelengths than the corresponding ones in the spectrum in *n*-heptane. The magnitude of the bathochromic shift is about 4.5 mμ for the γ-band and about 5.5 or 6 mμ for the β-band. These values probably corresponding to the "normal red-shift"[12] of the conjugation band are considerably smaller than those (about 8 mμ for the γ-band and about 9 mμ for the β-band) anticipated from the regular relation between the magnitude of the shift and the position of the band determined by Dale[12] for rigid molecules. This fact may be considered to indicate that the most probable spatial configuration of *trans*-stilbene in solution does not significantly differ from the one in the crystalline state and hence is planar or nearly planer.

Therefore, in order to infer the most probable spatial configurations of *cis*-stilbene and some related compounds of stilbene in solution by application of our method, the spectrum of *trans*-stilbene in *n*-heptane is taken as the spectrum of the planar reference compound, and the spectra of the *n*-heptane solutions are compared in principle as far as the data are available. In cases of absence of the data of the spectrum of the *n*-heptane solution, the data of the ethanol solution are used. As already mentioned, the spectra of *cis*-stilbene and the stilbene derivatives with substituents at the α- and α′-positions or at the ortho positions treated in this series all exhibit the structureless conjugation bands in contrast to that of *trans*-stilbene. Therefore, the question arises which maximum of fine structure of the conjugation band in the spectrum of *trans*-stilbene should be taken as the reference for the comparison. In the present treatment the γ-band at 294.1 mμ is tentatively chosen as the reference. This band is not only the most intense maximum of fine structure of the conjugation band in the spectrum of the *n*-heptane solution but also probably the central one.

Besides the above mentioned spectra by the pressed KCl-disk technique, the author attempted to measure the crystal spectrum of *trans*-stilbene also on thin films prepared on quartz plates by sublimation of crystals as well as by evaporation of a thin layer of solution, but these attempts were unsuccessful. Thus, the absorption curves obtained were very diffuse and indicated only indistinctly the presence of a band or bands at near 295~335 mμ. This failure of revelation of the conjugation band is probably due to the effect of the orientation of the molecules in the crystals as discussed by Dale[12] in the case of biphenyl.

Pesteil[13] measured the spectrum of *trans*-stilbene on thin crystal plates with polarized light and found a feeble band with two principal maxima at 367 and 387 mμ in addition to the stronger bands below 360 mμ. Jaffé and others[14] have stated that it appears reasonable to assume this feeble band to be the singlet-triplet absorption. Brodin and others[15] measured the spectrum of crystalline *trans*-stilbene at 20°K and found many vibrational frequencies.

Vapor Spectrum of *trans*-Stilbene.—According to Kanda[16], the vapor spectrum of *trans*-stilbene prossesses a discontinuous band with nine maxima at the region from 284.4 to 265.6 mμ, of which the most intense maxima are at 284.4 and 283.4 mμ, and a discontinuous band with ten maxima at the region from 244.3 to 233.5 mμ, of which the most intense maximum is at 240.5 mμ. The former band may be considered to be the conjugation band, viz. the A-band, and the latter the B-band. It is noteworthy that the conjugation band in the vapor spectrum is at considerably shorter wavelengths than the corresponding one in the solution spectra as well as the crystal spectrum. This fact probably indicates that the most likely configuration of *trans*-stilbene in the vapor state deviates considerably from the coplanarity, analogously to biphenyl[6].

Calculation

The relation between the spatial configurations and the electronic absorption spectra of stilbenes can be determined by the following calculations. The procedures of the calculations are the same in principle as the ones described previously[1]. The description is given here in a somewhat more refined form as the basis for the treatments not only in the present part but also in the succeeding parts of this series.

Determination of the Parameters for the Resonance Integrals as Functions of the Bond Length and the Interplanar Angle.—The $\pi-\pi$ resonance integral for the central ethylenic bond, namely the $\alpha-\alpha'$ bond, is denoted by $\eta\beta$, and the one for the $\alpha-1$ bond as well as the $\alpha'-1'$ bond by $\rho\beta$. (Symbols α and γ in the previous paper were replaced by ρ and η, respectively). Symbol β represents the $\pi-\pi$ resonance integral for the C–C bond in the benzene ring, and η and ρ are parameters by which allowances are made for changes of the resonance integrals associated with changes of the bond length and the interplanar angle.

The length of the $\alpha-\alpha'$ bond in *trans*-stilbene was estimated at 1.33±0.04 Å by Robertson and Woodward[4]. The length of the C=C bond in ethylene was recently found to be 1.337 Å[17], and the length of the "double" bonds in butadiene to be 1.337±0.005 Å[18]. Therefore, it may be presumed that the length of the ethylenic "double" bond does not significantly vary with the extent of conjugation. Hence the round value of 1.34 Å is taken as the length of the $\alpha-\alpha'$ bond in *trans*-stilbene as well as the related compounds throughout the present treatment. Consequently, the value of the parameter η is estimated at 1.080 from Mulliken's Tables[19] on the basis of the approximate proportionality of the $\pi-\pi$ resonance integral for C–C bond to the $\pi-\pi$ overlap integral.

The parameter ρ can be expressed approximately by the following equation, quite analogously to Eq. 1 in the first part[6] of this series;

$$\rho = S(R,\ 0^\circ)\cos\theta / S(1.39,\ 0^\circ) \qquad (1)$$

where $S(1.39,0^\circ)$ represents the $\pi-\pi$ overlap integral for the C–C bond in the benzene ring and $S(R,\ 0^\circ)$ represents the one in the case where the bond length is R and the interplanar angle is 0°.

According to the result of the X-ray crystal analysis of *trans*-stilbene by Robertson and Woodward[4], two molecules contribute to the asymmetric unit of the crystal, and these molecules have different appearances in the electron density maps. Thus, the length of the "single" bonds joining the phenyl groups to the ethylenic carbon atoms, namely the $\alpha-1$ and $\alpha'-1'$ bonds, and the interplanar angle were estimated at 1.44±0.02 Å and 3°, respectively, for one molecule and at 1.45±0.02 Å and 10°, respectively, for the other. Robertson and Woodward have, however, concluded that the apparent differences are due to the relative orientation of the

13) (a) P. Pesteil, *Compt. rend.*, **233**, 377 (1951). (b) Idem., ibid., **233**, 924 (1951).
14) H. H. Jaffé, Si-Jung Yeh and R. W. Gardner, *J. Molecular Spectroscopy*, **2**, 120 (1958).
15) M. S. Brodin, O. S. Pakhomova and A. F. Prikhot'ko, *Optika i Spektroskopiya*, **5**, 123 (1958); *Chem. Abstr.*, **53**, 48 (1959).
16) Y. Kanda, *Mem. Faculty Sci., Kyushu Univ. Ser. C, Chem.*, **1**, 189 (1950).
17) (a) L. S. Bartell and R. A. Bonham, *J. Chem. Phys.*, **27**, 1414 (1957). (b) H. C. Allen and E. K. Plyler, *J. Am. Chem. Soc.*, **80**, 2673 (1958). (c) J. M. Dowling and B. P. Stoicheff, *Bull. Am. Phys. Soc.*, **II3**, 373 (1958).
18) A. Almenningen, O. Bastiansen and M. Traetteberg, *Acta Chem. Scand.*, **12**, 1221 (1958).
19) R. S. Mulliken, C. A. Rieke, D. Orloff and H. Orlott, *J. Chem. Phys.*, **17**, 1248 (1949).

molecules and not to any appreciable differences in their shape or dimensions, and that the molecules are nearly planar and may be exactly planar within the limits of experimental error.

Therefore, the values of θ (the interplanar angle) and of R (the length of the $\alpha-1$ bond) may safely be assumed in the present treatment to be 0° and 1.445 Å, respectively, in the configuration of *trans*-stilbene in the crystalline state and hence in the most probable configuration of the molecule in solution. Accordingly, the relation between θ and R is assumed as follows, quite analogously to Eq. 4 in Part I[6].

$$\{S(R,\ 0^\circ)-S(1.54,\ 0^\circ)\}/\{S(1.445,\ 0^\circ)-S(1.54,\ 0^\circ)\}=\cos\theta \qquad (2)$$

Then, from Eqs. 1 & 2 and Eq. 3 in Part I, one obtains

$$\rho=\cos\theta\times 0.77108+\cos^2\theta\times(1.54-1.445)\times 1.4458 \qquad (3)$$

which is quite analogous to Eq. 7 in Part I. Accordingly, the value of ρ is computed to be 0.9084 when θ is 0° and R is 1.445 Å. It is evident that the value of ρ becomes smaller with increasing θ and that it is 0 when θ is 90°.

Solution of the Secular Equation for the Determination of the Molecular Orbitals.— By solving the secular equation for the determination of the molecular orbitals as linear combinations of $2p\pi$ atomic orbitals, one can obtain the values of energies of the molecular orbitals corresponding to the value of the parameter ρ. Consequently, the values of the extra-resonance energy (subsequently referred to as *R.E.*), of the coefficients of the $2p\pi$ atomic orbitals in the molecular orbital functions, and of the quantities such as the π-bond orders corresponding to the molecular configuration prescribed by the value of ρ can also be obtained by the usual procedures.

The stilbene-type conjugated system can be considered as belonging to the symmetry group D_2 in the present treatment. Then, the highest occupied π-orbital (π_1) belongs to the representation B_1, and coincides with the φ_1 orbital in benzene when ρ is 0. On the other hand, the lowest vacant π-orbital (π_1^*) belongs to B_3, and coincides with the φ_2 orbital in benzene when ρ is 0. (The notation for orbitals in benzene is according to Sklar[20].) Transitions from orbitals belonging to B_1 to those belonging to B_3 are allowed by absorption of light polarized along the direction of the long axis of the molecule. Accordingly, the energy difference between the lowest vacant orbital π_1^* and the highest occupied orbital π_1 (referred to as ΔE_A) is considered to be the transition energy corresponding to the conjugation band (viz. the A-band). The value of ΔE_A (in $-\beta$) is, of course, twice the absolute value of the enegy (in $-\beta$) of one of the two orbitals.

In addition to the ten orbitals belonging to B_1 and B_3, whose energies vary with ρ (cf. Fig. 2 in Ref. 1), there are two sets of doubly degenerate orbitals belonging to A_1 and B_2, whose energies do not vary with ρ. These orbitals may be considered as ones localized in the benzene rings. Thus, one (φ) of the two orbitals belonging to either A_1 or B_2 has the energy of $+\beta$ and corresponds to the φ_{-1} orbital in benzene, while the other orbital (φ^*) has the energy of $-\beta$ and corresponds to the φ_{-2} orbital in benzene. Transitions from the π_1 orbital (B_1) to the φ^* orbital belonging to B_2 or from the φ orbital belonging to A_1 to the π_1^* orbital (B_3) are allowed by absorption of light polarized along the direction of the short-axis of the molecule. These transitions may be considered as corresponding to the B-band, as suggested by Dale[21]. The value of the corresponding transition energy $\Delta E_B(-\beta)$ can evidently be expressed as $1+\Delta E_A(-\beta)/2$.

Transitions between the orbitals belonging to A_1 and those belonging to B_2 are allowed by absorption of light polarized along the direction of the long-axis of the molecule, and correspond probably to the C-band at about 200 mμ.

The results of the calculations are summarized in Table IV. In this table, $\Delta E_A(-\beta)$ and *R.E.*$(-\beta)$ are values obtained by ignoring the $\pi-\pi$ overlap integral, and $\Delta E_A(-\gamma)$ and *R.E.*$(-\gamma)$ are values obtained by taking the overlap integral into account, assuming the value of the overlap integral for the C–C bond in benzene as 0.25. The symbols $p_{\alpha-\alpha'}$ and $p_{\alpha-1}$ represent the π-bond orders of the $\alpha-\alpha'$ bond and of the $\alpha-1$ as well as the $\alpha'-1'$ bond, respectively.

It is evident that the values of ΔE_A and hence of ΔE_B increase with decreasing ρ and agree with the values for benzene when ρ is 0. This means that A-band as well as the B-bond is gradually shifted toward shorter wavelengths as the value

20) A. L. Sklar, ibid., 7, 984 (1939).

21) J. Dale, *Acta Chem. Scand.*, 11, 971 (1957).

TABLE IV

ρ	1.1	1.0	0.9	0.8	0.7	0.6
$\Delta E_A(-\beta)$	0.9920	1.0680	1.1492	1.2352	1.3262	1.4216
$\Delta E_A(-\gamma)$	1.0075	1.0874	1.1734	1.2654	1.3637	1.4679
$R.E.(-\beta)$	1.0252	0.8500	0.6904	0.5464	0.4190	0.3084
$R.E.(-\gamma)$	0.3532	0.2922	0.2368	0.1870	0.1432	0.1048
$p_{\alpha-\alpha'}$		(0.829)	0.858	0.8865	0.912	0.934
$p_{\alpha-1}$		(0.423)	0.381	0.340	0.298	0.255
ρ	0.5	0.4	0.3	0.2	0.1	0
$\Delta E_A(-\beta)$	1.5212	1.6246	1.7306	1.8376	1.9398	2
$\Delta E_A(-\gamma)$	1.5783	1.6945	1.8156	1.9400	2.0610	2.1333
$R.E.(-\beta)$	0.2140	0.1372	0.0772	0.0342	0.0084	0
$R.E.(-\gamma)$	0.0726	0.0466	0.0262	0.0118	0.0028	0
$p_{\alpha-\alpha'}$	0.954	(0.9705)				1
$p_{\alpha-1}$	0.213	(0.170)	(0.1275)	(0.085)	(0.0425)	0

The values of the π-bond orders in parentheses were obtained by either interpolation or extrapolation.

TABLE V

Stilbene	λ_A mμ	ν_A cm^{-1}	ΔE_A $-\beta$	ρ	θ°	R Å	$R.E.$ $-\beta$	$p_{\alpha-1}$	$p_{\alpha-\alpha'}$
trans-	294.1	34002	1.1423	0.9084	0	1.445	0.704	0.384	0.8555
cis-	280	35714	1.247	0.787	28	1.456	0.530	0.333	0.890

ρ decreases and therefore as the value of θ increases, and that these bands will coincide with those of benzene when ρ is 0 and therefore when θ is 90°.

It appears that there is no simple quantitative relation between ρ and ΔE_A, or between ΔE_A and $R.E.$ On the other hand, $R.E.(-\beta)$ is almost completely proportional to ρ^2 and can approximately be expressed as $0.8473\times\rho^2$. In addition, $p_{\alpha-1}$ is roughly proportional to ρ and can roughly be expressed as $0.425\times\rho$.

Correlation of the Calculated Transition Energy with the Observed Position of the Conjugation Band.—The value of ρ when θ is 0° and R is 1.445 Å is 0.9084, and the corresponding value of ΔE_A is $1.1423(-\beta)$, which is subsequently referred to as ΔE_L. The value of the wave number corresponding to ΔE_L, namely ν_L, is assumed to be 34002 cm^{-1} (294.1 mμ) which is the wave number of the A-γ-band in the spectrum of *trans*-stilbene in *n*-heptane, on the basis of the considerations mentioned already.

On the other hand, the value of ΔE_A when ρ is 0, namely ΔE_S, is $2(-\beta)$, and the corresponding value of the wave number, namely ν_S, is assumed to be 48000 cm^{-1} (208.3 mμ), the center of gravity of singlets of benzene, as usual.

Then, the value of ΔE_A $(-\beta)$ for a given compound of the stilbene-type is obtained from the observed position (ν_A in wave number) of the conjugation band by Eq. 8 in the first part[6] of this series. Consequently, the corresponding value of the parameter ρ and then the values of θ, $R.E.$, p, etc. can be obtained in turn.

Spectrum of *cis*-Stilbene

The solution spectrum of *cis*-stilbene (cf. Table I and Fig. 1 and also Refs. 1 and 7) differs considerably from that of the *trans*-isomer. The conjugation band (A-band) in the former is structureless in contrast to the one in the latter, and at a considerably shorter wavelength and of lower intensity than the one in the latter. This hypsochromic shift of the band is explained as being due to the non-planarity of the most probable configuration of *cis*-stilbene. The B-band of *cis*-stilbene is also structureless and at a shorter wavelength than the corresponding band of the *trans*-isomer, while the former is more intense than the latter.

Application of Calculation and Discussion

Data of the spectrum of the *n*-heptane solution of *cis*-stilbene are not available. Hence, the position of the conjugation band (280 mμ) in the spectrum of the ethanol solution is used as the basis of calculation for *cis*-stilbene, since the solvent effect of ethanol on the position of the band is considered not to differ significantly from

that of *n*-heptane on the analogy of the observation in the case of *trans*-stilbene. The results of application of the calculations to *cis*- and *trans*-stilbenes are shown in Table V.

The value of about 28° for the interplanar angles in *cis*-stilbene is in fairly good agreement with the value of about 25° estimated from the scale model[1].

At these values of the interplanar angles the steric repulsion between the two phenyl groups may be almost completely relieved. The difference between the stabilities of the isomers may be considered as the sum of the difference of extra-resonance (stabilization) energy and the difference of steric repulsion (destabilization) energy. If it is assumed that the difference of steric repulsion energy is small in the most probable configurations of the two isomers, the difference of stability is ascribed mainly to the difference of extra-resonance energy. When the value of $-\beta$ is tentatively assumed as 20 kcal./mol., the extra-resonance energy in *trans*-stilbene is evaluated as 14.07 kcal./mol. and that in the *cis*-isomer as 10.60 kcal./mol. The former value agrees fairly well with the value of 15 kcal./mol.[22] estimated from the heat of formation as well as the value of 12.5 kcal./mol.[23] estimated from the heat of hydrogenation[24], although the estimations of resonance energy, in general, do not seem to be entirely free from ambiguity. The difference between the extra-resonance energies of the two isomers is evaluated as about 3.5 kcal./mol. This value is also in satisfactory agreement with the experimental value of the energy difference between the isomers, 3 kcal./mol., estimated from the equilibrium of the thermal isomerization by Kistiakowsky and Smith[25] and by Taylor and Murray[26].

With a view to explaining the fact that the conjugation band of *cis*-stilbene is at a shorter wavelength and is of lower intensity than the corresponding one of the *trans*-isomer, Braude and other[27] have stated as follows: "Assuming that the wavelength shift of 150 Å from *trans*- to *cis*-stilbene is wholly due to steric hindrance, the differential de-stabilization amounts to about 6 kcal./mol., a value remarkably close to the resonance energy of *trans*-stilbene". That is, it seems that they have attempted to correlate the shift with the resonance energy or/and the steric repulsion energy. However, as already mentioned, there is no direct relation between the resonance energy and the electronic transition energy. And further, as mentioned in the earlier parts[6,28] of this series, there is also no direct relation between the steric repulsion energy and the transition energy. It seems evident that Braude and other's attempt was unsuccessful.

The values of $\Delta E_B(-\beta)$ for *trans*- and *cis*-stilbenes are estimated at 1.571 and 1.624, respectively. From these values the B-bands of these compounds are expected to be at 41001 cm^{-1} (243.9 mμ) and 41864 cm^{-1} (238.9 mμ), respectively, by application of the relation between ΔE and ν postulated above originally for the A-band. Considering the approximation used, it may be said that the agreement between these expected positions and the observed positions of the B-bands is nearly perfect.

Experimental

Measurements of Spectra. — All the spectra were measured with a Cary recording spectrophotometer Model 14 M-50.

The crystal spectra of *trans*-stilbene were measured by the pressed KCl-disk technique described by Dale[12]. The potassium chloride used had been precipitated from water solution with hydrochloric acid to obtain small particle size and dried at 400 to 450°C for about 6 hr., according to Hales and Kynaston[29]. As an example of the procedures of the preparation of the mixtures, that for the disks on which the spectra shown in Fig. 4 as well as Table III were measured will be described below. About 3.5 mg. of pure *trans*-stilbene was thoroughly ground in an agate mortar with about 200 mg. of potassium chloride. About 10.5 mg. of the mixture was then ground with about 350 mg. of potassium chloride, and pressed under vacuum in the usual manner into transparent disks (a radius, 0.65 cm.). The disk (a) weighed 140.4 mg. (the thickness, about 0.532 mm.), and the disk (b) weighed 111.1 mg. (the thickness, about 0.421 mm.).

Preparations of *p*-Substituted *trans*-Stilbenes. — *p*-Methoxy-*trans*-stilbene was prepared by the

22) L. Pauling and J. Sherman, *J. Chem. Phys.*, **1**, 606 (1933).
23) M. M. Kreevoy and R. W. Taft, Jr., *J. Am. Chem. Soc.*, **79**, 4016 (1957).
24) G. W. Wheland, "Resonance in Organic Chemistry", John Wiley & Sons, Inc., New York (1955), p. 80.
25) G. B. Kistiakowsky and W. R. Smith, *J. Am. Chem. Soc.*, **56**, 638 (1934).
26) T. W. J. Taylor and A. R. Murray, *J. Chem. Soc.*, **1938**, 2078.
27) W. Klyne (Ed.), "Progress in Stereochemistry", Vol. 1, Butterworths Scientific Publications, London (1954), p. 131, (E. A. Braude and E. S. Waight).
28) H. Suzuki, This Bulletin, **32**, 1350 (1959).
29) J. L. Hales and W. Kynaston, *Analyst*, **79**, 702 (1954).

Meerwein reaction[30] after the procedure of the preparation of *p*-methoxycarbonyl-*trans*-stilbene described by Fuson and Cooke[31]. The diazonium salt of *p*-anisidine was prepared by adding dropwise a solution of 27 g. of sodium nitrite in 45 ml. of water to a mixture of 150 ml. of 25% hydrochloric acid, 46.2 g. of *p*-anisidine, and 150 g. of ice. Throughout this experiment the reaction mixture was well stirred. An ice bath was placed around the reaction flask and 91.8 g. of crystalline sodium acetate was added. A solution of 55.5 g. of cinnamic acid in 450 ml. of acetone was added and the ice bath was removed. Five minutes later a solution of 20.3 g. of cupric chloride in 45 ml. of water was added dropwise and the mixture was stirred for about two hours at room temperature. After removal of a large amount of acetone, the residue was extracted with benzene. The benzene solution was washed in turn with a dilute solution of sodium carbonate, with dilute hydrochloric acid, and with water, and then dried on calcium chloride. After removal of the solvent, about 33 g. of a dark brown solid product was obtained. Treatment of the crude product with activated charcoal and repeated recrystallization from ethanol gave 23 g. of white crystals of *p*-methoxy-*trans*-stilbene, m.p. 136.8~137.5°C; yield, 29.2%.

p-Nitro-*trans*-stilbene was prepared from *p*-nitroaniline by the Meerwein reaction, quite analogously to the synthesis of the methoxy-analogue mentioned above. The purified product, yellow crystals, melted at 156~157°C; yield, about 15%.

Summary

(1) The quantitative relations between the degree of deviation from the coplanarity of the molecular configuration and the ultraviolet absorption spectrum as well as the quantities such as the extra-resonance energy and the π-bond orders have been determined for the stilbene-type compounds by calculations based on the simple LCAO molecular orbital method.

(2) The ultraviolet absorption spectra of *trans*-stilbene in the crystalline state, in the solution state, and in the vapor state have been discussed in reference to the spatial configurations of the molecule in the various states. The conjugation band in the vapor spectrum is at considerably shorter wavelengths than that in the solution spectra as well as the crystal spectra, a fact which has been considered as probably indicating that the most likely configuration of the molecule in the vapor state deviates considerably from coplanarity. The magnitude of the red-shift of the conjugation band in the crystal spectra measured by the pressed KCl-disk technique relative to the band in the spectrum of the *n*-heptane solution has been found to be smaller than the value anticipated for the rigid molecule. From this fact it has been inferred that the most probable configuration of *trans*-stilbene in solution does not significantly differ from the one in the crystalline state and is planar or nearly planar.

(3) On the basis of the above inference, the calculations have been applied to *cis*- and *trans*-stilbenes, and the interplanar angles in the most probable configuration of *cis*-stilbene have been estimated at about 28° from the position of the conjugation band, in fairly good agreement with the value estimated from the scale model. The results of the calculations have been discussed.

(4) In addition, the solvent effects of various solvents on the spectra of *trans*-stilbene and its *p*-methoxy- and *p*-nitro-derivatives have been discussed with special reference to the effect of benzene which has been found to cause a large bathochromic displacement of the conjugation band and a remarkable redistribution of intensity among the vibrational bands of the conjugation band of each compound.

The author desires to thank Professor Osamu Simamura for his encouragement, Dr. Yoshiya Kanda of Kyushu University for valuable advice, and also Professor Kengo Shiomi for reading the manuscript and for valuable advice.

Department of Chemistry
College of General Education
The University of Tokyo
Meguro-ku, Tokyo

30) H. Meerwein, E. Buchner and K. van Emster, *J. prakt. Chem.*, **152**, 237 (1939); *Chem. Abstr.*, **33**, 6261. See also: F. Bergmann et al., *J. Org. Chem.*, **6**, 134 (1941); **9**, 408, 415 (1944); **12**, 57 (1947).

31) R. C. Fuson and H. G. Cooke, Jr., *J. Am. Chem. Soc.*, **62**, 1180 (1940).

Relations between Electronic Absorption Spectra and Spatial Configurations of Conjugated Systems. VI. Triphenylethylene, Tetraphenylethylene and Tolan

By Hiroshi SUZUKI

(Received August 15, 1959)

The method developed in the preceding part[1] of this series is applied to triphenylethylene, tetraphenylethylene and tolan, and the relation between the ultraviolet absorption spectra and the spatial configurations of these compounds is discussed.

Triphenylethylene and Tetraphenylethylene

Spectra. — The ultraviolet absorption spectra of tri- and tetraphenylethylene in chloroform were formerly measured by Arends[2]. According to the results, the spectra differ only slightly from the spectrum of *trans*-stilbene. Jones[3] explained this spectral similarity as follows. "The three phenyl groups of triphenylethylene and the four phenyl groups of tetraphenyl ethylene can not be accommodated in a strainless planar structure; the strain can be eased either by a small rotation of all of the phenyl groups along their 1, 4-axes, or by a larger displacement of one of the phenyl groups of triphenylethylene or two of the *trans*-related phenyl groups of tetraphenylethylene, leaving two remaining *trans*-phenyl groups in the plane of the ethylenic bond. This second hypothesis leaves the molecule of tetraphenylethylene with a *trans*-stilbene chromophoric system together with two *insulated* phenyl groups, the absorption of which is too feeble to affect the spectrum".

The spectra of these compounds in *n*-heptane and in benzene have been newly measured by the present author. The results are shown in Table I and Fig. 1, in which the spectra of *trans*-stilbene[1] are included for comparison.

The A-band (conjugation band) of triphenylethylene as well as that of tetraphenylethylene has no distinct fine structure in contrast to that of *trans*-stilbene. The B-band, on the other hand, of triphenylethylene has a pattern of fine

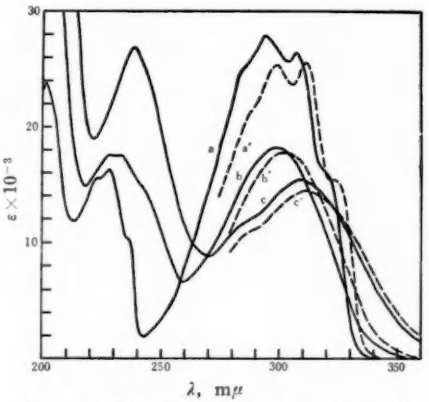

Fig. 1. Ultraviolet absorption spectra of *trans*-stilbene (a, in *n*-heptane; a', in benzene), triphenylethylene (b, in *n*-heptane; *b'*, in benzene), and tetraphenylethylene (c, in *n*-heptane; *c'*, in benzene) (cf. Table I).

structure closely similar to that of *trans*-stilbene.

Assuming that the maxima of the A-bands in the spectra of tri- and tetraphenylethylene in *n*-heptane are to be compared with the most intense maximum, viz. the γ-band, of fine structure of the A-band of *trans*-stilbene in the same solvent, the position of the maximum of the conjugation band is progressively shifted toward longer wavelengths as the number of phenyl groups in a molecule increases. The B-band is also shifted toward longer wavelengths in the same sequence. On the other hand, while the molecular extinction coefficient of the A-band decreases in the sequence, that of the B-band as well as that of the C-band increases markedly in the sequence.

Calculation and Discussion. — When it is assumed that triphenylethylene as well as tetraphenylethylene has a configuration in which the two *trans*-related phenyl groups are coplanar with the plane of the ethylenic bond according to Jones' second

1) H. Suzuki, This Bulletin, **33**, 379 (1960).
2) B. Arends, *Ber.*, **64**, 1936 (1931).
3) R. N. Jones, *J. Am. Chem. Soc.*, **65**, 1818 (1943).

TABLE I. ULTRAVIOLET ABSORPTION SPECTRA OF *trans*-STILBENE, TRIPHENYLETHYLENE AND TETRAPHENYLETHYLENE

Compound	A-band		B-band		C-band	
Solvent	λ_{max}, mμ	ε	λ_{max}, mμ	ε	λ_{max}, mμ	ε
trans-Stilbene						
n-Heptane	α (320.5)	16000	(236)	10400	201.5	23900
	β 306.9	26500	228.5	16200		
	γ 294.1	27950	(222)	15500		
Benzene	α (324.5)	15400				
	β 311.2	25600				
	γ 298.8	25340				
Triphenylethylene						
n-Heptane	298.5	18220	(242.5)	14570	(200)	40200
			232.0	17580		
			(228)	17540		
Benzene	301.8	17700				
Tetraphenylethylene						
n-Heptane	308.7	15300	238.5	26800	(203)	62500
	(285.8)	11700				
Benzene	311.2	14350				
	(288)	10900				

Wavelengths in parentheses denote inflections.

TABLE II. RESULTS OF CALCULATIONS

	trans-Stilbene		*Triphenylethylene*		*Tetraphenylethylene*	
	(γ)	(β)	(γ)	(β)	(γ)	(β)
λ_{max}, mμ	294.1	306.9	298.5		308.7	
$\Delta E_A(-\beta)$	1.1423		1.112	1.193	1.044	1.132
ρ	0.9084		0.946	0.849	1.032	0.922
ρ'	—		0.669	0.529	0.730	0.652
θ°	0		40	52	34.5	42
R, Å	1.445		1.467	1.481	1.462	1.469
$R.\ E.\ (-\beta)$	0.704		0.764	0.610	0.906	0.720
$p_{\alpha-\alpha'}$	0.8555		0.845	0.873	0.820	0.852
$p_{\alpha-1}$	0.384		(ρ) 0.400	0.359	0.310	0.277
			(ρ') 0.285	0.225		
$\Delta E_B(-\beta)$	1.571		1.556	1.597	1.522	1.566

hypothesis, it is evident that calculations quite similar to the one for stilbene described in the preceding part of this series can be applied to these compounds.

Alternatively, when it is assumed that in tetraphenylethylene all of the phenyl groups are rotated out of the plane of the ethylenic bond to the same extent as each other according to Jones' first hypothesis, the secular equation for the determination of the molecular orbitals as linear combinations of $2p\pi$ atomic orbitals is factorized into one equation identical in form with the one for stilbene and two equations for benzene, when ρ' is $1/\sqrt{2}\times\rho$, $\rho'\beta$ representing the $\pi-\pi$ resonance integral for each bond connecting a phenyl group to a ethylenic carbon atom.

Similarly, when it is assumed that ρ' is equal to $1/\sqrt{2}\times\rho$ also in triphenylethylene, in which the $\pi-\pi$ exchange integral for each of the bonds connecting two phenyl groups to the same ethylenic carbon atom and that for the bond connecting the other phenyl group to the other ethylenic carbon atom are denoted by $\rho'\beta$ and $\rho\beta$, respectively, the secular equation for this molecule can be factorized into an equation identical in form with the one for stilbene and the equation for benzene.

Therefore, whichever the configurations may be, the calculation based on the same equation as the one for stilbene can be applied to these compounds. Thus, after the procedure described in the preceding part of this series, the values of ρ can be computed from the observed positions of the A-bands.

Since the A-bands of these compounds

are at longer wavelengths than the A-γ-band of *trans*-stilbene as the reference, the values of ρ for the former compounds should be larger than that for the latter. If the models according to Jones' second hypothesis are chosen, the large values of ρ for tri- and tetraphenylethylene relative to the value for *trans*-stilbene must be explained only by the assumption that the lengths of the bonds linking the coplanar *trans*-related phenyl groups to the ethylenic carbon atoms in tri- and tetraphenylethylene were shorter than the corresponding one in *trans*-stilbene, since the most probable configuration of *trans*-stilbene is considered to be already planar. This is undoubtedly implausible.

The inference that Jones' second hypothesis is implausible seems to be supported also by the following consideration. Thus, as is seen in Table I and Fig. 1, the molecular extinction coefficient of the A-band decreases markedly in the order *trans*-stilbene > triphenylethylene > tetraphenylethylene. If there were any *trans*-stilbene chromophore in these compounds, all these compounds would show the almost identical molecular extinction coefficient at least approximately.

Now, when the alternative models according to Jones' first hypothesis are assumed for the most probable configurations of tri- and tetraphenylethylene, the values of ρ' are obtained from the values of ρ, and then, from the values of ρ' the values of θ, R and $p_{\alpha-1}$ can be obtained by the procedure analogous to the one for stilbene in the preceding part of this series. The results of calculations are shown in Table II, in which those for *trans*-stilbene are included for comparison. (The symbols have the same significance as in the preceding part.)

The fact that the calculated value of θ in triphenylethylene is apparently greater than that in tetraphenylethylene is, needless to say, due to the probably unreal starting assumption that one of the phenyl groups in triphenylethylene is coplanar with the plane of the ethylenic bond. The most probable configuration of triphenylethylene is presumed to be the one in which all of the phenyl groups are rotated out of the plane of the ethylenic bond to certain extents. Therefore, no reliance is to be placed on the values of θ, R and $p_{\alpha-1}$ for this compound, while the values of $R.E.$, $p_{\alpha-\alpha'}$ and ΔE_B can probably be considered as rough approximations.

The above mentioned calculations are based on the assumption that the maxima of the A-bands of tri- and tetraphenylethylene are to be compared with the γ-band in the A-band of *trans*-stilbene. However, as is seen in Table I and Fig. 1, while the maxima in the spectra of tri- and tetraphenylethylene in benzene are considered to correspond to the maxima in *n*-heptane, the most intense maximum in the spectrum of *trans*-stilbene in benzene is the β-band and not the γ-band as in *n*-heptane. Accordingly the possibility that the β-band instead of the γ-band is to be taken as the reference can not perhaps be ruled out. In Table II, the results of the calculations carried out by taking the β-band as the reference are also shown, being denoted by symbol β, in addition to those mentioned already, which are denoted by symbol γ. However, in view of the correlations of these results with some properties of the compounds, results γ seems more adequate, and hence subsequently the results of the calculations refer solely to results γ.

The B-bands are probably due to the allowed transitions from the highest occupied orbitals to the vacant orbitals with the energy of $-\beta$, or from the occupied orbitals with the energy of $+\beta$ to the lowest vacant orbitals, similarly to the case of stilbene. The C-bands are probably due to the allowed transitions from the orbitals with the energy of $+\beta$ to the orbitals with the energy of $-\beta$.

The B-band as well as the C-band increases the intensity in the order *trans*-stilbene < triphenylethylene < tetraphenylethylene, with an increasing number of benzene nuclei. It is interesting that the ratio of the molecular extinction coefficients of the C-bands of these compounds are roughly 1:2:3, in accordance with the ratio of the numbers of the orbitals which are considered to participate in these transitions.

In addition, it is of interest that the magnitude of the red-shift of the conjugation band associated with the change of solvent from *n*-heptane to benzene is appreciably smaller in the cases of tri- and tetraphenylethylene than in the case of *trans*-stilbene as well as some para-substituted *trans*-stilbenes which are presumed to be planar. If the presumption in the preceding part of this series that the shift is due to the special interaction between the π-orbitals of benzene and

those of the solute molecule is correct, this fact may be related to the nonplanarity of the configurations of tri- and tetraphenylethylene. This subject will be discussed more fully in a later part of this series.

Correlations between the Spatial Configurations and Some Properties of the Compounds.—The melting point of tetraphenylethylene is 223~224°C, and is considerably lower than that of its positional isomer, *p*, *p'*-diphenyl-*trans*-stilbene (about 300°C). In addition, the solubilities of the former compound in usual organic solvents are much greater than those of the latter. These facts are probably due to the nonplanarity of the configuration of tetraphenylethylene. The melting point of triphenylethylene is 68~69°C and markedly lower than that of its positional isomer, *p*-phenyl-*trans*-stilbene (about 220°C), and even than that of *trans*-stilbene (125°C). This fact is probably due to the nonplanarity and the unsymmetrical nature of the configuration of triphenylethylene.

According to Everard and others[4], the exaltation of the molecular refraction ($E[R]_D$) of *trans*-stilbene is +6.6, and that of triphenylethylene is about the same as, or only 0.1 at most less than, that of *trans*-stilbene. This fact may be considered to indicate that the extent of conjugation in triphenylethylene is almost equal to that in *trans*-stilbene, almost in complete accordance with the present conclusion deduced from the ultraviolet absorption spectra.

Next, the relations between the spatial configurations and the reactivities of these compounds will be discussed. In general, steric effects in reactions of olefinic compounds may be divided into the two main types: the steric hindrance to the approach of the reagent to the reaction site and the steric hindrance to resonance. The former may be illustrated by the fact that the rate of bromination of neopentylethylene is smaller than that of *t*-butylethylene[5]. That is, the steric effect of this type retards the reactions in most cases.

Tetraphenylethylene does not add bromine[6,7]. This is probably due to the steric effect of the first type mentioned above. That is, it seems that the phenyl groups rotated out of the plane of the central ethylenic bond inhibit the approach of the reagent to the bond.

According to Leavitt and others[8], the "methyl affinity" is 205 for *trans*-stilbene, 85 for triphenylethylene, and less than 25 for tetraphenylethylene. The "methyl affinity" is considered as a measure of reactivity of compounds to the methyl radical, although it is not clear which atoms of the compounds are attacked. The order of the "methyl affinity" mentioned above appears to be well explained in terms of the steric effect of the first type.

The reaction of olefins with perbenzoic acid in nonpolar solvents gives excellent yields of the corresponding epoxides. It has been presumed that in this reaction perbenzoic acid acts as a "double-bond reagent". According to Lynch and Pausacker[9], the reactivity of the series of phenyl-substituted ethylenes toward perbenzoic acid follows the double-bond orders of the olefinic links calculated by Coulson and Jacobs[10] (i.e. styrene>*trans*-stilbene > triphenylethylene> tetraphenylethylene). However, the calculations by Coulson and Jacobs are unacceptable because they are based on unreal planar molecular models even in the cases of tri- and tetraphenylethylene.

In spite of this, the sequence of the π-bond orders calculated by Coulson and Jacobs agrees qualitatively with the sequence of the π-bond orders as well as that of the extra-resonance energies (i.e. the bond localization energies of the ethylenic bonds) calculated here by taking the spatial configurations into account. (The π-bond orders of the ethylenic bonds calculated by Coulson and Jacobs are: *trans*-stilbene, 0.820; triphenylethylene, 0.752; tetraphenylethylene, 0.685. On the other hand, those calculated by the present author are 0.8555, 0.845 and 0.820, respectively.) Therefore, the sequence of the bond order and hence the sequence of the bond localization energy are presumed to determine at least partly the sequence of the reactivity. However, judging from the fact that the differences of the bond order and of the bond localization energy among these compounds are small, the steric effect of the first type may also be a contributory factor to the reactivity. This subject will be discussed in somewhat

4) K. B. Everard, L. Kumar and L. E. Sutton, *J. Chem. Soc.*, **1951**, 2807.
5) P. W. Robertson, J. K. Heyes and B. E. Swedlund, ibid., **1952**, 1014.
6) H. Bauer, *Ber.*, **37**, 3317 (1904).
7) J. Meisenheimer, *Ann.*, **456**, 139 (1927).
8) F. Leavitt, M. Levy, M. Szwarc and V. Stannett, *J. Am. Chem. Soc.*, **77**, 5493 (1955).
9) B. M. Lynch and K. H. Pausacker, *J. Chem. Soc.*, **1955**, 1525.
10) C. A. Coulson and J. Jacobs, ibid., **1949**, 2805.

TABLE III. ULTRAVIOLET ABSORPTION SPECTRA OF TOLAN

Solution in n-heptane

	A-band		B-band		C-band	
	λ_{max}, mμ	ε	λ_{max}, mμ	ε	λ_{max}, mμ	ε
α	297.2	27500	237.2	6930	196.5	38000
β	288.5	20800	232.2	6520		
γ	279.9	30800	222.0	16500		
δ	272.7	22400	217.2	18500		
ε	265.3	20600	(212)	19000		

Crystals (pressed KCl-disk)

	A-band				B-band			
	λ_{max}, mμ	$\Delta\lambda$	A	ε	λ_{max}, mμ	$\Delta\lambda$	A	ε
α	301.6	+4.4	0.282	1920	(239.0)	+1.8	0.100	680
β	292.4	+3.9	0.247	1680				
γ	283.3	+3.4	0.350	2380	(223.5)	+1.5	0.227	1540
δ	(275.8)	+3.1	0.288	1960	(218.5)	+1.3	0.264	1790
ε	268.0	+2.7	0.259	1760				

Wavelengths in parentheses denote inflections.
$\Delta\lambda$ denotes the magnitude of the wavelength displacement (in mμ) of each band relative to the corresponding band in the spectrum in *n*-heptane.
A denotes the absorbance (optical density).

greater detail in the succeeding part of this series.

In the reactions discussed so far, the reactivity decreases in the order *trans*-stilbene > triphenylethylene > tetraphenylethylene. This order coincides not only with the order in which the steric hindrance to the approach of the reagent to the ethylenic bond increases, but also with the order in which the π-bond order decreases and hence the bond localization energy increases. Both the factors, steric and electronic, will contribute to the reactivity in the same direction.

On the other hand, in the polarographic reduction the effect of conjugation operates in the opposite direction. Thus, the reduction takes place more easily with an increasing extent of conjugation, and the isolated double bond is not reducible. Maccoll[11] has found that there exists a linear relationship between the reduction potential and the energy required to place one or two electrons in the lowest vacant orbital of the molecule, that is, the energy (in $-\beta$) of the lowest vacant orbital, which is evidently half of $\Delta E_A(-\beta)$ in the present treatment. That is, the reduction potential should be related directly to the transition energy corresponding to the conjugation band. According to Laitinen and Wawzonek[12], in the series of phenylated ethylenes the ease of electro-reduction increases with increasing substitution in the order styrene < 1,1-diphenylethylene < *trans*-stilbene < triphenylethylene < tetraphenylethylene. The mean value of the reduction potential E (in V.) is -2.1425 for *trans*-stilbene, -2.1155 for triphenylethylene, and -2.046 for tetraphenylethylene. On the other hand, the energies of the lowest vacant orbitals (in $-\beta$) of these compounds are calculated to be 0.5712, 0.5558 and 0.5219, respectively. There exists a linear relationship between the reduction potential and the energy of the lowest vacant orbital at least in so far as these compounds are concerned. Tolan has a slightly more negative reduction potential (-2.195 V.) than *trans*-stilbene. This fact corresponds only qualitatively to the fact that the conjugation band of tolan is at shorter wavelengths than that of *trans*-stilbene as will be shown in the succeeding section (the energy of the lowest vacant orbital of tolan is calculated to be $-0.635\ \beta$).

trans-Stilbene forms a colored complex with 1, 3, 5-trinitrobenzene. According to the qualitative study by Ley and Rinke[13], when an aromatic compound is mixed with 1, 3, 5-trinitrobenzene in chloroform (both concentrations, 0.02 mol./l.), the solution colors as follows: *trans*-stilbene, intense yellow; triphenylethylene, yellow; tetraphenylethylene, very feeble yellow; (tetraphenylethane, colorless). The extent of coloration is considered to indicate

11) A. Maccoll, *Nature*, **163**, 178 (1949).
12) H. A. Laitinen and S. Wawzonek, *J. Am. Chem. Soc.*, **64**, 1765 (1942).
13) H. Ley and F. Rinke, *Ber.*, **56**, 771 (1923).

qualitatively the extent of the complex formation. Thus, the extent of the complex formation decreases with an increasing number of phenyl groups in the series of phenylated ethylenes, and accordingly may be related to the spatial configurations of these compounds.

Tolan

Spectra. — The ultraviolet absorption spectra of tolan (diphenylacetylene) are shown in Table III and Fig. 2. The spectra exhibit the conjugation band with well-resolved fine structure at considerably shorter wavelengths than the conjugation band of *trans*-stilbene. The spectrum of tolan in the crystalline state measured

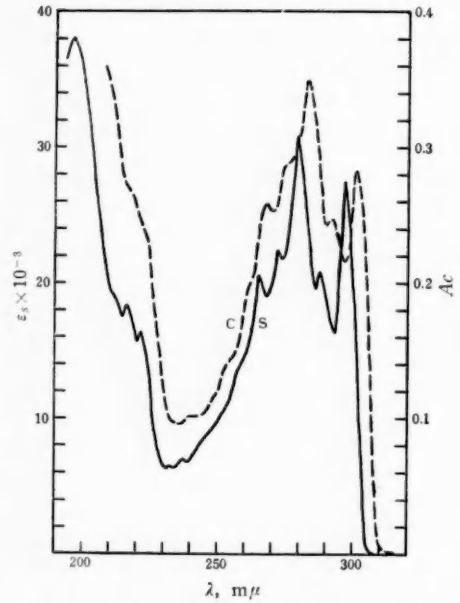

Fig. 2. Ultraviolet absorption spectra of tolan in solution in *n*-heptane (S) and in the crystalline state (the pressed KCl-disk) (C). Note separate ordinates for solution and crystals (cf. Table III).

by the pressed KCl-disk technique resembles the solution spectrum on the whole.

The red-shift of each band associated with the change of the state from the *n*-heptane solution to the crystalline state is seen to increase with almost complete regularity with the wavelength of the band from about 1.3 mμ at 217.2 mμ to about 4.4 mμ at 297.2 mμ, although these shifts are considerably smaller than the values determined by Dale[14] for naphthalene and anthracene (about 2 mμ at 220 mμ to 8 mμ at 300 mμ).

As seen already in the case of *trans*-stilbene in the preceding part of this series, also in the case of tolan, the apparent molecular extinction coefficients in the KCl-disk spectrum are much smaller than the corresponding molecular extinction coefficients in the solution spectrum, the former ones being only about 1/13 of the latter ones.

Calculation. — The notation used is as follows: the carbon atoms of the central triple bond, α and α'; the carbon atoms attached to α and α', 1 and 1'; the $2p\pi$ atomic orbitals at 1 and 1', ϕ_1 and $\phi_{1'}$; the two π-bonds in the triple bond, $(\alpha-\alpha')_x$ and $(\alpha-\alpha')_z$; the corresponding $2p\pi$ atomic orbitals, ϕ_x, $\phi_{x'}$, ϕ_z, and $\phi_{z'}$; the $\pi-\pi$ resonance integral for each of $(\alpha-\alpha')_x$ and $(\alpha-\alpha')_z$, $\eta_i\beta$; the $\pi-\pi$ resonance integral between ϕ_1 and ϕ_x as well as that between $\phi_{1'}$ and $\phi_{x'}$, $\rho_x\beta$; that between ϕ_1 and ϕ_z as well as that between $\phi_{1'}$ and $\phi_{z'}$, $\rho_z\beta$.

The secular equation for the determination of the molecular orbitals of tolan as linear combinations of the $2p\pi$ atomic orbitals can be factorized into the stilbene-type equation and the equation for an isolated π-bond, either when one of the parameters ρ_x and ρ_z is zero and the other is replaced by ρ, or when the parameters are equal to each other and both are replaced by $1/\sqrt{2}\times\rho$. The former requirement means that the two phenyl groups are in conjugation solely with one of the two π-bonds in the triple bond, leaving the other insulated. The alternative requirement means, needless to say, that the axes of ϕ_1 and $\phi_{1'}$ form an angle of 45° with the axes of ϕ_x and $\phi_{x'}$ as well as the axes of ϕ_z and $\phi_{z'}$.

According to the X-ray crystal analysis by Robertson and Woodward[15], tolan in the crystalline state has a planar configuration in which the lengths of the $\alpha-\alpha'$ bond and of the $\alpha-1$ as well as the $\alpha'-1'$ bond are 1.19 ± 0.02 and 1.40 ± 0.02 Å, respectively. The most probable configuration in solution is thought not to differ significantly from the configuration in the crystalline state, in view of the close similarity of the spectra in the two states. From the values of the bond lengths the values of the parameters η and ρ are

14) J. Dale, *Acta Chem. Scand.*, **11**, 650 (1957). See also Ref. 1 and Part I of this series: This Bulletin, **32**, 1340 (1959).

15) J. M. Robertson and I. Woodward, *Proc. Roy. Soc.* (*London*), **A164**, 436 (1938).

calculated to be 1.378 and 0.983, respectively, by the usual procedure based on the proportionality between the $\pi-\pi$ resonance integral and the $\pi-\pi$ overlap integral. By solving the secular equation, the following values are obtained: $\Delta E_A(-\beta)$, 1.270; $\Delta E_A(-\gamma)$, 1.303; *R. E.* $(-\beta)$, 0.732; *R. E.* $(-\gamma)$, 0.221; $p_{\alpha-\alpha'}$, 1.868; $p_{\alpha-1}=p_{\alpha'-1'}$, 0.372; $\Delta E_B(-\beta)$, 1.635. (The symbols have the same significance as in the preceding part of this series.)

Whereas the length of the $\alpha-1$ "single" bond in tolan is shorter than the length of the corresponding "single" bond (1.44 ± 0.02 or 1.45 ± 0.02 Å) in *trans*-stilbene, the π-bond order of the former is smaller than that of the latter (0.384). This fact is perhaps attributed to the difference of the hybridization of the σ-orbital at the α carbon atom in these two compounds (tolan, sp; stilbene, sp^2). Berthier and Pullman[16] reported somewhat different values for the π-bond orders of these compounds (tolan: $\alpha-\alpha'$, 1.909; $\alpha-1$, 0.307; *trans*-stilbene: $\alpha-\alpha'$, 0.879; $\alpha-1$, 0.352), but the relationship among the values is similar.

By using the linear relation between ΔE_A and ν_A postulated for the stilbene-type compounds in the precending part of this series (the longer-wavelength-side reference is the γ-band in the spectrum of *trans*-stilbene in *n*-heptane and the shorter-wavelength-side reference is the center of gravity of singlets of benzene), the wave number ν_A corresponding to the value of $\Delta E_A(-\beta)$ for tolan is calculated to be 36086 cm^{-1} (277.1 mμ). This is in good agreement with the observed position (279.9 mμ) of the γ-band of tolan in *n*-heptane, which is the most intense maximum of fine structure of the conjugation band. In addition, when the α-band or the β-band in the spectrum of *trans*-stilbene in *n*-heptane is taken as the longer-wavelength-side reference, the value of ν_A is computed to be 33702 cm^{-1} (296.7 mμ) or 34879 cm^{-1} (286.7 mμ), correspondingly, in agreement with the observed positions of the α-band (297.2 mμ) and the β-band (288.5 mμ) in the spectrum of tolan in *n*-heptane. The good agreement between the calculated wavelengths and the observed ones of the bands seems to justify the postulation of the linear relation between ΔE_A and ν_A.

16) G. Berthier and B. Pullman, *Compt. rend.*, **228**, 397 (1949).

Experimental

Measurements of Spectra.—All the spectra were measured with a Cary recording spectrophotometer Model 14 M-50.

The crystal spectrum of tolan was measured by the pressed KCl-disk technique quite analogously to the case of *trans*-stilbene in the preceding part of this series. About 3 mg. of tolan was thoroughly ground with about 200 mg. of potassium chloride and then about 10 mg. of the mixture was ground with about 350 mg. of potassium chloride and pressed. The disk used weighed 84.7 mg. (the thickness, about 0.321 mm.).

Materials.—Triphenylethylene was prepared by dehydration of 1,1,2-triphenylethanol obtained by the reaction of benzophenone with benzyl magnesium chloride[17]. From 27.3 g. (0.15 mol.) of benzophenone, 24.3 g. (0.095 mol.) of triphenylethylene, white crystals melting at 68~69°C, were obtained after recrystallization from 95% ethanol (63.3% of the theoretical amount).

Tetraphenylethylene was prepared by heating diphenyldichloromethane (benzophenone dichloride) with powdered copper in anhydrous benzene[18]. Diphenyldichloromethane was prepared from benzophenone and phosphorus pentachloride[19]. From 9.1 g. (0.05 mol.) of benzophenone, 4.7 g. (0.014 mol., 56.5% of the theoretical amount) of tetraphenylethylene, almost colorless crystals melting at 223~224°C, were obtained after recrystallization from a 1 : 1 by volume mixture of absolute ethanol and benzene.

Tolan was prepared, according to the directions of Schlenk and Bergmann[20], by oxidizing benzil dihydrazone with mercuric oxide. Benzil was prepared by oxidation of benzoin with nitric acid[21]. The yield of pure tolan, colorless crystals melting at 62°C, from 47 g. (0.219 mol.) of benzil was 16.4 g. (0.092 mol., 42% of the theoretical amount) after repeated recrystallization from ethanol.

Summary

The most probable configuration of triphenylethylene as well as that of tetraphenylethylene has been inferred to be the one in which all of the phenyl groups are rotated out of the plane of the ethylenic bond, on the basis of the analysis of the ultraviolet absorption spectra by application of the method based on the simple LCAO molecular orbital method described in the preceding part of this series. Some physical and chemical properties of these compounds have been

17) L. F. Fieser (Editor-in-Chief), "Organic Syntheses", Vol. XVII, John Wiley & Sons, Inc., New York (1937), p. 89.
18) R. S. Schreiber (Editor-in-Chief), ibid., Vol. 31 (1951), p. 104.
19) C. S. Marvel (Editor-in-Chief), ibid., Vol. XI (1931), p. 95.
20) W. Schlenk and E. Bergmann, *Ann.*, **463**, 76 (1928).
21) R. Adams (Editor-in-Chief), "Organic Syntheses", Vol. I, John Wiley & Sons. Inc., New York (1921), p. 25.

discussed with reference to the spatial configurations.

The method has been applied also to tolan (diphenylacetylene), and it has been shown that the calculated wavelengths of the bands agree fairly well with the observed ones.

In addition, it has been shown that the spectrum of tolan in the crystalline state measured by the pressed KCl-disk technique resembles the spectrum of the solution in *n*-heptane on the whole, and that the red-shift of each band associated with the change of the state from the *n*-heptane solution to the crystalline state increases with almost complete regularity with the wavelength of the band from about 1.3 mμ at 217.2 mμ to about 4.4 mμ at 297.2 mμ, the shifts observed here being appreciably smaller than the analogous shifts observed by Dale in the spectra of naphthalene and anthracene.

The author thanks Professor Kengo Shiomi for reading the manuscript and for advice.

Department of Chemistry
College of General Education
The University of Tokyo
Meguro-ku, Tokyo

Relations between Electronic Absorption Spectra and Spatial Configurations of Conjugated Systems. VII. α-Substituted and α,α'-Disubstituted Stilbenes

By Hiroshi SUZUKI

(Received August 15, 1959)

The method developed in Part V[1] of this series is applied to α- and α,α'-substituted stilbenes, some of which were preliminarily treated in an earlier paper[2], and the relations between the ultraviolet absorption spectra and the spatial configurations of these compounds are discussed. Further, the relations between the spatial configurations and some physical and chemical properties of these compounds are discussed in detail with special reference to α,α'-dimethylstilbene.

Ultraviolet Absorption Spectra.—The ultraviolet absorption spectra of α-alkyl- and α,α'-dialkylstilbenes in ethanol were reported previously[2]. The spectra of some of these compounds as well as α,α'-dihalostilbenes in *n*-heptane have newly been measured. These are shown in Figs. 1 and 2. In Table I, the data of the spectra are summarized.

The spectra of the alkylated stilbenes in *n*-heptane do not differ significantly from the corresponding spectra in ethanol. Thus, the following generalizations, some of which were not explicitly stated in the earlier paper, can be deduced. (1) The conjugation band is shifted toward shorter wavelengths and is reduced in intensity with increasing number and increasing size of substituents at the ethylenic

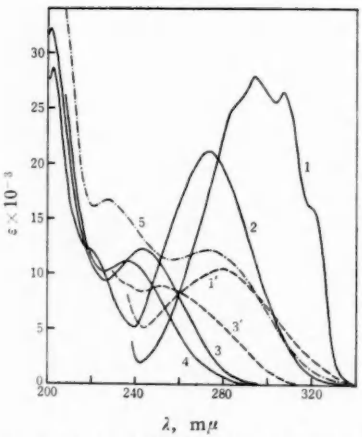

Fig. 1. Ultraviolet absorption spectra of stilbenes in *n*-heptane: 1, *trans*-stilbene; 1', *cis*-stilbene (in ethanol); 2, *trans*-α-methylstilbene; 3, *trans*-α,α'-dimethylstilbene; 3', *cis*-α,α'-dimethylstilbene; 4, *trans*-α,α'-diethylstilbene; 5, methyltriphenylethylene.

1) H. Suzuki, This Bulletin, **33**, 379 (1960).
2) H. Suzuki, ibid., **25**, 145 (1952).

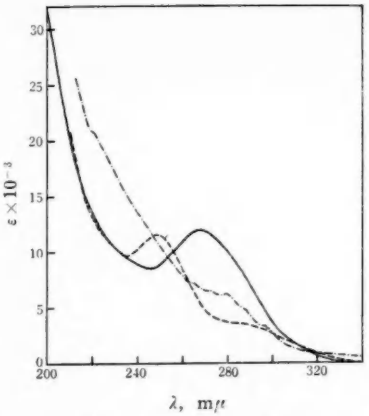

Fig. 2. Ultraviolet absorption spectra of *trans*-α,α'-dihalostilbenes in *n*-heptane: ——, dichlorostilbene; ------, dibromostilbene; —·—·—, diiodostilbene.

carbon atoms in each of the *trans* and the *cis* series. (2) The conjugation band of a *trans* isomer is invariably more intense than that of the corresponding *cis* isomer. (3) With stilbene as well as α-methylstilbene, the conjugation band of the *trans* isomer is at longer wavelengths than that of the *cis* isomer. On the other hand, with α,α'-dimethyl- as well as α,α'-diethylstilbene, the conjugation band of the *trans* isomer is at shorter wavelengths than that of the *cis* isomer. (4) The conjugation bands of these stilbene derivatives have, similarly to that of *cis*-stilbene, no fine structure, in contrast to that of *trans*-stilbene.

Also with *trans*-α,α'-dihalostilbenes, the conjugation band is structureless, and is shifted toward shorter wavelengths as the substituents become larger. *trans*-α,α'-Diiodostilbene in *n*-heptane dissociates

TABLE I. ULTRAVIOLET ABSORPTION MAXIMA

Stilbene	Solvent	*trans*			*cis*		
		λ, mμ	ε	Ref.	λ, mμ	ε	Ref.
Unsubstituted	H	294.1*	27950	1)			
		(B 228.5*	16200)				
		(C 201.5	23900)				
	E	294.5*	27850	1)	280	10450	a)
		(B 228.8*	16400)		(B 224	24400)	
		(C 201.0	23800)				
α-Methyl-	H	273.5	21100	b)			
		(B (217)	12530)				
		(C 202.3	28700)				
	E	272	21000	2)	267	9340	2)
α,α'-Dimethyl-	H	243.3	12270	b)	252.0	8880	b)
		(C (201.3)	32250)				
	E	243.5	12260	2)	252	8780	2)
α-Methyl-α'-ethyl-	E	240	11950	2)			
α,α'-Diethyl-	H	236.6	11090	b)			
	E	237.5	11020	2)	244	7740	2)
α-Methyl-α'-phenyl-	H	274.5	12200	b)			
		(B 227.5	16800)				
	E	275	9860	2)			
		(B 226	13720)				
α,α'-Dichloro-	H	268.0	12000	b)			
α,α'-Dibromo-	H	248.5	11570	b)			
α,α'-Diiodo-	H	(220.5)	20800**	b)			

Solvent: H, *n*-heptane; E, ethanol.

Symbols B and C in parentheses denote the B-band and the C-band, respectively. All the maxima other than the B- and C-bands refer to the conjugation bands (viz. A-bands). Wavelengths in parentheses denote inflections.

* The most intense maximum of fine structure.

** The apparent value. The accurate molecular extinction coefficient could not be determined, because this compound dissociates partly in this solvent into tolan and iodine.

a) R.N. Beale and E.M.F. Roe, *J. Chem. Soc.*, **1953**, 2755.

b) The present work.

TABLE II. RESULTS OF CALCULATION

Stilbene	Solvent	λ_A	ΔE_A	ρ	θ°	R	$R.E.$
		mμ	$-\beta$			Å	$-\beta$
trans-α-Methyl-	H	273.5	1.299	0.730	34.5	1.462	0.457
cis-α-Methyl-	E	267	1.354	0.671	40	1.467	0.387
trans-α,α'-Dimethyl-	H	243.3	1.577	0.446	58	1.490	0.173
cis-α,α'-Dimethyl-	H	252.0	1.490	0.531	51.5	1.481	0.243
trans-α-Methyl-α'-ethyl-	E	240	1.612	0.412	60.5	1.493	0.146
trans-α,α'-Diethyl-	H	236.6	1.649	0.378	63	1.497	0.124
cis-α,α'-Diethyl-	E	244	1.570	0.453	57.5	1.489	0.178
trans-α,α'-Dichloro-	H	268.0	1.345	0.680	39	1.467	0.397
trans-α,α'-Dibromo-	H	248.5	1.525	0.497	54.5	1.485	0.212
trans-α,α'-Diiodo-	H	220.5	1.838	0.200	75.7	1.517	0.034

gradually into tolan and iodine, and consequently the absorption due to tolan is detected in the spectrum (cf. Fig. 2 with Fig. 2 in the preceding part[3] of this series). The inflection at near 220.5 mμ probably indicates the vestigial conjugation band of *trans*-α,α'-diiodostilbene.

Application of Calculation.—In the application of the method developed in Part V of this series to these stilbene derivatives, the data of the spectra of *n*-heptane solutions newly measured are used. For the compounds, the spectra of which in *n*-heptane have not yet been measured, the data of the spectra of ethanol solutions are used, since the positions of the bands may be considered not to vary significantly in either of the solvents (cf. Table I and also Parts I[1] and V of this series).

The effects of the substituents upon the spectra must include not only the steric hypsochromic effect due to the steric interferences between the substituents and the phenyl groups but also the electronic (probably bathochromic) effect of the substituents (cf. Part II[5] of this series). However, in view of the fact that the substituents in the compounds treated here are at the positions of cross-conjugation to the conjugated system of the stilbene skeleton, this possible electronic effect is considered to be probably very small compared with the steric hypsochromic effect, especially in the cases of the alkyl substituents, and therefore, is ignored in the present treatment.

In the cases of the halogen substituents, the electronic effect of the lone pair electrons of the halogen atoms may be relatively large campared with the electronic (probably hyperconjugation) effect of the alkyl substituents, and perhaps it should not be ignored. Nevertheless, the possible electronic effect of all the substituents is ignored, for simplification, in the present treatment. That is, it is assumed that the position of the conjugation band is determined solely by the spatial configuration of the stilbene skeleton.

The results of the calculations are shown in Table II. The notation used here is the same as in Part V of this series.

In α-methylstilbene as well as α-methyl-α'-ethylstilbene, the positions of the two phenyl groups are not equivalent, and therefore, their angles of twist must differ from each other. In spite of this, the results for these compounds, obtained on the basis of the assumption that the angles of twist of the two phenyl groups are equal, are also shown for comparison.

It is to be noted that the calculated values of the angle of twist θ (interplanar angle) in Table II are possibly rather smaller than the actual values because of the neglect of the electronic effect of the substituents mentioned above. In addition, when the β-band instead of the γ-band of *trans*-stilbene is taken as the "longer-wavelength-side reference", the calculated values of θ will evidently become greater than those in Table II.

Discussion

As will be expected, Table II shows that the calculated interplanar angle becomes larger with the increasing number and size of substituents. It is of interest that the change of the substituents from methyl groups to ethyl groups affects only rather slightly the position of the conjugation band and consequently the interplanar angle. A somewhat similar phenomenon has been seen in the comparison between *o*-methyl- and *o*-ethylbiphenyl[5]. On the

3) H. Suzuki, ibid., **33**, 389 (1960).
4) H. Suzuki, ibid., **32**, 1340 (1959).
5) H. Suzuki, ibid., **32**, 1350 (1959).

other hand, the replacement of the methyl group in β-methylcinnamic acid by an ethyl group has a greater steric consequence. According to Takahasi[6], the wavelengths (mμ) of the conjugation bands and the molecular extinction coefficients (in parentheses) of the bands of cinnamic acid and its β-alkyl derivatives in 94% ethanol are as follows: cinnamic acid, 273 (22000); β-methylcinnamic acid, 260 (15000); β-ethylcinnamic acid, 244 (10000).

The conjugation band of methyltriphenylethylene (1,1,2-triphenylpropene) is at a considerably shorter wavelength than that of triphenylethylene (cf. the preceding part of this series) and coincides in position almost completely with that of *trans*-α-methylstilbene. From this fact, it would be inferred that the most probable configuration of methyltriphenylethylene might be the one in which the phenyl group at the *trans*-position to the methyl group was completely rotated out of the plane of the ethylenic bond, or in other words, was insulated, leaving the two remaining *trans*-related phenyl groups in the configuration analogous to the most probable configuration of *trans*-α-methylstilbene. However, the fact that the intensity of the conjugation band of methyltriphenylethylene is much smaller than that of *trans*-α-methylstilbene suggests that this inference is unlikely. This situation is very similar to that observed in the comparison between the spectra of triphenylethylene and of *trans*-stilbene[3].

As mentioned already, it is especially noteworthy that the conjugation band of *trans*-α,α'-dimethylstilbene as well as its diethyl a analogue is at a shorter wavelength than that of the *cis* isomer, contrary to the generally accepted view that *trans* isomers of conjugated compounds should exhibit the conjugation bands at longer wavelengths than the corresponding *cis* isomers. A similar phenomenon has been observed by Nagai and Simamura[7] with some *p,p'*-disubstituted α,α'-dimethylstilbenes. These facts are considered to indicate that with these compounds the *trans* isomers are less conjugated than the corresponding *cis* isomers. In fact, as is seen in Table II, the calculated interplanar angles in the *trans* isomers of α,α'-dimethylstilbene and its diethyl analogue are larger than those of the corresponding *cis* isomers, and the calculated extra-resonance energies of the *trans* isomers are smaller than those of the *cis* isomers. This conclusion deduced here from the absorption spectra seems to be supported by some pieces of information on the properties of these compounds such as the reactivities, the nuclear magnetic resonance spectra, and the exaltations of molecular refraction. Accordingly, the relations between the spatial configurations and some physical and chemical properties of the stilbenes will be discussed in a later section with special emphasis on those for *trans*- and *cis*-α,α'-dimethylstilbenes.

Correlation of the Calculated Interplanar Angles with the Values Estimated from Scale Models.—That the calculated interplanar angle (58°) for *trans*-α,α'-dimethylstilbene agrees fairly well with the value estimated from scale models has been described in the earlier paper[2]. Thus, according as one assumes a twisted structure for this compound in which the ortho hydrogen atom of each phenyl group just touches the methyl group attached to the same ethylenic carbon atom as the phenyl group or a structure in which that hydrogen atom just touches the other methyl group, the interplanar angle is estimated at 60° or 56°, in good agreement with the calculated value.

For *trans*-α,α'-dibromostilbene, the interplanar angle is estimated at 48° or 51.5° from analogous models in which the interference radius of a bromine atom is 1.95 Å[8] (van der Waals radius) and the length of a C-Br bond is 1.91 Å[8] (the length of an Alkyl-Br bond). The actual length of the C-Br bond may be shortened more or less from the above normal value by interaction between the bromine atom and the ethylenic bond[9]. When the possible shortening of the bond is taken into account, the interplanar angle estimated from models will become slightly larger. The agreement of the calculated value (54.5°) of the interplanar angle with the value estimated from scale models is not so good as in the case of the dimethyl analogue; still it may be said to be fairly good.

6) M. Takahasi, ibid., **31**, 756 (1958).
7) Y. Nagai and O. Simamura, presented at the 11th Annual Meeting of the Chemical Society of Japan, Tokyo, April, 1958.
8) L. Pauling, "The Nature of the Chemical Bond", Cornell University Press, Ithaca, N. Y. (1940).
9) (a) H. de Laszlo, *Proc. Roy. Soc.* (*London*), **A146**, 690 (1934). (b) J. A. C. Hagill, I. E. Coop and L. E. Sutton, *Trans. Faraday Soc.*, **34**, 1518 (1938).

For the dichloro analogue, the interplanar angle is estimated at 43° or 48° from the analogous medels in which the interference radius of a chlorine atom is 1.80 Å[8] (van der Waals radius) and the length of a C–Cl bond is 1.77 Å[8] (the length of a normal Alkyl-Cl bond). The agreement of the calculated interplanar angle (39°) with the value estimated from models is worse than in the cases of the dimethyl and the dibromo analogues. The discrepancy is probably due mainly to the effect of the interaction of the lone pair electrons of the chlorine atoms with the ethylenic bond on the position of the conjugation band, which has been ignored in the present calculations. The interaction may affect not only the estimation of the interplanar angle from scale models by the contraction of the C–Cl bond (the length of the C–Cl bond in chloroethylene, for example, is 1.69 Å[10]), but also may exert a bathochromic effect on the conjugation band. Thus, if it were not for this effect, this compound would exhibit the conjugation band at a shorter wavelength than the observed position, and consequently the calculated interplanar angle would become larger than the value in Table II.

Correlation of Some Properties with the Spatial Configurations. — *Exaltation of molecular refraction.*—As Mulliken[11] stated for the case of alkylstyrenes, the exaltation of molecular refraction can be considered as a measure of the extent of conjugation. Some relevant data selected from the data by Auwers[12,13] are shown in Table III.

The exaltation is markedly greater in *trans*-stilbene than in the *cis* isomer. On the other hand, in contrast to the case of stilbene, the exaltation is, though slightly, smaller in *trans*-α,α'-dimethylstilbene than in the *cis* isomer. This reversal is similar to what happens to the electronic absorption spectra.

Nuclear magnetic resonance. — Curtin and others[14] measured the proton magnetic resonance spectra of stilbene, azobenzene, and diphenylcycloalkanes, and found that the positions of the aromatic proton resonance and those of the α-protons provide a new method of assignment of configuration of such compounds.

According to the results of the measurements by them, the α-hydrogens of *cis*-stilbene give rise to resonance at a higher magnetic field than those of the *trans* isomer, indicating that the α-hydrogens of the *cis* isomer are more shielded than those of the *trans* isomer.

Recently, we measured the proton magnetic resonances of *trans*- and *cis*-α,α'-dimethylstilbenes and related compounds[15]. A relevant part of the results are shown in Table IV, together with the data by

TABLE III

Compound	EM_α	EM_D	$E\Sigma_\alpha$	$E\Sigma_D$	Ref.
trans-Stilbene			+3.24	+3.57	12, 13)
cis-Stilbene	+2.26	+2.74	+1.26	+1.52	13)
trans-α-Methylstilbene			+2.04	+2.17	12)
trans-α,α'-Dimethylstilbene	+2.10	+2.22	+1.01	+1.07	13)
cis-α,α'-Dimethylstilbene	+2.12	+2.27	+1.02	+1.09	13)
Triphenylethylene	+5.17	+5.68	+2.02	+2.22	12)
Methyltriphenylethylene	+3.64	+3.98	+1.35	+1.47	12)

EM_α and EM_D are exaltations of molecular refraction.
$E\Sigma_\alpha$ and $E\Sigma_D$ are specific exaltations.

TABLE IV. CHEMICAL SHIFTS OF PROTON MAGNETIC RESONANCE (in c.p.s.)

Compound	Proton	Solvent	*trans*	*cis*		Standard
Stilbene	α-H	CT	−90	−70	(at 40 Mc.)	M
α,α'-Dimethylstilbene	CH_3	B	− 8	−19	(at 27 Mc.)	Cy
α,α'-Diethylstilbene	CH_2	B	−22	−25	(at 27 Mc.)	Cy
	CH_3	B	+13	+ 5	(at 27 Mc.)	Cy

Solvent: CT, carbon tetrachloride; B, benzene.
Standard substance: M, an external methylene chloride; Cy, cyclohexane.

10) L. O. Brockway, J. Y. Beach and L. Pauling, *J. Am. Chem. Soc.*, **57**, 2693 (1935).
11) R. S. Mulliken, *J. Chem. Phys.*, **7**, 356 (1939).
12) K. v. Auwers, *Ber.*, **62**, 693 (1929).
13) K. v. Auwers, *Ann.*, **499**, 123 (1932).
14) D. Y. Curtin, H. Gruen and B. A. Shoulders, *Chem. & Ind.*, 1205 (1958).
15) M. Katayama, S. Fujiwara, H. Suzuki, Y. Nagai, and O. Simamura, presented at the 12th Annual Meeting of the Chemical Society of Japan, Kyoto, April, 1959.

Curtin and others for *trans*- and *cis*-stilbenes.

In contrast to the α-hydrogens of *trans*- and *cis*-stilbenes, the hydrogens of the α-methyl groups of *cis*-α,α'-dimethylstilbene and of the α-ethyl groups of *cis*-α,α'-diethylstilbene give rise to resonance at lower fields than the corresponding hydrogens of the *trans* isomers. That is, the hydrogens are less shielded in the *cis* isomers than in the corresponding *trans* isomers.

Katayama calculated the magnetic fields due to the circulating π-electrons' currents for these compounds by making an allowance for the spatial configurations, and found that the calculated differences of the magnetic fields for the *trans* isomers and for the *cis* isomers are smaller than the observed ones. Accordingly, the observed differences may be partly due to the differences of the π-electron densities at carbon atoms and of the electron densities at the hydrogen atoms concerned, which is, in turn, probably due to the differences of the extent of conjugation as well as hyperconjugation. That is, it appears that the conjugation in the π-electron systems affects the chemical shift of the nuclear magnetic resonance. At any rate, it is of interest that the observations on the proton resonance mentioned above are considered to correspond to the fact that the sequence of the positions of the conjugation bands of *trans* and *cis* isomers in the case of stilbene is reversed in the cases of α,α'-dimethyl- and α,α'-diethylstilbene.

Thermal isomerization. — As mentioned already in Part V of this series, *trans*-stilbene is thermodynamically much more stable than the *cis* isomer. Thus, according to Taylor and Murray[16], the equilibrium mixture of the *cis-trans* thermal isomerization at 200°C consists of 96% of the *trans* isomer and 4% of the *cis* isomer. In addition, according to Kistiakowsky and Smith[17], the equilibrium mixture at 320~340°C contains 92~94% of the *trans* isomer. The heat of the thermal *cis-trans* isomerization ($-\Delta H$) is about 3 kcal./mol. (In addition, the heat of isomerization at 25°C has been estimated at 7.0 ± 0.4 kcal./mol. for *p*-nitrostilbene and at 4.6 ± 0.3 kcal./mol. for *p,p'*-dinitrostilbene from the heats of combustion[18]. Also with these compounds, the *trans* isomers are, of course, much more stable than the *cis* isomers.)

The difference of stability between the isomers is by far smaller in the case of α,α'-dimethylstilbene than in the case of stilbene. Thus, according to the previous study by Simamura and the present author[2,19], the equilibrium mixture yielded by heating either *trans*- or *cis*-α,α'-dimethylstilbene with a little concentrated sulfuric acid for 20 hr. at 210°C contained the *trans* and the *cis* isomers in the ratio of the amounts 55 : 45 or 60 : 40.

The fact that the *trans* isomer is still, though slightly, also more stable in this case than the *cis* isomer would appear, at first sight, to be rather surprising, being contrary to the anticipation from the absorption spectra. As discussed already in the previous paper[2], however, this fact is understandable if one considers that the steric repulsion between the two methyl groups in the *cis* isomer, which can not be reduced by the rotation of the phenyl groups, is also an important contributory factor to the stability besides the resonance stabilization.

According to Taylor and Murray[16], the equilibrium mixture of the *cis-trans* isomerization of α,α'-dichlorostilbene at 220~230°C contains 75% of the *cis* isomer. The large stability of the *cis* isomer relative to the *trans* isomer may be partly due to the attractive (London) force between the chlorine atoms in the *cis* isomer as Taylor and Murray stated, and may be partly due to the fact that the difference of the resonance stabilization energy between the two isomers is considered, on the analogy of the case of α,α'-dimethylstilbene, to be not so great as in the case of stilbene, the resonance being considerably suppressed in both isomers by the steric factors.

Reaction with bromine.—As seen in Tables IV and V in Part V of this series and Table II in the present paper, the extra-resonance energy *R.E.*, i.e. the bond localization energy of the central ethylenic bond, decreases and the π-bond order of the ethylenic bond $p_{\alpha-\alpha'}$ increases, with decreasing ρ, and hence with the increasing interplanar angle. In Table V, the calculated values of *R.E.* and $p_{\alpha-\alpha'}$ for

16) T. W. J. Taylor and A. R. Murray, *J. Chem. Soc.*, **1938**, 2078.
17) G. B. Kistiakowsky and W. R. Smith, *J. Am. Chem. Soc.*, **56**, 638 (1934).
18) C. M. Anderson, L. G. Cole and E. C. Gilbert, ibid., **72**, 1263 (1950).
19) O. Simamura and H. Suzuki, This Bulletin, **27**, 231 (1954).

TABLE V

Entry No.	Compound	ρ	*R.E.* $(-\beta)$	$p_{\alpha-\alpha'}$
1	Tetraphenylethylene	1.032	0.906	0.820
2	Triphenylethylene	0.946	0.764	0.845
3	*trans*-Stilbene	0.908	0.704	0.856
4	*cis*-Stilbene	0.787	0.530	0.890
5	*trans*-α-Methylstilbene	0.730	0.457	0.904
6	*cis*-α,α'-Dimethylstilbene	0.531	0.243	0.948
7	*trans*-α,α'-Dimethylstilbene	0.446	0.173	0.963
8	(Unconjugated olefin)	0	0	1

trans- and *cis*-stilbenes and some related compounds are summarized. The variation of the bond localization energy as well as of the π-bond order of the ethylenic bond should affect the rates of the reactions of these compounds with the "double-bond reagents"[20]. Thus, the decrease in the bond localization energy as well as the increase in the π-bond order should facilitate such reactions. This effect is subsequently referred to as the bond localization effect.

On the other hand, the substituents themselves or the phenyl groups rotated out of the plane of the ethylenic bond owing to steric necessities may hinder the approach of the reagent to the reaction site in such reactions. This effect, being purely steric in nature, is referred to as the steric (hindrance) effect in a narrow sense. This effect should, of course, retard such reactions. For example, the fact that α-*t*-butylstilbene does not add bromine[21] in contrast to α-methyl[19] and α-ethyl analogues[22] which add bromine is probably due to this effect.

In addition to the effects mentioned above, the substituents may, of course, exert an electronic effect (e. g. the inductive, mesomeric, or hyperconjugation effect) on the reactions. Therefore, in consideration of the reactions of these stilbene-type compounds, all the effects of the above three types are to be taken into account.

Simamura and the present author found in the earlier study[19] on the action of bromine on stilbenes that *trans*-α-methyl stilbene adds bromine much faster than *trans*-stilbene. The extreme slowness of the reaction of *trans*-stilbene with bromine is partly due to the retarding effect of atmospheric oxygen, and when a little catechol is added, the rate increases appreciably. On the other hand, the fastness of the reaction of *trans*-α-methylstilbene is ascribed partly to the accelerating effect of a little hydrogen bromide formed as a by-product by substitution, which starts the chain addition reaction of bromine by producing, in co-operation with oxygen, bromine atoms, and this effect is considered to be also suppressed by catechol. However, even when a little catechol is added, the rate of the reaction of *trans*-α-methylstilbene with bromine is still much greater than that of *trans*-stilbene[23]. This difference of the rates may be partly due to the electron-donating effect of the methyl group, partly to the unsymmetrical nature of the electronic state of the ethylenic bond in methylstilbene, and partly (perhaps mainly) to the bond localization effect due to the nonplanarity of the configuration of methylstilbene.

The π-bond order of the ethylenic bond in *trans*-α,α'-dimethylstilbene is greater than that in methylstilbene, so that dimethylstilbene would be expected to add bromine more rapidly than methylstilbene. In fact, however, the action of bromine on dimethylstilbene leads to the facile substitution at the methyl groups rather than the addition at the ethylenic bond[19]. This fact seems to be attributable to the steric effect in a narrow sense or the unstability of dimethylstilbene dibromide as the possible intermediate due to the steric strain in the molecule caused by the crowding of bulky groups.

Methyltriphenylethylene does not add bromine, but is substituted at the methyl group only slowly[19]. The absence of the addition is probably due to the steric hindrance effect in a narrow sense.

Reaction with hydrogen bromide and oxygen.—It was reported previously that the steric effect plays a predominant role in the

20) G. M. Badger, "The Structures & Reactions of the Aromatic Compounds", The University Press, Cambridge (1954).
21) Ramart-Lucas, *Ann. Chim.*, [8] **30**, 394 (1913).
22) A. Klages and S. Heilmann, *Ber.*, **37**, 1447 (1904).
23) H. Suzuki, unpublished.

TABLE VI. EPOXIDATION OF OLEFINS WITH PERBENZOIC ACID IN BENZENE

Entry No.	Olefin	$10^4 k$	$\Delta H^{\ddagger}$	$\Delta F^{\ddagger}$	$-\Delta S^{\ddagger}$	Ref.
1	Tetraphenylethylene	0.28	17.2	24.1	22.6	25)
2	Triphenylethylene	3.075	15.7	22.6	22.7	25)
3	*trans*-Stilbene	4.27	15.25	22.2	22.8	25)
			13.8			26)
4	*cis*-Stilbene	13.35	14.1	21.75	25.2	25)
5	*trans*-α-Methylstilbene	37.42	12.6	21.1	28.1	26)
6	*cis*-α,α'-Dimethylstilbene	219.5	10.8	20.0	30.5	26)
7	*trans*-α,α'-Dimethylstilbene	228	11.0	20.0	29.8	26)
8	Cyclohexene	263.5	12.7	19.95	24.0	25)

The values of k (in mol^{-1} l. sec^{-1}) are those at 30°C. The values of $\Delta F^{\ddagger}$ (in kcal. mol^{-1}) and of $\Delta S^{\ddagger}$ (in cal. deg^{-1} mol^{-1}) are those calculated from the rates at 30°C. The values of $\Delta H^{\ddagger}$ are in kcal. mol^{-1}.

reactions of stilbene and stilbene derivatives with hydrogen bromide and oxygen[24]. The conclusions are summarized as follows.

(1) *trans*-Stilbene and *trans*-α-methylstilbene can produce bromine atoms by the combined action of hydrogen bromide and oxygen, and thus can initiate chain reactions, the former yielding mainly its dibromide, and the latter yielding its dibromide along with ω-bromoacetophenone and benzoic acid as the final products.

(2) On the other hand, both *trans*- and *cis*-α,α'-dimethylstilbenes as well as *trans*-α,α'-diethylstilbene undergo no such reaction in the absence of a catalyst, because they are unable by themselves to produce bromine atoms from hydrogen bromide and oxygen, probably owing to the steric effect which hinders the approach of hydrogen bromide and oxygen to the ethylenic bond. However, once bromine atoms have been produced from hydrogen bromide and a peroxidic initiator, they are active enough to attack the ethylenic bonds of these stilbene derivatives, producing radicals as chain carriers, and resulting in the oxidative cleavage of the double bonds.

(3) Further, methyltriphenylethylene and α,α'-bisbromomethylstilbene (1,4-dibromo-2,3-diphenyl-2-butene) appear not to react with hydrogen bromide and oxygen even in the presence of a peroxidic catalyst. That is, the steric hindrance is so great in these compounds that they are not only incapable of such initiation, but also unsusceptible even to the action of bromine atoms, or, if a bromine atom adds to the double bond, unable to propagate the chain reactions efficiently.

24) H. Suzuki, O. Simamura and T. Ichihashi, This Bulletin, **27**, 235 (1954).

Reaction with perbenzoic acid (epoxidation).—The reaction of olefins with perbenzoic acid gives excellent yields of the corresponding epoxides. It has been presumed that perbenzoic acid acts as a double-bond reagent, i.e. that the reaction involves attack on the olefinic bond and not on one of the constituting carbon atoms[25]. The correlation of the reactivities of *trans*-stilbene, triphenylethylene and tetraphenylethylene to perbenzoic acid with the π-bond orders as well as the bond localization energies of the ethylenic bonds of these compounds was briefly discussed already in the preceding part[3] of this series. The discussion will be extended here to other stilbene derivatives.

The relevant data selected from the results of the kinetic studies by Lynch & Pausacker[25] and by Simamura, Fukuyama & Nagai[26] are shown in Table VI.

While *cis*-stilbene is epoxidized much more rapidly than the *trans* isomer, *cis*-α,α'-dimethylstilbene is epoxidized slightly more slowly than the *trans* isomer, in accordance with the expectration from the calculated bond localization energies. The difference in the reaction rate among the compounds may, of course, depend not only on the difference of the bond localization energy, but also on the steric effect in a narrow sense (that is, the degree of unfavorableness of the steric situation to the approach of the reagent, or the magnitude of the steric strain in the transition state), and also on the electronic

25) B. M. Lynch and K. H. Pausacker, *J. Chem. Soc.*, **1955**, 1525.

26) The author is indebted to Professor O. Simamura, Dr. M. Fukuyama and Mr. Y. Nagai for communicating with him and allowing him to quote these results in advance of publication. They were presented first by them at the Symposium on the Organic Reaction Mechanism held under the auspices of the Chemical Society of Japan, Fukuoka, October, 1958.

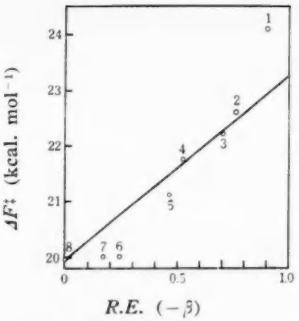

Fig. 3. Relation between the free energy of activation for the reaction of olefins with perbenzoic acid and the bond localization energy. Olefins are represented by the entry numbers in Table V as well as in Table VI.

effect of the substituents (e. g. the electron-donating effect of methyl groups). In spite of this, the sequence of the free energy of activation ($\Delta F^{\ddagger}$) shown in Table VI agrees completely with the sequence of the calculated bond localization energy (*R.E.*) shown in Table V. This fact is seen more clearly in Fig. 3, which shows the values of *R.E.* and $\Delta F^{\ddagger}$ for each compound plotted against one another and numbered according to the entry number in Table VI.

Considering the discrepancy between the experimental value of $\Delta H^{\ddagger}$ for *trans*-stilbene determined by Lynch and Pausacker and that by Simamura and others, it may be somewhat doubtful to compare the data of the different sources. On the other hand, it may also be doubtful to place much reliance on the absolute magnitude of the individual calculated bond localization energy. However, Fig. 3 appears to lead to the following discussions.

The points for *trans*-α-methylstilbene and especially for *trans*- and *cis*-α,α'-dimethylstilbenes are deviated down from the straight correlation line drawn nearly through the points for cyclohexene, *cis*- and *trans*-stilbenes. That is, the values of $\Delta F^{\ddagger}$ for these methylated stilbenes are smaller than those anticipated from the values of *R.E.* on the basis of the correlation line. These vertical deviations may be considered to indicate the facilitation of the reaction by the hyperconjugation effect or the electron-donating effect of the methyl groups. The steric interference with the approach of the reagent may also exist to some extent in these methylated stilbenes. This interference seems to be revealed by the large absolute values of the entropy of activation for these compounds as compared with *trans*-stilbene.

Tetraphenylethylene and triphenylethylene have greater free energies of activation than anticipated from the calculated bond localization energies on the basis of the correlation line. This fact appears to suggest that the low reactivities of these compounds as compared with *trans*-stilbene are not only due to the larger bond localization energies but also partly to the steric effect in a narrow sense caused by the greater crowding of phenyl groups or by the nonplanarity of the configurations of these compounds. However, in view of the fact that the values of the entropy of activation for these compounds are nearly equal to that for *trans*-stilbene, this possibility may be questionable. Perhaps, the so-called electron-withdrawing effect of the phenyl group relative to the hydrogen atom may be a contributory factor.

Simamura and others measured also the rates of the reaction of many 4,4'-disubstituted α,α'-dimethylstilbenes with perbenzoic acid, and found that there exists a linear relation between the logarithms of the rate constants and the sum of the values of Hammett's substituent constant for the 4- and 4'-substituents for each of the *trans* and the *cis* series. According to them, the proportionality constant (Hammett's reaction constant ρ) for the *cis* isomers is -0.88 at 30°C, -0.90 at 20°C, and -0.93 at 10°C, and, on the other hand, the value for the *trans* isomers is -0.80 at 30°C, -0.83 at 20°C, and -0.86 at 10°C, meaning that the effect of the 4- and 4'-substituents on the reaction rate constant is stronger in the *cis* series than in the *trans* series. This fact coincides with the present conclusion that the *cis* isomer of α,α'-dimethylstilbene is more conjugated than the *trans* isomer. The above mentioned values of Hammett's reaction constant for 4,4'-disubstituted dimethylstilbenes are appreciably smaller than those for 4-substituted *trans*-stilbenes (about $-1.07\sim1.16$, estimated from the data by Lynch and Pausacker). This fact may be correlated with the fact that *trans*-stilbene is more conjugated than *trans*- and *cis*-dimethylstilbenes.

Experimental

All the spectra were measured with a Cary recording spectrophotometer Model 14 M-50.

The alkylstilbenes were prepared as reported previously[2,19].

trans-α,α'-Dichlorostilbene was prepared by the addition of chlorine to tolan. To a solution of 10 g. of tolan in 100 cc. of acetic acid, 140 cc. of a 0.4 mol./l. solution of chlorine in acetic acid was added. The reaction mixture was left to stand for about a month, and then poured into water. The crystalline deposits were collected, pressed on a porous plate to remove some adhering oily matter, and repeatedly recrystallized from ethanol. The substance was obtained in colorless crystals melting at 138.5~139.8°C; yield, 2.4 g. (17.2% of the theoretical amount).

trans-α,α'-Dibromostilbene was prepared by the addition of bromine to tolan. To a solution of 3.4 g. of tolan in 70 cc. of ether, about 2 cc. (in exess) of bromine was added dropwise. The crystalline deposits were collected and washed twice with ether. The substance was obtained in colorless prisms melting at 205~206°C; yield, 5.1 g. (79% of the theoretical amount).

trans-α,α'-Diiodostilbene was prepared by the addition of iodine to tolan. To a solution of 356 mg. (2×10^{-3} mol.) of tolan in 10 cc. of acetic acid, a solution of 508 mg. (2×10^{-3} mol.) of iodine in 22.5 cc. of acetic acid was added and the reaction mixture was left to stand for about a month. The crystalline deposits were collected and carefully recrystallized from acetic acid. The substance was obtained in colorless, bright prisms hardly soluble in most organic solvents and decomposing at about 199°C with the evolution of iodine vapor; yield, 744 mg. (86% of the theoretical amount).

Summary

The ultraviolet absorption spectra of some α- and α,α'-substituted stilbenes have been analyzed, and the most probable spatial configurations of these compounds have been inferred from the spectra by application of the calculation method described in the earlier part of this series.

It is especially noteworthy that with α,α'-dimethylstilbene as well as its diethyl analogue the *trans* isomer shows the conjugation band at a shorter wavelength than the *cis* isomer, contrary to the generally accepted view that *trans* isomers of conjugated compounds should exhibit the conjugation bands at a longer wavelength than the corresponding *cis* isomers. This fact is considered to indicate that with these compounds the *trans* isomers are less conjugated than the corresponding *cis* isomers, and that the angle of twist of the "single" bond (interplanar angle) is larger in the *trans* isomers than in the corresponding *cis* isomers. This has been confirmed by the results of the calculations. Further, this is supported also by some pieces of information on the properties of these compounds, such as the reactivities, the exaltation of molecular refraction, and the nuclear magnetic resonance. With special emphasis on this respect, the correlation of some physical and chemical properties of these compounds with the spatial configurations of the molecules has been discussed in detail.

The author desires to thank Professor Osamu Simamura and Professor Kengo Shiomi, for reading the manuscript and for valuable advice, and Dr. Makoto Takahasi for encouragement throughout this study.

Department of Chemistry
College of General Education
The University of Tokyo
Meguro-ku, Tokyo

Relations between Electronic Absorption Spectra and Spatial Configurations of Conjugated Systems. VIII. Stilbene Derivatives with Methyl Groups on the Benzene Nuclei

By Hiroshi SUZUKI

(Received August 15, 1959)

The method developed in Part V[1] of this series is applied to some stilbene derivatives with methyl groups on the benzene nuclei. With such compounds, the electronic bathochromic effect of the methyl groups on the benzene nuclei should not be ignored. Accordingly, an allowance for this effect is made, analogously to the case of *o*-alkyl- and *o*,*o*'-dialkylbiphenyls in Part II[2] of this series, by choice of the references for correlation between the calculated transition energy ΔE_A and the observed wave number ν_A of the conjugation band.

4-Methyl- and 4, 4'-Dimethyl-*trans*-stilbene.—In order to determine the longer-wavelength-side reference, the ultraviolet absorption spectra of 4-methyl- and 4, 4'-dimethyl-*trans*-stilbene in *n*-heptane were measured. The results are shown in Table I and Fig. 1. The spectra resemble the spectrum of *trans*-stilbene, on the whole showing fine structures (cf. Table I and Fig. 1 in Part V). The introduction of a methyl group into a para-position of *trans*-stilbene causes the red-shift of about 4.2 mμ of the maxima of the conjugation band, and the introduction of the second methyl group into the other para-position results in a further red-shift of about 3 mμ.

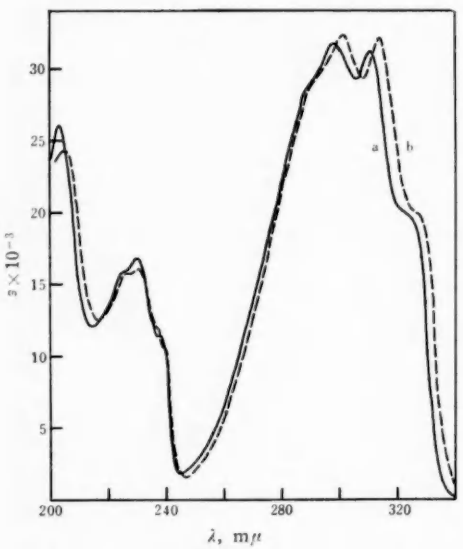

Fig. 1. Ultraviolet absorption spectra (in *n*-heptane): a ——, 4-methyl-*trans*-stilbene; b ------, 4, 4'-dimethyl-*trans*-stilbene.

4,4',*α*,*α*'-Tetramethylstilbene.—According to Nagai and Simamura[3], the spectrum of *trans*-4, 4', α, α'-tetramethylstilbene shows the absorption maximum at 245 mμ (ε = 15000), and that of the *cis* isomer shows the maximum at 258 mμ (ε = 10000). These maxima are considered as the conjugation bands. Thus, with these compounds, similarly to α, α'-dimethylstilbene[4], the conjugation band of the *cis* isomer is at a longer wavelength and of lower intensity than that of the *trans* isomer.

In application of our method to these compounds, the possible bathochromic effect of the α- and α'-methyl groups is provisionally ignored for the same reasons as in the preceding part[4] of this series, and then, in order to make allowance for the bathochromic effect of the *p*- and *p*'-methyl groups, *trans*-4, 4'-dimethylstilbene is taken as the longer-wavelength-side reference compound. That is, the value of ν_L [wave number corresponding to the calculated transition energy for planar *trans*-stilbene, ΔE_L, 1.1423 $(-\beta)$] is assumed in this case to be 33190 cm^{-1} (301.3 mμ, the γ-band of *trans*-4, 4'-dimethylstilbene). On the other hand, as the shorter-wavelength-side reference, the value for toluene corresponding to the center of gravity of singlets of benzene is taken. That is, the value of ν_S [wave number corresponding to the value of ΔE_A when ρ is 0, ΔE_S,

1) H. Suzuki, This Bulletin, **33**, 379 (1960).
2) H. Suzuki, ibid., **32**, 1350 (1959).
3) Y. Nagai and O. Simamura, presented at the 11th Annual Meeting of the Chemical Society of Japan, Tokyo, April, 1958.
4) H. Suzuki, This Bulletin, 33, 396 (1960).

TABLE I. ABSORPTION MAXIMA OF METHYLATED STILBENES (IN *n*-HEPTANE)

Compound	A-band		B-band		C-band	
	λ, mμ	ε	λ, mμ	ε	λ, mμ	ε
4-Methylstilbene	α (324.5)	19800	(238.0)	11450	203.3	26100
	β 311.2	31200	△230.2	16800		
	γ △298.3	31800	(225.0)	15800		
	δ (292.0)	29550				
4,4'-Dimethylstilbene	α (327.5)	19900	(239.5)	10550	204.8	24350
	β 314.2	32100	(237.0)	11980		
	γ △301.3	32400	△230.7	16100		
	δ (293.5)	29950	225.9	15730		
2,4,6-Trimethylstilbene	282.7	19200			208.5	29600
					201.5	29700
2,4,6,2',4',6'-Hexamethylstilbene	262.7	16000			214.0	35700

Wavelengths in parentheses denote inflections.
Symbol △ denotes the most intense maximum of fine structure.

TABLE II. RESULTS OF CALCULATION

Compound	λ_A mμ	$\Delta E_A/-\beta$	ρ	$\theta°$	R Å	$R.E./-\beta$	$p_{\alpha-\alpha'}$
trans-Stilbene	294.1	1.1423	0.9084	0	1.445	0.704	0.856
trans-4,4',α,α'-Tetramethylstilbene	245	1.620	0.404	61	1.494	0.140	0.970
cis-4,4',α,α'-Tetramethylstilbene	258	1.491	0.530	51.7	1.481	0.242	0.948
trans-2,4,6,2',4',6'-Hexamethylstilbene	262.7	1.523	0.498	54.3	1.485	0.212	0.954

$2(-\beta)$] is assumed to be 46882 cm^{-1} (213.3 mμ) (cf. Table II in Part II).

On the basis of the above references, calculation by the usual method has been carried out. The results are shown in Table II, in which the notation is the same as in Part V of this series. The calculated values of the interplanar angle θ (the angle of twist of each "single" bond) for *trans*- and *cis*-4,4',α,α'-tetramethylstilbenes agree fairly well with the values for *trans*- and *cis*-α,α'-dimethylstilbenes (58° and 51.5°), respectively (cf. Table II in the preceding part of this series).

2,4,6-Trimethyl- and 2,4,6,2',4',6'-Hexamethyl-*trans*-stilbene.—The ultraviolet absorption spectra of 2,4,6-trimethyl-*trans*-stilbene (*trans*-1-mesityl-2-phenylethylene) and 2,4,6,2'4',6'-hexamethyl-*trans*-stilbene (*trans*-1,2-dimesitylethylene) measured in *n*-heptane are shown in Table I and Fig. 2. A comparison of these spectra with the spectrum of *trans*-stilbene[1] reveals that the conjugation band shifts progressively toward shorter wavelengths and reduces the intensity with the increasing number of methyl substituents. This fact is undoubtedly due to the steric interferences

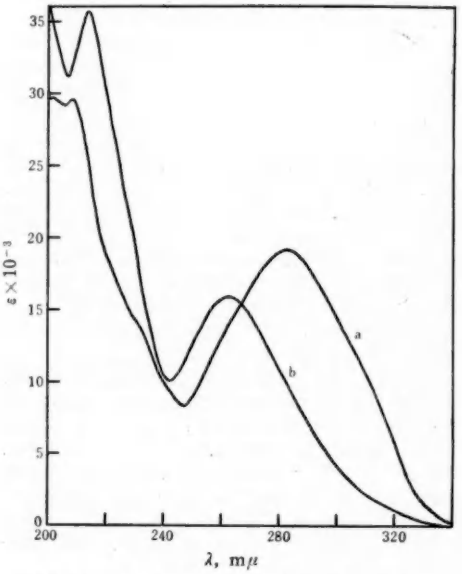

Fig. 2. Ultraviolet absorption spectra (in *n*-heptane): a, 2,4,6-trimethyl-*trans*-stilbene; b, 2,4,6,2',4',6'-hexamethyl-*trans*-stilbene.

of the substituents which prevent the molecule from assuming a planar configuration. It is noteworthy that the conjugation bands of these substituted stilbenes have, similarly to those of *cis*-stilbene[1] and α-substituted stilbenes[4], no fine structure, in contrast to that of *trans*-stilbene.

Now, it is assumed that the mean value of the magnitude of the red-shift of the conjugation band caused by substitution of a methyl group at the *o*- or *p*-position of *trans*-stilbene is 3 mμ, and that the effect of methyl substitution is additive analogously to the case of methylbenzenes[5]. Then if the configuration of dimesitylethylene were planar, this compound whould show the conjugation band at a longer wavelength than that of *trans*-stilbene by about 18 mμ (3×6 mμ). That is, the conjugation band of the hypothetical planar molecule of this compound would be at about 312 mμ ($294+18$ mμ). Accordingly, the value of ν_L is assumed in this case to be 32051 cm^{-1} (312 mμ).

On the other hand, as the shorter-wavelength-side reference compound, mesitylene is taken. While the approximate center of the low-intensity band of benzene in the region between 230 and 270 mμ is at 255 mμ, the corresponding one of mesitylene is at 266 mμ[6]. In addition, while the 0-0 band of benzene is at 262.54 mμ, that of mesitylene is at 274.06 mμ[5]. That is, the band of mesitylene is at longer wavelengths by about 11 or 11.5 mμ than that of benzene. On the analogy of the case of toluene as well as ethylbenzene (cf. Table II in Part II), it may be considered that the other bands of mesitylene are probably at longer wavelengths by about 11 or 11.5 mμ than the corresponding bands of benzene. Accordingly, the value for mesitylene corresponding to the center of gravity of singlets of benzene (48000 cm^{-1}, 208.3 mμ) is presumed to be 45600 cm^{-1} (219.3 mμ= $208.3+11$ mμ). Therefore, the value of ν_S for treatment of dimesitylethylene is assumed to be 45600 cm^{-1}.

The results of calculation carried out by the usual procedure on the basis of the above references are shown in Table II. From scale models, it is inferred that the interplanar angle in *trans*-dimesitylethylene should be approximately equal to that in *trans*-α,α'-dimethylstilbene. The value calculated here is slightly smaller than that for dimethylstilbene; still it may be said that the agreement is fairly good.

2,4,6-Trimethylstilbene is unsymmetrical, so that the two interplanar angles should be different, and therefore, the resonance integral for the Mes-C bond and that for the Ph-C bond should be different from one another. Therefore, the present method can not be applied to this compound. However, it must be sure that this compound is nonplanar, since the conjugation band is at a considerably shorter wavelength than that of *trans*-stilbene. On the basis of the above assumption that the red-shift caused by a *p*- or *o*-methyl group is about 3 mμ, it is presumed that the conjugation band of this compound would be at about 273.7 mμ ($282.7-9$ mμ) if it were not for the red-shift by the electronic effect of the methyl groups. It is of interest that this presumed position coincides almost completely with the observed position of the conjugation band of *trans*-α-methylstilbene (273.5 mμ)[4]. It may, therefore, be presumed that the value of the extra-resonance energy *R. E.* of mesitylphenylethylene is approximately equal to that of α-methylstilbene [$0.457(-\beta)$][4] and hence is smaller than that of *trans*-stilbene. This presumption seems to be supported by the following fact. According to Everard and others[7], the exaltation of molecular refraction of *trans*-stilbene is +6.6, and that of 2,4,6-trimethylstilbene is smaller by 1.3 than that of *trans*-stilbene. This fact is considered to indicate that the extent of conjugation is smaller in trimethylstilbene than in stilbene.

Everard and Sutton[8] have found with 4-dimethylaminostilbenes a similar depression of the exaltation caused by *o*-substituents attributable to steric inhibition of resonance. According to them, the exaltation of 4-dimethylaminostilbene is 7.5, and, on the other hand, the values for its 2,2'-dimethyl- and 2',4',6'-trimethyl-derivatives are 3.3 and 1.6, respectively (the values of the exaltation are expressed relative to that of *trans*-stilbene). The value for the 2'-chloro-derivative is much the same as that for the parent compound, indicating that there is negligible inhibition of conjugation in the chloro-compound in contrast to the methyl compounds.

4-Dimethylaminostilbene and related compounds have been studied by several

5) K. F. Herzfeld, *Chem. Revs.*, **41**, 233 (1947).
6) A. E. Gillam and E. S. Stern, "An Introduction to Electronic Absorption Spectroscopy", 2nd Ed., Edward Arnold Publishers, Ltd., London (1957), p. 134.
7) K. B. Everard, L. Kumar and L. E. Sutton. *J. Chem. Soc.*, **1951**, 2807.
8) K. B. Everard and L. E. Sutton, ibid., **1951**, 2816.

workers in England, probably in connection with the carcinogenic activity. Haddow and others[9] have found that the derivatives of 4-dimethylaminostilbene with methyl groups at two *o*-positions in a benzene nucleus are biologically ineffective probably because of the nonplanarity of the molecular configurations of these compounds. Beale and Roe[10] have found that the oscillator strength of the longest wavelength band (conjugation band) of *trans*-stilbene as well as 4-dimethylaminostilbene is markedly lowered by substitution of methyl groups at the *o*-positions. Thus, in the 2'-position a methyl group causes a decrement of 0.04 in *f*-value, and successive introductions of further methyl groups into the *o*-positions cause larger decrements in *f* of magnitude varying with the position of substitution. This effect has been attributed to the steric hindrance to planarity of the molecular configuration.

Regarding the reactions of the *o*-methyl substituted stilbenes, only a few data are available. According to the present author's preliminary study[11], the rate of bromination of 2,4,6-trimethylstilbene in carbon tetrachloride is markedly greater than that of trans-stilbene, even when a little catechol is added to suppress the retarding effect of atmospheric oxygen[4]. The high reactivity of trimethylstilbene as compared with stilbene is probably partly due to the larger π-bond order of the ethylenic bond or the lower bond localization energy in trimethylstilbene relative to stilbene.

On the other hand, according to Fuson and others[12], the reactivity to potassium permanganate falls in the order *trans*-stilbene > 2,4,6-trimethylstilbene > 2,4,6,2',4',6'-hexamethylstilbene. Thus, when 0.1 cc. of a 2% solution of potassium permanganate in water is added to a solution of 0.05 g. of the stilbene in 4 cc. of acetone, the time required for discharging the permanganate color is as follows: *trans*-stilbene, less than one minute; trimethylstilbene, four and one-half hours; hexamethylstilbene, 60 hr. In the methylated stilbenes, there should be a considerably large steric hindrance to the approach of the reagent to the ethylenic bond due to the mesityl or phenyl groups rotated out of the plane of the ethylenic bond. The order of the reactivity can be considered to be in conformity with the magnitude of the steric hindrance.

9) A. Haddow, R. J. C. Harris, G. A. R. Kon and E. M. F. Roe, *Trans. Roy. Soc.* (*London*), **A241**, 147 (1948).
10) R. N. Beale and E. M. F. Roe, *J. Am. Chem. Soc.*, **74**, 2302 (1952).
11) H. Suzuki, unpublished.
12) R. C. Fuson, J. J. Denton and C. E. Best, *J. Org. Chem.*, **8**, 64 (1943).

Experimental

All the spectra were measured with a Cary recording spectrophotometer Model 14 M-50.

p-Methylstilbene was prepared by the Meerwein reaction, quite analogously to the synthesis of *p*-methoxystilbene described in Part V of this series. From 53.5 g. of *p*-toluidine, 25.8 g. of the purified product, colorless crystals melting at 121~122°C, was obtained after repeated recrystallization from ethanol (26.5% of the theoretical amount).

p,p'-Dimethylstilbene was prepared by reduction of *p,p'*-dimethylbenzoin (*p*-toluoin), quite analogously to the synthesis of *trans*-stilbene from benzoin described in Organic Syntheses[13]. From about 15 g. of *p*-toluoin, the purified product, colorless crystals melting at 177~178°C, was obtained after repeated recrystallization from ethanol; yield, 4.7 g. (32% of the theoretical amount).

Found: C, 92.34; H, 7.86. Calcd. for $C_{16}H_{16}$: C, 92.26; H, 7.74%.

p-Toluoin was prepared by the benzoin condensation of *p*-tolualdehyde. To a solution of 82.7 g. of *p*-tolualdehyde in 165 ml. of ethanol, a solution of 18 g. of potassium cyanide in 120 ml. of water was added. The reaction mixture was refluxed for about two hours, and then left to stand for about a month in a refrigerator. The crystalline deposits contaminated with a considerably large amount of orange-colored oily matter were collected and pressed on a porous plate to remove the adhering oily matter. After recrystallization from ethanol, *p*-toluoin was obtained in colorless crystals melting at 87~88°C; yield, 15 g. (18.1% of the theoretical amount).

p-Tolualdehyde was prepared according to the method described in Organic Syntheses[14].

2,4,6-Trimethylstilbene was prepared, after the procedure described by Fuson and others[12], by dehydration of 1-mesityl-2-phenylethanol prepared by the Grignard reaction of mesitaldehyde with benzyl magnesium chloride. The product was purified by repeated recrystallization from ethanol, and obtained in colorless crystals melting at 56.5~57.5°C.

Mesitaldehyde was prepared, according to the method described in Organic Syntheses[15], by the action of hydrogen chloride on mesitylene in tetrachloroethane in presence of anhydrous aluminum chloride and zinc cyanide.

13) L. I. Smith (Editor-in-Chief), "Organic Syntheses", Vol. 23, John Wiley & Sons, Inc., New York (1943), p. 86.
14) F. C. Whitmore (Editor-in-Chief), ibid., Vol. XII (1932), p. 81.
15) L. I. Smith (Editor-in-Chief), ibid., Vol. 23 (1943), p. 57.

Mesitylene was prepared according to the method described in Organic Syntheses[16].

2,4,6,2',4',6'-Hexamethylstilbene was prepared, according to the method described by Fuson and Best[17], by heating thiomesitaldehyde with copper powder. To a solution of 8.5 g. of mesitaldehyde in 80 ml. of anhydrous ethanol cooled by a freezing mixture, hydrogen chloride was passed for 50 min., and then hydrogen chloride and hydrogen sulfide were passed for one and a third hours at −5∼+5°C. The reaction mixture was left to stand for about two hours. The white deposits were collected and washed repeatedly with anhydrous ethanol. Thus, after being dried in a desiccator, the crude thiomesitaldehyde was obtained as white, apparently amorphous, powder; yield, 4.3 g. About 4.2 g. of the crude thiomesitaldehyde was mixed thoroughly with 3.6 g. of copper powder, and heated for about one hour over an oil bath at 220∼230°C. The copper powder turned black. Repeated extraction with hot ligroin afforded, after removal of the solvent, the crude dimesitylethylene. After repeated recrystallization from ethanol and treatment with activated charcoal, the substance was obtained in colorless fine needles melting at 131∼132°C; yield, 1.85 g.

The preparation of this compound by dehydration of 1,2-dimesitylethanol was reported by Fuson and others[12]. However, an attempt by the present author to prepare 1,2-dimesitylethanol, according to the directions of Fuson and others, by the Grignard reaction of mesitaldehyde with 2,4,6-trimethylbenzyl magnesium chloride was unsuccessful. 2,4,6-Trimethylbenzyl chloride was prepared from mesitylene according to the directions of Vavon and Bolle[18].

The author desires to thank Professor Kengo Shiomi for reading the manuscript and for advice.

Department of Chemistry
College of General Education
The University of Tokyo
Meguro-ku, Tokyo

16) H. Gilman (Editor-in-Chief), ibid., Col. Vol. 1. (1932), p. 334.
17) R. C. Fuson and C. E. Best, *J. Am. Chem. Soc.*, **67**, 155 (1945).
18) G. Vavon and J. Bolle, *Compt. rend.*, **204**, 1826 (1937).

Relations between Electronic Absorption Spectra and Spatial Configurations of Conjugated Systems. IX. p-Phenylstilbene, p,p'-Diphenylstilbene, and their Related Compounds

By Hiroshi SUZUKI

(Received September 21, 1959)

In this part of the series, the results of the measurements of the ultraviolet absorption spectra of *p*-phenylstilbene (1-phenyl-2-*p*-biphenylylethylene), 1-phenyl-2-(2-fluorenyl)-ethylene, *p,p'*-diphenylstilbene (1,2-di-*p*-biphenylylethylene), and its *a,a'*-dimethyl derivative (2,3-di-*p*-biphenylyl-2-butene) are reported, and the calculations based on the simple LCAO molecular orbital method analogous to those for stilbene and related compounds described in the earlier parts[1-4] of this series are applied to these spectra.

In addition, the red-shifts of the conjugation bands observed with these compounds as well as stilbene and related compounds when the solvent is changed from *n*-heptane to benzene are summarized, and the correlation of these shifts with the spatial configurations of the molecules is discussed.

p-Phenylstilbene and 1-Phenyl-2-(2-fluorenyl)-ethylene

The spectra of these compounds (both are probably *trans*) in solutions in benzene and in *n*-heptane are shown in Fig. 1, and the data of the absorption maxima are recorded in Table I. The notation of the bands is analogous to the one in the earlier parts of this series. Thus, the A-band denotes the conjugation band.

These spectra are somewhat similar in shape to that of *trans*-stilbene (cf. Fig. 1 in Part V[1] of this series). The fine

1) H. Suzuki, This Bulletin, **33**, 379 (1960).
2) H. Suzuki, ibid., **33**, 389 (1960).
3) H. Suzuki, ibid., **33**, 396 (1960).
4) H. Suzuki, ibid., **33**, 406 (1960).

TABLE I. ABSORPTION MAXIMA

Compound	In benzene		In *n*-heptane			
	A-band		A-band		B- & C-bands	
	λ, mμ	ε	λ, mμ	ε	λ, mμ	ε
p-Phenylstilbene						
	[(343.5)]	22200	[(338)]	23200	225.5	13100
	△327.8	35500	△322.5	36000		
	(317.4)	32900	(311.5)	33200	200.3	31900
1-Phenyl-2-(2-fluorenyl)-ethylene						
	356.5	28450	351.2	29100	258.9	2170
	△341.5	42900	△335.8	43100	230.0	15230
	[(330.5)]	37000	[(327.5)]	37200	223.7	15420
	[(321)]	30800	(318.5)	32450	210.0	26950
	[(307)]	19430	[(303.5)]	21000	204.5	27800
p, p'-Diphenylstilbene						
	[(362)]	31300	[(357)]	0.126*	[(243)]	0.042*
	△343.0	49900	△337.4	0.214*	(220.5)	0.078*
	(332.5)	46200	(327.5)	0.199*	(201.8)	0.254*
p, p'-Diphenyl-α, α'-dimethylstilbene						
	276.2	29000	273.3	0.838*	203	1.826*

Symbol △ denotes the most intense maximum of fine structure. Wavelengths in parentheses denote inflections, and those in double parentheses denote very indistinct inflections.
Symbol * denotes the intensity in absorbance.

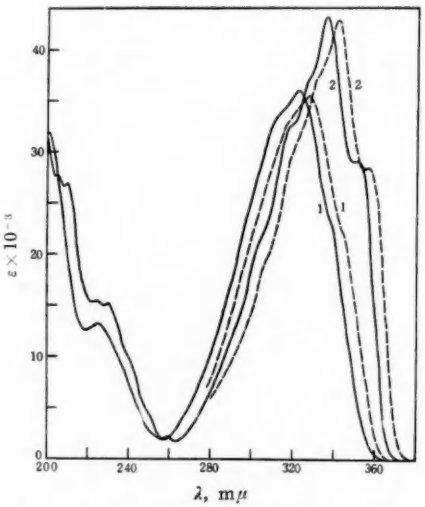

Fig. 1. Ultraviolet absorption spectra: 1, *p*-phenylstilbene; 2, 1-phenyl-2-(2-fluorenyl)-ethylene: ——, in *n*-heptane; ----, in benzene.

structure of the conjugation band of *p*-phenylstilbene is, however, more blurred than that of stilbene. The pattern of the fine structure of the conjugation band of the fluorenyl compound may be said to resemble that of fluorene (cf. Fig. 1 in Part III[5] of this series).

5) H. Suzuki, ibid., **32** 1357 (1959).

The maximum of the conjugation band of *p*-phenylstilbene is at a longer wavelength by about 28.4 mμ relative to the most intense maximum (the γ-band) of fine structure of the conjugation band of stilbene, in accordance with the expectation from the length of the conjugated system. The most intense maximum of fine structure of the conjugation band of the fluorenyl compound is at a still longer wavelength by about 13.3 mμ than that of the biphenylyl compound, a fact which may be considered to correspond to the fact that the most intense maximum of fine structure of the conjugation band of fluorene is at a longer wavelength by about 14.5 mμ than the maximum of the conjugation band of biphenyl[5].

Now, the calculation method analogous to the one used so far in this series is applied to these compounds. In the calculation the data of the spectra in *n*-heptane are used as before. The resonance integral for the ethylenic bond is denoted by η_β, and as the value of η the value of 1.080, corresponding to the bond length 1.34 Å, is taken. The resonance integral for the bonds connecting the benzene rings to the ethylenic carbon atoms is denoted by $\rho\beta$, and as the value of ρ, the value of 0.908, corresponding to the bond length 1.445 Å, is tentatively taken as in the case of *trans*-stilbene[1]. The resonance integral for the bond

between the two benzene rings in the biphenyl part is denoted by $\mu\beta$.

When as the value of the variable μ the corresponding value for fluorene 1.060 is used, the electronic transition energy ΔE_A (the energy difference between the lowest vacant orbital and the highest occupied orbital) is calculated to be 1.018 $(-\beta)$, by the usual procedure of the simple LCAO molecular orbital method. This calculated value of the transition energy, which is referred to as ΔE_L, is considered to correspond to the wave number of the most intense maximum of the conjugation band of the fluorenyl compound, 29780 cm^{-1} (335.8 mμ), which is referred to as ν_L.

On the other hand, when μ is zero, the value of ΔE_A is 1.142 $(-\beta)$, which corresponds conceivably to the wave number of the γ-band of *trans*-stilbene, 34002 cm^{-1} (294.1 mμ)[1]. These values of the calculated and the corresponding observed transition energies are referred to as ΔE_S and ν_S, respectively.

On the basis of the above determination of the longer-wavelength-side and the shorter-wavelength-side references, the value of ΔE_A corresponding to the wave number of the maximum of the conjugation band of the biphenylyl compound, 31008 cm^{-1} (322.5 mμ), is calculated to be 1.054 $(-\beta)$, and the corresponding value of μ is calculated to be 0.877. This calculated value of μ is slightly greater than the corresponding value for biphenyl in solution obtained in Part I[6] of this series. This fact would appear to suggest that the length of the bond concerned is shortened and the angle of twist of the bond is decreased in the biphenylyl compound compared with those in biphenyl in solution, owing to the increase in the extent of conjugation. However, it should not be so asserted, since it may be doubtful whether much reliance can be placed on these numerical values, because of the many assumptions made for simplification in the calculation and especially of the peculiar nature of the parameter μ for fluorene.

p,p'-Diphenylstilbene and its *α, α'*-Dimethyl Derivative

The spectra of these compounds (both are probably the *trans* isomers) in solutions in benzene and in *n*-heptane are shown in Fig. 2, and the data of the absorption maxima are summarized in

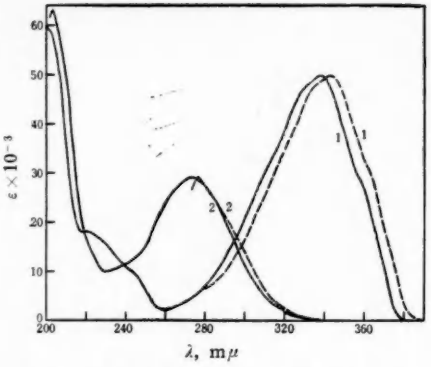

Fig. 2. Ultraviolet absorption spectra: 1, *p,p'*-diphenylstilbene; 2, *p,p'*-diphenyl-*α,α'*-dimethylstilbene: ——, in *n*-heptane; ----, in benzene.

Table I. The solubilities of these compounds in *n*-heptane are so low that the concentrations of the solutions in *n*-heptane and hence the molecular extinction coefficients of the spectra could not be determined. Accordingly, in Table I the intensities of the absorption bands of these compounds in *n*-heptane are represented in absorbance (the solution of the parent compound used is an almost saturated solution, and the solution of the dimethyl derivative is a solution of very roughly quarter the concentration of the saturated solution ; the cell path length is 1 cm.). In Fig. 2, the extinction of the main band of each compound in *n*-heptane has been arbitrarily set to be equal to its extinction in benzene. From these data, it is evident that the solubility of the *α,α'*-dimethyl compound is considerably higher than that of the parent compound. In addition, the melting point of the dimethyl compound (about 240~245°C) is considerably lower than that of the parent compound (about 303~305°C). These facts are very similar to those observed in the comparison between *trans*-stilbene and its *α,α'*-dimethyl derivative[3].

The fine structure of the conjugation band of the diphenylstilbene is further more blurred when compared with that of the phenylstilbene, and the maximum of the former is shifted further toward the longer wavelength than that of the latter. On the other hand, the conjugation band of the dimethyl derivative is almost structureless, and is at a considerably shorter wavelength and of lower intensity than that of the parent compound. This situation is also very similar to that

6) H. Suzuki, ibid., **32**, 1340 (1959).

observed in the comparison between *trans*-stilbene and its α,α'-dimethyl derivative[3], and is undoubtedly explained in terms of the steric effect of the methyl substituents.

Similarly to the treatment in the preceding section, the resonance integral for the ethylenic bond is denoted by $\eta\beta$, and the value of η is assumed to be 1.080. The resonance integral for the "single" bond between the two benzene rings in each biphenyl part is denoted by $\mu\beta$, and the value of μ is assumed to be 0.780, being equal to the corresponding value for biphenyl in solution[6]. (This choice of the value is not conclusive, but it is believed that a small change of this value does not alter significantly the final result of the present calculation). The resonance integral for each "single" bond in the stilbene part of the molecule is denoted by $\rho\beta$, in which ρ is the variable in the present calculation.

When as the value of ρ the corresponding value for planar *trans*-stilbene, 0.9084, is taken, the energy of the allowed transition from the highest occupied orbital to the lowest vacant orbital, ΔE_A, is calculated to be 1.0181 $(-\beta)$. This value is ΔE_L in the present treatment, and is considered to correspond to the wave number of the maximum of the conjugation band of *p,p'*-diphenylstilbene, 29638 cm^{-1} (337.4 $m\mu$). This compound should be more conjugated than *trans*-stilbene as well as biphenyl, and consequently, the lengths of the "single" bonds, the angles of twist of the bonds, and hence the values of ρ and μ are possibly different from the corresponding ones in *trans*-stilbene and in biphenyl. In spite of this, since it is believed that small changes of the values of ρ and μ will not significantly alter the final result, on the analogy of the calculation for terphenyls described in Part IV[7] of this series, the calculation is carried out on the basis of the above assumptions.

When ρ is zero, the value of ΔE_A is 1.523 $(-\beta)$. This value is ΔE_S in the present calculation, and corresponds to the wave number of the maximum of the conjugation band of biphenyl in *n*-heptane, 40486 cm^{-1} (247.0 $m\mu$)[6].

On the basis of the above references, from the wave numer of the conjugation band of the α,α'-dimethyl derivative in *n*-heptane, 36590 cm^{-1} (273.3 $m\mu$), the corresponding value of ΔE_A is calculated to be 1.342 $(-\beta)$, and then the following corresponding values are obtained by the usual procedure: ρ, 0.461; θ, 57°; R, 1.488 Å. The calculated value of the interplanar angle θ between the benzene ring and the ethylenic bond, 57°, for this compound coincides almost completely with the value for *trans*-α,α'-dimethylstilbene, 58°[3].

In this connection, it was planned originally to apply a similar method also to 1,2-di-(2-fluorenyl)-ethylene and its 1,2-dimethyl derivative. However, the attempts to prepare these compounds regrettably resulted in failure.

Lastly in this section, the spectra of ketazines may be briefly referred to. Compounds which are probably *p*-biphenylyl methyl ketazine and 2-fluorenyl methyl ketazine were obtained as by-products in the processes of preparation, or in attempts at preparation, of the corresponding dimethylstilbenes, as will be described in the experimental part. The spectra of these ketazines are shown in Fig. 3. These compounds are only

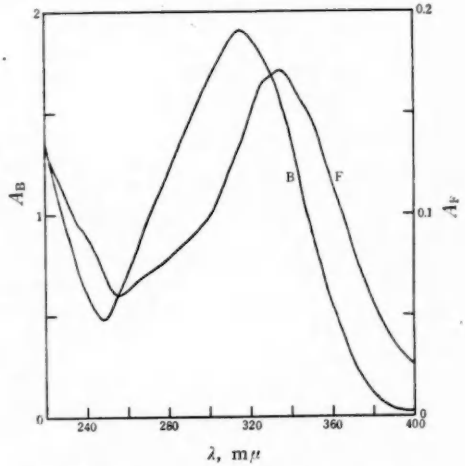

Fig. 3. Ultraviolet absorption spectra: B, *p*-biphenylyl methyl ketazine; F, 2-fluorenyl methyl ketazine. Note separate ordinates for the compounds.

very slightly soluble in *n*-heptane, so that the concentrations of the solutions used could not be determined. Consequently, the intensities of absorption are expressed in absorbance (for very roughly saturated solutions; the cell path length, 1 cm.).

Also in this case, the absorption maximum of the fluorenyl compound (335 $m\mu$) is at a longer wavelength than that of the

7) H. Suzuki, ibid., **33**, 109 (1960).

TABLE II. THE SOLVENT EFFECT OF BENZENE ON THE ULTRAVIOLET ABSORPTION SPECTRA. —The red-shifts of the conjugation bands associated with the change of the solvent from *n*-heptane to benzene.

Compound	Absorption max. (in *n*-heptane)		$\Delta\lambda$ mμ	$\Delta\nu$ cm^{-1}	Molecular configuration
	λ, mμ	ε			
p-Nitrostilbene	345.0	23820	+5.5	−455	planar
p, p'-Diphenylstilbene	337.4	49900[b)]	+5.6	−483	planar
1-Phenyl-2-(2-fluorenyl)-ethylene	335.8	43100	+5.7	−497	planar
p-Phenylstilbene	322.5	36000	+5.3	−502	planar
Tetraphenylethylene	308.7	15300	+2.5	−260	nonplanar
p-Methoxystilbene	302.7	28950	+5.0	−537	planar
Triphenylethylene	298.5	18220	+3.3	−366	nonplanar
trans-Stilbene	294.1	27950	+4.7	−535	planar
p, p'-Diphenyl-α, α'-dimethylstilbene	273.3	29000[b)]	+2.9	−384	nonplanar

The values of ε denoted by symbol b represent the values for benzene solutions.

corresponding biphenylyl compound (315 mμ). If these compounds were planar, they would be expected to show the conjugation bands at considerably longer wavelengths than *p,p'*-diphenylstilbene. In fact, however, it is not so. This fact is considered to indicate that these ketazines are conceivably nonplanar.

Correlation of Solvent Effects of Benzene with Spatial Configurations of Aromatic Solute Molecules

It was previously reported that the conjugation bands of *trans*-stilbene and some related componds are shifted toward considerably longer wavelengths when the solvent is changed from *n*-heptane to benzene[1,2]. A similar phenomenon is observed also with the compounds treated in the present paper. In Table II, the data of the red-shifts observed hitherto are summarized, in which symbols $\Delta\lambda$ and $\Delta\nu$ denote the magnitude of the displacement of the band in wavelength (mμ) and that in wave number, respectively, associated with the change of the solvent from *n*-heptane to benzene. In this table, solely the data on the most intense maximum of the conjugation band of each compound are assembled, the data on the inflections or vestigial bands being excluded.

It is to be noted here that whether or not the apparent absorption maximum of *p,p'*-diphenyl-α,α'-dimethylstilbene in benzene at 276.2 mμ is the true maximum may be somewhat doubtful, because the apparent maximum is so near the shorter-wavelength-side limit (about 270 mμ) of the range in which the measurement of the spectra by using benzene as the solvent is possible. If it is not so, the intrinsic absorption maximum of this compound must be at a shorter wavelength than the apparent maximum. Accordingly, the value of $\Delta\lambda$ for this compound listed in Table II may be considered rather as the upper limit.

Because of inevitable uncertainty in determination of the positions of the absorption maxima, the numerical values of $\Delta\lambda$ as well as $\Delta\nu$ may not be decisive. With such a reservation, however, it seems that the following generalization can be drawn from Table II: whereas the red-shifts for the planar molecules are about 5 mμ, the red-shifts for the probably nonplanar molecules are about 3 mμ and considerably smaller than the values for the planar molecules.

According to Bayliss[8], the magnitude (in cm^{-1}) of the red-shift of an absorption band of a nonpolar solute by a nonpolar solvent depends directly on the oscillator strength of the band, inversely on the frequency of the band, therefore, directly on the wavelength of the band, and is related to the refractive index n of the solvent at the frequency concerned, depending directly on $(n^2-1)/(2n^2+1)$. Thus, the band is shifted toward lower frequencies and therefore toward longer wavelengths with the increasing refractivity of the solvent.

The refractive index of benzene is greater than that of *n*-heptane. It seems, however, that the great bathochromic effect of benzene relative to *n*-heptane observed here can not be attributed wholly to the difference of refractivity. For

8) N. S. Bayliss, *J. Chem. Phys.*, **18**, 292 (1950).

example, by the use of Eq. 12 in Bayliss' paper, the magnitude of the red-shift of the conjugation band of *trans*-stilbene associated with the change of solvent from *n*-heptane to benzene is roughly calculated to be only about 60 cm^{-1}. This calculated value is by far smaller than the observed value.

In general, the intensity of the conjugation band of a non-planar compound is considerably smaller than that of the corresponding planar compound. Hence it would be expected that the difference of the magnitude of the red-shift between the planar compounds and the nonplanar compounds might be rather related to the difference of the intensity of the band. This is, however, unlikely, in view of the fact that the conjugation band of *p,p'*-diphenyl-α,α'-dimethylstilbene, which is undoubtedly nonplanar, shows a relatively small red-shift in spite of considerably high intensity. Further, as will be evidently seen in Table II, there is no regular relation between the magnitudes of the red-shifts and the wavelengths of the bands.

Therefore, it seems most natural after all to correlate the magnitude of the red-shift with the spatial configuration of the solute molecule, and this correlation seems to suggest, as already mentioned in Part V[1], the presence of a special interaction between the π-orbitals (or π-electrons) of the solute molecule and those of benzene.

Experimental

Measurements of Spectra.—The ultraviolet absorption spectra of the olefins were measured with a Cary recording spectrophotometer Model 14 M-50. The spectra of the ketazines were measured with a Beckman type spectrophotometer.

***p*-Phenylstilbene.** — This compound was prepared by the Meerwein reaction. The diazonium salt of *p*-aminobiphenyl was prepared by adding dropwise with stirring a solution of 27 g. of sodium nitrite in 45 ml. of water to a mixture of 300 ml. of 25% hydrochloric acid, 63.4 g. of *p*-aminobiphenyl, and 300 g. of ice. An ice bath was placed around the reaction flask and 235 g. of crystalline sodium acetate was added. A solution of 55.5 g. of cinnamic acid in 900 ml. of acetone was added and the ice bath was removed. Five minutes later a solution of 40.6 g. of cupric chloride in 90 ml. of water was dropwise added and the mixture was stirred for about three hours at room temperature. After being left to stand overnight, the copious green precipitate was collected on a filter and dissolved in a large amount of benzene. The benzene solution was washed in turn with a dilute solution of sodium carbonate, with water, with dilute hydrochloric acid, and then with water, dried on calcium chloride, and treated with activated charcoal. On concentrating the solution by evaporation, pale orange-yellow crystals separated. The crystals were repeatedly recrystallized from benzene. Thus, about 34.5 g. of *p*-phenylstilbene, colorless crystals melting at 220.0~220.5°C, was obtained (about 36% of the theoretical amount). A solution of this compound in benzene shows violet fluorescence.

p-Aminobiphenyl was prepared after the procedure described by Schlenk[9] by reducing *p*-nitrobiphenyl in ethanol with stannous chloride and concentrated hydrochloric acid. From 77 g. of *p*-nitrobiphenyl, 64.5 g. of *p*-aminobiphenyl, pale brown-yellow leaflets melting at 53~55°C, was obtained after recrystallization from ethanol (98.6% of the theoretical amount).

p-Nitrobiphenyl was prepared, according to the directions of Maki and his coworker[10], by nitration of biphenyl in acetic acid. From 154.2 g. of biphenyl, 91 g. of *p*-nitrobiphenyl, pale yellow needles melting at 114.5~115.3°C, was obtained after recrystallization from ethanol.

1-Phenyl-2-(2-fluorenyl)-ethylene. — This compound was prepared by the Meerwein reaction, quite analogously to the preparation of *p*-methoxystilbene described in Part V[1] of this series. From 22.8 g. of 2-aminofluorene, 5.1 g. of the product was obtained after a series of purification processes by treatment with activated charcoal and by repeated recrystallization from benzene; colorless needles melting at 219.5~221.0°C (15.1% of the theoretical amount).

Found: C, 94.04; H, 6.17. Calcd. for $C_{21}H_{16}$: C, 93.99; H, 6.01%.

2-Aminofluorene was prepared by the method described in Organic Syntheses[11], by reducing 2-nitrofluorene in ethanol with zinc dust together with calcium chloride. From 106.3 g. of 2-nitrofluorene, 66.3 g. of 2-aminofluorene, orange-brown needles melting at 125~126.5°C, was obtained (72.7% of the theoretical amount).

2-Nitrofluorene was prepared according to the directions described in Organic Syntheses[11] by nitration of fluorene. From 120 g. of fluorene, 108 g. of the probably somewhat crude product, yellow needles melting at 151~154°C, was obtained (about 71% of the theoretical amount).

***p,p'*-Diphenylstilbene.**—This compound was prepared, after the procedures of preparation of some symmetrical diarylethylenes described by Wood and his coworkers[12] and also the procedures of preparation of 1,2-dimesitylethylene described by Fuson and Best[13], by heating polythio-*p*-phenylbenzaldehyde with copper powder.

9) W. Schlenk, *Ann.*, **368**, 303 (1909).
10) T. Maki and K. Obayashi, *J. Chem. Soc., Japan, Ind. Chem. Sec.* (*Kogyo Kagaku Zasshi*), **54**, 375 (1951).
11) W. H. Carothers (Editor-in-Chief), "Organic Syntheses", Vol. XIII, John Wiley & Sons, Inc., New York (1933) p. 74.
12) J. H. Wood, J. A. Bacon, A. W. Meibohm, W. H. Throckmorton and G. P. Turner, *J. Am. Chem. Soc.*, **63**, 1334 (1941).
13) R. C. Fuson and C. E. Best, ibid., **67**, 155 (1945).

A solution of 9.1 g. of *p*-phenylbenzaldehyde in 340 ml. of absolute ethanol was saturated with dry hydrogen chloride. Hydrogen chloride and hydrogen sulfide were then passed into the solution for two and one-half hours at −3∼0°C. The almost white (or pale pink) powder produced in this way was isolated, washed several times with absolute ethanol, and dried in a vacuum desiccator; m. p. 80∼88°C; yield, 9 g. A mixture of 9 g. of the crude thioaldehyde and 26 g. of copper-bronze powder was heated for thirty minutes in a small flask by means of a sand bath at 260∼310°C. The copper powders turned black, and white crystals separated on the surface of the mixture. After cooling, the ethylenic compound was repeatedly extracted with large quantities of boiling xylene. The xylene solution was concentrated to bring about crystallization. Repeated recrystallization from xylene and treatment with activated charcoal gave 0.7 g. of pure *p,p'*-diphenylstilbene, colorless thin plates melting at 301.5∼304.5°C (8.4% of the theoretical amount from the aldehyde). This compound proved to be only slightly soluble in benzene and in xylene, and hardly soluble at all in *n*-heptane and in ethanol. A dilute solution in xylene, benzene, as well as *n*-heptane shows intense violet fluorescence.

Found: C, 94.02; H, 6.28. Calcd. for $C_{26}H_{20}$: C, 93.94; H, 6.06%.

The preparation of *p*-phenylbenzaldehyde, white thin plates melting at 60∼61°C, will be reported in the succeeding part of this series.

The author attempted also to prepare *p,p'*-diphenylstilbene by reducing *p,p'*-diphenylbenzoin with zinc amalgam and hydrochloric acid after the procedures to prepare *trans*-stilbene from benzoin described in Organic Syntheses[14], and also by the method analogous to the one to prepare *trans*-stilbene described by Fieser[15], which involves three steps: replacement of the hydroxyl group of benzoin by chlorine (with thionyl chloride), reduction of the carbonyl group with sodium borohydride to give the chlorohydrin, and elimination of the elements of hypochlorous acid with zinc and acetic acid. These attempts resulted in failure. Thus, by either method, solely an unidentified product, colorless thin plates melting at 227.0∼227.5°C, was obtained in good yield. The ultraviolet absorption spectrum of this compound in *n*-heptane shows a structureless band with the maximum at 275 mμ.

p,p'-Diphenylbenzoin was prepared, according to the directions of Gomberg and Natta[16], by the benzoin condensation of *p*-phenylbenzaldehyde. From 42.5 g. of *p*-phenylbenzaldehyde, 25.9 g. of the product purified by repeated recrystallization from xylene and by treatment with activated charcoal, almost colorless or faint yellow crystals melting at 166∼169.5°C, was obtained (61% of the theoretical amount). As a by-product, about 2 g. of *p*-phenylbenzoic acid, colorless needles melting at 219.5∼222°C, was obtained.

p,p'-Diphenyl-α,α'-dimethylstilbene.—This compound was prepared from *p*-phenylacetophenone (*p*-biphenylyl methyl ketone) after the Vargha Kovács' method[17]. A mixture of 10 g. of *p*-phenylacetophenone, 100 ml. of isopropyl alcohol, and 25 g. of 80% hydrazine hydrate was refluxed for about 30 hr. A thick white precipitate of the hydrazone was collected and dried in a vacuum desiccator. The hydrazone proved to be soluble with difficulty in petroleum ether. To a solution of the crude hydrazone in about 500 ml. of benzene, 18.1 g. of yellow mercuric oxide was added, and the mixture was stirred for about 9 hr. at room temperature. After filtration, into the pale red-orange solution sulfur dioxide was passed for thirty minutes. After removal of the solvent, the yellow residual solid was extracted with petroleum ether (b.p. 80∼100°C). Repeated recrystallization of the residue from xylene gave 5.8 g. of a compound, yellow, bright, thin plates melting at 274.5°C, which is probably *p*-biphenylyl methyl ketazine. On the other hand, the petroleum ether extract solution was filtered through a chromatographic column of alumina, and then concentrated to bring about crystallization. Fractional recrystallization of the crystals from petroleum ether gave very small quantities of colorless prisms melting at 240∼245°C and small quantities of pale yellow needles melting at about 260∼290°C. Although both the quantities were far too small for complete identification, the former compound (the colorless prisms) is considered probably to be the desired compound. On the other hand, the ultraviolet absorption spectrum of the latter in *n*-heptane shows a band with maxima at 289 and 313.5 mμ, and the spectrum in benzene shows a structureless band at 300 mμ.

The poorness of the yield of the desired compound in the above experiment is considered to originate in imperfection of the oxidation of the hydrazone. The author attempted to oxidize the hydrazone by using lead dioxide instead of mercuric oxide, and also by using petroleum ether as solvent (suspension). However, these attempts resulted in failure, the only isolated product in each experiment being the ketazine.

The author attempted to prepare this dimethyl compound also after the procedures described by Cline and his coworkers[18] to prepare α,α'-dimethylstilbene by heating trithioacetophenone with Raney nickel in xylene in an atmosphere of nitrogen. From 6.3 g. of *p*-phenylacetophenone, about 4 g. of the corresponding thio compound, pale grayish yellow powder, was obtained after the procedures of the preparation of trithioacetophenone described by Baumann and Fromm[19].

14) L. I. Smith (Editor-in-Chief), "Organic Syntheses", Vol. 23, John Wiley & Sons, Inc., New York (1943), p. 86.
15) L. F. Fieser, "Experiments in Organic Chemistry", 3rd. Ed., D. C. Heath and Company, New York (1955), p. 179—180.
16) M. Gomberg and F. J. Van Natta, *J. Am. Chem. Soc.*, **51**, 2238 (1929).
17) L. v. Vargha and E. Kovács, *Ber.*, **75B**, 794 (1942).
18) J. K. Cline, E. Campaign and J. W. Spies, *J. Am. Chem. Soc.*, **66**, 1136 (1944).
19) E. Baumann and E. Fromm, *Ber.*, **28**, 895 (1895).

However, the final product obtained by heating the thio compound with Raney nickel was yellow, bright crystals melting at 328.5~330.0°C and soluble with difficulty in usual organic solvents. The ultraviolet absorption spectrum of this product in benzene showed a structureless band with the maximum at 354 mμ.

The preparation of *p*-phenylacetophenone, m.p. 119~121.5°C, will be described in the succeeding part of this series.

Unsuccessful Attempts to Prepare 1,2-Di-(2-fluorenyl)-ethylene. — Preparation of this compound by heating polythio-2-formylfluorene with copper powder after the preparation of *p,p'*-diphenylstilbene described above was attempted. However, the only product isolated was pale yellow needles melting at 289~290.5°C, whose spectrum in *n*-heptane resembles the spectum of 2-formylfluorene as well as that of 2-acetylfluorene (cf. the succeeding part of this series), showing a band with well-resolved fine structure, the most intense maximum of which is at about 310.5 mμ. This product is probably not the desired compound, as was revealed by the spectrum.

The preparation of 2-formylfluorene, faint yellow needles melting at 85.5~86.5°C, will be described in the succeeding part of this series.

Unsuccessful Attempts to Prepare 2,3-Di-(2-fluorenyl)-2-butene. — Preparation of this compound by the Vargha and Kovács' method analogously to the preparation of 2,3-di-*p*-biphenylyl-2-butene (*p,p'*-diphenyl-α,α'-dimethylstilbene) described above was attempted. However, the attempts to oxidize the hydrazone of 2-fluorenyl methyl ketone (2-acetylfluorene) with mercuric oxide and with lead dioxide were unsuccessful, and the only isolated product was an orange-yellow crystalline compound melting at 301~302°C, which is considered to be 2-fluorenyl methyl ketazine.

The preparation of 2-acetylfluorene, colorless crystals melting at 127.5~128°C, will be described in the succeeding part of this series.

The author desires to thank Professor Kengo Shiomi for reading the manuscript and for advice, and Dr. Makoto Takahasi for his interest and encouragement. The micro-analyses were carried out by Mr. Shozo Masuda.

Department of Chemistry
College of General Education
The University of Tokyo
Meguro-ku, Tokyo

The Formation Constants of Metal Acetate Complexes. II. Polarographic Determination of the Formation Constants of Acetatocopper(II), Acetatolead(II) and Acetatozinc(II) Complexes

By Nobuyuki TANAKA and Kiyoko KATO*

(Received September 18, 1959)

In the previous paper[1], a new method for the determination of the formation constants of metal acetate complexes and its application to the study of acetatonickel(II) complexes were presented. The method is based on the polarographic measurement of the sum of the equilibrium concentrations of hydrated metal ions and metal acetate complexes in the presence of an appropriate auxiliary complex-forming substance. Although it has advantages over the conventional methods, its application to other metal acetate complexes seems to be difficult.

In this paper are presented the procedure and the results of the determination of the formation constants of acetatocopper(II), acetatolead(II) and acetatozinc(II) complexes. The procedure is applicable when the formation constants of certain metal acetate complexes are known and can be used as standards.

Theoretical

Let us consider the acetate buffer solution which contains two different metal ions, M^{m+} and $M'^{m'+}$, and ethylenediaminetetraacetate (EDTA) ions. There exist the following equilibria:

$$M^{m+} + M'Y^{(m'-4)+} \rightleftarrows MY^{(m-4)+} + M'^{m'+} \quad (1)$$

$$MY^{(m-4)+} + H^+ \rightleftarrows MHY^{(m-3)+} \quad (2)$$

* Present address: The Women's Department, Tokyo College of Pharmacy, 31, Uenosakuragi-cho, Taito-ku, Tokyo.

1) N. Tanaka and K. Kato, This Bulletin, **32**, 516 (1959).

$$M'Y^{(m'-4)+} + H^+ \rightleftarrows M'HY^{(m'-3)+} \quad (3)$$

$$M^{m+} + nOAc^- \rightleftarrows M(OAc)_n^{(m-n)+} \quad (4)$$

$$M'^{m'+} + n'OAc^- \rightleftarrows M'(OAc)_{n'}^{(m'-n')+} \quad (5)$$

where Y^{4-} means a completely dissociated EDTA anion. The overall substitution reaction between M^{m+} and $M'Y^{(m'-4)+}$ in the acetate buffer solution, therefore, may be represented as

$$\left\{\begin{matrix} M^{m+} \\ \uparrow\downarrow \\ M(OAc)_n^{(m-n)+} \end{matrix}\right\} + \left\{\begin{matrix} M'Y^{(m'-4)+} \\ \uparrow\downarrow \\ M'HY^{(m'-3)+} \end{matrix}\right\} \rightleftarrows \left\{\begin{matrix} M'^{m'+} \\ \uparrow\downarrow \\ M'(OAc)_{n'}^{(m'-n')+} \end{matrix}\right\} + \left\{\begin{matrix} MY^{(m-4)+} \\ \uparrow\downarrow \\ MHY^{(m-3)+} \end{matrix}\right\} \quad (6)$$

In the polarographic measurement, the diffusion current of metal ions obtained in acetate media corresponds to the sum of the diffusion current of the hydrated metal ions and that of the acetato complexes[1]. Consequently, the concentrations that can be determined polarographically are $[M^{m+}]_{app}$ and $[M'^{m'+}]_{app}$ given by the equations

$$[M^{m+}]_{app} = [M^{m+}] + \sum_1^n [M(OAc)_n^{(m-n)+}] \quad (7)$$

and

$$[M'^{m'+}]_{app} = [M'^{m'+}] + \sum_1^{n'} [M'(OAc)_{n'}^{(m'-n')+}] \quad (8)$$

respectively.

The total concentrations of metals and EDTA, $[M]_t$, $[M']_t$ and $[EDTA]_t$, in the solution are given in terms of the concentrations of the ionic and molecular species present:

$$[M]_t = [M^{m+}]_{app} + [MY^{(m-4)+}] + [MHY^{(m-3)+}] \quad (9)$$

$$[M']_t = [M'^{m'+}]_{app} + [M'Y^{(m'-4)+}] + [M'HY^{(m'-3)+}] \quad (10)$$

$$[EDTA]_t = [EDTA]_f + [MY^{(m-4)+}] + [MHY^{(m-3)+}] + [M'Y^{(m'-4)+}] + [M'HY^{(m'-3)+}] \quad (11)$$

where $[EDTA]_f$ represents the concentration of the uncomplexed EDTA. Under the condition that $[M]_t + [M']_t > [EDTA]_t$, $[EDTA]_f$ is negligibly small as compared with the concentrations of other species in the solution.

From the polarographic measurement of either $[M^{m+}]_{app}$ or $[M'^{m'+}]_{app}$, the equilibrium constant of Eq. 6

$$K_{M,app}^{M'} = \frac{[M'^{m'+}]_{app}\{[MY^{(m-4)+}] + [MHY^{(m-3)+}]\}}{[M^{m+}]_{app}\{[M'Y^{(m'-4)+}] + [M'HY^{(m'-3)+}]\}} \quad (12)$$

is obtained with the relations given by Eqs. 9 to 11, provided that the values of $[M]_t$, $[M']_t$, and $[EDTA]_t$ are known. The constant $K_{M',app}^{M}$ may be called the apparent equilibrium constant of the substitution reaction in question. On the other hand, the equilibrium constant of the substitution reaction given by Eq. 1 is expressed as

$$K_{M'}^{M} = \frac{[M'^{m'+}][MY^{(m-4)+}]}{[M^{m+}][M'Y^{(m'-4)+}]} \quad (13)$$

Introducing Eqs. 7, 8 and 13 into Eq. 12, $K_{M',app}^{M}$ is rewritten as

$$K_{M',app}^{M} = K_{M'}^{M} \frac{\beta}{\beta'} \frac{1 + \sum_1^{n'} K_{M'(OAc)_{n'}} [OAc^-]^{n'}}{1 + \sum_1^{n} K_{M(OAc)_n} [OAc^-]^n} \quad (14)$$

$$\beta = 1 + K_{MHY}^{H}[H^+]$$

$$\beta' = 1 + K_{M'HY}^{H}[H^+]$$

where $K_{M(OAc)_n}$ and $K_{M'(OAc)_{n'}}$ represent the overall formation constants of $M(OAc)_n^{(m-n)+}$ and $M'(OAc)_{n'}^{(m'-n')+}$, respectively, and K_{MHY}^{H} and $K_{M'HY}^{H}$, the equilibrium constants of the reactions of Eqs. 2 and 3, respectively.

If the formation constants of acetato complexes of one of the metals are known, those of the other can be determined with Eq. 14 by the measurement of $K_{M',app}^{M}$ at various acetate concentrations. When the values of $K_{M(OAc)_n}$ are known, Eq. 14 is conveniently arranged as

$$F_0 \equiv K_{M',app}^{M}\left\{1 + \sum_1^n K_{M(OAc)_n}[OAc^-]^n\right\} = K_{M'}^{M}\frac{\beta}{\beta'}\left\{1 + \sum_1^{n'} K_{M'(OAc)_{n'}}[OAc^-]^{n'}\right\} \quad (15)$$

From the extrapolation of the plot of F_0 vs. $[OAc^-]$ to zero acetate concentration, $\frac{\beta}{\beta'}K_{M'}^{M}$ is obtained. Then, the functions $F_1, F_2, \cdots, F_{n'}$ are defined, which are written as follows:

$$F_1 \equiv \frac{F_0 - \frac{\beta}{\beta'}K_{M'}^{M}}{\frac{\beta}{\beta'}K_{M'}^{M}[OAc^-]} = K_{M'OAc} + K_{M'(OAc)_2}[OAc^-] + \cdots\cdots \quad (16)$$

$$F_2 \equiv \frac{F_1 - K_{M'OAc}}{[OAc^-]} = K_{M'(OAc)_2} + K_{M'(OAc)_3}[OAc^-] + \cdots\cdots \quad (17)$$

.....

$$F_{n'} \equiv \frac{F_{n'-1} - K_{M'(OAc)_{n'-1}}}{[OAc^-]} = K_{M'(OAc)_{n'}} \quad (18)$$

F_1 is plotted against $[OAc^-]$ and the value of $K_{M'OAc}$ is determined by extrapolating the plot to zero acetate concentration. Further treatment leads to the determination of $K_{M'(OAc)_{n'}}$, if higher acetato complexes are present in the solution.

When the formation constants of $M'(OAc)_{n'}^{(m'-n')+}$ are known, similar relations are derived:

$$F_0' \equiv \frac{1 + \sum_1^{n'} K_{M'(OAc)_{n'}} [OAc^-]^{n'}}{K^{M}_{M',app}} = \frac{\beta'}{\beta K^{M}_{M'}} \left\{ 1 + \sum_1^{n} K_{M(OAc)_n} [OAc^-]^n \right\} \quad (15')$$

$$F_1' \equiv \frac{F_0' - \frac{\beta'}{\beta K^{M}_{M'}}}{\frac{\beta'}{\beta K^{M}_{M'}} [OAc^-]} = K_{MOAc} + K_{M(OAc)_2} [OAc^-] + \cdots\cdots \quad (16')$$

$$F_2' \equiv \frac{F_1' - K_{MOAc}}{[OAc^-]} = K_{M(OAc)_2} + K_{M(OAc)_3} [OAc^-] + \cdots\cdots \quad (17')$$

The values of $K_{M(OAc)_n}$ can be determined by the same procedure as for those of $K_{M'(OAc)n'}$.

Experimental

Reagent. — Standard solutions of copper(II) nitrate and zinc nitrate were prepared by dissolving known amounts of pure copper and zinc metals, respectively, in a reagent-grade nitric acid. A standard solution of nickel nitrate was the same as used in the previous study[1]. The solution of disodium ethylenediaminetetraacetate was standardized against the standard solution of copper(II) nitrate by amperometric titration[2]. A standard solution of lead nitrate was prepared by dissolving an appropriate quantity of reagent-grade lead nitrate. Its concentration was determined amperometrically with the standardized EDTA solution[2]. For buffers and supporting electrolytes, guaranteed reagents were used without further purification.

Apparatus and Procedure. — The polarograph and the dropping mercury electrode used were the same as those described in the previous paper[1]. The dropping mercury electrode had an m value of 1.27 mg./sec. and a drop time τ of 3.69 sec. in an air-free 0.1 M potassium chloride solution at 25°C with open circuit. The measurements of the diffusion currents of copper(II) in acetate buffer solutions were carried out with the following three reaction mixtures:

(a) copper(II)-nickel(II)-EDTA
(b) copper(II)-lead(II)-EDTA
(c) copper(II)-zinc(II)-EDTA

The measurements were made at 15, 25 and 35°C in acetate buffers of pH 4.7±0.1 in which the acetate concentrations were varied from 0.01 M to 0.2 M. The ionic strength was adjusted to be 0.2 with potassium nitrate. Gelatin was added as a maximum suppressor by 0.01% in concentration.

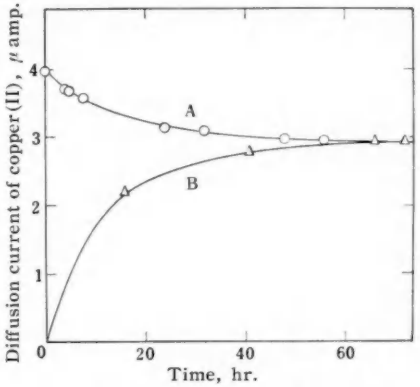

Fig. 1. Relation between the diffusion current of copper(II) and time in the forward (curve A) and the reverse (curve B) reactions of the substitution reaction $Cu^{2+} + NiY^{2-} \rightleftarrows CuY^{2-} + Ni^{2+}$, measured in acetate buffer solutions of pH 4.7 at 15°C. Total concentrations are: $[Cu]_t = 1.00 \times 10^{-3}$ M; $[Ni]_t = 1.50 \times 10^{-3}$ M; $[EDTA]_t = 1.00 \times 10^{-3}$ M.

The substitution reactions involving the EDTA complexes are not always completed instantaneously. The rates of these reactions vary widely according to the system investigated. In systems (b) and (c), the reactions are nearly completed within a few minutes under the experimental conditions. The reaction mixtures, therefore, were subjected to the measurement approximately 3 hours after the preparation. On the other hand, it has often been stated that the exchange or substitution reactions involving the nickel-EDTA complexes proceed at a relatively slow rate[3-7]. This was confirmed also in this study by the fact that the reaction mixtures of system (a) reach the equilibrium extremely slowly. One of the examples is given in Fig. 1, where the change of the polarographic diffusion current of copper(II) in the reaction mixture is plotted against

2) N. Tanaka, M. Kodama, M. Sasaki and M. Sugino, *Japan Analyst (Bunseki Kagaku)*, **6**, 86 (1957).

3) F. A. Long, S. S. Jones and M. Burke, *Brookhaven Conf. Rept. BNE-C-8*, **2**, 106 (1948).

4) C. M. Cook, Jr. and F. A. Long, *J. Am. Chem. Soc.*, **80**, 33 (1958).

5) G. Schwarzenbach, R. Gut and G. Anderegg, *Helv. Chim. Acta*, **37**, 937 (1954).

6) K. Bril and P. Krumholz, *J. Phys. Chem.*, **57**, 874 (1953).

7) N. Tanaka and Y. Sakuma, This Bulletin, **32**, 578 (1959).

the time for the forward and reverse reactions. Fig. 1 shows that the reaction equilibrates approximately 60 hours after the initiation of the reaction. In system (a), therefore, all measurements were made about 3 days after the solutions had been prepared.

Results

The apparent diffusion current constants of copper(II) were determined by measuring the diffusion current at various acetate concentrations. The values of $[Cu^{2+}]_{app}$ were calculated with the aid of those apparent diffusion current constants from the diffusion currents obtained with the reaction mixtures of systems (a), (b) and (c). Then, the apparent equilibrium constants $K^{M}_{M',app}$ given by Eq. 12 were calculated, with which F_0, F_1……$F_{n'}$ (or F_0', F_1'……F_n') were successively obtained. The results obtained for systems (a), (b) and (c) are given below. The values of β/β' (or β'/β) in Eq. 14 were calculated with the equilibrium constants K^{H}_{MHY} and $K^{H}_{M'HY}$ given by Schwarzenbach et al.[5], with the result that they are approximately unity for all three systems at pH of the present experiments.

Copper(II) - Nickel(II) - EDTA System. — In the solution containing acetate up to 0.2 M in concentration, nickel(II) forms only a monoacetato complex, its formation constant K_{NiOAc} at ionic strength 0.2 being 2.6, 2.6 and 2.4 at 15, 25 and 35°C, respectively[1]. With the aid of these values, the formation constants of acetatocopper(II) complexes were obtained by determining the values for $K^{Cu}_{Ni,app}$ at various acetate concentrations. The $K^{Cu}_{Ni,app}$ is given by the equation

$$K^{Cu}_{Ni,app}=\frac{[Ni^{2+}]_{app}[CuY^{2-}]}{[Cu^{2+}]_{app}[NiY^{2-}]}$$

F_0' and F_1' given by Eqs. 15′ and 16′ respectively were calculated and plotted against the acetate ion concentration. These plots for 25°C are shown in Fig. 2, in which the F_1' plot gives a straight line. This fact clearly indicates that no appreciable amount of complexes with three acetates or more co-ordinated is present in the solution under the experimental conditions. From the F_1' plot the formation constants of mono- and diacetatocopper(II) complexes, K_{CuOAc} and $K_{Cu(OAc)_2}$, were determined, the former being determined by the intercept at zero acetate concentration and the latter, by the slope.

Similar relations were also found at 15 and 35°C. The formation constants obtained at various temperatures are given in Table I.

Copper(II)-Lead(II)-EDTA System. — The formation constants of acetatolead(II) complexes were determined by the measurement of $K^{Cu}_{Pb,app}$ at various acetate concentrations with the aid of the formation constants of $CuOAc^+$ and $Cu(OAc)_2$ obtained in this study, where $K^{Cu}_{Pb,app}$ is given by the equation

$$K^{Cu}_{Pb,app}=\frac{[Pb^{2+}]_{app}[CuY^{2-}]}{[Cu^{2+}]_{app}[PbY^{2-}]}$$

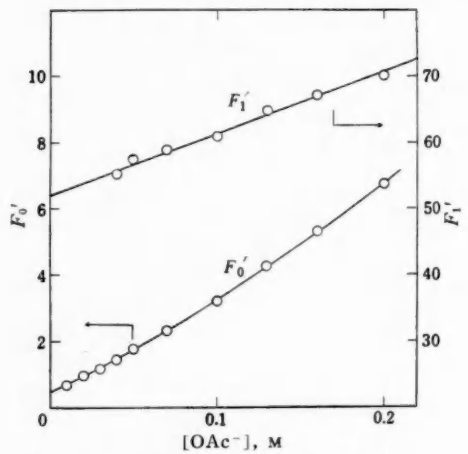

Fig. 2. F_0' (Eq. 15′) and F_1' (Eq. 16′) as a function of the acetate ion concentration in copper(II)-nickel(II)-EDTA system at 25°C.

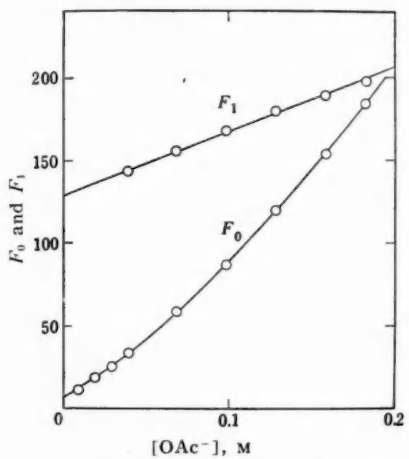

Fig. 3. F_0 (Eq. 15) and F_1 (Eq. 16) as a function of the acetate ion concentration in copper(II)-lead(II)-EDTA system at 25°C.

In this case F_0 and F_1 given by Eqs. 15 and 16 were calculated and plotted instead of F_0' and F_1'. In Fig. 3 these plots for 25°C are shown, where the F_1 plot gives a straight line indicating that $PbOAc^+$ and $Pb(OAc)_2$ are appreciable species of acetatolead(II) complexes present in the solution. Similar plots were obtained at 15 and 35°C. The formation constants of $PbOAc^+$ and $Pb(OAc)_2$ were determined. These are given in Table I.

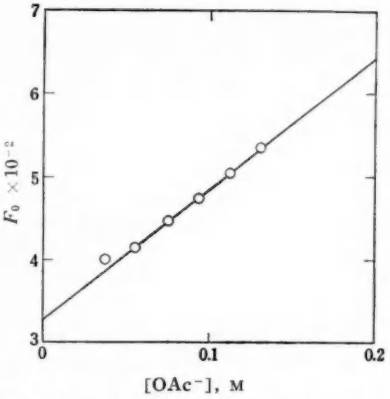

Fig. 4. F_0 (Eq. 15) as a function of the acetate ion concentration in copper(II)-zinc(II)-EDTA system at 25°C.

Copper(II) - Zinc(II) - EDTA System. — The formation constants of acetatozinc(II) complexes were determined with the same procedure as for the acetatolead(II) complexes. $K^{Cu}_{Zn,app}$ which is given by the equation

$$K^{Cu}_{Zn,app} = \frac{[Zn^{2+}]_{app}[CuY^{2-}]}{[Cu^{2+}]_{app}[ZnY^{2-}]}$$

was determined at various acetate concentrations. In this case it was found that

TABLE I. FORMATION CONSTANTS OF ACETATOCOPPER(II), ACETATOLEAD(II) AND ACETATOZINC(II) COMPLEXES AT VARIOUS TEMPERATURES

Metal ion	Temp., °C	K_{MOAc}	$K_{M(OAc)_2}$
Copper(II)	15	41	190
	25	52	93
	35	69	82
Lead(II)	15	130	750
	25	130	390
	35	120	380
Zinc(II)	15	5.7	—
	25	4.6	—
	35	3.7	—

TABLE II. SOME EXAMPLES OF THE REPORTED VALUES OF FORMATION CONSTANTS OF ACETATOCOPPER(II), ACETATOLEAD(II) AND ACETATOZINC(II) COMPLEXES

Metal ion	Investigator	Method	Temp., °C	Ionic strength	K_{MOAc}	$K_{M(OAc)_2}$	Ref.
Copper(II)	Pedersen	Potentiometric	18	0.2	46.7	316	8
	Fronæus	Ion-exchange	20	1	45	440	9
	Sircar et al.	Potentiometric	29~33	0	250	2000	10
				0.2	83*	350*	(10)
Lead(II)	Aditya et al.	Potentiometric	30	0	270	9000	11,12
				0.2	76*	1300*	(11,12)
	Burns et al.	Polarographic	25	1.98	150	840	13
	Siddhanta et al.	Potentiometric	31~34.5	0	302	9700	14
				0.2	85*	1500*	(14)
Zinc(II)	Cannan et al.	Potentiometric	—	0.2	10.7	—	15
	Bardhan et al.	Solubility	35	0	39	—	16
				0.2	13*		(16)
	Bardhan et al.	Potentiometric	35	0	29	—	16
				0.2	9.6*		(16)

* Those values are the formation constants which were calculated by the present authors with the values reported in the literature referred to. In the calculation, the activity coefficients of copper(II), lead(II), zinc(II) and acetate ions were estimated to be 0.33, 0.28, 0.33 and 0.73, respectively, and the activity coefficient of monoacetato complexes was assumed to be equal to that of acetate ions.

8) K. J. Pedersen. *Det Kgl. Danske Viedenskab. Selskab. Math-Fys. Medd.*, **22**, No. 12 (1945).
9) S. Fronæus, *Acta Chem. Scand.*, **5**. 859 (1951).
10) S. C. Sircar. S. Aditya and B. Prasad, *J. Indian Chem. Soc.*, **30**, 633 (1953).
11) N. K. Das, S. Aditya and B. Prasad, ibid., **29**, 169 (1952).
12) S. Aditya and B. Prasad, ibid., **30**, 213 (1953).
13) E. A. Burns and D. N. Hume, *J. Am. Chem. Soc.*, **78**, 3958 (1956).
14) S. K. Siddhanta and S. N. Banerjee, *J. Indian Chem. Soc.*, **35**, 323 (1958).
15) R. K. Cannan and A. Kibrick, *J. Am. Chem. Soc.*, **60**, 2314 (1938).
16) S. Bardhan and S. Aditya, *J. Indian Chem. Soc.*, **32**, 105 (1955).

TABLE III. EQUILIBRIUM CONSTANTS FOR THE SUBSTITUTION REACTION (EQ. 1) AT VARIOUS TEMPERATURES COMPARED WITH SCHWARZENBACH'S VALUES

		15°C	20°C	25°C	35°C
Copper(II)-Nickel(II)	K^{Cu}_{Ni} a)	2.0	—	2.2	2.5
	$K^{Cu}_{Ni,app}$ b)	—	1.5	—	—
	$K^{Cu}_{Ni,cor}$ c)	—	2.1	—	—
Copper(II)-Lead(II)	K^{Cu}_{Pb} a)	3.2	—	5.0	8.0
	$K^{Cu}_{Pb,app}$ b)	—	6.3	—	—
	$K^{Cu}_{Pb,cor}$ c)	—	4.4	—	—
Copper(II)-Zinc(II)	K^{Cu}_{Zn} a)	3.2×10^2	—	3.3×10^2	3.4×10^2
	$K^{Cu}_{Zn,app}$ b)	—	2.1×10^2	—	—
	$K^{Cu}_{Zn,cor}$ c)	—	2.9×10^2	—	—

a) Values obtained in the present investigation.
b) Values obtained by Schwarzenbach et al.
c) Values calculated from Schwarzenbach's values with Eq. 14.

the F_0 plot gave a straight line, which is shown in Fig. 4. This fact led to the conclusion that at acetate concentration up to 0.2 M, $ZnOAc^+$ is the only species which exists in the solution at an appreciable concentration. Similar relations were obtained also at 15 and 35°C. The formation constants of $ZnOAc^+$ are listed in Table I.

Discussion

The formation constants of the acetato complexes of copper(II), lead(II) and zinc(II) have been determined by various researchers. Some of them are given in Table II. These are compared with the formation constants given in Table I.

Recently, Yasuda and Yamasaki[18] studied the complex formation of some carboxylic acids by the pH titration method. They compared the stabilities of the complexes of bivalent metal ions and found that the order of Pb > Cu > Zn, Cd > Ni is valid for the complexes which contain co-ordinating groups such as benzoate, phthalate and succinate. The magnitude of the first formation constants of acetato complexes of nickel(II), copper(II), lead(II) and zinc(II) determined by the present authors are in accordance with the above order. This fact supports the validity of the rule proposed by Yasuda and Yamasaki.

The equilibria of the substitution reaction represented by Eq. 1 have been studied. The equilibrium constants so far obtained, however, are considered to be not $K^M_{M'}$, but $K^M_{M',app}$, because they were determined in the acetate media but not corrected for the effect of acetate ions on the equilibria. In the present paper, the values of $K^M_{M'}$ given in Eq. 13 were determined by the extrapolation of the F_0 (or F_0') plot to zero acetate concentration. In Table III, the values of $K^M_{M'}$ for the three substitution reactions obtained in this study are summarized together with those obtained by Schwarzenbach et al.[5] for the same reactions. Schwarzenbach and his co-workers studied these equilibria at 20°C in the solution of ionic strength 0.1 with 8×10^{-3} M sodium acetate. The effect of acetato complex formation can be corrected with the relation given by Eq. 14. The original values given by Schwarzenbach et al. were converted to the $K^M_{M'}$ values using the formation constants $K_{M(OAc)_n}$ and $K_{M'(OAc)_{n'}}$ determined in this study. The resulting constants are also given in Table III, which are in satisfactory agreement with the $K^M_{M'}$ values observed experimentally in this study. This fact proves clearly the validity of the procedure and the results presented in this paper.

Summary

A new procedure for the determination of the formation constants of metal acetate complexes was developed. The procedure is

17) J. Kielland, *J. Am. Chem. Soc.*, **59**, 1675 (1937).
18) M. Yasuda and K. Yamasaki, presented at the Symposium on Metal Complexes, Tokyo, November, 1958.

based on the polarographic measurements of the sum of the equilibrium concentrations of the hydrated metal ions and the metal acetate complexes in the presence of an appropriate auxiliary complex-forming substance and of the reference metal ions of which the formation constants of acetate complexes are known.

The procedure was applied to the study of acetatocopper(II), acetatolead(II) and acetatozinc(II) complexes, EDTA being used as an auxiliary complex-forming substance. The overall formation constants $K_{M(OAc)_n}$ ($n=1$ and 2) for these metal acetate complexes were determined at an ionic strength of 0.2 at 15, 25 and 35°C.

The authors thank the Ministry of Education for the financial support granted for this research.

Department of Chemistry
Faculty of Science
Tohoku University
Katahira-cho, Sendai

SHORT COMMUNICATIONS

Confirmation of the Catalytic Deuteration of Methyl Groups of p-Xylene by the Use of the Infrared and NMR Methods

By Kozo Hirota, Hazime Kusumoto and Tomiko Ueda

(Received November 11, 1959)

It has been considered generally that the catalytic isotopic exchange reaction of hydrogen atoms with deuterium oxide occurs much more difficultly at paraffinoid hydrocarbons than at benzenoid hydrocarbons. However, as reported already[1] the exchange reaction of *p*-xylene catalyzed by nickel powders occurs also at the hydrogen atoms of the methyl groups, judging from the mass-spectrometric and infrared data of the products. In order to confirm such an expected result, the same samples were analyzed by the NMR apparatus of high resolution type (Varian V-4300 B). The conclusion was the same as already obtained. However, it was found that the proton signal of the methyl groups splitted into three or five components. Such a splitting may be not only interesting as a sure evidence of the above conclusions, but also would be noteworthy as a rare case where spin-spin coupling between H and D nuclei attached to the same carbon atom was observed. Although the similar splitting phenomenon has been reported by some researchers[2], the NMR results also will be presented here preliminarily in connection with the essential point of the research.

Nickel powders were prepared by decomposing nickel formate, oxidizing with air at 300°C and reducing at 400°C with hydrogen for 8 hr. Exchange reaction was carried out in a sealed glass tube, which contained a known amount of pure *p*-xylene and deuterium oxide (99.7% D_2O) as well as nickel catalyst. During the reaction, the tube was kept in a thermostat without shaking. After the definite time the reaction was stopped, and the *p*-xylene was separated from both heavy water and catalyst.

As an example of the experiment the most deuterated run, (No. 5), in which the reactants *p*-xylene and D_2O, were 0.4792 g. and 0.4864 g., respectively, and which were carried out for 150 hr. at 100°C will be referred. The numbers of deuterium (d_i) atoms in *p*-xylene molecules, determined by the mass-spectrometer, were as follows (%):

$$d_0=0.2,\ d_1=2.0,\ d_2=9.0,\ d_3=23.5,\ d_4=32.6,$$
$$d_5=24.7,\ d_6=7.9,\ d_7=0.1,\ d_8=d_9=d_{10}=0.0.$$

1) Abstracts of the 12th Annual Meeting of the Chemical Society of Japan (1959), p. 85.

2) (a) M. Karplus, D. H. Anderson, T. C. T. Farrer and H. S. Gutowsky, *J. Chem. Phys.*, **27**, 597 (1957); M. Karplus and D. H. Anderson, ibid., **30**, 6 (1957). (b) J. N. Schoolery, *Svensk. Kem. Tidskr.*, **69**, 185 (1957). (c) G. V. D. Tiers, *J. Chem. Phys.*, **29**, 963 (1958).

By the infrared method, three bands could be observed at the region of the C-D stretching bands, i. e. 2187, 2118 and 2047 cm^{-1} (broad). They can be ascribed to the bands of deuterated methyl groups, because in the case when the exchange reaction had been carried out by use of D_2SO_4 in order to deuterate the hydrogen atoms at the benzene ring[2], one C-D band appeared at 2254 cm^{-1}. This conclusion is not contradictory to the mass-spectrometric data, because *p*-xylene molecules highly deuterated more than six were negligibly small. Therefore it may be concluded that the exchange reaction proceeded practically at the six hydrogen atoms of the methyl groups (cf. Fig. 1).

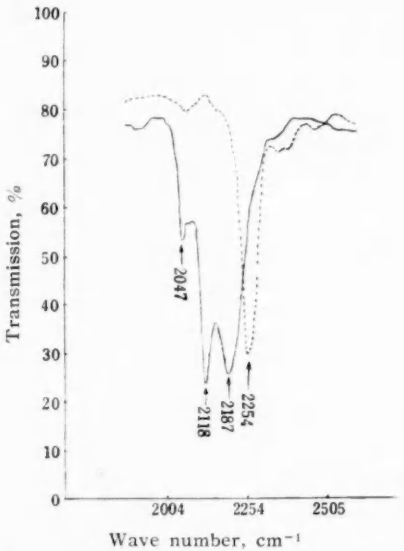

Fig. 1. Infrared absorption spectra of the deuterated samples.
——: Ni catalyst (deuterated degree = 39%)
------: H_2SO_4 catalyst (deuterated degree = 23%)[3]

By the NMR measurements relative intensity ratio of the proton signals of the methyl and ring groups in the original *p*-xylene should be expected to be 3 : 2 in singlet. This ratio would be expected to change as the deuteration proceeded. Actually the sample in medium process changed it, and moreover the methyl group spectrum had a structure which could be considered as superposed singlet and triplet components. These structures may be assigned to spectra from protons in CH_3 groups and those in CH_2D groups, respectively. Though exact measurements were hard, the relative intensity ratio of the ring protons and the methyl ones (CH_3 and CH_2D) seemed to be almost the same. There was observed no appreciable change in the line shape of the ring protons. It may be difficult to decide whether the ring protons also were exchanged or not. However, the obtained results would suggest that the exchange reaction proceeded easily at the methyl groups. The other features of this spectrum was slight shift of the proton signals of CH_2D to higher field as reported by Tiers[2]. Unfortunately a strong signal from CH_3 groups prevented exact measurements of this kind, but the distorted line shape and the slight hump on the central strong component suggested this fact. This tendency was observed more clearly with the more deuterated sample (No. 5). The large sharp central line of the triplet disappeared, and a very weak quintet if compared with the singlet of the ring protons which remained still sharp and strong was observed on the methyl protons. This would suggest at least that the deuteration had proceeded more easily at the two methyl groups than at the ring groups. The observed quintet was very weak and distorted considerably. The observed J_{H-D} was about 2 c. p. s. The distortion might be caused by superimposed structures like singlet, triplet and quintet being slightly shifted each other. These features of NMR measurements confirmed clearly that the deuteration by this method would occur easily at the methyl groups and that the deuteration may take place step by step at the two methyl groups; i. e., roughly speaking, according to the scheme, $CH_3 \rightarrow CH_2D \rightarrow CHD_2 \rightarrow CD_3$.

The authors express their sincere thanks to Professor J. Itoh who gave them valuable suggestions on the NMR spectra.

Department of Chemistry
Faculty of Science
Osaka University
Nakanoshima, Osaka
(K. H.) (T. U.)

Research Institute of Industry & Science
Osaka University
Sakai-shi, Osaka (H. K.)

3) T. Ueda. *Catalysts* (*Shokubai*), **1**, 1 (1959).

Cyclopentadienyl Cobalt Cyclooctatetraene

By Akira NAKAMURA and Nobue HAGIHARA

(Received February 4, 1960)

The present authors have previously reported the synthesis of cyclooctatetraene iron tricarbonyl and related compounds[1]. In continuation of the present study, the authors now wish to report a new synthesis of cyclopentadienyl cobalt cyclooctatetraene. Cyclopentadienyl cobalt dicarbonyl was heated at reflux in an excess of cyclooctatetraene under nitrogen for 6 hr. After removal of the unreacted starting materials, brown crystals were obtained by sublimation at 80°C under reduced pressure in 7% yield. These crystals were purified by recrystallization from petroleum ether and by sublimation. The purified sample had a m. p. of 81~82°C. Found: C, 68.32; H, 5.66; mol. wt. (Rast), 256. Calcd. for $C_{13}H_{13}Co$: C, 68.42; H, 5.74%, mol. wt., 228.

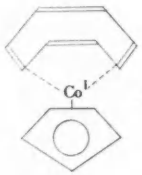

(I)

The elemental analysis apparently conformed to the structure, $(C_5H_5)Co(C_8H_8)$, cyclopentadienyl cobalt cyclooctatetraene (I). The same compound (I) could be obtained by irradiation of a mixture of cyclopentadienyl cobalt dicarbonyl and cyclooctatetraene with ultraviolet light under nitrogen for many hours.

I was soluble in common organic solvents and was stable in air. It was also soluble in cold concentrated sulfuric acid and in warm concentrated hydrochloric acid. The solution of I in carbon tetrachloride was decomposed by bromine and by iodine to give green and black precipitates, respectively. I reacted with cyclopentadienyl cobalt dicarbonyl in refluxing dioxane to give dark brown crystals, m. p. >300°C (with decomposition). I readily absorbed 2 mol. of hydrogen in the presence of Raney nickel catalyst at room temperature under ordinary pressure. Orange crystals, m. p. 102°C, were isolated from the hydrogenation mixture by sublimation in a reduced pressure at 80°C. These products of the reaction of I with bromine, iodine, hydrogen, cyclopentadienyl cobalt dicarbonyl and other reagents are now being studied in this laboratory and the results will be reported at a later date.

Three distinct proton resonance peaks were found at 82, 123 and 159 c. p. s, (ratio of the areas; 4.1 : 5 : 4.1), respectively, on the low field side from the proton resonance of cyclohexane. The result of this nuclear magnetic resonance study indicates that three different kinds of protons are present in I in a ratio of 4 : 5 : 4.

The infrared spectrum of I (in Nujol) showed a strong band at 1637 cm^{-1} due to C=C stretching similar to the corresponding 1635 cm^{-1} band of cyclooctatetraene. In the ultraviolet region it had an absorption maximum at 245 mμ ($\log \varepsilon$: 4.32, in 95 % alcohol).

These spectral and NMR data together with the chemical reactivity of I are essentially different from those of cyclooctatetraene iron tricarbonyl[1-3]. The double bonds in I which are presumably not used in π-bonding with the cobalt show usual properties of olefinic double bonds as described above. In contrast to this fact all four double bonds of the cyclooctatetraene moiety in cyclooctatetraene iron tricarbonyl do not show the usual properties of double bonds and they were thought to be affected by π-complex formation[3]. Accordingly the cyclooctatetraene moiety in I should be different from that of cyclooctatetraene iron tricarbonyl in its spacial and electronic structures. From the above evidences the authors propose the structure shown in the figure for I.

The Institute of Scientific and Industrial Research
Osaka University
Sakai-shi, Osaka

1) A. Nakamura and N. Hagihara, This Bulletin, **32**, 880 (1959); *J. Chem. Soc. Japan, Pure Chem. Sec.* (*Nippon Kagaku Zasshi*), in press; *Mem. Inst. Sci. and Ind. Res. Osaka Univ.*, in press.

2) T. A. Manuel and F. G. A. Stone, *Proc. Chem. Soc.*, **1959**, 90.

3) M. D. Rausch and G. N. Schrauzer, *Chem. & Ind.*, **1959**, 957.

The Use of Recoil Fission Rare Gas for the Study of the Change in Crystal Structure

By Seishi Yajima, Sumio Ichiba, Yuichiro Kamemoto and Koreyuki Shiba

(Received February 5, 1960)

Hahn[1] first investigated the emanation method which used radioactive inert gases $^{222}Rn(T_{1/2}=3.83\ d.)$, $^{220}Rn(T_{1/2}=54.5\ sec.)$ and $^{219}Rn(T_{1/2}=3.92\ sec.)$ as tracers. Since then, crystal structure changes and decomposition reactions were studied by this method[2]. In this method a parent of the radon nuclides is usually incorporated into a solid by coprecipitation with the solid or by deposition on the solid and the correlation between the escaped radioactive inert gas and crystal structure changes was studied.

In the present work, the radioactive fission product rare gases are used in place of radioactive radon nuclides. Uranium dioxide powder (particle size $\sim 0.2\ \mu$) is mixed with the solid powder to be examined, and the mixture is irradiated with thermal neutrons. When the weight ratio of uranium dioxide to the solid is 1 : 30, the fission recoil energy enables about 90% of the fission products to be caught by the surrounding solid powder. The captured fission product rare gases will behave in a similar manner as radon mentioned above, and they will be easily detected because of the relatively high fission-yield of radioactive xenon and krypton.

γ-Hematite or α-hematite and uranium dioxide powder of which the weight ratio is 30 : 1 were mixed and the mixture 500 mg. was irradiated for a total nvt of $\sim 3.5 \times 10^{15}$ thermal neutrons per cm^2 in an experimental hole of the JRR-1 reactor. After one-day cooling, the sample was placed in a quartz boat in a quarz tube which was connected with a phosphorus pentoxide drying tube, a dry ice trap (for radioactive iodine), a spiral counting cell inserted into an NaI scintillation crystal well of a γ-ray spectrometer and a flow rate meter, in the order mentioned. Pure helium gas was passed over the sample at a flow rate of 70 ml./min., and the sample was heated by a furnace surrounding the quartz tube at a rate of 5°C per minute. The radioactive xenon escaping from hematite was carried by helium and the radioactivity was measured by the γ-ray spectrometer which was previously adjusted to detect 250 keV. γ-ray of xenon-135 only. The plots of the radioactivity of xenon-135 escaped from γ-hematite and α-hematite versus temperature are shown in Figs. 1 and 2, respectively.

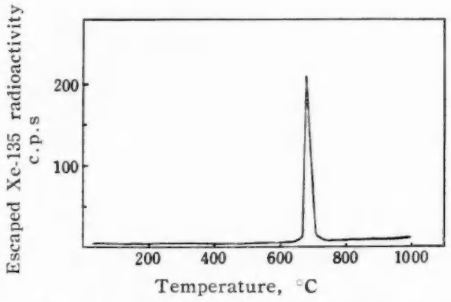

Fig. 1. Heating curve of γ-hematite. Heating rate, 5°C/min.

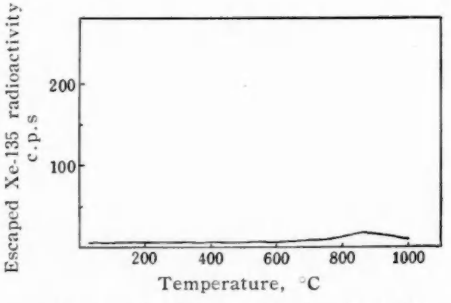

Fig. 2. Heating curve of α-hematite. Heating rate, 5°C/min.

The peak at 680°C of γ-hematite is considered to be related with the crystal change of γ-hematite to α-hematite. An X-ray diffraction method has shown that γ-hematite changes to α-hematite when the former is heated above the temperature at which a peak appears. In the case of α-hematite, the peak was not observed, because the crystal structure change is irreversible.

The previous data on the temperature of crystal structure change of γ-hematite to α-hematite are not in good agreement with the present result. The observed peak by the present method may shift with the heating rate, and the temperature

1) O. Hahn and O. Müller, *Z. Elektrochem.*, **29**, 189 (1923).
2) e. g., K. Zimens, *Z. physik. Chem.*, **B37**, 231 (1937).

of crystal structure change may be dependent on the preparation method and on impurities in γ-hematite.

The emanation method by the use of radioactive fission product rare gases will be applicable to many solids, even metals, because the samples can be prepared without chemical treatment, which are prerequisite to the radon emanation method.

Division of Chemistry
Japan Atomic Energy Research Institute
Tokai, Ibaraki-ken

Intramolecular Interaction between Hydroxyl Group and π-Electrons. IX[1]*. The Energy of the Interaction in Benzyldimethylcarbinol*

By Michinori Ōki and Hiizu Iwamura

(Received February 8, 1960)

The determination of the energy of the intramolecular interaction between hydroxyl group and π-electrons in this laboratory has so far been confined to the phenolic series[1,2]. In a preceding paper[1], it was referred that alcohols having internal interaction show rather complicated O–H stretching absorption bands (ν_{O-H}) consisting of two free ν_{O-H} corresponding to rotational isomers about the C_α–O bond and an interacting ν_{O-H}, and that the present technique[3] of separating the apparent curve into three Lorentz function type curves leaves some ambiguity and makes the evaluation of the energy inaccurate. However, current studies[1] on the effect of molecular conformations on the intramolecular interaction between the alcoholic hydroxyl group and π-electrons have shown that, in order to make more detailed discussions, the strength of the interaction should be expressed quantitatively. To overcome the aforementioned difficulty the authors took advantage of the observation that the rotational isomers of tertiary alcohols can not be distinguished by the present dispersion of the spectrometer[5], and expected that, unlike 2-phenylethanol, the free ν_{O-H} of benzyldimethylcarbinol would be single[6] and that the apparent ν_{O-H} curve could be exactly separated into a free and an interacting ν_{O-H} by the usual method of Ramsay[6]. This expectation proved to be the case and the energy of the interaction was determined by measuring the temperature variation of the absorption as described previously[1]. The least square method was adopted to determine the six parameters; a_1, b_1, ν_1, a_2, b_2 and ν_2, in the Lorentz function;

$$D(\nu)=\frac{a_1}{(\nu-\nu_1)^2+b_1^2}+\frac{a_2}{(\nu-\nu_2)^2+b_2^2}$$

The data are summarized in Table I.

TABLE I. THE EFFECT OF TEMPERATURE ON THE ν_{O-H} ABSORPTION OF BENZYLDIMETHYLCARBINOL

$1/T\times10^3$	ν_{O-H}	ν	a	b	$\ln(A_1/A_2)$
3.37	1	3593.5	16.13	8.14	−0.292
	2	3614.9	25.11	9.46	
3.25	1	3594.3	18.46	8.97	−0.268
	2	3615.9	26.24	9.76	
3.16	1	3594.9	17.23	9.11	−0.340
	2	3616.0	25.93	9.76	
3.04	1	3595.4	17.22	9.28	−0.349
	2	3615.7	25.67	9.76	
2.94	1	3596.3	15.86	9.14	−0.397
	2	3617.4	24.95	9.67	

The energy difference ($-\Delta H$) was found to be 0.54±0.13 kcal./mol. This is far less than that of ordinary hydrogen bondings which range from 2.3 to 7 kcal./mol.[7] The energy value is not consistent with those estimated by Goldman and Crisler[8] and by Schleyer and coworkers[9], but is in good agreement with some conformational observations accumulated in this laboratory[10] for β-tetralol, cyclohexen-3-ol and ergosterol. Namely, these compounds only exhibit the free hydroxyl band and

1) Part VIII: M. Ōki and H. Iwamura, This Bulletin, in press.
2) M. Ōki, H. Iwamura and Y. Urushibara, ibid., **31**, 769 (1958).
3) M. Ōki and H. Iwamura, ibid., **32**, 1135 (1959).
4) M. Ōki and H. Iwamura, ibid., **32**, 307 (1959); P. von Schleyer, D. S. Trifan and R. Bacskai, *J. Am. Chem. Soc.*, **80**, 6691 (1958).
5) M. Ōki and H. Iwamura, This Bulletin, **32**, 950 (1959).
6) D. A. Ramsay, *J. Am. Chem. Soc.*, **74**, 72 (1952).
7) C. A. Coulson, *Research*, **10**, 149 (1957).
8) I. M. Goldman and R. O. Crisler, *J. Org. Chem.*, **23**, 751 (1958).
9) While the present work was in progress, P. von Schleyer and his coworkers [*Tetrahedron Letters*, No. 14, (1959), p. 1] alluded that the energy of the intramolecular interaction in 2-phenylethanol was estimated to be about 1.4 kcal./mol. through temperature variation.
10) M. Ōki, H. Iwamura and T. Onoda, unpublished work.

lack the interacting ν_{O-H}. These molecules could have been able to possess an internal interaction if the hydroxyl groups were oriented axially, while the axial conformation is known to be less stable than the equatorial conformation by about one kcal./mol.[11] Thus, if the energy of interaction were more than or at least nearly equal to one kcal./mol., the interaction should have been certainly permitted to exist to some extent. Therefore, the energy of the interaction in these cases must be fairly smaller than one kcal./mol. A full discussion will be given in the near future.

Department of Chemistry
Faculty of Science
The University of Tokyo
Hongo, Tokyo

11) D. H. R. Barton, R. C. Cookson, W. Klyne and C. W. Shoppe, *Chem. & Ind.*, **1954**, 21.

NMR Study of α, β-Unsaturated Fatty Acids

By Shizuo Fujiwara, Hiroshi Shimizu*, Yoji Arata* and Sachio Akahori**

(Received February 10, 1960)

The NMR spectra of six sorts of α, β-unsaturated acids were measured by the 27 Mc. high-resolution spectrometer constructed in this laboratory. The acids used in this experiment were crotonic acid (I), isocrotonic acid (II), methacrylic acid (III), β-methylcrotonic acid (IV), angelic acid (V) and tiglic acid (VI). Among these, II and III were studied in pure liquids and others as saturated solutions in carbon tetrachloride at 25°C. The observed and calculated spectra are shown in Fig. 1, and the approximate values of chemical shifts and spin coupling constants derived from observed spectra are given in Table I, where the spin coupling constants between H and H, and between H and CH_3 are about the same as in ethylenic compounds[1]. From the spectra

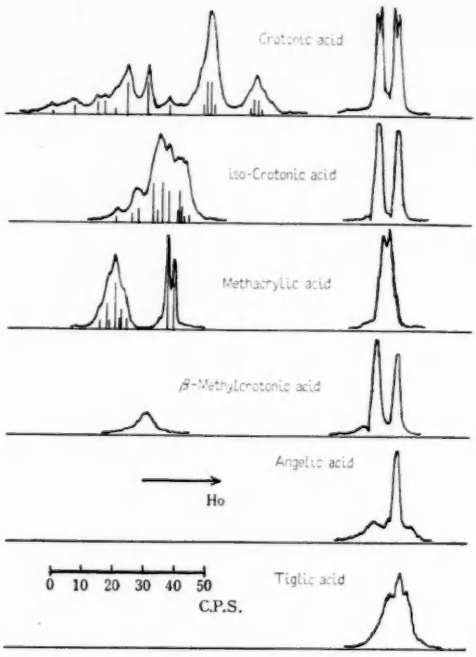

Fig. 1

of I and II, it will be concluded that the α-proton signal appears at the field higher than the β-proton, and that the β-proton *trans* to the carboxyl group is about 1 p.p.m. higher than the *cis* proton. The observed chemical shift between gem protons in methacrylic acid is 0.62 p.p.m., which is considerably larger than that between gem protons in the simple ethylenic compounds with the values of 0.1~0.2 p.p.m.[1] This fact seems to be consistent with the conclusion mentioned above on the chemical shifts for the β-protons of crotonic and isocrotonic acids. The magnitudes of the chemical shifts between the two methyl groups attached to the same carbon atom are not so large as the values between the gem protons.

An interesting solvent effect was observed in the system of β-methylcrotonic acid and benzene; where as the acid was diluted by benzene, the chemical shift between gem methyl groups was observed to increase, and the dilution shift at zero concentration was about 0.45 p.p.m. As reported by Shimizu[2,3] and Fujiwara[2], the active methyl group of saturated fatty

* Faculty of Pharmaceutical Sciences, The University of Tokyo, Hongo, Tokyo.
** Shizuoka College of Pharmacy, Koroku-cho, Shizuoka.

1) J. A. Pople, W. G. Bernstein and H. J. Schneider, "High Resolution Nuclear Magnetic Resonance", McGraw-Hill Book Co., Inc., New York (1959), p. 242.

2) H. Shimizu and S. Fujiwara, *Chem. Pharm. Bull. (Tokyo)*, to be published.

3) H. Shimizu, *J. Chem. Soc. Japan, Pure Chem. Sec. (Nippon Kagaku Zasshi)*, to be published.

TABLE I. SPIN COUPLING CONSTANTS AND CHEMICAL SHIFTS OF α,β-UNSATURATED FATTY ACIDS

(3) (2) C=C (4) COOH	Chemical shift p.p.m.	Spin coupling constant, c.p.s. H–H			H–CH_3		
		J_{23}	J_{24}	J_{34}	J_{23}	J_{24}	J_{34}
CH_3, H, H, COOH	$\delta_{H_2}-\delta_{H_3}=1.28$		15.5		1.2		6.1
H, H, CH_3, COOH	$\delta_{H_2}-\delta_{H_3}=0.19$	9.0				≤1.0	7.0
H, CH_3, H, COOH	$\delta_{H_3}-\delta_{H_4}=0.62$			1.9	~0	1.7	
CH_3, H, CH_3, COOH	$\delta_{Me_2}-\delta_{Me_4}=0.27$				≤1.0	≤1.0	
H, CH_3, CH_3, COOH	$\delta_{Me_2}-\delta_{Me_4}=0.2$				~0		6.5
CH_3, H, CH_3, COOH	$\delta_{Me_2}-\delta_{Me_3}\simeq 0$					≤1.0	6.0

acid, such as acetic acid shows the high field shift as the result of π complex formation with benzene molecule. The *trans* methyl group which is relatively unaffected from a steric point of view will tend to form π complex more easily than the *cis* methyl group and, hence, to show the dilution shift. The fact that the CH_3–CH_3 shift was increased by the dilution will be explained if the methyl group whose signal appeared at the field higher than the other is more shifted toward a high field. Thus, it is suggested from these considerations that the signal at the higher field may be assigned to the *trans* methyl group and the one at the lower field to the *cis* group. This conclusion may seem contrary to the expectation that the active methyl usually resonates at the field lower than the inactive one owing to the less density of the electronic cloud around it. As these unsaturated molecules have planar structures, however, the magnitude of the paramagnetic effect due to the carbonyl group at the *cis* position will exceed that of the paramagnetic effect at the *trans* position whose effect is mainly caused by inductive force of the carbonyl group.

More refined values of chemical shifts and spin coupling constants will be reported in the near future[4] by H. Shimizu, Y. Arata and S. Fujiwara concerning the general discussion of the analyses of the complex NMR spectra.

University of Electro-Communications
Chofu-shi, Tokyo

4) It will appear in This Bulletin.

Remarks on the Mechanism of Ammonia Synthesis

By Kenzi TAMARU

(Received February 8, 1960)

The importance of adsorption measurements during surface catalysis has recently been emphasized[1] and the adsorption measurements during ammonia synthesis on a doubly promoted iron catalyst has been carried out in a closed circulating system. The apparatus was almost the same with that schematically illustrated in a previous paper[1]. The reaction vessel is 12 cm. in length and 3.5 cm. in internal diameter. The circulation pump has a circulation rate between 4.5 and 8.0 l. (stp) per hour depending upon the pressure,

1) K. Tamaru, This Bulletin, **31**, 666 (1958); *Trans. Faraday Soc.*, **55**, 824, 1191 (1959); *Nature*, **183**, 319 (1959).

reaction temperature and composition of the reaction mixture. The reaction usually proceeded in such a way that the ammonia produced was collected in a trap cooled with liquid oxygen. The composition of the circulating mixture of nitrogen and hydrogen was determined with a thermal conductivity cell connected to the circulating system. The amount of ammonia trapped was determined by releasing it into a space between two stopcocks at room temperature. The amounts of the gases adsorbed on the catalyst surface were estimated from the amount of reactants introduced, the pressure and the composition of the circulating gas, and amount of ammonia trapped. Due allowance was made for the analytical samples removed from the apparatus. The promoted iron catalyst employed was obtained from the Government Industrial Research Institute, Tokyo, and contains 5% Al_2O_3 and 1% K_2O. The catalyst (198 g.) was powdered to smaller than 20 mesh and was reduced at 500°C for about 1000 hr. in a hydrogen flow of about 36 l. per hour at about atmospheric pressure, water vapor being removed by means of dry ice or liquid oxygen traps in the reaction system. Before each run the catalyst was evacuated for a few hours, treated with circulating hydrogen for 15 hr. in the system, with the traps maintained at liquid oxygen temperature, and then degassed for one hour. All these operations were carried out at 500°C.

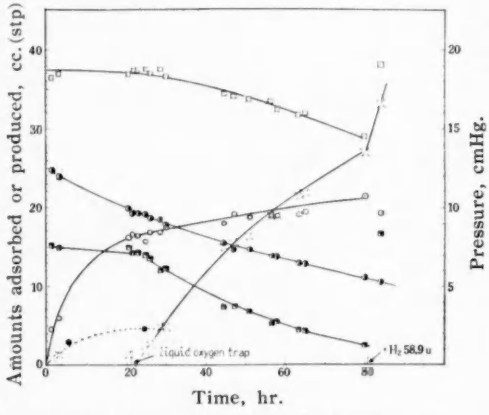

Fig. 1. Adsorption measurements during ammonia synthesis at 180°C. Amounts introduced: Hydrogen, 80.4 cc., Nitrogen, 71.8 cc. (stp).
◉: Hydrogen adsorbed (cc.).
•: Nitrogen adsorbed (cc.).
×: Ammonia produced (cc.).
◥: Ambient hydrogen pressure (cm.).
◑: Ambient nitrogen pressure (cm.).
●: Nitrogen adsorption in the absence of hydrogen at $P_{N_2}=15.13$ cmHg.

TABLE I

Flow rate l.(stp)/hr.	Relative reaction rate
11.23	1.00
5.58	0.95
10.18	1.00
4.98	1.06
12.27	1.00
5.56	0.89
7.70	1.00
3.37	0.98
7.39	1.00
2.98	0.95

Typical results for the experiments at 180°C are shown in Fig. 1 which illustrates experiments in which the ammonia trap was not cooled during the first 21 hr. The reaction rate was measured at a variety of circulation rates including alternately slow and fast rates at 250°C, and the results are shown in Table I, where the total pressure of the circulating reactant was between 22.61 and 11.36 cmHg and the nitrogen content was 28~38%. It is shown in the table that the reaction rate is not very sensitive to the circulation rate in the region in which adsorption was studied. It would appear that in the present studies the circulation rate is so high compared to the reaction rate that the partial pressure of the ammonia produced in the reaction vessel is very small.

According to Scholten and Zwietering[2], the rate of chemisorption of nitrogen on a singly promoted iron catalyst is proportional to the pressure. Hence, if allowance is made for the difference in nitrogen pressure, the results of Fig. 1 show that the rate of adsorption of nitrogen *in the absence of hydrogen* almost corresponds to the rate of ammonia synthesis reported by Emmett and coworkers[3]. This is one reason why they consider nitrogen adsorption to be the rate-determining step in the synthesis. However, as is brought out in Fig. 1, hydrogen causes a marked acceleration in the rate of adsorption of nitrogen. This conclusion is in accordance with the

2) J. J. F. Scholten and P. Zwietering, *Trans. Faraday Soc.*, **53**, 1363 (1957).
3) P. H. Emmett and S. Brunauer, *J. Am. Chem. Soc.*, **56**, 35 (1934); S. Brunauer, K. S. Love and R. G. Keenan, ibid., **64**, 751 (1942).

observations of Joris & Taylor, and Kummer & Emmett[4], that isotopic exchange of nitrogen is accelerated by hydrogen.

As shown in Fig. 1, the removal of ammonia from an equilibrated mixture of nitrogen, hydrogen and ammonia has little effect on the adsorption of either hydrogen or nitrogen. Suppose, for example, that all the nitrogen on the catalyst surface takes part in the reaction, then, if all the ammonia in the equilibrated mixture is removed, the adsorbed nitrogen should be rapidly consumed to form ammonia if nitrogen chemisorption is slow compared to all the other surface reaction, including hydrogen adsorption and that ammonia in the reacting gas is negligible. In actual experiments it may be unrealistic to neglect the ammonia pressure completely, but it is to be expected that if all the gaseous ammonia is trapped out the amount of adsorbed nitrogen should fall by an amount corresponding to the distance from equilibrium. But no sign of this tendency could be detected. Consequently, it seems unlikely, as far as one limits his own discussion to the behavior on the whole surface, that the nitrogen chemisorption only is rate determining, though commonly so accepted at present time[5].

This work was carried out with the financial support from the Mitsubishi Chemical Industries, Ltd., to which the author's thanks are due.

Department of Chemistry
Yokohama National University
Minami-ku, Yokohama

4) G. G. Joris and H. S. Taylor, *J. Chem. Phys.*, **7**, 893 (1939); J. T. Kummer and P. H. Emmett, ibid., **19**, 289 (1951).

5) C. Bokhoven, C. van Heerden, R. Westrik and P. Zwietering, "Catalysis", edited by Emmett, Vol. III, Reinhold Publishing Corp., New York (1955), p. 265.

*Polymerization of Styrene with the Ziegler-Natta Catalysts in the Presence of Molecular Hydrogen**

By Shunsuke Murahashi, Shun'ichi Nozakura and Yutaka Utsuhara**

(Received December 22, 1959)

It appears very important matter to have measures of controlling the molecular weight of isotactic polystyrenes in the polymerization with the Ziegler-Natta catalysts. Isotactic polystyrenes hitherto obtained in this laboratory according to the usual way[1] had the molecular weight of the order of several millions. In the course of this study, polymers having lower molecular weight was needed for the study of solution properties.

Among various factors affecting on molecular weight, such as the concentration of monomer, that of catalysts, and that of transfer agents, molecular hydrogen was chosen in the present work as one of the possible transfer agents, which had been known to be effective for controlling the molecular weight of polyethylene[2].

Recently, Natta has revealed in a paper the effectiveness of molecular hydrogen as controlling agents of molecular weight of polypropylene[3].

It has been found in the present work that isotactic polystyrenes of the low molecular weight could actually be obtained in the presence of hydrogen, although in addition to this there has been found another reaction which is competitive to the polymerization reaction, i.e. hydrogenation of styrene to ethylbenzene.

Polymerizations were carried out in an stainless steel autoclave of 200 ml. capacity. After the autoclave was flashed with nitrogen, $TiCl_3$ (3.0 g., the product of Stauffer Chemical Co.) washed with *n*-heptane was poured in with 30 ml. of *n*-heptane, and $AlEt_3$ (0.6 to 0.7 g.) was injected into the bottom of the autoclave

* Part V in a series on "Stereoregular Polymers": Presented at the 8th Annual Meeting of Society of Polymer Science (Japan), May 30, 1959.

** Present address: Research Laboratories, Kanebo Spinning Co. Ltd., Tomobuchicho, Miyakojima-ku, Osaka.

1) S. Murahashi, S. Nozakura, M. Sumi and K. Hatada, This Bulletin, **32**, 1094 (1959).

2) G. Natta, *Chem. & Ind.*, **1957**, 296

3) G. Natta, *J. Polymer Sci.*, **34**, 531 (1959).

from an injection syringe, and then styrene that was placed in a glass bottle was set in the autoclave. Dry hydrogen was charged to the desired pressure, the temperature was raised to 70°C, and then the shaking was commenced to make styrene contact with the catalyst suspension. Isotactic polymer was purified by the usual extraction procedure with methyl ethyl ketone.

It was found that both yields of total polymer and isotactic fraction in total polymer decreased markedly with increasing hydrogen pressure under the condition otherwise unaltered. As expected, however, intrinsic viscosities of isotactic fractions in toluene at 70°C also decreased as illustrated in Fig. 1.

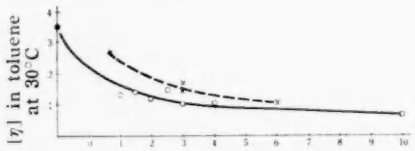

Fig. 1. Variation of intrinsic viscosities of isotactic polystyrenes with hydrogen pressure.
○: Polymerization time, 5 hr.
×: Polymerization time, 21 hr.
●: Polymerization for 5 hr. under a nitrogen atmosphere.

It was also found that the decreasing yields of polymer with increasing hydrogen pressure was mainly attributable to the occurrance of the competitive reaction, i. e. hydrogenation of styrene catalysed by the Ziegler catalyst. In one run, where styrene (9.1 g., 0.087 mol.) was heated with the catalytic system ($AlEt_3$, 0.71 g.; $TiCl_3$, 3 g.) at the constant hydrogen pressure of 8.9 kg./cm², 0.068 mol. of hydrogen was absorbed and gave a product, in which 3.7 g. of ethyl benzene was identified together with 0.474 g. of a pasty polymer and 0.499 g. of a solid polymer.

A modified catalyst system, $AlEt_3$ $Ti(OBu\text{-}n)_4$, produced no appreciable amount of polymer, but smoothly catalyzed the hydrogenation of styrene. Styrene alone, styrene and $AlEt_3$, and styrene and $TiCl_3$ did not show any absorption of hydrogen at the similar conditions.

From the above results, the observed decrease of molecular weight of isotactic polystyrenes with increasing hydrogen pressure may be considered to be due to following two reasons: the first is the effect of hydrogen as a chain transfer agent. Hydrogen probably cleaves a growing carbon-metal bond giving a metal-hydrogen bond and a saturated dead polymer, and the former would be still capable of initiating a new polymer chain. The second is the early lowering of monomer concentration due to the consumption of monomer by the hydrogenation reaction. Dependence of molecular weight on monomer concentration had been definitely demonstrated in the polymerization of propylene with the Natta catalysts[4] and hence the similar feature might be held in this case.

Propylene and butene-1 did not suffer such a hydrogenation reaction and the molecular weights of their polymers were found to be effectively controlled by the hydrogen pressure.

Department of Polymer Science
Faculty of Science
Osaka University
Nakanoshima, Osaka

4) G. Natta, I. Pasquon and E. Giachetti, *Makromol. Chem.*, **24**, 258 (1957).